ABSTRACT

Title of Thesis: EVALUATION OF SMOKE DETECTOR

RESPONSE ESTIMATION METHODS

Justin Aaron Geiman, Master of Science, 2003

Thesis directed by: Professor James A. Milke
Department of Fire Protection Engineering

Approximation methods exist to provide estimates of smoke detector response based on optical density, temperature rise, and gas velocity thresholds. The objective of this study was to assess the uncertainty associated with these estimation methods. Experimental data was used to evaluate recommended alarm thresholds and to quantify the associated error. With few exceptions, less than 50 percent of the predicted alarm times occurred within ± 60 seconds of the experimental alarms. At best, errors of 20 to 60 percent (in under-prediction) occurred for smoldering fires using an optical density threshold. For flaming fires, errors in predicted alarm times on the order of 100 to 1000 percent in over-prediction of the experimental alarms were common. Overall, none of the approximation methods distinguished themselves as vastly superior. Great care must be exercised when applying these approximation methods to ensure that the uncertainty in the predicted alarm times is appropriately considered.

EVALUATION OF SMOKE DETECTOR RESPONSE ESTIMATION METHODS

by

Justin Aaron Geiman

Thesis submitted to the Faculty of the Graduate School of the
University of Maryland, College Park in partial fulfillment
of the requirements for the degree of
Master of Science
2003

Advisory Committee:
      Professor James A. Milke, Chair
      Professor Frederick W. Mowrer
      Dr. Daniel T. Gottuk

ACKNOWLEDGEMENTS

TABLE OF CONTENTS

LIST OF TABLES

LIST OF FIGURES

CHAPTER 1: INTRODUCTION

Smoke detection has become a fundamental component of the active fire protection strategy of most modern buildings, particularly residential occupancies. However, this was not always the case. The smoke detection industry experienced explosive growth in the use of smoke detectors in the 1970's, driven by advances in technology and manufacturing that greatly reduced prices [Bukowski & Mulholland, 1978]. This explosive growth was accompanied, and likely furthered, by several significant research projects that reinforced the life safety protection provided by smoke detectors [Heskestad, 1974; Bukowski, et al., 1975] and provided evidence that supported increased requirements for smoke detectors in buildings. In addition, significant research efforts were undertaken to understand the environments to which detectors are exposed and the response of these detectors to such environments [Heskestad, 1974; Heskestad, 1975; Bukowski, et al., 1975; Heskestad & Delichatsios, 1977]. Many of the means by which to estimate the response of smoke detectors were formulated during this period of important smoke detection research (1970's) and have not advanced significantly since then; they are still the only available means for engineers to even approximate the response of smoke detectors. However, the practicality of these methods is severely limited by the significant fact that the uncertainty in the methods is generally unknown. The current research addresses this shortcoming and provides guidance on modeling the response of smoke detectors. The goals and scope of this research are detailed in subsequent sections of this chapter.

1.1 Research Goals

The overall goal of the present research is to assess and provide guidance on the currently available methods of smoke detector response prediction. Specific goals of this study are as follows.

Evaluation of the recommended thresholds of various measurements used in smoke detector response estimation techniques based on experimental data is the initial objective of this research. Subsequently, the predictive capabilities of these methods at estimating smoke detector response are examined and the uncertainty quantified. Finally, guidance is provided to engineers on the use of smoke detector response estimation techniques.

1.2 Research Scope

The focus of this research will be on methods of smoke detector response estimation provided in the *SFPE Handbook of Fire Protection Engineering* [Schifiliti, et al., 2002] and the *National Fire Alarm Code*, NFPA 72 [2002]. These sources are considered to be the most likely sources of guidance for engineers in the United States on the design and analysis of smoke detection systems.

The current research is divided into two phases. Phase 1 of the project focuses on the validation of thresholds used in smoke detector response estimation. Phase 2 of the project examines the predictive capability of smoke detector response estimation techniques and quantifies the associated uncertainty. Each of these phases is developed further in the subsections to follow.

1.2.1 Phase 1 – Threshold Evaluation

Thresholds commonly presented in the literature for estimating the response of smoke detectors are examined in Phase 1 by comparing them to the experimental measurements adjacent to smoke detectors at the time of alarm. Threshold values for optical density, temperature, and velocity are examined. The database for this examination is comprised of two independent series of tests, designated in this report as the Navy [Harrison, et al., 2003; Gottuk, et al., 2003] and Kemano [Su, et al., 2003] data sets, respectively. These data sets encompass a range of smoke sources, test conditions, smoke detector manufacturers, and models. Both flaming and smoldering fire sources are considered in each series of tests.

The Navy data, which was provided by the Naval Research Laboratory (NRL), includes a total of 41 tests and approximately 360 smoke detector alarms. Multiple smoke detectors were used in each test, which led to a large number of smoke detector alarms relative to the number of tests conducted. Only those detectors that alarmed during the course of a test were examined. Values of the local optical density, temperature rise, and velocity adjacent to each detector were determined at the time each smoke detector alarmed during the tests. Optical density and temperature rise values at the time of detector alarm are available for the vast majority of tests and detectors. Unfortunately, the velocity at detector alarm was only available for a small number of tests and detectors.

The Kemano data, which was provided by the National Research Council of Canada (NRCC), includes a total of 13 tests. Again in this study multiple smoke alarms were

used in each test and only those smoke alarms that alarmed are considered. Note that in

the Navy test series smoke detectors were used, while in the Kemano test series smoke

alarms were used. For simplicity, both smoke alarms and smoke detectors are referred to

as smoke detectors in this report. Values of the local optical density and temperature rise

adjacent to each detector will be determined at the time each smoke detector alarmed

during the tests. Unfortunately, velocity measurements were not taken as a part of the

Kemano study.

Further information on test conditions and experimental setup used in each test series is

discussed in Chapter 3, Experimental Setup.

1.2.2 Phase 2 – Threshold Uncertainty

Based on a review of current guidance provided in the literature (See Chapter 2),

recommended thresholds for optical density, temperature rise and velocity at the time of

detection were used to calculate alarm times from the test data. For example, the optical

density data adjacent to a smoke detector that alarmed was analyzed to determine the

time at which a certain optical density threshold value associated with detection was

exceeded; this time was taken as the *predicted* alarm time using the given optical density

alarm threshold. This analysis was completed for all smoke detectors that alarmed during

each test series. Although the conditions outside detectors that did not alarm could also

be analyzed in the same manner (i.e. to determine if an alarm would be predicted where

no actual alarm occurred during the test), the process of quantifying the uncertainty in

such predictions was unclear and was therefore avoided. The thresholds used in Phase 2 are the same as those analyzed in Phase 1.

Phase 2 serves as a means to assess the uncertainty uniquely inherent to the estimation technique (i.e. threshold) used without the complication of additional modeling errors (i.e. whether the model is predicting the measurement correctly). Any error associated with the experimental measurements used to make the predictions is assumed to be small in comparison to the estimated errors in modeling smoke detector response using one of the estimation techniques examined. The uncertainty related to each predicted smoke detector alarm response will be determined based on the difference between the predicted and experimental alarm times, normalized by the experimental alarm time.

CHAPTER 2: LITERATURE REVIEW

As stated in Chapter 1, the decade following 1970 was a period of tremendous growth in the popularity of smoke detectors. A growth in research and the general knowledge base regarding the operation of smoke detectors accompanied this. Most of the practical means of estimating the response of smoke detectors were derived from this era and have remained largely unchanged. By itself, this fact is not significant. However, there have been significant advances in detector technology since that time, including more uniform smoke entry characteristics among detector technologies, reduced sensitivity to nuisance (i.e., non-fire) sources, algorithm-based detection and multi-sensor, multi-criteria detection. Research into the current trend toward the development of fire detection algorithms and multi-sensor, multi-criteria fire detectors is prevalent in the literature in the last decade [e.g. Gottuk, et al., 1999; McAvoy, et al., 1996; Milke, 1995; Milke and McAvoy, 1996; Milke and McAvoy, 1997; Rose-Pehrsson, et al., 2000; Wong, et al., 2000]. However, advancement in the research behind predicting the response of common spot-type ionization and photoelectric detectors has been minimal. More fundamental approaches exist to model the detectors, though these methods have not been advanced sufficiently to prove practically useful for modeling smoke detectors.

This chapter will address many of the issues mentioned in the previous paragraph in more detail as well as some fundamental topics related to the prediction of smoke detector response.

2.1 Detector Operating Principles

Before any attempt is made to understand the means by which smoke detector response is

predicted, an understanding of the fundamental operating principles of smoke detectors is

required. For this study, only spot-type ionization and photoelectric detectors are

considered and are therefore the only technologies addressed in this section. For the sake

of brevity, from this point forward the use of the phrase *smoke detectors* will refer only to

spot-type ionization and photoelectric smoke detectors. More information on detector

operating principles, both those included here and some that are not, is available from

[Bukowski & Mulholland, 1978; Schifiliti & Pucci, 1996].

Ionization smoke detectors operate as a result of the reduction of electrical current in their

ionization chamber below a given threshold in the presence of smoke. The ionization

chamber consists of a tiny amount of radioactive material (typically Americium-241)

located between two metal plates, one with a positive electrical charge and one with a

negative electrical charge. The voltage across the two plates is maintained via a 9-volt

battery or 120-volt alternating current (typical household current). The Americium

contained in the chamber emits alpha particles, positively-charged ions consisting of two

protons and two neutrons, which *ionize* molecules in air (e.g., nitrogen and oxygen

molecules). Ionization of the oxygen and nitrogen molecules simply means that electrons

from these molecules are "knocked off" by the positively charged alpha particles. As a

result of this collision, the neutral atoms that lose an electron become positively charged

and the free electrons (i.e. the ones that were knocked off) attach to neutral gas molecules

7

to form negative ions. The ions are then drawn to the metal plate containing the opposite charge of the ion. A small current (on the order of 10^{-11} amperes) occurs as the result of this normal transfer of charge between these ions and the metal plates of the ionization chamber [Bukowski and Mulholland, 1978]. When smoke particles enter the chamber they become attached to ions (just as occurred with the gas molecules of the clean air). However, since these particles are significantly larger than the ions formed from the gas molecules, the velocity at which they are drawn to the metal plates is orders of magnitude slower, which allows the ionized smoke particles to be carried out of the sensing chamber by convection before they reach the metal plates [Bukowski and Mulholland, 1978]. As a result, a reduction in the current between the metal plates occurs and the smoke detector triggers an alarm when this current falls below a preset level.

Photoelectric smoke detectors operate on a significantly different principle than ionization smoke detectors – light scattering. Light scattering results from the interference of smoke particles with a beam of light. Photoelectric smoke detectors contain a light source, typically a light-emitting diode (LED), and a light receiver, such as a photocell. Meacham reported that two photoelectric detector manufacturers use LEDs with peak wavelengths in the range of 880 – 950 nm [Meacham, 1992]. The photocell is arranged at such an angle that it does not normally receive any light from the LED. The volume defined by the intersection of the viewing angles of the light beam from the LED and the photocell is termed the scattering volume [Bukowski & Mulholland, 1978]. As smoke enters the scattering volume, light from the LED is scattered onto the photocell. Photocells generate a current when a luminous flux (the scattered light) is applied. The

luminous flux received by the photocell increases in proportion with the smoke

concentration in the scattering volume. When the amount of scattered light reaching the

photocell exceeds a preset threshold, an alarm is triggered. The signal produced by

photoelectric detectors is sensitive to a number of physical characteristics of both the

detector and smoke including the number concentration, size distribution, shape, and

refractive index of the smoke particles as well as the scattering volume and wavelength of

light used in the detector [Schifiliti, et al., 2002].

2.2 Smoke Measurements

There are numerous experimental measurements that are used to characterize smoke.

The most common measurement of smoke is in terms of light attenuation or extinction.

Light attenuation, the decrease in luminous intensity due to the absorbtion, reflection, and

refraction of light by particles (smoke), is commonly referred to as *obscuration*. This

measurement is relevant to evaluating visibility through smoke and is also used as a

means of grossly estimating the response of smoke detectors (despite the fact that neither

ionization nor photoelectric detectors operate based on light attenuation) [Schifiliti, et al.,

2002]. Light attenuation is measured by aligning a light beam and photocell at a given

distance apart (the pathlength of the light, *l*). Such a device is called by several names

including optical density meter (the terminology used in this report) and smoke meter.

The attenuation of light by smoke is measured by the intensity of light received by the

photocell, *I*, relative to the intensity of light received by the photocell in the absence of

smoke (I_0). The light attenuation is typically normalized by the path length of the light

(*d*). In this way, light attenuation is typically measured as the average light attenuation

over a unit path length of light. Various forms of this are calculated as follows [Schifiliti, et al., 2002]:

Percent obscuration per unit distance, O_u

$$O_u = 100 * \left[1 - \left(\frac{I}{I_0} \right)^{1/d} \right]$$

Optical Density per unit distance, D_u

$$D_u = \frac{1}{d} \log_{10} \left(\frac{I_0}{I} \right)$$

Extinction Coefficient, K

$$K = \frac{1}{d} \ln \left(\frac{I_0}{I} \right)$$

The optical density of smoke per meter of path length (m^{-1}) will be the measurement used throughout this analysis. For brevity, the term *optical density* will used to refer to the optical density per meter.

The extinction coefficient calculation comes directly from an integrated form of Bouguer's Law of light attenuation assuming a constant extinction coefficient over the path length. As Mulholland points out, Bouguer's law is strictly valid only for monochromatic light sources (i.e., light sources emitting a single wavelength of light) [Mulholland, 2002]. However, many researchers, and even the standards used to evaluate smoke detectors, use polychromatic (white light) sources to measure light extinction. Foster examined the uncertainty in applying Bouguer's Law to a polychromatic light source for wood smoke and predicted a 22 percent deviation over the mass concentrations examined [Foster, 1959]. Mulholland [1982] presented the general design of a light

extinction instrument that satisfies Bouguer's law by using a monochromatic light source and eliminating forward scattered light at the receptor. More recently, Putorti [1998] described in more detail the characteristics, performance guidelines, and expected uncertainty of a similar device. Mulholland, et al. [2000] extended this research by constructing and testing such an instrument.

It should also be noted that optical density is simply a base 10 expression of Bouguer's Law and therefore the same disclaimer regarding potential errors from polychromatic light sources applies. The optical density, D_u can be calculated from the extinction coefficient, K, as follows

$$D_u = \frac{1}{d}\log_{10}\left(e^{Kd}\right) = \frac{Kd}{d}\log_{10}\left(e^1\right) \approx \frac{K}{2.303}$$

Other important smoke measurements include the particle size distribution, particle number concentration, mass concentration, and refractive index. These measurements are representative of fundamental physical properties of the smoke aerosol, but are rarely measured despite their potential value. Measuring smoke in this way is a difficult experimental problem due to the vast range of particles sizes (0.005 – 5 μm) and particle concentrations (10^4 – 10^{10} particles/cm^3) expected from smoke; the dynamic nature of each due to particle coagulation and agglomeration (smoke aging) only adds to the difficulty [Bukowski & Mulholland, 1978].

Lee and Mulholland [1977] provide a thorough review of the physical properties of smoke and instrumentation to obtain such properties. The level of detail provided by Lee

and Mulholland is not repeated here, but the highlights of their work are summarized below. The single most important property of smoke is its size distribution, which is highly dependant on the mode of combustion (i.e., flaming or smoldering fire). Particle size measurements are typically made using an Electrical Aerosol Analyzer (EEA) for particle sizes of 0.006 – 1 μm and an optical particle counter is employed for particle sizes of 0.5 – 5 μm. The size distribution is important due to the fact that the smoke generated by a fire typically contains a range of particle sizes, with a peak concentration of particles of a certain size (often referred to as the *peak particle size* of the smoke). Flaming fire sources tend to produce particles with significantly smaller peak particle sizes than smoldering (non-flaming) fire sources. In addition, the peak particle size tends to decrease with increasing temperature and velocity, due to more complete combustion and less time for particle growth due to coagulation, respectively. A condensation nuclei monitor is typically used to monitor the particle number concentration of smoke. The number concentration decreases rapidly over time due to particle coagulation. The mass concentration of smoke is typically measured by a particle mass monitor and by filter collection. Losses to the surrounding surfaces (wall losses) are the most significant loss mechanism for mass concentration, however even these losses are generally orders of magnitude lower than the reduction of number concentration due to coagulation. The mass concentration, therefore, appears to relatively constant as a function of smoke age.

Seader and Einhorn present a value they term as the particle optical density, which is the ratio of optical density per meter to mass concentration. They found the particle optical density, D_p, is approximately constant for a variety of wood and plastic fuels at 1.9 m^2/g

for smoldering fires and 3.3 m²/g for flaming fires [Seader and Einhorn, 1977].

However, as Mulholland [2002] notes, these values are based on the optical density

measured with a polychromatic white light source, to which Bouguer's Law is not strictly

valid. Despite this limitation, these values can be used as a rough guide if no other data is

available. The specific extinction coefficient, σ_s (m²/g), is the equivalent of the particle

optical density in terms of base e (i.e. $\sigma_s = 2.303 * D_p$). The results from Seader and

Einhorn are more commonly presented in terms of specific extinction coefficient as $\sigma_s =$

7.6 m²/g for flaming combustion and $\sigma_s = 4.4$ m²/g for smoldering combustion. More

recently, Mulholland and Croarkin found a mean specific extinction coefficient of

8.7m²/g with an expanded uncertainty of $\pm$ 1.1 m²/g (95 percent confidence level) using a

632.8 nm (He-Ne) laser for over-ventilated flaming fires [Mulholland & Croarkin, 2000].

Their analysis included a variety of fuel sources and fire sizes, with measurements

conducted by several laboratories. One significant conclusion from this work is that the

variation in specific extinction coefficient between laboratories was greater than the

variation found from a single laboratory to different fire sources. The importance of the

particle optical density and the specific extinction coefficient are that they can be used to

model the optical density or extinction coefficient of smoke by calculating the mass

concentration of smoke.

Another measurement of interest related to the particle optical density is the mass optical

density, D_m (m²/g). Seader and Chien [1975] defined the mass optical density as the

optical density of smoke produced per unit mass of fuel consumed. The particle optical

density is converted to the mass optical density by the following equation

$$D_m = D_p * y_s$$

where: y_s = fraction of particulate matter (smoke) produced relative to the mass

loss of the fuel (also commonly referred to as the soot yield)

D_m is typically used to predict the optical density of smoke based on the equation

$$D_u = \frac{D_m \Delta m_f}{V_c} = \frac{D_m \dot{m}_f}{\dot{V}}$$

where:

D_u = Optical density per meter (m^{-1})

D_m = Mass optical density (m^2/g (fuel))

Δm_f = Mass loss of fuel (g)

V_c = Volume into which smoke mass is dispersed (m^3)

$\dot{m}_f$ = Mass loss rate of fuel (g/s)

$\dot{V}$ = Volumetric flow rate (m^3/s)

The mass optical density is typically determined using small-scale tests. Results for D_m

for a variety of materials are presented by Mulholland [2002]. Quintiere [1982] has

reported that the correlation between small-scale measurements of D_m and the optical

density values from full-scale fires breaks down with complex fires.

2.3 Smoke Detector Modeling Approaches

The approaches used to predict smoke detector response are categorized into first-

principles methods and approximation methods. First principles methods are the more

scientific methods of predicting detector response, however none of these are currently

practical for use by engineers. Approximation methods, which are the focus of this study, may not correspond to the actual operational principle employed by the detector, but are indications of conditions likely present when the detector alarms. The uncertainty in these approximations is expected to be significant. Schifiliti and Pucci [1996] provide a thorough review of the state-of-the-art in fire detection modeling.

2.3.1 First-Principles Methods

Scientific first-principles approaches to predicting smoke detector response do exist. However, due to the lack of sufficient specific experimental data, including certain properties of both the smoke and smoke detector, these models are effectively useless to engineers. Nevertheless, these models do warrant discussion in that they hold the potential to provide smoke detector response predictions with much greater accuracy.

Mulholland [2002] presented an empirical model for the electrical signal from a smoke detector, S, for either ionization or photoelectric smoke detectors as the integrated product of the size distribution and the response function, $R(d)$, of the detector according to the equation

$$S = \int_{d_{\min}}^{d_{\max}} R(d) \frac{\delta N}{\delta d} \delta d$$

where:

S =   Electrical signal from smoke detector (μV)

$R(d)$ =   Response function for the smoke detector (μVcm^3)

$\dfrac{\delta N}{\delta d}$ =   Number size distribution function (cm$^{-3}\mu$m^{-1})

d =   Particle diameter (μm)

The difficulty in applying this knowledge is that the response function, $R(d)$, is particular to the detector design and only determined through specific testing. Mulholland and Liu [1980] determined the response function for one ionization detector to be the product of a constant multiplied by the particle diameter, $R(d) = 7d$. However this relationship holds only for the detector under test in their research.

Models are available that address the specific operating principles of the detector design – ionization or light scattering. A semi-empirical equation for the signal from an ionization chamber in the presence of smoke was developed by Hosemann [1970] for relatively low smoke densities. Although Hosemann's work is not readily accessible, his work is discussed by Scheidweiler [1976], Litton [1977], and Helsper, et al. [1983]. The equation developed by Hosemann is

$$y \cdot \eta = N \cdot \bar{d}$$
$$y = x \frac{2 - x}{1 - x}$$
$$x = \frac{\Delta I}{I_0}$$

where:

N =   Particle number concentration

$\bar{d}$ =   Mean particle diameter

η =   chamber constant

Hosemann's theory was found to agree within a few percent of the mathematical model derived by Litton [1977]. Helsper, et al. [1983] quantitatively verified the ionization chamber theory of Hosemann experimentally. Therefore, with knowledge of particle size distribution and concentration of the smoke, the chamber constant of the particular detector, and the threshold alarm signal for the detector, an ionization smoke detector can be modeled using this theory. A complicating factor in this modeling exercise is that as the smoke ages, the number concentration and size distribution change due to coagulation [Lee & Mulholland, 1977] and therefore these dynamics must also be modeled.

In a further refinement of this work, Newman [1994] modified the theory to include the charge fraction of soot particles. As Newman remarks, the fraction of charged particles produced by combustion, X_e, had been shown to be highly material-dependant. Newman found a notable correlation between experimental data and the ionization chamber theory when modified to account for particle charge fraction. The modified equation presented by Newman is

$$y \cdot \eta = \left(1 - X_e\right) \cdot N \cdot \bar{d}$$

Newman recognized that this model was somewhat difficult to apply in that it required knowledge of smoke particle number concentrations, particle size and charge fraction.

He reformulated the previous equation in terms of the soot volume fraction, f_v, and a detector/material sensitivity factor, α.

$$y = \alpha \cdot f_v$$

Newman found that the sensitivity factor was related to the soot yield (y_s) by

$$\alpha = -[0.62\ln(y_s) + 0.74] \times 10^8$$

Although this result may seem fortuitous, Newman noted that the main source of ions in flames was due to chemi-ionization and that the increase in soot formation and chemi-ionization with increasing bond unsaturation and aromaticity as support for this correlation. Furthermore, based on previous work, Newman showed that the soot volume fraction can be related to the extinction coefficient at a particular wavelength by

$$f_v = \frac{K_\lambda \lambda}{7.0}$$

Finally, combining the above equations, Newman's model of ionization detector response allows the prediction of ionization detector response based on the soot yield, the light extinction coefficient, and the change of current required to cause an alarm according to the following equation:

$$y = -\frac{K_\lambda \lambda[0.62\ln(y_s) + 0.74] \times 10^8}{7.0}$$

The first principles approach to modeling photoelectric (light-scattering) smoke detectors is significantly less advanced. To the author's knowledge, the only such attempt at fundamentally modeling photoelectric smoke detectors was conducted by Meacham [1992]. Meacham proposed the use of Mie light-scattering theory to predict smoke detector response in the following form:

$$I_s = I_0 \frac{\lambda^2 N V_s}{8\pi^2 l^2}(i_1 + i_2)$$

where:

I_s =   Intensity of light scattered (W/m^2)

I_0 =   Intensity of incident light(W/m^2)

λ =   Wavelength of light (m)

N =   Particle number concentration

V_s =   Sensing volume (m^3)

l =   Distance from the center of the particle to the light receptor

$(i_1 + i_2)$ =   Mie scattering coefficients (f{λ,d,θ,m})

θ =   Scattering angle

m   =   Real component of refractive index

d   =   Particle diameter

For a given detector, the values of I_s, I_0, λ, V_s, l, and θ are known (or at least could be obtained from the manufacturer). To calculate N, Meacham proposes using the relationship between the number concentration and mass concentration provided by Mulholland [2002]:

$$N = \frac{6C_s}{\pi\rho d_{gn}^3}\exp\left(-\frac{3}{2}\ln^2\sigma_g\right)$$

where:

N =   Particle number concentration (particles/m^3)

C_s =   Mass concentration of smoke (g/m^3)

ρ =   Density (g/m^3)

d_{gn} =   Geometric mean number diameter (μm)

σ_g =   Geometric standard deviation (–)

The Mie scattering coefficients could be determined for the smoke based on the small-scale Scattered Light Detection Instrument (SLDI) described by Meacham. Later, Loepfe, et al. [1997] present a device similar to the SLDI to determine the angle- and polarization-dependent scattered light intensities for high concentrations of fire and non-fire aerosols at a fast sampling rate. Although, Meacham provided much of the necessary exploratory work on modeling the response of photoelectric smoke detectors, his suggestions for future work on this topic have not been acted upon.

Research programs are needed that develop databases of smoke measurements (e.g., particle number concentration, mass concentration, refractive index) required by the models discussed for a variety of common fuels. Once a sufficient knowledge base of these measurements is obtained, specific properties of the smoke detectors required by these models needs to be determined as part of the listing procedure of smoke detectors or be made readily available by manufacturers. Only when all of these future needs are met will these first-principles smoke detector response models be practical tools for engineers to use.

2.3.2 Approximation Methods

The approximation methods available for the prediction of smoke detector response are a product of necessity. Out of a desire to have some practical means of estimating the response of smoke detectors, early researchers in this area developed methods of approximation based on measurements that could be modeled with reasonable accuracy and obtained experimentally with minimal additional effort. This section will outline the development of the current state-of-the-art in approximating smoke detector response and provide the basis on which much of the remainder of this research is based.

2.3.2.1 Optical Density Method

The optical density method of estimating detector response compares a calculated optical density outside a detector to a threshold value of optical density indicative of detector response. Various measurements that are used to calculate optical density were discussed in section 2.2. To review, one common method of calculation relies on the empirically determined quantity mass optical density, D_m, which is assumed to be constant for a given fuel. Using the mass loss of the fuel, the volume into which the smoke is dissipated, as well as D_m an optical density can be determined. Likewise, the optical density can be calculated based on the mass concentration of the smoke produced by a fire. Based on knowledge of the mass loss of the fuel, the smoke yield, and volume into which the smoke is dissipated, the mass concentration can be calculated. From this mass concentration, the values of particle optical density by Seader & Einhorn [1977] (or the specific extinction coefficient vales reported by Mulholland and Croarkin [2000]) can be used to calculate the optical density. The previously discussed methods could be

calculated by hand or, more likely, be incorporated into zone model or field model calculations.

Once the optical density is calculated, the threshold optical density for detection needs to be known in order to estimate detector response. Approaches that have been considered include using the nominal sensitivity of the smoke detector (the alarm level marked on the detector as determined by the appropriate detector sensitivity test (i.e. UL 217 [2001] or 268 [2003]); using the specified upper limit black smoke concentration of $0.14m^{-1}$ formerly used in the smoke detector approval standards UL 217 [2001] and UL 268 [2003]; and determining the threshold values based on experimental measurements in which both optical density meters and smoke alarms were present. The two former approaches will be discussed in more detail later.

In one of the early examinations of detector response, Heskestad and Delichatsios [1977] calculated the optical densities at detector response for several materials under flaming conditions. In Volume I of their report, Heskestad and Delichatsios [1977] provide "representative" values of optical density at response for *active fire spread* for flaming fires. This table is reproduced below in metric units.

Table 1 - Representative optical density values at alarm for flaming fires from Heskestad and Delichatsios [1977].

	Optical Density at Response, D_{ur} (m^{-1})	
Fire Source	**Ionization**	**Photoelectric**
Wood (Sugar Pine, 5% moist.)	0.016	0.049
Polyurethane Foam	0.164	0.164
Cotton Fabric (Unbleached Muslin)	0.002	0.026
PVC Wire Insulation	0.328	0.328

As Table 1 shows and as Heskestad and Delichatsios [1977] point out, there is significant variation in the optical density at response values with respect to the fire source (material) and the detector operating principle. What is not evident from Table 1, nor presented by Heskestad and Delichatsios [1977], is exactly how these "representative" values were determined and the degree of variation in these values. Heskestad and Delichatsios do report that they gave little weight to the generally high optical density values at detector response at the furthest distance from the fire for the polyurethane and cotton fires and the near-zero values of optical density at detector response for the PVC fires obtained before vigorous flame spread occurred. Additional details on the variation in the optical density at response values for flaming wood crib fires is also reported. Heskestad and Delichatsios [1977] report an average optical density at response of 0.014 m^{-1}, with minimum and maximum values of 0.003 m^{-1} and 0.032 m^{-1} respectively, for ionization detectors. Likewise, for photoelectric detectors responding to flaming wood fires, the average optical density at response was 0.053 m^{-1}, with minimum and maximum values of 0.018 m^{-1} and 0.101 m^{-1} respectively. Despite the "representative" values corresponding fairly well with the mean values for the wood crib fires, it is not clear whether this is the case for all the materials considered. Furthermore, even the overall variation noted for the wood crib fires is significant and needs to be considered when predicting smoke detector response.

In more recent work, Geiman and Gottuk [2003] examined the optical densities at response for UL-listed smoke detectors under full-scale fire test conditions from three different series of tests. The data sets used encompass a range of smoke sources, detector

sensitivity levels, test conditions, and detector manufacturers. In total, a database of 875 detector responses was compiled and examined. Major variables evaluated included smoke detector type (ionization/photoelectric), fire type (flaming/smoldering) and nominal detector sensitivity. The optical density alarm threshold defined by Geiman and Gottuk [2003] is the smoke optical density level at which a certain percentage of detectors would have alarmed based on the test data. Geiman and Gottuk [2003] examined all the optical density at detector response data and presented optical density alarm threshold values corresponding to when 20, 50 and 80 percent of the detectors alarmed in the full-scale tests. These percentages of the population of detector responses were selected based on providing a range of thresholds at a justifiable resolution; i.e., defining thresholds at 5 or 10 percent increments of the available population was not sound given the small sample sizes. The vast majority of the data sets did not include more than 50 detectors for a given fire, detector type, and nominal sensitivity, with some only in the range of 10 to 20 detectors. Based on an informal sensitivity analysis, it was concluded that using a percentage greater than 80 percent or less than 20 percent of the population could result in one or two anomalous tests inappropriately skewing the thresholds presented.

Table 2 presents the 20, 50, and 80 percent optical density alarm thresholds presented by Geiman and Gottuk [2003]. In addition, the arithmetic mean optical density at the detector response for each case is also presented with the standard deviation. These values are provided to demonstrate the large variation in the data and to establish a rationale for using percentiles of the population for this analysis. In fact, examining the

24

range within one standard deviation of the mean can result in non-physical, negative

values for the optical density at alarm. This is an artifact of the statistics due to the

presence of values much larger than the mean. The last column in the table is the number

of detectors examined. The three test series presented in Table 2 are designated as the

Indiana Dunes [Bukowski, et al., 1975], Navy [Gottuk, et al., 1999; Rose-Pehrsson, et al.,

2000; Wong, et al., 2000], and Fire Research Station (FRS) [Spearpoint and Smithies,

1997] data sets.

Table 2 - 20th, 50th, and 80th percentile values of optical density at detector response from Geiman and Gottuk [2003].

Test Series	Detector Type	Nominal Sensitivity (OD/m)	Fire Source[a]	ODM Alarm Thresholds (OD/m)			ODM Value at Alarm (OD/m)		# Dets
				20%	50%	80%	Mean	Std Dev	
Indiana Dunes	Ion	0.0143	F	0.003	0.015	0.090	0.060	0.117	49
Indiana Dunes	Photo	0.0143	F	0.018	0.045	0.118	0.138	0.237	42
Indiana Dunes	Ion	0.0288	F	0.003	0.024	0.116	0.081	0.133	54
Indiana Dunes	Photo	0.0288	F	0.022	0.057	0.118	0.138	0.227	41
Indiana Dunes	Ion	0.0143	S	0.032	0.078	0.186	0.111	0.098	83
Indiana Dunes	Photo	0.0143	S	0.021	0.040	0.087	0.074	0.111	69
Indiana Dunes	Ion	0.0288	S	0.057	0.127	0.186	0.149	0.136	96
Indiana Dunes	Photo	0.0288	S	0.033	0.057	0.118	0.082	0.084	76
Navy	Ion	0.0071	F	0.007	0.015	0.044	0.025	0.026	46
Navy	Photo	0.0071	F	0.012	0.028	0.056	0.031	0.026	43
Navy	Ion	0.0186	F	0.011	0.022	0.065	0.034	0.037	45
Navy	Photo	0.0361	F	0.028	0.049	0.057	0.055	0.046	14
Navy	Photo	0.0508	F	0.044	0.068	0.121	0.082	0.049	22
Navy	Ion	0.0071	S	0.028	0.081	0.116	0.079	0.049	18
Navy	Photo	0.0071	S	0.028	0.042	0.066	0.061	0.057	25
Navy	Ion	0.0186	S	0.025	0.090	0.138	0.082	0.057	14
Navy	Photo	0.0361	S	0.030	0.065	0.076	0.074	0.065	6
Navy	Photo	0.0508	S	0.063	0.079	0.125	0.093	0.046	20
FRS	Ion	0.0129	F	0.013	0.025	0.062	0.039	0.039	15
FRS	Ion	0.023	F	0.006	0.023	0.053	0.032	0.034	15
FRS	Photo	0.027	F	0.056	0.120	0.165	0.117	0.061	15
FRS	Photo	0.0295	F	0.034	0.072	0.104	0.069	0.038	15
FRS	Ion	0.0129	S	0.098	0.205	0.267	0.212	0.125	11
FRS	Ion	0.023	S	0.032	0.094	0.164	0.100	0.074	12
FRS	Photo	0.027	S	0.038	0.089	0.160	0.100	0.058	13
FRS	Photo	0.0295	S	0.014	0.044	0.136	0.103	0.146	13

[a] F = Flaming Fires; S = Smoldering Fires

In addition to providing representative optical density values at detector response, Geiman and Gottuk [2003] also compared the optical densities at detector response to two of the alarm thresholds mentioned earlier – the nominal sensitivity of the detector and the maximum black smoke optical density in UL 217 and UL 268 (0.14 m^{-1}). The nominal sensitivity of the detector was found to be a suitable alarm threshold only for ionization detectors detecting flaming fires. In contrast, an optical density threshold of 0.14 m^{-1} was found to generally provide a conservative estimate of detector response for all modes of combustion and detection principles examined.

2.3.2.2 Temperature Rise Method

Other than presenting the optical density at response, Heskestad and Delichatsios [1977] did not promote the use of the optical density at response as a means of estimating detector response. Instead they promoted the concept of a characteristic temperature rise associated with smoke detector response, which they believed varied less between materials than optical density.

The theory that Heskestad and Delichatsios [1977] developed to be able to relate detector response to the temperature rise at the detector requires numerous assumptions. Heskestad and Delichatsios [1977] assume that the ratio of mass concentration to temperature rise is constant with respect to both time and space. This claim assumes that:

- the mass generation of smoke is equal to the mass loss of fuel,

- turbulent convection is solely responsible for the movement of combustion

  products (including smoke) (i.e. diffusion and gravitational settling are

  insignificant),

- combustion products do not react after they leave the source, and

- heat transfer from the smoke particles due to radiation and between the

  ceiling jet flow and the ceiling material is insignificant.

Heskestad and Delichatsios [1977] also used the (now) generally accepted assumption

that the optical density per unit length is proportional to mass concentration (see section

2.2).

Given the previously mentioned assumptions, Heskestad and Delichatsios [1977] claim

that the ratio of optical density to temperature rise ($D_u/\Delta T$) is constant with respect to

both time and space for a given material fuel and burning mode (i.e., flaming,

smoldering, vertical, or horizontal combustion). However, the data they present does not

bear this out. For the wood crib fires with the 29 ft ceiling height the presented $D_u/\Delta T$

increases almost linearly with time, with little variation in space. The wood crib fires at

the 8 ft ceiling exhibited a similar trend with the exception of the data from the 40 ft

radial distance from the fire axis, which were significantly higher than at the 10 ft and 20

ft radii. Convective heat losses were blamed for the anomaly and it was suggested that

heat transfer to the ceiling could begin invalidating their theory at ratios of radial distance

to ceiling height greater than four (which Heskestad and Delichatsios point out is

supported by the theory for steady ceiling jets [Alpert, 1971]). For the other materials

studied, $D_u/\Delta T$ exhibited various behaviors including decreasing with time and increasing

to a maximum until steady burning is achieved then decreasing. In none of the data

presented was $D_u/\Delta T$ invariant enough to be considered constant in time *or* space.

Nevertheless, Heskestad and Delichatsios [1977] recommend using a constant $D_u/\Delta T$ as a

rough approximation and present "representative" values of $D_u/\Delta T$. The term

representative is used in quotation marks because this is the wording that Heskestad and

Delichatsios use, but this claim is not necessarily supported nor explained by them.

Schifiliti and Pucci [1996] reexamined this data and provided the range of values of

$D_u/\Delta T$ for each fuel. Table 3 shows the "representative" values of $D_u/\Delta T$ provided by

Heskestad and Delichatsios [1977] and the range of $D_u/\Delta T$ values added by Schifiliti and

Pucci [1996], both of which been converted into metric units. Be aware that temperature

rise values less than 3 ºC (5 ºF) were not considered when calculating these ratios, due to

the fairly severe temperature stratification observed in test facility used by Heskestad and

Delichatsios [1977].

Table 3 - Ratio of optical density to temperature rise for various fuels

	$D_u/\Delta T \ ((\text{m}^\text{o}\text{C})^{-1})$	
Material	**"Representative" Value**	**Range of Values**
Wood (Sugar Pine, 5% moist.)	1.2E-3	8.9E-4 – 3.2E-3
Cotton (Unbleached Muslin)	5.9E-4 / 1.2E-3	3.0E-4 – 1.8E-3
Paper (in Trashcan)	1.8E-3	Data not available
Polyurethane Foam	2.4E-3	1.2E-2 – 3.2E-2
Polyester Fiber (Bed Pillow)	1.8E-2	Data not available
PVC Wire Insulation	3.0E-2 / 5.9E-2	5.9E-3 – 5.9E-2
Foam Rubber / PU (Sofa Cushion)	7.7E-2	Data not available

In order to determine the temperature rise at detector response, ΔT_r, Heskestad and

Delichatsios [1977] did *not* rely directly on the recorded data. It was thought that ΔT_r

values based on the recorded data would include significant contributions of the ignitor

(or sustainer) fuel, which would unnecessarily increase ΔT_r. However, the actual ΔT_r

values from the data were never calculated (or at least not presented) by Heskestad and

Delichatsios for comparison. Instead, Heskestad and Delichatsios [1977] calculate ΔT_r as

$$\Delta T_r = \frac{D_{ur}}{D_u / \Delta T}$$

In other words, the "representative" values of D_{ur} from Table 1 were combined with the

"representative" values of $D_u/\Delta T$ from Table 3, by means of the equation above, to

determine the "representative" temperature rises at detection. The "representative"

values of ΔT_r provided by Heskestad and Delichatsios [1977], converted into metric units,

are summarized in Table 4.

Table 4 - Representative temperature rise to detection for flaming, spreading fires
from Heskestad and Delichatsios [1977].

	ΔT_r (°C)	
Fire Source	Ionization	Photoelectric
Wood (Sugar Pine, 5% moist.)	14	42
Polyurethane Foam	7	7
Cotton Fabric (Unbleached Muslin)	2	28
PVC Wire Insulation	7	7

The values presented in Table 4 still appear in Annex B of NFPA 72 [2002], however,

they are no longer included in the *SFPE Handbook of Fire Protection Engineering*

[Schifiliti, et al., 2002]. It is also interesting to note that the representative temperature

rise of the ionization detector to the flaming cotton fabric fire which is reported as 3 °F by

Heskestad and Delichatsios [1977] is below the 5 °F minimum temperature rise they

established for much of their analysis.

An ad hoc committee of the Fire Detection Institute, which included Benjamin, Heskestad, Bright, and Hayes [1979], was formed in order to formulate the research by Heskestad and Delichatsios [1977] into a form that would be useful for smoke detector standards. In this report, the authors promote the concept of the detector material response number (DMR), the temperature rise from burning a given material required to cause a selected smoke detector to alarm. The DMR values presented in this report are identical to those found in Table 4. Benjamin, et al. [1979] note that the DMR numbers are not sufficient when smoke entry resistance is present and that an equation utilizing the characteristic length, L, of the detector (identical in form to Heskestad's model of smoke entry resistance presented in section 2.3.2.3, but with the temperature rise substituted for optical density). However, because manufacturers and approval laboratories never adopted a test to determine L numbers, the DMR (temperature rise at detection) values by themselves became used as a means of predicting smoke detector responses.

In 1984 when Appendix C of NFPA 72E was published, a temperature rise of 13 °C (20 °F) was used to indicate detector response [NFPA 72, 2002]. This recommendation has since been clarified in NFPA 72 to more accurately portray the original recommendations of Heskestad and Delichatsios [1977]. In addition, the previous edition of the *SFPE Handbook of Fire Protection Engineering* briefly mentioned that for higher energy flaming fires, detectors often alarm at a temperature rise of 10 to 15 °C [Schifiliti, et al., 1995]. However, even based on these references in the literature, the origin of the assumption that 13 ºC corresponds to the temperature rise at detection for all detectors is unclear. Benjamin, et al. [1979] make reference to the fact that if the burning material is

not known or readily predictable, then a conservative approach would be to assume a wood crib is burning and use the DMR value for wood for the given detector. Later, when Evans and Stroup [1985] developed the DETACT model, they discussed how the calculated temperature rise (such as that determined by DETACT), could be used along with the analysis of Heskestad and Delichatsios [1977] to calculate the response time of smoke detectors (See section 4 of [Evans and Stroup, 1985]). In their discussion, they note that a specific ionization smoke detector (tested by Heskestad and Delichatsios [1977]) could be represented as a low temperature heat detector alarming at 13 ºC above ambient for a wood fire. The difference between this temperature rise and the DMR value for the ionization detector and wood fire listed in Table 4 is due to conversion to metric units and rounding. Evans and Stroup [1985] converted the optical at response value (from 0.005 ft^{-1} to 0.016 m^{-1}) and ratio of optical density to temperature rise (from 2.0E-4 (ft ºF)$^{-1}$ to 1.2E-3 (m ºC)$^{-1}$) from Heskestad and Delichatsios [1977] and then calculated the temperature rise at detection from these converted values. The presentation of the 13 ºC temperature rise for detection by Evans and Stroup [1985], when taken in addition to the comments by Benjamin, et al. [1979] regarding a DMR for wood for an unknown fire source, led to the incorrect conclusion by many that any given fire and detector could be approximated as a heat detector alarming at 13 ºC. It is the author's belief that Heskestad and Delichatsios, Bejamin, et al., and Evans and Stroup never intended for 13 ºC to be used to predict response for all detectors to all fires, however this is how their work was interpreted.

Numerous studies have questioned, or outright disputed, both the use of a constant temperature rise for detection, as well as the temperature rise method in general. After an article by Milke [1990] appeared in *Fire Technology* regarding the technical basis of the (then) new smoke management standard for malls and atria (NFPA 92B [1990]), Beyler and DiNenno [1991] responded with a Letter to the Editor citing numerous technical questions on this article including the recommendation of using a temperature rise at detection of approximately 10 ºC for all burning materials and detectors. Due to the increasing use of the temperature rise method, which Beyler and DiNenno [1991] remark was based on "very weak data", they reexamined the data from Heskestad and Delichatsios [1977]. Unlike the method used by Heskestad and Delichatsios [1977] to determine ΔT_r, Beyler and DiNenno [1991] examined the actual gas temperature data adjacent to the detectors at the time of response. They found that ΔT_r was not even close to constant for a specific detector responding to a given material, much less for all materials and detectors. Numerous studies have since reported similar conclusions (e.g., Schifiliti and Pucci, 1996; Luck and Seivert, 1999; Cholin and Marrion, 2001).

Additionally, Mowrer and Friedman [1998], Gottuk, et al. [1999], and Wakelin [1997] have shown smoke detector alarms occurring at temperature rises as low as 1 to 3 °C. Furthermore, Bukowski and Averill [1998] point out that Collier [1996] found that when using CFAST a 4 ºC temperature rise best matched detector alarms from experiments, while Davis and Notarianni [1996] recommended a temperature rise of 5 ºC for ionization detectors with a nominal sensitivity of 0.025 m^{-1} in a high bay hangar space. Bukowski

32

and Averill [1998] go on to conclude that using a temperature rise at detection of 4-5 ºC for modern detectors may be sufficient.

2.3.2.3 Critical Velocity Method

Numerous early researchers noted that often smoke detectors seemed to just "quietly disappear in the smoke" in the absence of sufficient convective flow near detectors [Bukowski, 1992]. The phenomenon to which they were referring is particularly prevalent in slow smoldering fires. Such fires often produce significant quantities of smoke without producing sufficient buoyancy; buoyancy is required to drive the flow. Without a significant driving force, the velocity of the smoke reaching the smoke detector can be quite low and as a result the optical density outside the smoke detector can be significantly greater than that in the sensing chamber of the smoke detector due to a smoke entry lag. Smoke entry lag can be significant and can cause the response of the smoke detector to be appreciably delayed.

Heskestad attempted to account for this well-observed phenomenon of smoke entry lag in his early work on modeling the response of smoke detectors. As an initial phase of some of his work on the early-warning performance of residential fire detectors, Heskestad developed an equation to correlate the response of smoke detectors to the optical density of smoke at detector response [Heskestad, 1974]. This equation accounted for the entry lag of smoke. The equation for the optical density at smoke detector response is based on a characteristic optical density inside the smoke detector to a given smoke (D_{uo}), the rate

of rise of the optical density $\left(\dfrac{dD_u}{dt}\right)$, a characteristic length of the smoke detector that is

independent of the smoke properties (*L*), and the local gas velocity (u):

$$D_{ur} = D_{uo} + \left(\frac{L}{u}\right)\left(\frac{dD_u}{dt}\right)$$

Heskestad [1975] formalized and documented this theory in more detail. The equation

presented above is actually a simplified form of the actual response equation. Bjorkman,

et al. [1992] provide a concise derivation of the detector response equation as well as the

simplified form noted above.

Bjorkman, et al. [1992], Marrion [1989], and Oldweiler [1995] have all since studied

Heskestad's detector response equation and determined L for various detectors. Schifiliti

and Pucci [1996] have compiled the characteristic lengths (L) of detectors determined by

these researchers. The characteristic lengths ranged from 1.8 to 14.2 m for ionization

detectors and 2.6 to 18.4 m for photoelectric smoke detectors across all researchers

studying a variety of detectors, smokes/aerosols, and flow velocities. In studying

Heskestad's detector response equation Bjorkman, et al. [1992], Marrion [1989], and

Oldweiler [1995] all observed variation in L for low velocity flows [Schifiliti and Pucci,

1996]. This observation implies that a single L value is not sufficient to characterize the

smoke entry for both low and high velocity flows. In addition, a possible dependence of

L on smoke characteristics was implied by the data of Marrion and Oldweiler [Schifiliti

and Pucci, 1996]. Each of these last two points questions fundamental assumptions of the

characteristic length used in Heskestad's theory – independence of L from the properties

of the smoke and ceiling jet.

Modern smoke detectors are expected to have more uniform entry resistance characteristics due to the addition of variable velocity and smoldering fire sensitivity tests into smoke detector approval standards [Bukowski, 1992]. Based on this fact and the observed variation in L at lower flow velocities, more recent research into smoke entry lag into smoke detectors has moved away from Heskestad's model. Recently, Cleary, et al. [2000] presented a two-parameter entry lag model that correlates each parameter to velocity using power-law equations. The first parameter is termed the dwell time, the delay associated with the decrease in flow caused by entrance screens and baffles, which is modeled as a plug flow. The second parameter is a mixing time, the delay associated with the sensing chamber volume, which occurs in series after the dwell time and is modeled as a perfectly-stirred volume. Cleary, et al. examined two different ionization and photoelectric smoke detectors over approximately 25 tests, with velocities ranging from 0.02 to 0.55 m/s, to determine the correlations for the dwell and mixing times for each detector. As might be expected from Heskestad's model, Cleary, et al. found that the exponent of the power-law velocity correlation between both the dwell time and mixing was close to −1 (i.e. both parameters varied approximately inversely proportional to the velocity – at low velocities smoke entry delays are significant). However, there was significant scatter in the model parameters, possibly due in part to uncertainty in the velocity measurements. Finally, for velocities greater than approximately 0.5 m/s, a single parameter model or simply a small constant lag time may be appropriate, since the dwell time drops below 10 seconds and the mixing time is essentially zero (at least for the detector designs studied). Although the research by Cleary, et al. provides an

advancement in the state-of-the-art of understanding smoke entry lag, they only examined one smoke source (a propene diffusion burner that provides black smoke), specific testing of a detector is still required to determine the correlations for the two-parameter model, and no further verification of this technique has been done by other researchers.

Brozovski [1991] approached the smoke entry problem differently, attempting to determine a velocity below which delays due to smoke entry resistance would become significant or prevent detector operation. In his research, a low velocity wind tunnel was used to determine that a critical velocity, u_c, of approximately 0.15 m/s exists below which smoke detector response can become delayed. Coincidentally, this critical velocity corresponds to the velocity used in the approval standard for smoke detectors (UL 217 [2001]). Schifiliti and Pucci [1996] caution that the critical velocity may vary with smoke detector design or that it is simply an artifact of the detectors, test parameters or test apparatus used. Nevertheless, Schifiliti, Meacham, and Custer in the *SFPE Handbook of Fire Protection Engineering* [2002] and Annex B of NFPA 72 [2002] propose using the critical velocity approach as a means of estimating the response of smoke detectors. The critical velocity threshold is compared to a calculated ceiling jet velocity (e.g., a velocity from a ceiling jet velocity correlation) and once this threshold is exceeded, it is assumed that sufficient smoke concentration is present to cause the detector to alarm.

CHAPTER 3: OVERVIEW OF EXPERIMENTAL DATA

The experimental data examined in this research was not conducted by the author, but graciously provided by other researchers. Two series of tests were examined, designated as the Navy [Harrison, et al., 2003; Gottuk, et al., 2003] and Kemano [Su, et al., 2003] tests. Both test series are described in further detail later in this chapter. The rationale for selecting these tests as part of this study was that both test series included full-scale fire tests in which modern smoke detectors and several environmental variables (e.g. optical density, temperature, and velocity) were examined in close proximity to one another. Additionally, all of the data from these tests was provided electronically in order to facilitate the analysis and modeling efforts of this project. Overall, these tests provided a reasonable cross-section of smoke sources, test conditions, and smoke detectors likely in modern buildings.

3.1 Navy Tests

The Navy tests were conducted aboard the ex-USS *Shadwell*, the Naval Research Laboratory's full-scale fire research facility in Mobile, Alabama [Carhart, et al., 1992]. The tests were conducted as two series, the first test series was conducted April 7-18, 2003 and the second test series was conducted April 21-25, 2003. The details of these tests are described below.

3.1.1 Test Spaces

Fire tests were performed in small- and medium-size test compartments onboard the ex-USS *Shadwell*. The overall dimensions of the small test compartment were 6.05 m from

forward to aft, 3.61m from port to starboard and 3.05 m in height. The medium test

compartment was 5.94 m forward to aft, 8.08 m port to starboard, and 3.05 m in height.

The medium size test space also contained a vestibule, which was not part of the test

space, in the front, starboard corner that measured 1.13 long, 2.22 m wide, and 2.59 m

high.

Both the small and medium test spaces aboard the ex-USS *Shadwell* have beams

spanning port to starboard at 1.22 m spacing and depths of 30.5 cm from the ceiling. In

addition, the medium test space was split into two zones separated by a 49.5 cm beam

that runs forward to aft through the compartment.

Two ventilation scenarios were used in this test series: no ventilation and 12 air changes

per hour of 100 percent outside air (maximum ventilation conditions in the

compartment). From a fire testing standpoint, these ventilation scenarios are

representative of conditions that remove the least and greatest amounts of heat and

smoke. The compartment doors were closed for each test series.

3.1.2 Fire Sources

Multiple fire exposures were used in the full-scale fire tests onboard the ex-USS

Shadwell. For the first test series, fires were performed both in the space where the

detectors were located as well as in an adjacent space to the test compartment. Since

there were no vents that allowed the passage of smoke between the adjacent spaces and

the spaces in which the detectors were located, the adjacent space fire tests were excluded

from this analysis. Each of the 13 in-space fires in the first test series consisted of one of

four different wood crib fires, with approximate energy release rates of 12, 25, 50 or 125

kW.

For the second test series, fairly small fire and nuisance sources were used to challenge

the detection systems. Of the 40 total tests conducted in the second test series, nuisance

sources were used in 12 of these tests; these tests were not considered in this analysis.

Table 5 presents the fire sources used in the second series of Navy tests. The sources

were initiated at various locations throughout the test space (the detailed locations are

provided in [Gottuk, et al., 2003]).

Table 5 - Fire sources used in the second series of Navy tests

Fire Source	Description
Smoldering Cable Bundle	Five one foot pieces of cable (Monroe Cable Co., LSTSGU-9, M24643/16-03UN XLPOLYO) in a bundle. A 500 W cartridge heater (Vulcan, TB507A) is placed in the middle of this bundle energized to 70 percent of its maximum voltage, initially. The power was increased to 500 W (100%) after 25 to 30 minutes. For tests 2-37 to 2-40, the heater was energized to 500 W from the start of the test.
Lactose/Chlorate	Based on British Standard BS6266, an equal mixture by mass of potassium chlorate and of lactose powder were mixed thoroughly and ignited with a butane lighter.
Cardboard Box	Four 0.26 x 0.26 x 0.11m cardboard boxes were loosely filled with brown paper and arranged in a two-tiered stack with a 2.5 cm flue space between the two stacks. A butane lighter was used to light a bottom corner of a box in the flue space.

3.1.3 Smoke Detectors

A variety of smoke and fire detection systems were evaluated in the Navy tests, of which

only Simplex and Edwards Systems Technology Inc. (EST) spot-type ionization and

photoelectric detectors were used in this analysis. The Simplex detectors used included

Model 4098-9717 ionization detectors and Model 4098-9714 photoelectric detectors.

The EST detector models used were SIGA-IS (ionization) and SIGA-PS (photoelectric).

To provide anonymity to the manufacturers, the detectors were arbitrarily assigned

identification numbers for this analysis. The nominal sensitivity (manufacturer default

sensitivity) values of the detectors used in this test series are shown in Table 6 along with

the corresponding identification number and detector type.

Table 6 - Smoke detectors used in the Navy tests

Test Compartment	ID	Detector Type	Nominal Sensitivity	
			m^{-1}	%Obs/ft
Small	1	Ionization	0.023	1.6
	2	Photoelectric	0.051	3.5
	3	Ionization	0.019	1.3
	4	Photoelectric	0.036	2.5
	5	Ionization	0.023	1.6
	6	Photoelectric	0.051	3.5
	7	Ionization	0.019	1.3
	8	Photoelectric	0.036	2.5
Medium	9	Ionization	0.023	1.6
	10	Photoelectric	0.051	3.5
	11	Ionization	0.019	1.3
	12	Photoelectric	0.036	2.5
	13	Ionization	0.023	1.6
	14	Photoelectric	0.051	3.5
	15	Ionization	0.019	1.3
	16	Photoelectric	0.036	2.5
	17	Ionization	0.023	1.6
	18	Photoelectric	0.051	3.5
	19	Ionization	0.019	1.3
	20	Photoelectric	0.036	2.5
	21	Ionization	0.023	1.6
	22	Photoelectric	0.051	3.5
	23	Ionization	0.019	1.3
	24	Photoelectric	0.036	2.5

Detectors were positioned in groups at several locations throughout the space, with a general spacing of 0.3 m between detectors within each grouping. The detector locations remained constant throughout the two Navy test series. The smoke detectors were installed to industry standards (i.e. NFPA 72 [2002]). One smoke detector from each manufacturer of each type was installed at every grouping. For the largest wood crib fires, some of the detectors were removed to avoid damage from gas temperatures exceeding 100 °C.

3.1.4 Instrumentation

Only instrumentation that pertains to the optical density, temperature and velocity measurements adjacent to the smoke detectors is discussed in this section. For details on additional instrumentation not discussed here, refer to Harrison, et al. [2003] and Gottuk, et al. [2003].

The smoke optical density was measured with an optical density meter (ODM). Each ODM utilized an 880 nm infrared light emitting diode (IRLED) and receptor arrangement over a 1.0 m path length. Before each test all ODMs were adjusted such that the ambient optical density measurement were near zero.

Temperature measurements in the Navy tests were made with Inconel-sheathed, type K thermocouples located adjacent to each smoke detector group. All thermocouples were positioned approximately 9 cm below the overhead.

A sonic anemometer (Model No. SPAS/2Y) from Applied Technologies, Inc. was used to measure the gas velocity in two orthogonal directions. The vertical (floor to ceiling) velocity component was not measured. The velocity along each direction is computed based on the transit times for sonic pulses that are generated at the probe's sonic transducers and received 15 cm away by opposing transducers. The listed wind speed measurement range for this probe was $0 - 50$ m/s, with a resolution of ± 0.01 m/s according to the manufacturer's specifications. One limitation of this velocity probe was that the operating temperature range is -30 to $+60$ºC. Procedures were in place during the test to remove the probe from the hot smoke when (if) the gas temperature approached the maximum safe operating temperature of the probe. The sonic anemometer was originally calibrated by the manufacturer. A formal calibration of the instrument for this test series was not conducted, however informal examinations of its operation were made.

3.2 Kemano Tests

The National Research Council of Canada (NRC) recently had the unique opportunity of conducting full-scale fire detection experiments in residential dwellings in Kemano, British Columbia [Su, et al., 2003]. A total of 13 fire detection tests were conducted as part of that study from May 18 – 22, 2001. Details on the test spaces, fire sources, smoke detectors, and instrumentation used in these tests will be outlined in the remaining sections of this chapter.

3.2.1 Test Spaces

Tests were performed in two residential dwellings, identified as BB-513 and K1-106 by Su, et al. [2003]. Both dwellings were of typical wood frame construction with common residential interior furnishings. The houses were unheated. Dimensioned schematics of each dwelling, which include detector, instrumentation, and fire source locations are found in Figures 8a, 8b, 29, and 30 of [Su, et al., 2003]. Dwelling BB-513 is a one-story bungalow, which also had a finished basement, with approximate internal dimensions of 7.7 m by 12.2 m. The ceiling height on the ground floor of BB-513, where the tests were conducted, was 2.44 m. Tests 1 – 9 were conducted in BB-513. The remaining 4 tests were conducted in K1-106, a two-story single-family home with approximate internal dimensions of 6.9 m by 8.9 m. The ground floor of K1-106 had a ceiling height of 2.5 m, the second floor ceiling height was 2.4 m, and the landing area of the staircase had a ceiling height of 3.0 m.

3.2.2 Fire Sources

Small, slow-growing flaming and smoldering fire sources were used in the Kemano tests to challenge the smoke detectors. Most fires began as smoldering combustion and later transitioned to flaming. Representative household fire sources (e.g. wood, paper, polyurethane foam, etc.) were used. The details of the fire sources used are summarized in Table 7. An electronic heating element was used as the source of ignition energy in all tests.

Table 7 - Fire sources used in the Kemano tests

Fire Source	Description
Wood	5 to 10 pine sticks (19 mm x 38 mm x 127 mm each)
Paper	20 - 0.50 m x 0.68 m sheets of newspaper (Each folded to 0.165 m x 0.23 m)
PU Foam with Cotton Flannel	0.10 m thick, 0.20 m diameter pieces of polyurethane foam, wrapped with a 0.57 m x 0.53 m sheet of cotton flannel
Cotton Flannel	0.86 m x 0.86 m cotton flannel sheet folded to 0.215 m x 0.215 m.
Upholstered Chair	Section of upholstered chair (arm / seat cushion); no further material details provided

Kemano test 12 is excluded from this analysis. Test 12 began as 450 mL of cooking oil in a pan, however a 75 percent heptane / 25 percent toulene mixture was added several times later in the test to the cooking oil to accelerate the fire development.

3.2.3 Smoke detectors

Underwriter's Laboratories of Canada (ULC) listed battery-powered ionization and photoelectric smoke detectors (compliant with the requirements of CAN/ULC-S531-M87 [1995]) were included in the Kemano tests. Additional fire detection technologies (i.e. multi-sensor and carbon monoxide detectors) were also present, but were not used in this analysis.

A total of 14 ionization and 14 photoelectric smoke detectors were used in Tests $1 - 9$ of the Kemano test series. However, not all of these detectors were collocated with optical density meters or thermocouples. Ionization detectors labeled I8, I14, and I28 and photoelectric detectors labeled P6, P16, and P26 all had optical density meters and

thermocouples located adjacent to their respective locations. Only thermocouples were collocated with ionization detector I18 and photoelectric detector P20. The remaining detectors were not located directly adjacent to any instrumentation and therefore were not used in this analysis. Each group of smoke detectors contained a single ionization and photoelectric detector and were located at the ceiling of Bedroom 1 (detectors P6 and I8), corridor (detectors I14 and P20), foyer (detectors I18 and P20), and living room (detectors P26 and I28). In general, all smoke detectors were spaced 0.3 m apart (center to center) within each detector grouping.

Kemano tests 10 – 13 included a total of 5 photoelectric and 8 ionization smoke detectors located on the ground and second floor of K1-106. Note that the fires were all conducted on the ground floor. Each smoke detector group consisted of an ionization detector and a photoelectric detector. Two smoke detector groups were located in the living room on the ground floor (detectors I1 and P3 in one group and detectors I4 and P6 in the other). Detectors I7 and P9 were located as a group in the staircase landing (between the ground and second floors). Two additional smoke detector groups were installed in the second floor corridor (detectors I10 and P12 in one group and detectors I13 and P15 in the other). Each group was located adjacent to both gas temperature and optical density instrumentation, with the exception of one of the living room detector groups (I1 and P3) and one of the second floor corridor groups (I13 and P15) that were collocated only with temperature measurement instrumentation.

3.2.4 Instrumentation

Optical density meters and thermocouples were used in the Kemano tests to measure the smoke optical density and temperature in the vicinity of the smoke detectors. No instrumentation was provided in the Kemano tests to measure the gas velocity near the smoke detectors.

Optical density meters used in the Kemano tests were designed and constructed by NRC. Each optical density meter used a 940 nm, pulsed, near-infrared LED light source with a photodiode, separated by a distance of 0.60 m. Calibrations were performed on all optical density meters using optical filters. For the nine tests conducted in BB-513, smoke optical meters were located in Bedroom 1, the corridor and the living room at both ceiling height and 1.68 m above the floor. Only the ceiling height (0.15 m below the ceiling) optical density meters are used in this study. Optical density meters were located in the living room, staircase landing, and corridor on the second floor for the remaining four Kemano tests performed in K1-106. Again, these instruments were located at the ceiling and 1.68 above the floor and only the ceiling height (0.15 m below the ceiling) optical density meters were considered in this analysis.

Temperature measurements in the Kemano tests were measured with 0.038 mm diameter (26 AWG), Type K, nickel-chromium and nickel-aluminum alloy thermocouples (TCs). Multiple TCs were arranged into trees (vertical arrays), to measure the gas temperature at various heights. Only the top-most TC in each tree, located 40 mm below the ceiling, was examined in this analysis. TC trees were located in the living room, corridor, and

Bedroom 1 adjacent to the smoke detector groups for the tests conducted in BB-513.

Likewise, for the final four Kemano tests in K1-106, TC trees were located in the living

room, corridor, staircase landing, and second floor corridor adjacent to the smoke

detector groups.

CHAPTER 4: PHASE 1 RESULTS

Experimental measurements of optical density, temperature, and velocity adjacent to

smoke detectors at the time of alarm are the basis for Phase 1 of this analysis. A

statistical description of the experimental measurements examined at the time of alarm is

provided in this section. In addition, thresholds commonly presented in the literature for

estimating the response of smoke detectors are compared to these experimental

measurements.

4.1 Variables Considered

A critical element in an engineering analysis, especially one that is not based on first-

principles, is careful selection of variables of interest. For each of the experimental

measurements (optical density, temperature, and velocity) that are used as alarm

thresholds, four variables are considered:

- Mode of Combustion

- Smoke Detector Type

- Nominal Sensitivity

- Ventilation Status

Each of these four variables may affect the optical density, temperature, or velocity at the

time of detector alarm. The significance of each of these variables will be examined and

insignificant variables will be eliminated.

The mode of combustion, in this context, refers to either smoldering or flaming

combustion of the burning item. Throughout the rest of this section the mode of

combustion will be referred to as the "fire type." Flaming and smoldering fires produce smoke with significantly different characteristics and smoldering fires are less likely to produce a strong buoyant plume than flaming fires, both of which could result in variations of optical density, temperature and velocity at alarm. The type of smoke detector refers to the operating principle of the smoke detector. For this research, only ionization and photoelectric smoke detectors were considered. Detectors with different operating principles respond with varying degrees of sensitivity to different characteristics of the smoke. As a result, differences in the optical density at alarm are likely between detector types. The nominal sensitivity of a smoke detector is the alarm level marked on the detector as determined by the appropriate detector sensitivity test (i.e. UL 217 [2001] or UL 268 [2003]). Although this singular value applies only to the performance of the detector under the specified test conditions and will not likely extrapolate to the performance of the detector under different conditions, it does serve as a point of reference to be considered. Finally, the status of the ventilation system may impact the values of optical density, temperature, and velocity at alarm. A functioning ventilation system may remove, or relocate, both smoke and heat from a fire and would likely affect the air velocity adjacent to the detector.

4.2 Development of Statistical Description

The statistical description of the optical density, temperature, and velocity at alarm values is based on that presented by Geiman and Gottuk [2003] for the optical density at alarm. See Table 2 for an example of the statistics they presented. Before proceeding further into this discussion, it is necessary to discuss the nature of the data used in the statistical

description. In the early stages of this investigation, both instantaneous as well as averaged (5 and 10 second average values around the time of alarm) were examined. No significant difference was found between the instantaneous and averaged values for the optical density and temperature rise at alarm; the instantaneous values were therefore used for these measurements throughout this study. Conversely, the variation in the velocity data required that a 10 second average value around the time of alarm be used for all velocity at alarm values in this study.

Typically, mean and standard deviation values can adequately describe a population of data for engineering calculations. However, for populations that are not normally distributed the mean and standard deviation alone may not be adequate. To illustrate this point and to provide evidence that the optical density values at alarm are not normally distributed, Figure 1, presents box plots of the optical density values at alarm for all tests examined. Note that the number of detector alarms incorporated in Figure 1 were 106, 93, 71, and 105 for the flaming-ion, flaming-photo, smoldering-ion, and smoldering-photo categories, respectively. In addition, a fictitious box plot labeled "Normal Distribution" has been added to the figure for comparison purposes only (i.e. the values used and variation shown have no meaning). From a previous study of optical density at alarm values [Geiman & Gottuk, 2003], the fire type and detector type are known to be significant variables, so these are the only variables considered at this point in the analysis.

A box plot provides a graphical representation of the data in the form of a five number summary (in Figure 1 the 10th, 25th, 50th, 75th, and 90th percentiles) [Devore, 2000]. The 25th and 75th percentiles, form a box representing the middle 50 percent of values (the interquartile range). The median is represented as the solid line that divides the previously mentioned box. The lines extending from the box to the 10th and 90th percentiles, respectively, are called the whiskers. Similar to the box, the middle 80 percent of the data is contained within the whiskers. To avoid plotting each outlier (i.e., value below the 10th percentile and above the 90th percentile) on the box plot, the 5th and 95th percentiles are shown. These points represent possible extreme values or "outliers." In addition to the normal five-point summary, the arithmetic mean of the data set is presented on the box plots as a dashed red line.
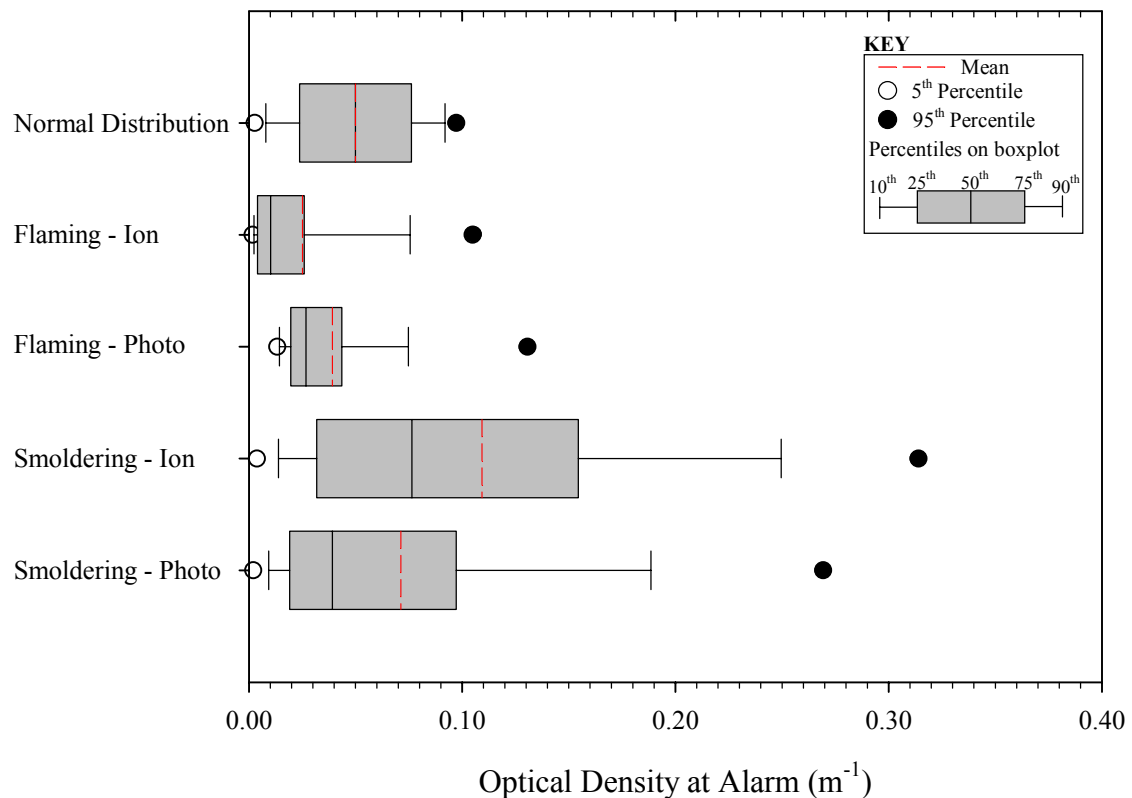
Figure 1 - Box plots illustrating the non-normal distributions of optical density at alarm data.

Box plots are a means to graphically represent the central tendencies and variation in the data. The mean and median are both representations of the central tendencies of the data, while the size of the box and whiskers reflect the variation in the data. Likewise, the skewness or asymmetry of the data can also be determined from the box plot. In a symmetric distribution, the mean and the median would be identical and the width of the box and whiskers on each side of the mean would be symmetrical (see "Normal Distribution" box plot in Figure 1). If the mean is higher than the median, the data is positive or right-skewed; if the mean is lower than the median then the data is negative or left-skewed. From Figure 1, the optical density is obviously a right-skewed distribution and not a normal distribution, since the box and whiskers are larger on the positive (right) side of the median than the other for each of the distributions of test data. This skewness is the result of the mean being "pulled" higher by unusually large values in the data set. Given this knowledge of the distributions of the optical density at alarm data, the use of percentiles of the population, as used by Geiman and Gottuk [2003], over a simple mean and standard deviation seems justified. However, to enable continued evaluation of this assumption throughout this work, the average and standard deviations of the populations will be provided. For simplicity, and comparison purposes, the temperature rise and velocity data will be treated in the same manner as the optical density.

Another aspect of the statistical treatment used by Geiman and Gottuk [2003], and adopted here, relates to the percentiles of the population presented. Through an informal sensitivity analysis, Geiman and Gottuk decided that the 20th, 50th, and 80th percentiles provided a reasonable description of the population at a justifiable resolution. They

found that using percentiles of the population examined lower than the 20th or greater

than the 80th may introduce complications given the small sample sizes where one or two

anomalous tests could inappropriately skew results. Figure 2 illustrates the deviation

from the majority of the population of optical density at alarm data below the 20th and

above the 80th percentile. The plots in Figure 2 use the same data set used in the box

plots in Figure 1.
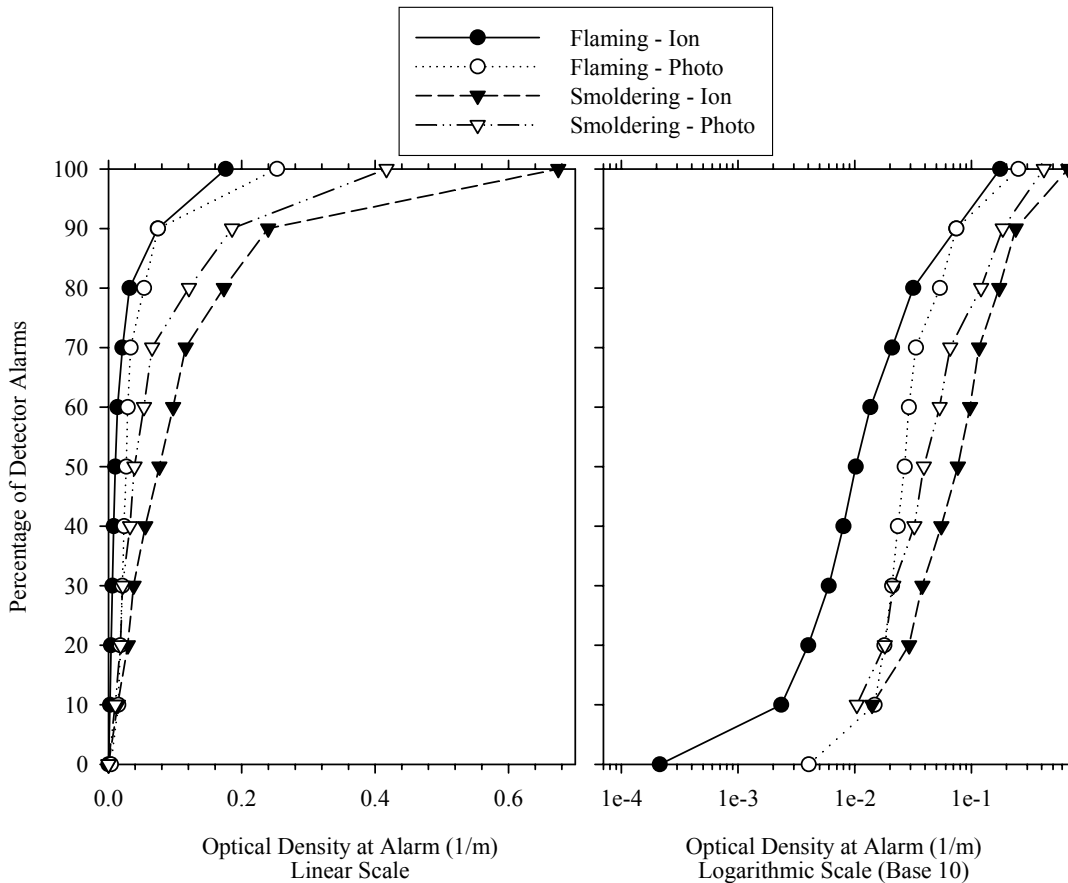
Figure 2 - Cumulative distribution of optical density at alarm to illustrate rationale for using 20th and 80th percentiles.

The two plots shown in Figure 2 are identical other than the scale used for the optical

density at alarm values. The plot on the left uses a linear scale and the deviation above

the 80th percentile is clearly visible. To better visualize the optical density at alarm below

the 20th percentile, the plot on the right uses a base-10 logarithmic scale.

4.3 Optical Density at Alarm

4.3.1 Statistical Description

Based on a previous study of optical density at alarm values [Geiman & Gottuk, 2003],

the fire type and detector type are known to be significant variables. However, the

significance of the nominal sensitivity of the detector and the ventilation status on the

optical density at alarm are unknown. A systematic evaluation of the significance of

these two remaining variables is performed before the final statistical description of the

optical density at alarm values is presented. The data from the Navy tests is the only data

suitable to perform this evaluation. The data from the Kemano tests will be presented

later in this section.

To determine the significance of the detector nominal sensitivity on the optical density at

alarm, a statistical description of the optical density at alarm data (described in section

4.2) was developed that considered the nominal sensitivity, in addition to the fire type

and detector type.

Table 8 - Statistical description of Navy optical density (m^{-1}) at alarm data, grouped according to fire type, detector type and detector nominal sensitivity.

Fire Type	Detector Type	Nominal Sensitivity	20%	50%	80%	Mean	Std Dev	Count
Flaming	Ion	0.019 m^{-1}	0.004	0.010	0.022	0.016	0.019	46
Flaming	Ion	0.023 m^{-1}	0.004	0.009	0.021	0.016	0.025	43
Flaming	Photo	0.036 m^{-1}	0.019	0.025	0.044	0.034	0.024	43
Flaming	Photo	0.051 m^{-1}	0.019	0.026	0.041	0.034	0.027	40
Smoldering	Ion	0.019 m^{-1}	0.015	0.021	0.070	0.049	0.067	14
Smoldering	Ion	0.023 m^{-1}	0.030	0.066	0.142	0.108	0.137	38
Smoldering	Photo	0.036 m^{-1}	0.018	0.034	0.087	0.056	0.065	38
Smoldering	Photo	0.051 m^{-1}	0.014	0.037	0.086	0.064	0.083	42

Based on Table 8, the nominal sensitivity of a detector does not appear to significantly influence the optical density at alarm for ionization detectors responding to flaming fires, photoelectric detectors responding to flaming fires, or photoelectric detectors responding to smoldering fires. In all three of these cases, the 20th, 50th, and 80th percentiles of these populations, as well as the average values, correlate well between the two nominal sensitivity values. It is also significant that for all three of these cases the sample sizes at each nominal sensitivity value were comparable. In contrast, the nominal sensitivity of the detector does appear to be significant for ionization detector responding to smoldering fires. The 20th and 80th percentiles of the population of optical density at alarm data differ by a factor of two, while the 50th percentiles of the population differ by almost a factor of three for the two nominal sensitivity values.

There are two caveats to these observations that need to be stated. First of all, the manufacturer and design of the detectors in each nominal sensitivity group are different. That is, the two nominal sensitivity values represent two detector models, one by EST and one by Simplex. Therefore, the differences between the two nominal sensitivity

values for the ionization detectors responding to smoldering fires could also be attributed to the difference in detector designs. Furthermore the sample size of the 0.019 m^{-1} nominal sensitivity ionization detector group responding to smoldering fires is only about one third the size of the population of detector alarms considered for the 0.023 m^{-1} nominal sensitivity group of ionization detectors responding to smoldering fires. This indicates a lack of sensitivity by the 0.019 m^{-1} nominal sensitivity ionization detectors in many tests in which the 0.023 m^{-1} nominal sensitivity ionization detectors did alarm; providing further evidence that the difference in optical density at alarm for the ionization detectors and smoldering fires is related to the detector model and not the nominal sensitivity of the detectors. The small sample size for the first group could possibly skew the results, although the magnitude of the difference between the groups suggests that this is unlikely.

Since the nominal sensitivity of the detectors only appeared significant for ionization detectors responding to smoldering fires, this variable will only persist for this case in subsequent analyses, but no longer be considered for the other cases (ionization detectors responding to flaming fires and photoelectric detectors responding to either flaming or smoldering fires). With the determination on the significance of the optical density complete, the effect of ventilation on the optical density at alarm is now examined. Table 9 provides a statistical description of the optical density at alarm considering the status of the ventilation system (on or off) as a variable in addition to the other variables already determined to be significant. When operating, the ventilation system used in the Navy tests produced a flow of approximately 12 air changes per hour in the test compartment.

Table 9 - Statistical description of Navy optical density (m^{-1}) at alarm data, grouped according to fire type, detector type, detector nominal sensitivity (where applicable), and ventilation.

Fire Type	Detector Type	Nominal Sensitivity	Ventilation Status	20%	50%	80%	Mean	Std Dev	Count
Flaming	Ion		Off	0.004	0.010	0.021	0.016	0.023	56
Flaming	Ion		On	0.003	0.010	0.024	0.017	0.021	33
Flaming	Photo		Off	0.018	0.025	0.032	0.032	0.025	54
Flaming	Photo		On	0.020	0.028	0.058	0.039	0.025	29
Smoldering	Ion	0.019 m^{-1}	Off	0.018	0.038	0.091	0.071	0.085	7
Smoldering	Ion	0.019 m^{-1}	On	0.006	0.018	0.030	0.028	0.037	7
Smoldering	Ion	0.023 m^{-1}	Off	0.029	0.104	0.189	0.148	0.168	20
Smoldering	Ion	0.023 m^{-1}	On	0.032	0.041	0.072	0.063	0.072	18
Smoldering	Photo		Off	0.021	0.054	0.133	0.086	0.093	42
Smoldering	Photo		On	0.009	0.028	0.049	0.032	0.026	38

The status of the ventilation system appears to have an effect on the response of both ionization and photoelectric detectors responding to smoldering fires. In contrast, there appears to be little difference in the results between the two ventilation conditions for the flaming fires, with the exception of the 80th percentile values of photoelectric detectors. For the smoldering fires, the 20th, 50th, and 80th percentiles of the optical density at alarm values, as well as the mean values, are a factor of two to three greater when the ventilation system is off, then for those tests in which the ventilation system was operating at 12 air changes per hour. Possible reasons for this outcome include an increased air velocity in the space with the ventilation system operating or that the operating ventilation system reduces the optical density in the space by dilution with fresh air or extraction of smoke. A similar trend is not seen for the detectors responding to flaming fires. For the flaming fires, the 20th, 50th, and 80th percentiles of the optical density at alarm values, as well as the mean values, correlate well for the two ventilation conditions. The 80th percentile optical density at alarm values for photoelectric detectors

responding to flaming fires with the ventilation on was almost twice as large as with the ventilation off. An explanation for this result is not obvious. However, since the 20th and 50th percentile values for the two ventilation conditions correlate so well, the effect of ventilation is considered negligible for flaming fires.

Having examined the variables believed to be relevant to the response of smoke detectors to optical density, a final statistical description of the optical density at alarm can be made. Table 10, below, provides quantitative data on the optical density at alarm for smoke detectors, while illustrating the general trends in the response of smoke detectors to several variables.

Table 10 - Final statistical description of Navy optical density (m^{-1}) at alarm data.

Fire Type	Detector Type	Nominal Sensitivity	Ventilation Status	20%	50%	80%	Mean	Std Dev	Count
Flaming	Ion			0.004	0.010	0.021	0.016	0.022	89
Flaming	Photo			0.019	0.026	0.044	0.034	0.025	83
Smoldering	Ion	0.019 m^{-1}	Off	0.018	0.038	0.091	0.071	0.085	7
Smoldering	Ion	0.019 m^{-1}	On	0.006	0.018	0.030	0.028	0.037	7
Smoldering	Ion	0.023 m^{-1}	Off	0.029	0.104	0.189	0.148	0.168	20
Smoldering	Ion	0.023 m^{-1}	On	0.032	0.041	0.072	0.063	0.072	18
Smoldering	Photo		Off	0.021	0.054	0.133	0.086	0.093	42
Smoldering	Photo		On	0.009	0.028	0.049	0.032	0.026	38

As seen in previous studies the fire type and detector type significantly affect the optical density at alarm for smoke detectors. To further summarize the trends seen in Table 10, the nominal sensitivity of the detector and status of the ventilation system did not significantly influence the optical density at alarm for either ionization or photoelectric smoke detectors responding to flaming fires. In contrast, the response of these same detectors to smoldering fires was affected by the nominal sensitivity of the detectors and

ventilation in the compartment. The response of the photoelectric detectors to smoldering fires was only influenced by the ventilation status, while ionization detectors appeared to be affected by both the ventilation of the compartment and the nominal sensitivity of the detector. As might be expected, the optical density at alarm values for smoldering fires with no ventilation were significantly (by a factor of two to three) greater than when the ventilation system was operating. An operating ventilation system provides additional momentum to the smoldering smoke, possibly reducing the smoke entry resistance into the sensing chamber of the detector, while at the same time reducing the concentration of the smoke in the compartment by dilution (i.e. the addition of clean outside air into the compartment or removal of smoke particles from the compartment). The difference in optical density at alarm values for ionization detectors responding to smoldering fires for different nominal sensitivity values was likely a result of different detector designs for these detectors. Geiman and Gottuk [2003], found no significant difference, or at least no recognizable trend in the difference, between detectors of varying nominal sensitivity values (including detectors of the same design with different nominal sensitivities). In general, smoldering fires, which tend to produce larger smoke particles, are more difficult for ionization detectors to detect. Therefore, it is reasonable to assert that in this more challenging smoke detection scenario for ionization detectors (i.e. detection of smoke from a smoldering fire) that the response of the detector could be more sensitive to the detector design. From a modeling standpoint, this presents a formidable challenge, in that the response of ionization detectors to smoldering fires may not be suitable for generalization across different detector models.

Unfortunately, the manufacturers and nominal sensitivity values of the detectors used in the Kemano tests were not available and all of the tests were performed in unconditioned space (i.e. no heating, air conditioning, or ventilation system was operating). This limits the application of the method used to analyze the Navy data and hinders the complete integration of these two datasets. Another complicating factor was that the Kemano tests were all small fires intended to challenge the detection systems that began as smoldering fires and transitioned to flaming fires later in the test. To address this issue, the fire type at the time of detection was determined for each smoke detector in each test. Detector alarm times within 120 seconds after the transition time (i.e. the time at which the fire transitioned from smoldering to flaming) were examined individually and a determination was made as to whether the detector was still receiving smoldering smoke or the smoke received by the detector was indeed the smoke from a flaming fire. This determination was made based on plots of the optical density and temperature data around the time of alarm, with consideration given to transit time from the room of fire origin to the detector location. With that being said, Table 11 provides the final statistical description of the Kemano data, grouped according to the fire type at the time of alarm and smoke detector type.

Table 11 – Final statistical description of Kemano optical density (m^{-1}) at alarm data.

Detector Type	Fire Type	20%	50%	80%	Mean	Std Dev	Count
Flaming	Ion	0.023	0.073	0.108	0.072	0.052	17
Flaming	Photo	0.012	0.067	0.134	0.081	0.078	10
Smoldering	Ion	0.089	0.154	0.213	0.157	0.072	19
Smoldering	Photo	0.022	0.068	0.195	0.106	0.094	25

The results presented in Table 10 and Table 11 can be compared to the results presented

by Geiman and Gottuk [2003]. Before doing so, an important distinction between these

two studies is that all the optical density at alarm data examined by Geiman and Gottuk

was from optical density meters using a white light source, whereas the optical density

meters used in the Navy and Kemano tests examined in this study used optical density

meters with an infrared light source. Overall, the optical density at alarm values from the

Navy data set examined by Geiman and Gottuk were greater than for the Navy data used

in this study. In contrast, the optical density at alarm values from the Kemano tests were

generally greater than the average optical density at alarm data across all test series and

nominal sensitivity values presented in Table 2 of Geiman and Gottuk [2003].

4.3.2 Comparison to Common Thresholds

In the previous section, a statistical description of optical density at alarm values was

provided. However, in order to fully evaluate the thresholds used to estimate the

response of smoke detectors, a direct comparison between the optical density at alarm

data from experiments and commonly used thresholds needs to be made. Two of the

optical density alarm thresholds considered here were also examined by Geiman and

Gottuk [2003] – the nominal sensitivity of the smoke detector and 0.14 m^{-1}. In addition,

the 20-, 50-, and 80-percent optical density alarm thresholds presented by Geiman and

Gottuk [2003] are evaluated. Each optical density alarm threshold is evaluated by

comparing it to the optical density measurements at the time of alarm. The figures that

follow in this section depict the percentage of detectors that would have been in alarm at

a smoke optical density less than or equal to the alarm threshold for each grouping of

significant variables presented in the final statistical descriptions of the data (Table 10 and Table 11).

The first alarm threshold evaluated for optical density measurements is the nominal sensitivity of the detector. The optical density at alarm of each individual detector is compared to the nominal sensitivity of that detector. Figure 3 presents the percentage of detectors that alarmed at or below their nominal sensitivity values. Only the Navy tests had detectors with known nominal sensitivity values and were therefore the only tests considered in the evaluation of the nominal sensitivity as an alarm threshold.

If the typical response of a smoke detector is considered to occur when 50 percent of the population of detectors alarm, then this provides a useful cutoff in evaluating the effectiveness of an alarm threshold. Therefore, the nominal sensitivity appears to be a reasonable threshold to evaluate the response of ionization and photoelectric detectors to flaming fires, as well as photoelectric detectors responding to smoldering fires with an operating ventilation system. The nominal sensitivity appears to barely capture the typical response of detectors for smoldering fires being detected by photoelectric detectors with no ventilation and for the 0.019 m^{-1} nominal sensitivity ionization detectors responding to smoldering fires with the ventilation on. For all other cases in Figure 3, the nominal sensitivity does not capture at least 50 percent of the smoke detector alarms. Geiman and Gottuk [2003] found that the nominal sensitivity only captured 50 percent of the smoke detector alarms for ionization detectors responding to flaming fires. Figure 4 contains their data for comparison to this study. The increased

percentages of detector alarms that occurred at optical densities less than or equal to the nominal sensitivity for the flaming fires and some of the smoldering fires in this study was surprising compared to the results of Geiman and Gottuk.
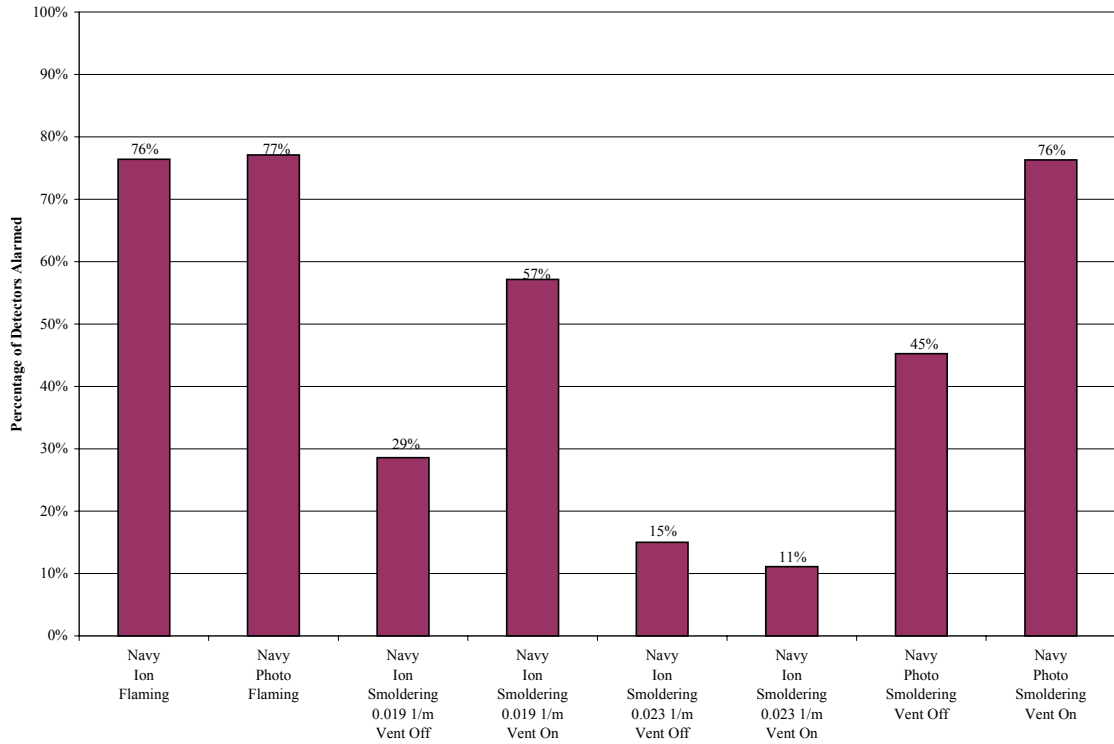
Figure 3 - Percentage of detectors that alarmed at an optical density less than or equal to the nominal sensitivity of each detector.
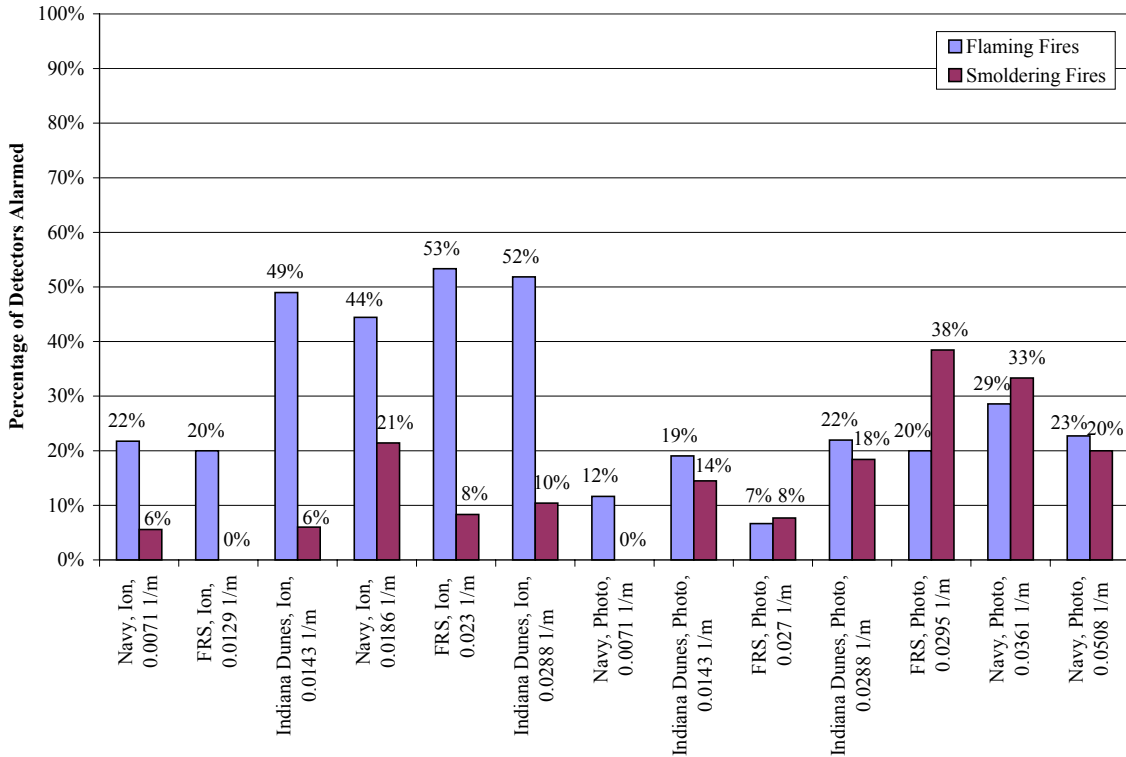
Figure 4 - Percentage of detectors that alarmed at an optical density less than or equal to the nominal sensitivity of each detector from the data of Geiman and Gottuk [2003].

An optical density equal to 0.14 m^{-1} is the next optical density alarm threshold evaluated. Figure 5 presents the percentage of detectors that alarmed at or below an optical density per meter of 0.14. Both the Navy and Kemano test data are used to evaluate this alarm threshold.

99% 99% 100% 94% 100%

Navy
Kemano

88% 86% 80% 81% 68% 65% 42%

Percentage of Detector Alarms

100%
90%
80%
70%
60%
50%
40%
30%
20%
10%
0%

Ion
Flaming

Photo
Flaming

Ion
Smoldering
0.019 1/m
Vent Off

Ion
Smoldering
0.019 1/m
Vent On

Ion
Smoldering
0.023 1/m
Vent Off

Ion
Smoldering
0.023 1/m
Vent On

Photo
Smoldering
Vent Off

Photo
Smoldering
Vent On

Ion
Smoldering

Photo
Smoldering
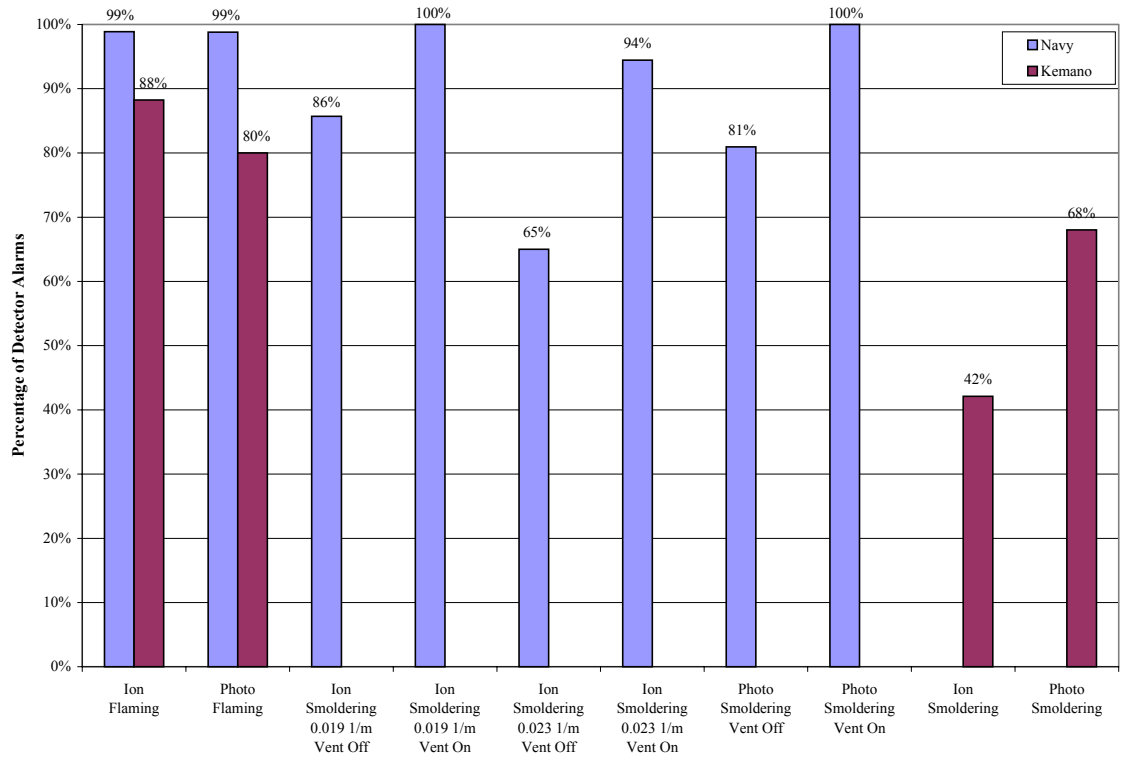
Figure 5 - Percentage of detectors that alarmed at an optical density less than or equal to 0.14 m^{-1}.

In contrast to the use of the nominal sensitivity as an alarm threshold, 0.14 m^{-1} easily captures the typical detector response in a vast majority of the cases examined. In fact, in 9 of the 12 cases examined at least 80 percent of detector alarms occurred at or below 0.14 m^{-1}. Consequently, 0.14 m^{-1} provides a relatively conservative estimate of detector response. In only one case, ionization detectors responding to smoldering fires in the Kemano test series, did an optical density alarm threshold of 0.14 m^{-1} not capture at least the typical (i.e. 50 percent) detector response. Another significant observation from Figure 5 is that the percentage of detectors that alarmed below an optical density of 0.14 m^{-1} decreases noticeably (from 100 percent to 86 percent, 94 percent to 65 percent, and 100 percent to 81 percent) for the detection of smoldering fires with no ventilation. This is not to say that it no longer captures the typical response in these situations, it clearly

captures a majority of alarms; but it does move further away from providing a

conservative alarm threshold in these situations.

The final set of alarm thresholds examined are the 20, 50, and 80 percent thresholds

based on the data used by Geiman and Gottuk [2003]. For the Navy tests in this study,

the 20, 50, and 80 percent alarm thresholds used are based on the 20, 50, and 80 percent

alarm thresholds for all nominal sensitivity values from the Navy test data used by

Geiman and Gottuk [2003]. These thresholds are not explicitly presented by Geiman and

Gottuk, but calculated for this study based on their data. The alarm thresholds used for

the Kemano tests were the average 20, 50, and 80 percent alarm thresholds for all test

series presented in Table 2 of Geiman and Gottuk [2003]. The average alarm thresholds

are not used for the Navy data because more representative thresholds are available (i.e.

the Navy data from Geiman and Gottuk [2003] is for similar detectors, test

compartments, and fire sources as the Navy data used in this study).

Table 12 - 20, 50, and 80 percent optical density alarm thresholds (m^{-1}) used in this study (based on data from Geiman and Gottuk [2003]).

Alarm Threshold	Fire Type	Navy		Kemano	
		Ion	Photo	Ion	Photo
20%	Flaming	0.008	0.018	0.007	0.031
20%	Smoldering	0.027	0.030	0.045	0.032
50%	Flaming	0.019	0.044	0.021	0.063
50%	Smoldering	0.090	0.061	0.113	0.059
80%	Flaming	0.050	0.069	0.072	0.106
80%	Smoldering	0.130	0.119	0.176	0.110

Table 5 presents the percentage of detectors that alarmed at or below the optical density

alarm thresholds presented in Table 12.
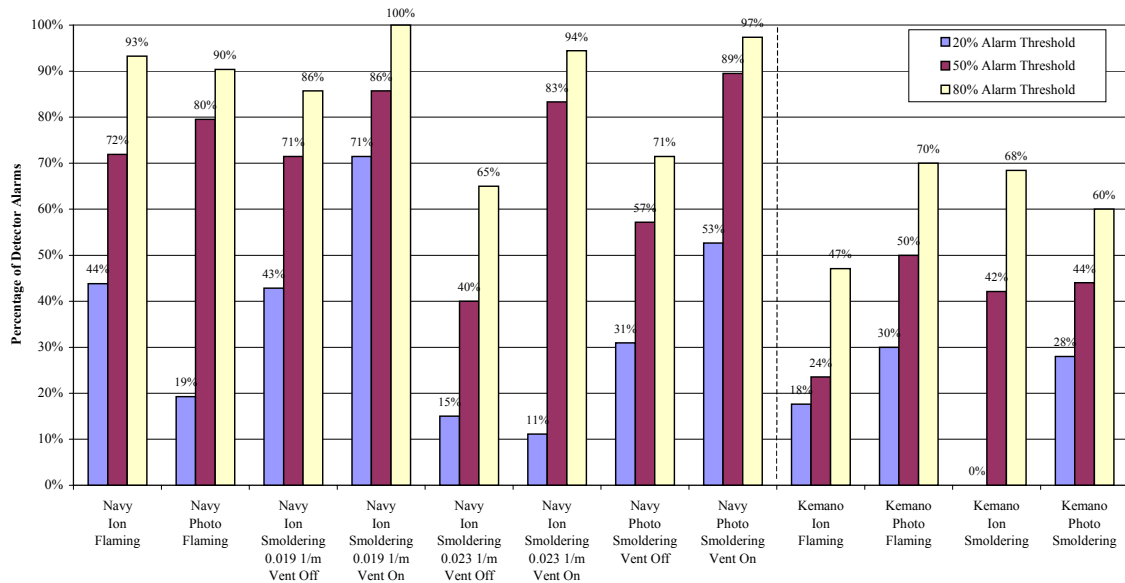
Figure 6 - Percentage of detectors that alarmed at an optical density less than or equal to the 20, 50, and 80 percent optical density alarm thresholds from Table 12.

One obvious conclusion from Figure 6 is that although the thresholds used represented

the 20th, 50th, and 80th percentile of that population of data, the percentages of detectors

that alarmed at or below these thresholds varied significantly in this study. For example,

the percentages of detector alarms that occurred at or below the 20 percent optical density

thresholds from Table 12 ranged from 0 to 71. However, the majority of the 20 percent

optical density alarm thresholds resulted in approximately 20 to 40 percent of detector

alarms occurring at or below these optical densities. The range of results for the 50

percent optical density alarm threshold was 24 – 86 percent. However, most of the

results for the 50 percent alarm threshold lied in the range of 40 – 70 percent. Similarly,

the 80 percent alarm thresholds resulted in 45 – 100 percent of alarms being captured,

with the majority of results in the range of approximately 70 – 90 percent. Although the

20, 50, and 80 percent optical density alarm thresholds from Table 12 do not provide

tremendous accuracy in the exact percentage of detector alarms captured, in general they

do capture lower, middle, and upper ranges of detector alarms in the general vicinity of these percentages as is there intended use.

4.4 Temperature Rise at Alarm

4.4.1 Statistical Description

Since no previous statistical description of temperature rise values at alarm exists, the process used for the optical density alarm presented in the previous section is adopted. The fire type and detector type are assumed to be significant. The significance of the nominal sensitivity of the detector and compartment ventilation status to the temperature rise at alarm are explored. The data from the Navy tests is the only data suitable to perform this evaluation. Later in this section, the data from the Kemano tests will be presented, separately.

To determine the significance of the detector nominal sensitivity on the temperature rise at alarm, Table 13 provides a statistical description of the temperature rise at alarm data that considered the nominal sensitivity, in addition to the fire type and detector type, for the flaming fires. Results for the smoldering fire tests were eliminated from this table due to the fact that there was no appreciable temperature rise for the smoldering fires. For the smoldering fire tests, the 80th percentile temperature rise at alarm was approximately 1°C for each detector type and nominal sensitivity presented in Table 13,. Furthermore, the maximum temperature rise at alarm values for each detector type and nominal sensitivity were only $2 - 3$°C. A temperature rise of 1°C is not only within the

normal range of ambient temperature variation, but also within the accuracy of the thermocouple.

Table 13 - Statistical description of Navy temperature rise (°C) at alarm data for flaming fires, grouped according to detector type and detector nominal sensitivity.

Fire Type	Detector Type	Nominal Sensitivity	20%	50%	80%	Mean	Std Dev	Count
Flaming	Ion	0.019 m^{-1}	1	2	4	2	3	54
Flaming	Ion	0.023 m^{-1}	0	1	2	1	2	49
Flaming	Photo	0.036 m^{-1}	1	11	19	11	10	51
Flaming	Photo	0.051 m^{-1}	1	7	15	9	10	47

Although there is some difference in the temperature rise at alarm between the nominal sensitivity values, the nominal sensitivity of the detectors does not appear to significantly influence the temperature rise at alarm. This determination is not based solely on the results presented in Table 13, but rather an examination of the entire population of temperature rise at alarm data in ten-percentile increments. The difference between the two nominal sensitivity values is never more than 2°C for the ionization detectors and never more than 4°C for the photoelectric detectors between the data for the two nominal sensitivities at the same percentile of the population. Therefore, the nominal sensitivity of the detectors is no longer considered as a variable affecting the temperature rise at alarm.

The effect of ventilation on the temperature rise at alarm is now examined. Table 14 presents a statistical description of the temperature rise at alarm for the flaming fires considering the detector type and ventilation status. The smoldering fires were excluded due to negligible temperature rises at alarm.

Table 14 - Statistical description of Navy temperature rise (°C) at alarm data for flaming fires, grouped according to detector type and ventilation status.

Fire Type	Detector Type	Ventilation Status	20%	50%	80%	Mean	Std Dev	Count
Flaming	Ion	Off	1	2	3	2	2	65
Flaming	Ion	On	0	1	3	2	3	38
Flaming	Photo	Off	2	8	16	10	8	63
Flaming	Photo	On	0	7	20	11	12	35

As with the nominal sensitivity, the temperature rise at alarm does not appear to be significantly influenced by the ventilation status. Due to the nominal sensitivity and ventilation not significantly affecting the temperature rise at alarm, only the detector type is considered in the final statistical description of the temperature rise at alarm for the flaming fires. Table 15 provides the final description of the data, as well as the maximum temperature rise at alarm for the smoldering Navy tests and the maximum temperature rise at alarm for the smoldering and flaming Kemano tests.

Table 15 - Statistical description of temperature rise (°C) at alarm data for both test series, grouped according to fire type and detector type.

Test Series	Fire Type	Detector Type	20%	50%	80%	Maximum	Mean	Std Dev	Count
Navy	Flaming	Ion	0	1	3	15	2	3	103
Navy	Flaming	Photo	1	8	16	38	10	10	98
Navy	Smoldering	Ion				3			58
Navy	Smoldering	Photo				3			83
Kemano	Flaming	Ion				1			20
Kemano	Flaming	Photo				3			10
Kemano	Smoldering	Ion				1			21
Kemano	Smoldering	Photo				1			31

For the flaming fires, ionization detectors alarm at lower temperature rises than photoelectric fires. This observation is consistent with the optical density at alarm data (see Table 10 and Table 11), where the optical density at alarm is generally higher for photoelectric detectors than ionization detectors for flaming fires. It should also be noted that for flaming fires detected by ionization detectors, the temperature rise at alarm was

barely noticeable, with approximately 80 percent of the alarms occurring at temperature rises of 3°C or less.

The shaded rows in Table 15 represent data in which no significant temperature rise at alarm is found. For these rows, even at the 80th percentile the temperature rise at alarm is approximately 1°C or less. The maximum values are only provided to demonstrate the lack of correlation between the temperature rise and detector alarm status for these cases. Interestingly, even the detector alarms that occurred during the flaming period of burning in the Kemano tests showed no substantial temperature rise at the time of alarm.   It is important to remember that the flaming fires in the Kemano tests began as slow smoldering fires and later transitioned to flaming combustion. Regardless, based on these results it does not appear prudent to use temperature rise alarm thresholds for smoldering fires or those that begin as smoldering fires and later transition to flaming fires.

4.4.2 Comparison to Common Thresholds

This section provides a direct comparison between the experimental temperature rise at alarm data and commonly used thresholds in order to fully evaluate the temperature rise thresholds used to estimate the response of smoke detectors. Temperatures rises of 4°C and 13°C are evaluated as temperature rise alarm thresholds. In addition, the material-specific temperature rises presented by Heskestad and Delichatsios [1977] (see Table 4) for flaming fires are evaluated. Based on the statistical description of the temperature rise at alarm data in the previous section, only the flaming fires from the Navy tests are presented in Figure 7. For the smoldering Navy tests and all the Kemano tests, there was

no observable temperature rise at the time of alarm. Therefore, for each of these cases

the percentage of detectors that alarmed at a temperature rise less than or equal to the

threshold would be 100 percent.
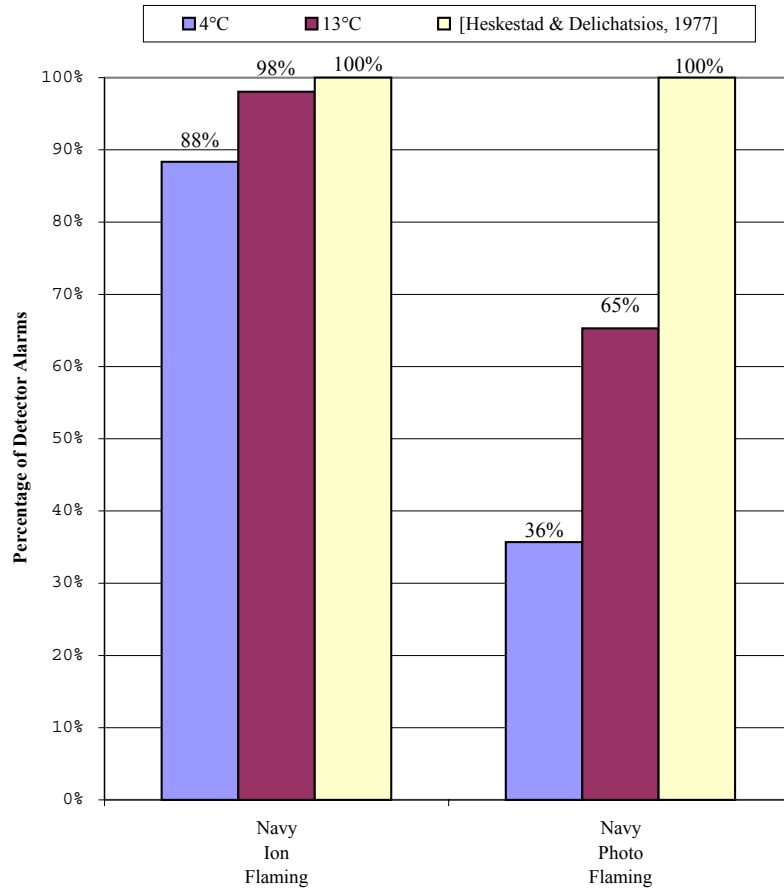
Figure 7 - Percentage of detectors that alarmed at a temperature rise less than or equal to each temperature alarm threshold for Navy tests with flaming fires.

As with the evaluation of the optical density alarm threshold, the *typical* response of

smoke detectors in Figure 7 is assumed to be at 50 percent (i.e. half of alarms occur at

greater temperature rises and half occur at lesser temperature rises). A temperature rise

threshold of 4°C therefore provides a more conservative estimate of the ionization

detector response to flaming fires than the typical detector with 88 percent of the alarms

occurring at or below the threshold. However, this same threshold does not capture the

typical detector response for flaming fires being detected by photoelectric detectors (only 36 percent of detectors alarmed below the threshold). At an alarm threshold of 13°C, the results are slightly different. As expected based on the performance of the 4°C threshold, an alarm threshold of 13°C provides a significantly conservative estimate of the detector response (i.e. 98 percent of alarms occurred at or below this threshold) as compared to the typical response. The 13°C threshold does capture the typical response of photoelectric detectors to flaming fires, in contrast to the 4°C threshold. Finally, for both ionization and photoelectric detectors responding to flaming fires, the material-specific temperature rises capture 100 percent of all detector alarms, meaning that all alarms occurred at temperature rises less than the threshold values. Although the percentage of detectors that had alarmed once the temperature rise thresholds had been reached was large in most cases, this does not necessarily translate into outstanding performance from a modeling standpoint. Since a vast number of alarms occurred at much lower temperature rises, the thresholds examined would possibly predict alarms much later than they actually occur or may never indicate an alarm occurred when it actually did. Phase 2 will hopefully demonstrate this possible shortcoming of using conservative alarm thresholds.

4.5 Velocity at Alarm

In comparison to the optical density and temperature data available at the time of detector alarms, there is relatively little available velocity data at the time of alarm. There are only a total of approximately 50 smoke detector alarms at which velocity data is available, all of which come from the Navy test series. No velocity measurement

instrumentation was used in the Kemano tests. Consequently, the results presented in this section are less certain than those presented in previous sections for the optical density and temperature rise at alarm.

4.5.1 Statistical Description

During an initial examination of the available velocity at alarm data, inconsistencies were noted for the smoldering fire tests. For that reason, the velocity data as a function of time was plotted for all tests in which alarms occurred. This exercise revealed that for 6 of the 9 smoldering tests for which velocity data was available and detectors near the velocity probe had alarmed there was no distinguishable difference between the velocity during the test and the ambient velocity before the fire source was ignited. Five of these six tests were tests in which there was no ventilation system in operation; a result that is expected. Figure 8 presents the velocity magnitude as a function of time (from ignition) for test NAVY-2-05, a smoldering lactose / potassium chlorate fire with no ventilation. The adjacent detector alarms are shown as vertical lines in this plot, labeled with the detector number that alarmed. Negative times shown in the plot reflect data taken before ignition of the fire source, which was taken to provide baseline conditions for each test.

For the three smoldering tests in which there were noticeable increases in the velocity magnitude, a peak velocity of approximately 0.15 m/s occurred as a brief spike(s) in the measured velocity magnitude for a period(s) of no more than 10 to 15 seconds at a time. These peaks typically occurred once or twice in close succession, with the remainder of the velocity data before and after the peak being similar to that shown in Figure 8. The

detector alarms in these tests (9 total alarms for the 3 tests) generally corresponded to the peaks in the velocity magnitude. However, the other 14 detector alarms that occurred during the 6 smoldering tests discussed earlier showed no distinguishable increase in velocity magnitude that could be attributed to the fire source. Therefore, it was concluded that evaluating the velocity at the time of alarm for the smoldering fire tests would not provide any information that would be useful for modeling the response of smoke detectors.
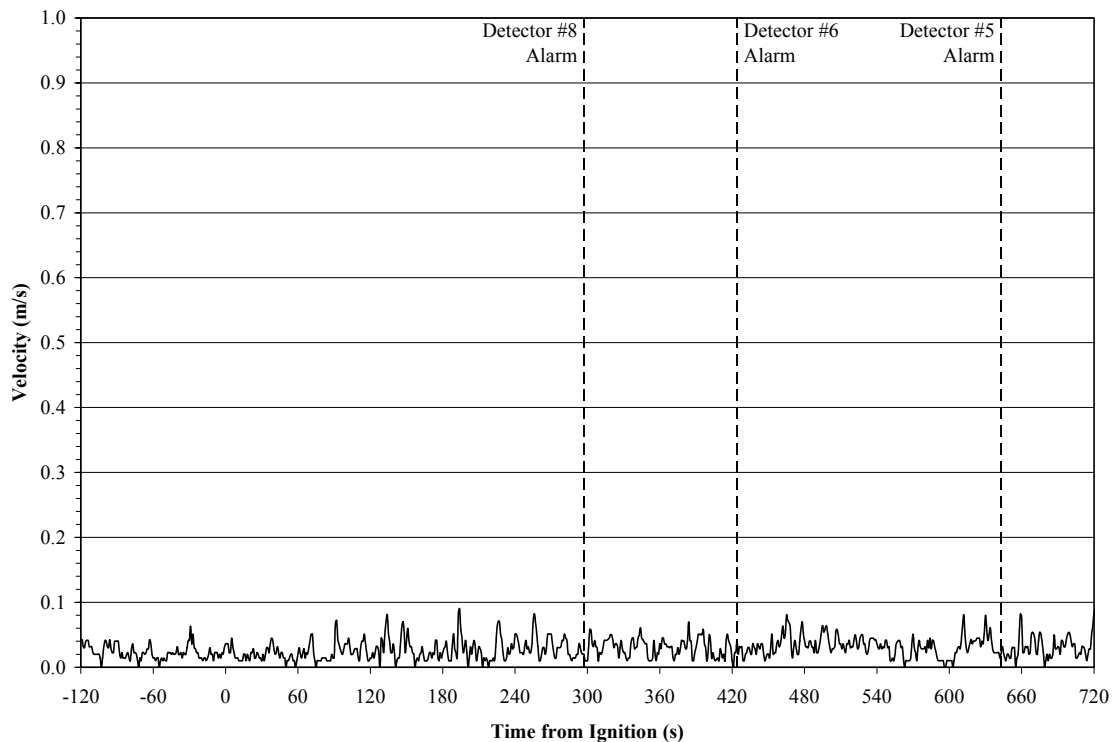
Figure 8 - Velocity magnitude as a function of time for test NAVY-2-05, a smoldering lactose / potassium chlorate fire with no ventilation.

In contrast to the velocity data from the smoldering fires, the velocity data from the flaming fires demonstrated an increase in velocity attributable to the fire source and therefore the velocity at detector alarm will be evaluated for these tests. This determination is again based on an examination of plots of the velocity magnitude as a

function of time. One additional interesting observation from this examination of the

velocity data from the flaming fires was that the noise in the data got progressively worse

as the velocity magnitude increased in some tests. After overlaying a plot of the gas

temperature (which is also measured by the sonic anemometer (i.e. velocity probe)), the

cause of the noise was determined to be signal degradation at elevated temperatures.

According to the manufacturer of the probe, the transducers used in the probe are

susceptible to damage at temperatures greater than 60ºC and the signal from the

instrument degrades at temperatures of 50 to 60ºC. This signal degradation (a reduction

of the signal to noise ratio) results in valid, but noisy data. Figure 9 provides an example

of the noisy velocity data, with the shaded region representing the period of time at which

the temperature exceeded 50 °C. Test procedures were in place to remove the probe from

the hot gases before temperatures exceeded 60ºC, however the probe was not always

removed soon enough to avoid noisy data.   Fortunately, most of the detector alarms

occurred before the noise in the velocity data became excessive and an 11-point (10

second) average around the time of alarm was used to determine the velocity at alarm

values, both of which should minimize noise problems. In summary, the statistical

description of the velocity at alarm will only be performed for the flaming fire tests, due

to the lack of significant velocity increase for the majority of smoldering fires.
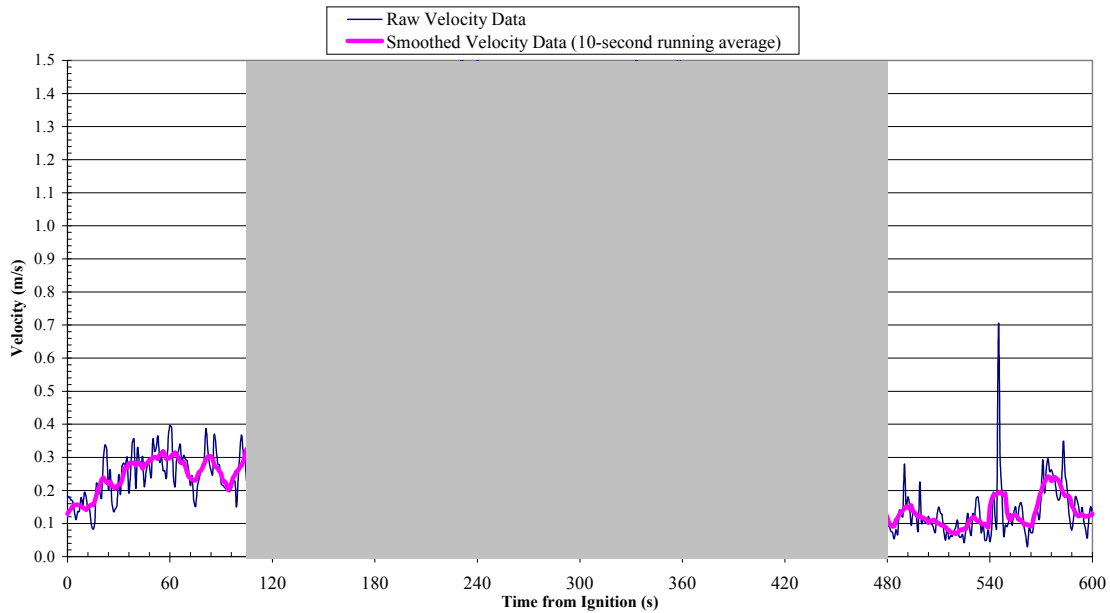
Figure 9 - Noisy velocity data at elevated temperatures for test NAVY-2-10.

The treatment of variables for the velocity at the time of alarm for the flaming fires is identical to that used for the optical density and temperature at alarm. The detector type is assumed to be a significant variable, at least initially, while the nominal sensitivity of the detectors and the status of the ventilation system are examined for their influence on the gas velocity magnitude at the time of alarm. Table 16 provides a statistical description of the available velocity magnitude data at the time of alarm considering the detector type and nominal sensitivity as variables.

Table 16 - Statistical description of velocity magnitude (m/s) at the time of alarm for flaming fires, grouped by detector type and nominal sensitivity.

Fire Type	Detector Type	Nominal Sensitivity	20%	50%	80%	Mean	Std Dev	Count
Flaming	Ion	$0.019 \ m^{-1}$	0.07	0.10	0.20	0.13	0.07	9
Flaming	Ion	$0.023 \ m^{-1}$	0.05	0.11	0.20	0.12	0.08	8
Flaming	Photo	$0.036 \ m^{-1}$	0.09	0.12	0.23	0.15	0.09	7
Flaming	Photo	$0.051 \ m^{-1}$	0.08	0.12	0.14	0.12	0.07	6

77

Based on the results in Table 16, the nominal sensitivity does not appear to significantly affect the velocity magnitude at alarm. In addition, the type of detector does not seem to affect the velocity magnitude at alarm, despite the initial assumption to the contrary. Considering the small samples sizes, the degree of correlation between the different types of detectors and nominal sensitivities within a fire type is somewhat remarkable.

Eliminating both the type and nominal sensitivity of the detectors as variables affecting velocity at alarm, the effect of the ventilation status on the velocity at alarm is examined. Table 17 provides a statistical description of the velocity magnitude at the time of detector alarm for flaming fires with and without the ventilation system in the compartment operating.

Table 17 - Statistical description of velocity magnitude (m/s) at the time of alarm for flaming fires, grouped by ventilation status.

Fire Type	Ventilation Status	20%	50%	80%	Mean	Std Dev	Count
Flaming	Off	0.06	0.11	0.20	0.12	0.07	18
Flaming	On	0.07	0.12	0.21	0.14	0.08	12

The results presented in Table 17 are, for all practical purposes, identical for the two ventilation conditions examined. Therefore, the only significant variable affecting the velocity at alarm is the fire type. For smoldering fires, there is no significant increase in velocity over ambient levels for the vast majority of tests. For flaming fires, the velocity at alarm values (in units of m/s) are 0.07, 0.12, and 0.21 for the 20th, 50th, and 80th percentiles of the population respectively, with the arithmetic mean value equal to 0.13 with a standard deviation of 0.07. Interestingly, unlike most of the optical density and temperature rise data, the mean and median velocity at alarm values are quite similar. In

addition, notice that the range of values within one standard deviation of the mean (0.06 –

0.20 m/s) captures approximately the middle 60 percent of the data. In combination,

these observations suggest that the population of velocity magnitude at alarm data is

likely normally distributed.

The lack of dependence of the velocity magnitude at alarm on any variables other than

the fire type suggests that the two models of ionization detectors and the two models of

photoelectric detectors tested in the Navy test series all have similar smoke entry

characteristics. Although there is not sufficient evidence to unconditionally extrapolate

this statement to all detector models, these results provide evidence that the difference in

smoke entry characteristics between operating principles and models of modern spot-type

smoke detectors has been greatly reduced over previous generations of smoke detector

technology. Consequently, a single velocity threshold (or threshold velocity range) may

be sufficient to predict all detector alarms to flaming fires.

4.5.2 Comparison to Common Thresholds

There is currently only one threshold related to the velocity at the time of alarm. This

threshold is often referred to as a *critical velocity* and is typically given as a value of 0.15

m/s. To evaluate the critical velocity as an alarm threshold, the percentage of detectors

that alarmed at a velocity magnitude less than or equal to this threshold is examined. As

expected from the discussion in this previous section regarding the lack of an increase in

velocity from the smoldering fires, 100 percent of alarms from smoldering fire tests

occurred below 0.15 m/s. In contrast, only 67 percent of alarms during flaming fire tests

occurred at or below 0.15 m/s. This result highlights the fact that although it has been

termed a *critical velocity*, alarms, in this case a majority of them, occur at velocities less

than this value.

4.6 Relationship between Optical Density and Temperature Rise at Alarm

One of the fundamental assumptions of the temperature rise method of estimating smoke

detector response is the constancy of the ratio of optical density to temperature rise in

both time and space. The data to support this assumption by Heskestad and Delichatsios

in their development of the temperature rise method does not conclusively confirm the

constancy of the optical density to temperature rise ratio. However, they believed that

"representative" values of the ratio of optical density to temperature rise were sufficiently

accurate for rough estimation purposes. The representative values they presented were

only for flaming spreading fires. The optical density and temperature rise values at alarm

from the Navy experiments can be used to some extent to either confirm or refute the

constancy of the optical density to temperature rise ratios. Unfortunately, the only

flaming fire source used in both the work by Heskestad and Delichatsios [1977] and the

experiments examined in this report is a wood crib. Flaming wood crib fires were

conducted in the Navy test series. Figure 10 shows the entire population of optical

density to temperature rise ratios at alarm for the Navy flaming wood crib fires, as well as

the representative ratio for this fire source provided by Heskestad and Delichatsios

[1977].
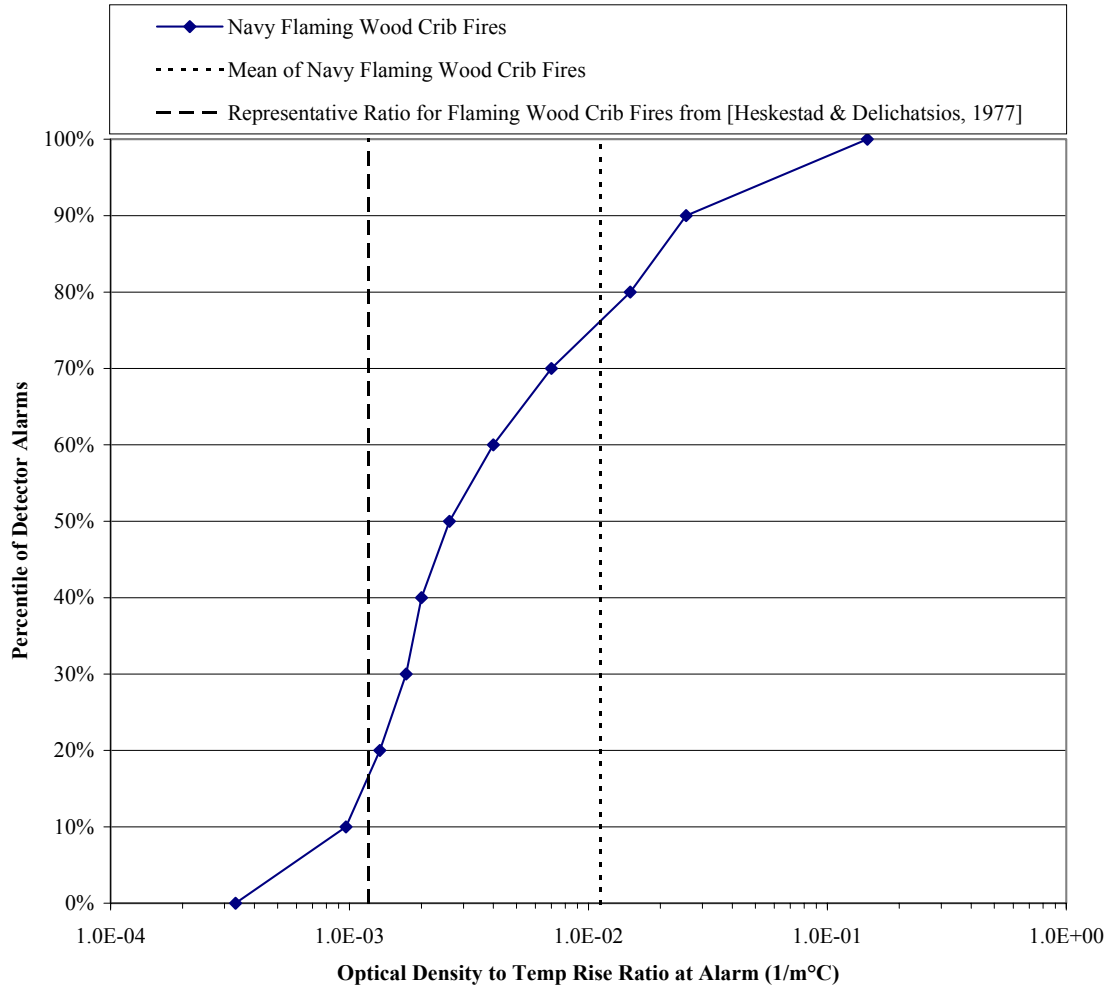
Figure 10 - Optical density to temperature rise ratios for flaming wood crib fires.

Despite the claim that the optical density to temperature rise ratio is constant in both time

and space, Figure 10 shows this ratio varying by over two orders of magnitude at the time

of alarm. The representative value determined by Heskestad and Delichatsios was for the

period of active fire growth and the data used to determine this ratio excluded

temperature rises less than 3 ºC (5 ºF). If this value was truly representative, one would

expect a narrow band around the representative value, not values differing by two orders

of magnitude. Although the data presented in Figure 10 is at the time of alarm and the

representative value is during active fire spread, this difference should be insignificant if

the value is constant in time and space. Furthermore, the value of the optical density to

temperature rise ratio at the time of alarm is the desired value for the intended purpose of the ratio – to calculate a temperature rise at detection based on a characteristic optical density at detection.

One explanation for the inconsistency between the data and the representative value in Figure 10 is that the smoke detectors are operating during periods other than the active fire growth period. The ratio of optical density to temperature rise before active fire growth occurs or during the decay period may vary. The data presented by Heskestad and Delichatsios showed variation as a function of time, but even this was not an orders of magnitude variation. The other possible explanation for the discrepancy seen in Figure 10 is due to the exclusion of temperature rise values less than 3 ºC. The rationale behind the exclusion of these small temperature rises was to prevent interference from ambient temperature variations and contributions of the ignitor fuels. While these are both judicious motives, for the Navy flaming fires 80 percent of ionization detectors and 40 percent of photoelectric detectors alarmed at temperature rises less than or equal to 3 ºC. This observation provides a motivation not to exclude small temperature rises from the determination of the optical density to temperature rise ratio in this study. As seen in Figure 11, small temperature rise values tend to increase the optical density to temperature rise ratio. This may explain why the representative optical density to temperature rise ratio from Heskestad and Delichatsios appears near the minimum value for all the ratios shown in Figure 10.
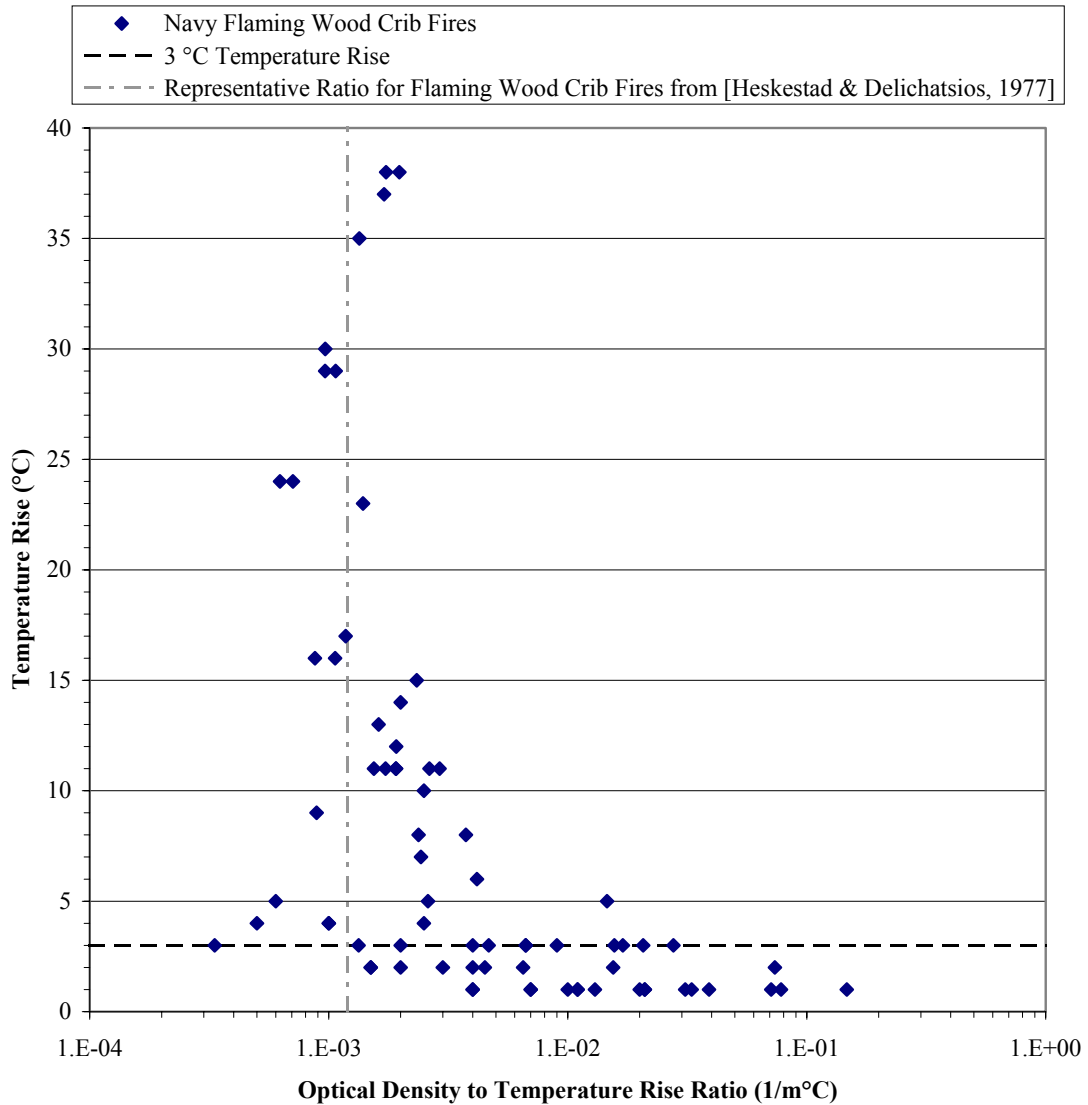
Figure 11 - Temperature rise at alarm plotted as a function of optical density to temperature rise ratio at alarm for the Navy flaming wood crib fires.

Based on the results for the optical density to temperature rise ratio at alarm presented in this section, the ratio is not constant and can vary over several orders of magnitude at the time of alarm. Since the constancy of the optical density to temperature rise ratio is one of the fundamental assumptions in using the temperature rise method, these results raise serious questions as to the validity of that approach, especially considering the prevalence of alarms occurring at nearly indistinguishable temperature rises for smoldering fires,

smoldering to flaming transitional fires, and to a lesser extent flaming fires being detected

by ionization detectors.

CHAPTER 5: PHASE 2 RESULTS

The second phase of this analysis uses the experimental measurements of optical density, temperature, and velocity adjacent to smoke detectors to estimate the response of smoke detectors based on typical alarm threshold values of these measurements. The goal of this phase is to assess the uncertainty in estimating smoke detector response based on the thresholds presented. A custom Microsoft Excel spreadsheet program was developed with Visual Basic for Applications that calculates the estimated alarm times and their associated errors with respect to the experimental alarm times for the threshold entered. This Threshold Evaluator program and the general analysis approach used are discussed in more detail in Section 5.1.

5.1 Description of Threshold Evaluator and Analysis Approach

Development of a tool to facilitate the prediction and analysis of detector alarms based on threshold measurements was the motivation behind the Threshold Evaluator. Microsoft Excel, with the aid of its Visual Basic for Applications (VBA) automation language, serves as the engine for the Threshold Evaluator. The Excel workbook consists of three worksheets: a user input screen; a template used to report the calculated alarm times; and a database of test information from the Navy and Kemano test series.

The user input screen, shown in Figure 12, allows the user to specify the threshold measurement type (i.e., optical density, temperature rise, or velocity) and value at the top of the screen. A checkbox is provided for cases where the nominal sensitivity is the desired optical density threshold. In this case, the alarm threshold used for each detector

alarm depends on the nominal sensitivity of the detector in the database. Tests and

detectors evaluated by the Threshold Evaluator are limited by user selections for the test

series, fire type, fire source material, and detector type. The default option for each of

these fields is "Any", indicating that the database should not be limited by this field.

However, if the user enters a threshold that only applies to flaming fires and ionizations

detectors, they select "Flaming" from the Fire Type field and "Ion" from the Detector

Type field to limit the predicted alarms to the desired tests and detectors.

Threshold Evaluator

Measurement	Optical Density (1/m)
Threshold	

☐ Use Nominal Sensitivity of Detector as Threshold

Limit Tests Examined by:

Test Series	Any
Fire Type	Any
Material	Any
Detector Type	Any

Instructions:

Select the desired threshold measurement and enter the threshold value. The tests examined by the Threshold Evaluator can be limited by the test series, fire type, material burning, and/or detector type.

Press the Evaluate button below when finished.

The evaluation process can be time consuming, please be patient. The progress of the evaluation will be displayed in the StatusBar (bottom, left of Excel window). A new report will be created for each evaluation performed.

Evaluate

Figure 12 - Screen shot of user input worksheet in the Threshold Evaluator.

Evaluation of the threshold (i.e. prediction of alarm times based on the entered threshold)

occurs when the "Evaluate" button is clicked at the bottom of the screen. The process of

predicting the alarm times is quite simple and could easily be done by hand for a limited

number of tests, detectors, and thresholds. However, the repetitive nature of this process

lends itself perfectly to VBA programming, particularly considering there are 425

experimental detector alarms in the database and there are numerous alarm thresholds to

evaluate. Instead of presenting the gory details of the VBA code used to predict alarm times, a rough outline of the steps taken by the code (i.e. pseudo-code) is presented.

- Verify user inputs for completeness (e.g. Was a threshold value entered?)
- Filter the database such that only tests meeting the user specifications are considered. Ensure that only detectors that were adjacent to instrumentation for the desired threshold measurement are examined.
- Create a new report for this evaluation from the template
- Loop through each record (i.e. experimental detector alarm) from the filtered database and predict an alarm time based on the user-specified threshold.
  - Open the data file for the test
  - Determine the first and last row of data to examine in the data file. For the smoldering-to-flaming transitional fires in the Kemano test series, the experimental alarms that occurred during the smoldering period use data from ignition to the transition time to predict alarms, whereas the experimental alarms that occur during flaming combustion use data from the transition time to the end of test to predict alarms. All other alarm predictions are based on data between the ignition time (time zero in the data files) and end of the data file.
  - Loop through each data point and compare that to the threshold entered. Once the threshold has been exceeded, the time associated with this data point is taken as the alarm time. To be consistent with Phase 1, only single point measurements were used for optical density and temperature. Due to the additional noise in the velocity data, an 11-point (10 second)

average around each data point was taken prior to evaluating whether the threshold was exceeded.

- o If the threshold was not exceeded, and no alarm was predicted, the maximum value and time at which it occurred are determined.
- o Copy the important test information and calculated alarm time to the report.
- o Calculate the percentage error in the predicted alarm time with respect to the experimental alarm time. For almost all cases, the error in the predicted alarm time is calculated as

$$\% \text{ Error} = \left| \frac{t_{predicted} - t_{experiment}}{t_{experiment}} \right| * 100\%$$

For the experimental detector alarms that occurred during flaming combustion, this equation is modified to account for the offset from the ignition time to the time of transition to flaming combustion ($t_{flaming}$)

$$\% \text{ Error} = \left| \frac{t_{predicted} - t_{experiment}}{t_{experiment} - t_{flaming}} \right| * 100\%$$

- o Repeat for each experimental detector alarm in the filtered database.
- Once predictions of all experimental alarms have been made, statistics for the predicted alarms are calculated, (e.g. the number of alarms predicted, the number of over- and under-predicted alarms, and the mean, standard deviation and percentiles of the population of error in the predicted alarm times) are added to the report.
- Finally, the user is alerted that the evaluation is complete along with the number of experimental alarms considered in the evaluation and the time

required to complete the evaluation. The most time required to complete an evaluation in this study was approximately 70 seconds.

The database of test information includes the following fields relevant to the prediction of detector alarm times: test series, test id, fire type, classification of the fire source, detector id, detector type, alarm time, the channel/column identifier for optical density, temperature and velocity measurements in the data files, the initial temperature, the detector nominal sensitivity, the status of the ventilation system, and the smolder-to-flaming transition time. The database, and the Threshold Evaluator itself, is easily extensible to include other data at a later time. To extend the use of the Threshold Evaluator to other test series, information on the additional tests first needs to be added to the database in the appropriate format (i.e. use the nomenclature already established in the database, alarm times should be in seconds, etc.) Secondly, the data files for the additional tests should be in Microsoft Excel format, containing only a single worksheet of test data, and placed in a directory whose name corresponds to the name of the test series entered in the database. The directory of test data for each test series is expected to be located in the same directory as the Threshold Evaluator. For example if the Threshold Evaluator is located at the path "C:\Phase 2\Threshold Evaluator.xls", then the data for the Navy test series is required to be located in the directory "C:\Phase 2\Navy\". In addition, Threshold Evaluator constructs the data filename and path based on the information in the database. Therefore, the standard naming convention adopted for all datafiles is *TestSeries-TestID*.xls. For example, the required filename of Navy test 2-12 is "NAVY-2-12.xls" and the required test name for Kemano test 9 is "KEMANO-09.xls"

according to the information in the database. The format of the data files is not nearly as rigid. Because of this flexibility, changes are required to the VBA code of the Threshold Evaluator before new test series are evaluated. In the subroutine "CalcAlarmTime", the format of the datafile must be declared. Modifications to the code need to be made in the code that is preceded by the comment "Specify the format of the datafiles". Two examples of the required modifications to the code (which is only three lines), along with a template version of the code are provided as comments in the code. The code specifies addresses of the first cells in the worksheet that contain the test times (topmost time cell on the spreadsheet) and instrument channel labels (leftmost channel label). The time data (in units of seconds) must be contained in a single column, in ascending order with time zero coinciding with the ignition time of the test. Data from each instrument must be placed in consecutive columns with a cell preceding (above) the data containing an identifying label for the instrument (the labels for all data columns must be in same the row). The label provided for each data column should match the channel/column identifiers used for optical density, temperature and velocity measurements in the database.

Having discussed the workings of the Threshold Evaluator, it is necessary to discuss how the results obtained from this program are used in the analysis. The goal of this phase of the research is to assess the uncertainty in estimating detector response based on threshold values of optical density, temperature rise, and velocity. To achieve this goal there are four metrics of the certainty in the predicted alarm times that are examined: the total percentage experimental alarms predicted; the percentages of experimental alarms

that are over- or under-predicted; the mean, median, and standard deviation of the mean

percentage error in the predicted alarm times with respect to the experimental alarm

times, and the percentage of alarm predictions that are within a given window of time

around the experimental alarm time. The first and second metrics are presented together,

as the first metric is simply a sum of the percentages of the under-predicted and over-

predicted alarms (the second metric). In addition to simply quantifying the error in the

associated prediction, the equations presented earlier in this section for the percentage

error are used to identify the direction of error in relation to the experimental alarm (i.e.

percentage errors less than zero indicate an under-prediction error, while those greater

than zero indicate an over-prediction error). To minimize the errors associated with the

predicted alarm time, the predicted alarm time would be less than the experimental alarm

time (under-predicted) in 50 percent of the cases and greater than the experimental alarm

time (over-predicted) in the remaining 50 percent. Although in some situations, only

over-predicted alarms may be desired and the inherent additional error is tolerated. The

purpose of the modeling exercise will dictate which approach is warranted. Quantifying

the uncertainty according to the calculated percentage error with respect to the

experimental alarm time is useful, but not uniquely so. In fact, the percentage error in the

predicted alarm time is insufficient, or rather misleading, when comparing errors in

predicted alarm times between smoldering and flaming fires. For example, assume that a

detector alarms 30 seconds after ignition and the predicted alarm time for this case is 60

seconds. The resultant error in the prediction would be +100 percent, despite the

predicted alarm time being within 30 seconds of the actual alarm. In contrast, assume

that fire and smoke growth rates were much smaller, as is typically the case with

smoldering fires and the experimental detector alarm did not occur until 1500 seconds, with the predicted alarm time at 1650 seconds. The resultant error in this prediction is only +10 percent, even though there is a difference of 150 seconds between the experimental and predicted alarm times. A comparison of detection times to when hazardous or untenable conditions occur is often the best approach in these situations, however a tenability analysis is beyond the scope of this paper.

In an attempt to address this issue two arbitrary windows of time around the experimental alarm are examined as the fourth metric of uncertainty in the predicted alarm times. Percentages of predicted detector alarms that are within ± 30 seconds and ± 60 seconds of the experimental alarm time are used. An estimated alarm time within a 60 second window around the actual alarm time (i.e. ± 30 s) is assumed to be a *great* prediction while estimated alarm times within a 120 second window around the actual alarm time (i.e. ± 60 s) is still assumed to be a *good* prediction. These measures are arbitrary and in some cases, depending on the expected growth rates of the fire and smoke or level of accuracy required for the application, a prediction that differs with the actual alarm by more than 60 seconds may be adequate.

5.2 Uncertainty in Alarm Predictions using Optical Density Thresholds
The same optical density alarm thresholds examined previously in this report are evaluated in this section: the nominal sensitivity of the detector; 0.14 m^{-1}; and the 20, 50, and 80 percent thresholds presented by Geiman and Gottuk [2003]. Each of these thresholds will be examined in turn.

Back in section 4.3.2, the percentage of detectors that alarmed at optical densities less than or equal to their nominal sensitivity values varied widely depending on the fire type, detector type, ventilation, etc. To further this analysis, alarm times were predicted for each detector based on their nominal sensitivity and the experimental optical density measurements. Figure 13 presents the percentages of experimental alarms under-predicted and over predicted on a stacked bar chart. The total height of each stacked bar represents the total percentage of experimental alarms that were predicted.
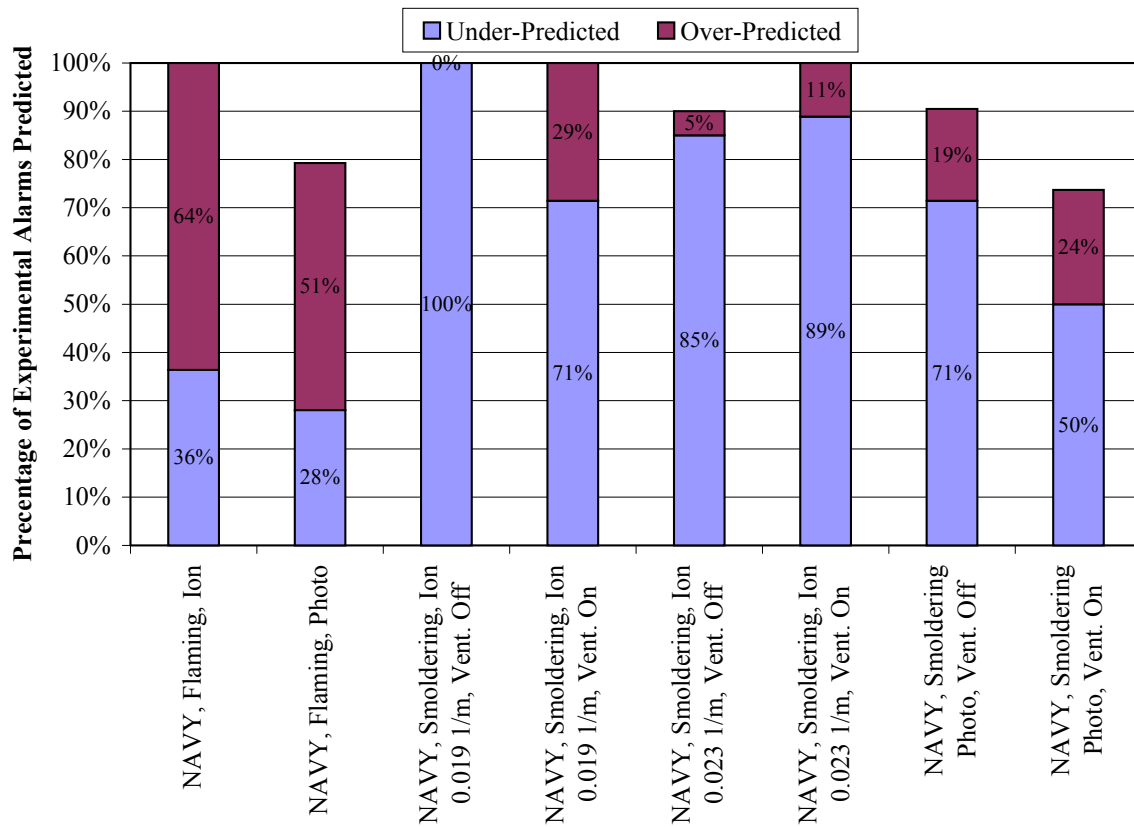
Figure 13 - Percentage of under-predicted and over-predicted alarms using the nominal sensitivity of the detectors as an alarm threshold.

For all but two of the cases shown in Figure 13, the nominal sensitivity predicted at least 90 percent of all alarms that occurred during the experimental testing. For the two remaining cases, at least 75 percent of alarms were predicted. The downside to this high of a successful percentage of predictions is that the vast majority of predicted alarms for the smoldering fires occurred before the alarms in the experiments. On the other hand, for the flaming fires there were more over-predicted alarms than under-predicted, with a ratio of under-predicted to over-predicted alarms closer to one.

Table 18 presents the calculated error in the predicted alarms based on the experimental alarm time. In addition to quantifying the error, the direction of error in relation to the experimental alarm can be determined (i.e. percentage errors less than zero indicate an under-prediction error, while those greater than zero indicate an over-prediction error). The median, mean, and standard deviation values are given in percentage error. Therefore, the range of error in the predicted alarm times within plus or minus one standard deviation of the mean for smoldering fires with the ventilation off and photoelectric detectors in Table 18 is −74 percent to +68 percent.

Table 18 - Mean and median error in predicted alarm times using the nominal sensitivity of the detectors as an alarm threshold.

Test Series	Fire Type	Detector Type	Nominal Sensitivity	Ventilation Status	Nominal Sensitivity Optical Density Threshold			
					Alarms Predicted	Error in Predicted Alarm Time		
						Median	Mean	Std Dev
NAVY	Flaming	Ion			88	90%	327%	513%
NAVY	Flaming	Photo			65	33%	103%	246%
NAVY	Smoldering	Ion	0.019 m^{-1}	Off	7	-59%	-56%	26%
NAVY	Smoldering	Ion	0.019 m^{-1}	On	7	-68%	-29%	79%
NAVY	Smoldering	Ion	0.023 m^{-1}	Off	19	-51%	-41%	38%
NAVY	Smoldering	Ion	0.023 m^{-1}	On	18	-35%	-28%	62%
NAVY	Smoldering	Photo		Off	38	-22%	-23%	35%
NAVY	Smoldering	Photo		On	28	-14%	-4%	70%

In general, the mean and median error associated with using the nominal sensitivity to estimate the response of smoke detector to smoldering fires is on the order of $20 - 60$ percent under-predicted. When the standard deviations for the mean errors are considered, the range of errors is substantially large. Despite a better balance between over-predicted and under-predicted alarms for flaming fires (see Figure 13), the errors associated with the predicted alarms are significantly greater than for the smoldering cases just discussed. The mean and median errors in the estimated detector responses to the flaming fires using the nominal sensitivity as an alarm threshold are on the order of $100 - 300$ percent over-prediction. On one hand, the fact that the errors are most over-prediction means that the predicted alarm times are fairly conservative. However, the concern is that they are overly conservative and that a $100 - 300$ percent over-prediction error is too large.

The percentage errors presented in the previous table do not necessarily fully describe how well the nominal sensitivity as an alarm threshold estimates detector responses. The reasons for this were discussed in the previous section. To remedy this situation, a

further step in the analysis was taken to examine the percentage of predicted alarms that occurred within ± 30 seconds and ± 60 seconds of the experimental alarm time. Figure 14 illustrates the percentages of predicted alarms (using the nominal sensitivity as an alarm threshold) that occurred within ± 30 seconds and ± 60 seconds of the experimental alarm time. Note that the percentages of predicted alarms within ± 60 seconds include the predictions within ± 30 seconds (e.g. in Figure 14 for the Navy flaming fires and ionization detectors, 20 percent of predicted alarms were within ± 30 seconds with an additional 20 percent of predicted alarms between ± 30 to 60 seconds such that the total percentage of predicted alarms within ± 60 seconds was 40 percent).
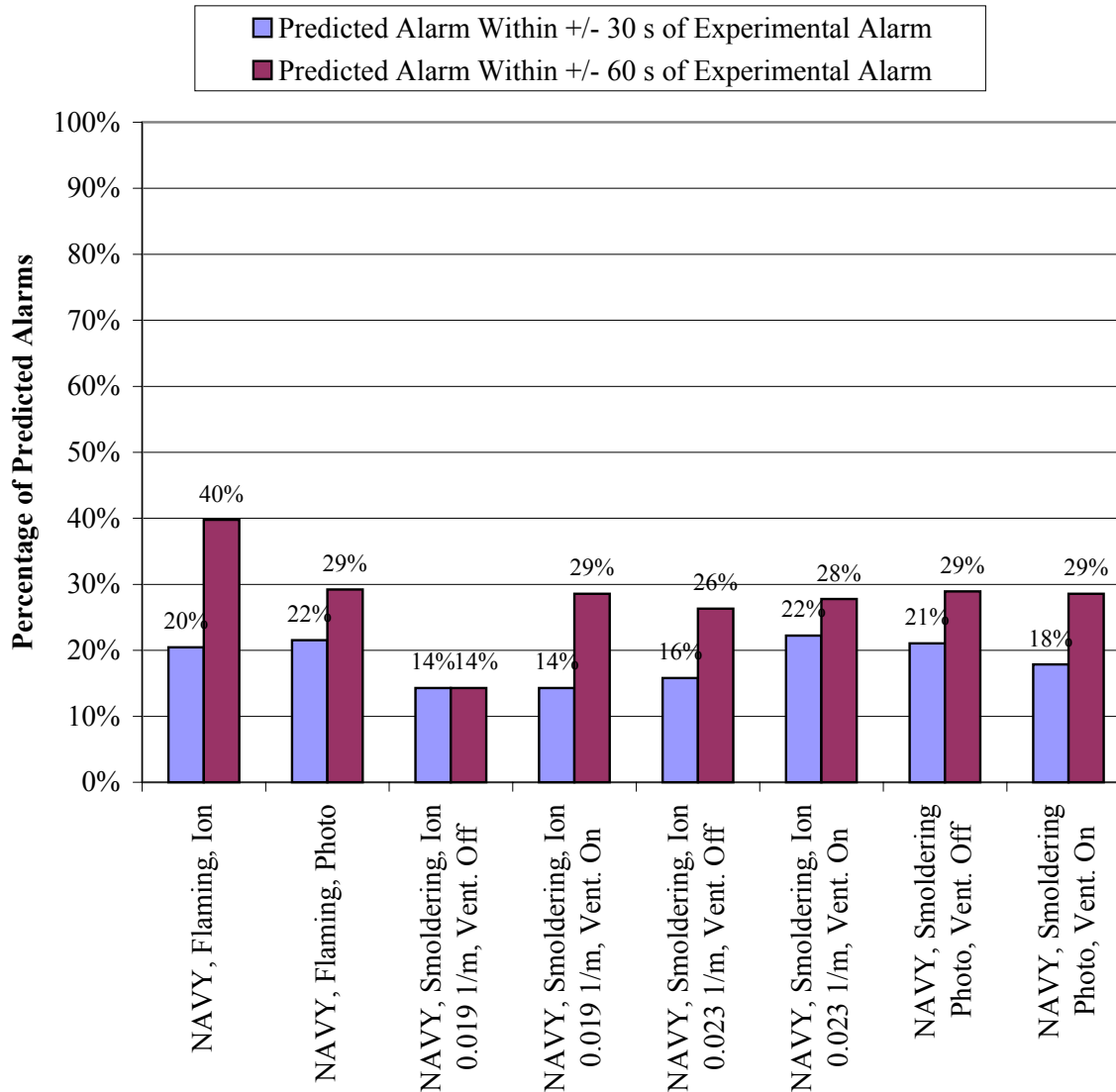
Figure 14 - Percentage of predicted alarms that occurred within ±30 and ±60 seconds of the experimental alarm with the nominal sensitivity of detectors used as an alarm threshold.

Interestingly, the percentage of alarms occurring within ± 30 and ± 60 seconds of the experimental alarm time was fairly constant across the cases considered. The percentage of predicted alarms within ± 30 seconds was generally in the range of 15 – 20 percent, while the percentage of predicted alarms within ± 60 seconds was generally in the range of 25 – 30 percent. In addition, despite a mean error of over 300 percent, 40 percent of

the predicted alarm times for ionization detectors responding to flaming fires were within ± 60 seconds of the experimental alarm time. Overall, the fact that only 20 − 30 percent of predicted alarm times were *good* predictions (as defined in the previous section) is not very encouraging for using the nominal sensitivity as an alarm threshold to estimate the response of smoke detectors.

The same process undertaken for examining the uncertainty in the estimated detector response using the nominal sensitivity as an alarm threshold is applied to the $0.14m^{-1}$ threshold. As before, the percentage of under-predicted and over-predicted alarms is evaluated first.
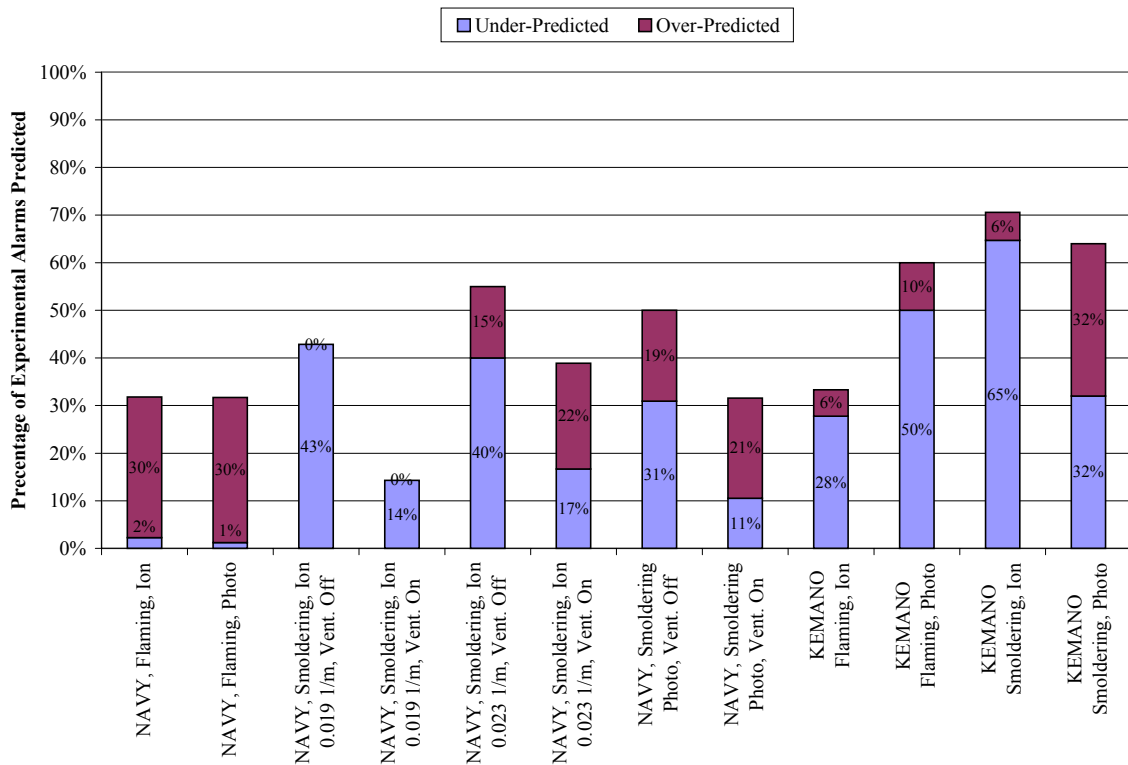
Figure 15 - Percentage of under-predicted and over-predicted alarms using an optical density of $0.14m^{-1}$ as an alarm threshold.

In contrast to Figure 13 for the nominal sensitivity alarm threshold where all of the cases predicted more than 75 percent of the experimental alarms, Figure 15 shows that for a majority of the cases shown less than 50 percent of the experimental alarms were predicted using 0.14 m^{-1} as an alarm threshold. This low percentage of predicted alarms was due to the optical density of the smoke during the test not exceeding 0.14 m^{-1} for many of the tests. For ionization and photoelectric detectors responding to flaming fires, the vast majority of alarms predicted using an optical density of 0.14 m^{-1} as an alarm threshold were over-predictions. Despite the fact that for flaming fires an optical density threshold of 0.14 m^{-1} over-predicts almost all alarms, it may provide a useful bounding condition. The propensity for this threshold to over-predict detector response times combined with the fact that 99 percent of ionization and photoelectric detector responses to flaming fires in the Navy test series occurred at an optical density less than or equal to 0.14 m^{-1} (See Figure 5) leads to the conclusion that if this threshold is exceeded for a flaming fire, then a detector response is highly likely to have occurred and the actual alarm time of the detector took place prior to the predicted alarm time.

The percentage of predicted alarms for the smoldering cases from the Navy tests and the transitional smoldering-to-flaming fires from the Kemano tests were varied. However, the percentage of predicted alarms that were over-predicted increased as compared to using the nominal sensitivity as an alarm threshold where almost all predicted alarms were under-predicted. It is also interesting to note that the overall percentage of alarms predicted was lower for the cases in which the ventilation system was operating as compared to when there was no ventilation. The operating ventilation system in many of

these tests limits the optical density below the threshold of 0.14 m^{-1} so fewer alarms are predicted.

The range of errors in the predicted alarm times varies significantly more for the 0.14 m^{-1} optical density threshold as compared to the detector nominal sensitivity threshold. The mean and median errors in the predicted alarm times for the 0.14 m^{-1} as an alarm threshold are shown in Table 19.

Table 19 - Mean and median error in predicted alarm times using an optical density of 0.14 m^{-1} as an alarm threshold.

Test Series	Fire Type	Detector Type	Nominal Sensitivity	Ventilation Status	0.14 m^{-1} Optical Density Threshold			
					Alarms Predicted	Error in Predicted Alarm Time		
						Median	Mean	Std Dev
NAVY	Flaming	Ion			28	1844%	2089%	1203%
NAVY	Flaming	Photo			26	152%	857%	1311%
NAVY	Smoldering	Ion	0.019 m^{-1}	Off	3	-11%	-31%	36%
NAVY	Smoldering	Ion	0.019 m^{-1}	On	1		-51%	
NAVY	Smoldering	Ion	0.023 m^{-1}	Off	11	-4%	-18%	36%
NAVY	Smoldering	Ion	0.023 m^{-1}	On	7	7%	-20%	42%
NAVY	Smoldering	Photo		Off	21	-8%	-7%	44%
NAVY	Smoldering	Photo		On	12	45%	75%	102%
KEMANO	Flaming	Ion		Off	8	-51%	-51%	50%
KEMANO	Flaming	Photo		Off	6	-61%	-52%	44%
KEMANO	Smoldering	Ion		Off	13	-26%	-27%	23%
KEMANO	Smoldering	Photo		Off	16	-8%	40%	159%

For flaming fires, the error associated with the predicted responses of ionization detectors was on average approximately 2000 percent, while that for photoelectric detectors was on average approximately 900 percent (with the errors in both cases being over-predictions). Again, the error in the predicted alarm times for the smoldering and smoldering-to-flaming transitional cases varied but was significantly less than for the flaming fires. In general, the mean error for these cases was in the range of 10 to 50 percent under-prediction, with the error in the responses of photoelectric detectors in the Navy

smoldering fires with ventilation and Kemano smoldering tests being the outliers in this

group with mean errors of 40 and 75 percent over-prediction, respectively. It is

worthwhile to note that due to small sample sizes of predicted alarms for some of these

cases (e.g. the 0.019 m^{-1} ionization detector responses to the Navy smoldering fires with

ventilation on) the results in Table 19 should be interpreted with caution.

The percentage of predicted alarms that are within $\pm$ 30 and $\pm$ 60 seconds of the

experimental alarm, as shown in Figure 16, provides another measure of uncertainty in

the predicted alarms using a threshold optical density of 0.14m^{-1}.
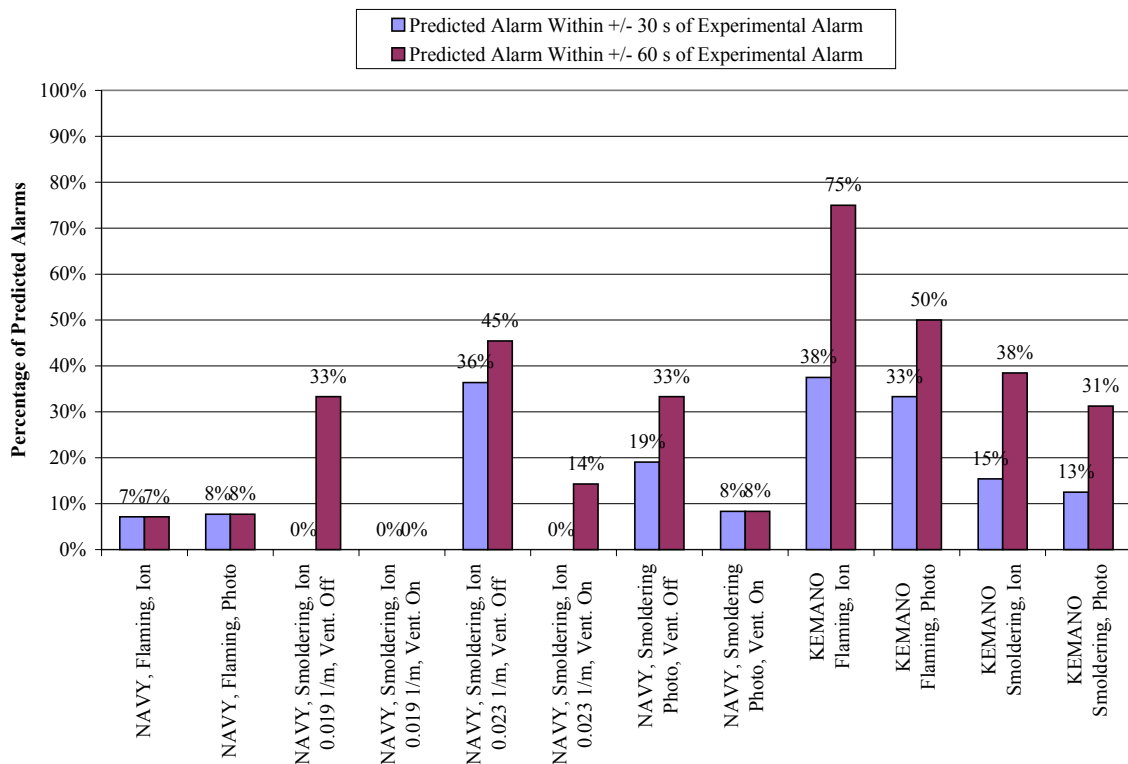
Figure 16 - Percentage of predicted alarms that occurred within ±30 and ±60 seconds of the experimental alarm with an optical density of 0.14 m^{-1} used as an alarm threshold.

As expected with mean errors in the predicted alarm times on the order of 1000 – 2000 percent for ionization and photoelectric detectors responding to the Navy flaming fires, less than 10 percent of the predicted alarms were within ± 30 and ± 60 seconds. The percentage of predicted alarms between these two windows of time varied. The cases in which none of the predicted alarms were within ± 30 and/or ± 60 seconds all had less than 10 predicted alarms. In addition, the favorable percentages of predicted detector responses within ± 30 and ± 60 seconds for flaming fires from the Kemano test series are surprising given the results from the Navy tests. The difference in the Kemano test series is that an appreciable concentration of smoke typically accumulated during the initial smoldering phase of combustion (before the fire transitioned to flaming) that would not normally have been present if the fires were flaming throughout their entire duration. As a result, the experimental alarms during the flaming period of the tests generally occurred soon after the transition to flaming. Since the predictions made for the experimental alarms that occurred during the flaming period only looked at data after the transition time and there was already a significant smoke concentration at this time, the majority of both experimental and predicted alarms occurred on or immediately following the time to transition. In this way, the methodology used to predict the alarms of detectors during the flaming period of the smoldering-to-flaming transitional fires results in alarm times artificially close to the experimental alarm time. This observation is not necessarily reflected in Table 19 where the reported median errors were –50 to –60 percent, but upon further exploration below the 20th to 30th percentile the percentage errors were –90 to – 100 percent (i.e. the predicted alarm occurred immediately on or soon after the transition to flaming combustion).

102

The 20, 50, and 80 percent optical density thresholds from Table 12 were also used to estimate detector responses from the Navy and Kemano tests. Optical density thresholds used to predict smoke detector alarm times from these tests were shown previously in Table 12. Figure 17 illustrates the percentages of experimental alarms that are over- and under-predicted for the 20, 50, and 80 percent optical density alarm thresholds. The total percentage of experimental alarms that are predicted ranged from 86 to 100 percent for all cases examined for the 20 percent threshold, with between 70 and 90 percent of all experimental alarms being under-predicted. Subsequently, the total percentage of predicted alarms diminishes for the 50 percent and 80 percent thresholds, as expected. In addition, for the flaming ionization and photoelectric predictions, the ratio of over-predicted to under-predicted alarms increased 1:3 or 1:6 at the 20 percent threshold to more than 4:1 at the 80 percent threshold. However, the trends in the smoldering cases were not nearly as well behaved. In many of the smoldering fires, both ionization and photoelectric detector responses were still predominantly under-predicted, even at the 50 percent and 80 percent alarm thresholds. It is important to remember though that the thresholds used in these predictions do not address all of the variables embodied here for smoldering fires; the status of ventilation in the compartment and the nominal sensitivity of the detectors were not considered significant variables by Geiman and Gottuk [2003].
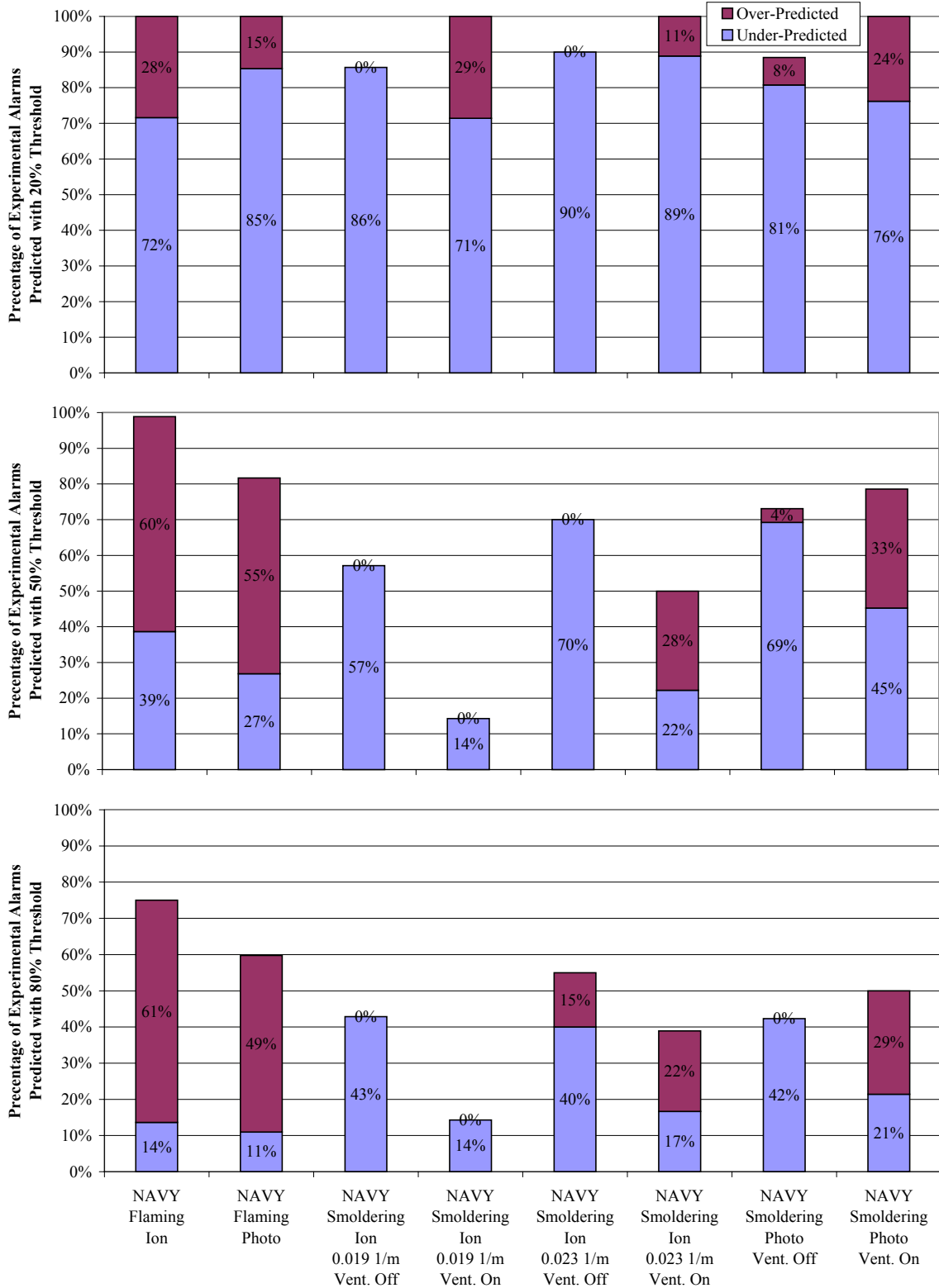
Figure 17 - Percentage of under-predicted and over-predicted alarms for the Navy tests using the 20 percent (top), 50 percent (middle), and 80 percent (bottom) optical density alarms thresholds from Table 12.

104

Mean and median error values are quantified in **Error! Not a valid bookmark self-reference.** for the Navy test series. In general, the errors for all cases at the 20 percent threshold were in the range of 20 to 60 percent under-predicted, with the exception to this being for ionization detectors with flaming fires where the mean error was in over-prediction due to a few large over-prediction errors. Moving to the 50 percent threshold there is not a reduction or minima of the predicted error at this threshold, as previously expected. For example, the magnitude of the error for the ionization and photoelectric detectors for flaming fires was at a minimum at the 20 percent threshold and continually increased to a maximum value at the 80 percent threshold. In addition, the mean and median predicted errors in the response of ionization and photoelectric detectors to flaming fires were all errors in over-prediction at the 50 percent and 80 percent thresholds. Finally, it is interesting to note the standard deviations of the mean error. For the flaming cases, the standard deviation increased from the 20 percent to the 80 percent threshold, while for the smoldering cases it remained fairly constant. The standard deviations in the error of the predicted alarm times for smoldering fires in which the ventilation was off were in the range of 20 to 30 percent for all the thresholds, however the standard deviations in the error of the predicted alarm times with the ventilation on were consistently 2 to 3 times higher.

Table 20 - Mean and median error in predicted alarm times for the Navy tests using the 20 percent (top), 50 percent (middle), and 80 percent (bottom) optical density alarm thresholds from Table 12.

Test Series	Fire Type	Detector Type	Nominal Sensitivity	Ventilation Status	20% Optical Density Threshold			
					Alarms Predicted	Error in Predicted Alarm Time		
						Median	Mean	Std Dev
NAVY	Flaming	Ion			88	-34%	43%	251%
NAVY	Flaming	Photo			82	-21%	-16%	64%
NAVY	Smoldering	Ion	0.019 m^{-1}	Off	6	-53%	-52%	28%
NAVY	Smoldering	Ion	0.019 m^{-1}	On	7	-66%	-19%	94%
NAVY	Smoldering	Ion	0.023 m^{-1}	Off	18	-53%	-45%	27%
NAVY	Smoldering	Ion	0.023 m^{-1}	On	18	-33%	-25%	63%
NAVY	Smoldering	Photo		Off	24	-39%	-36%	29%
NAVY	Smoldering	Photo		On	42	-20%	-8%	73%

Test Series	Fire Type	Detector Type	Nominal Sensitivity	Ventilation Status	50% Optical Density Threshold			
					Alarms Predicted	Error in Predicted Alarm Time		
						Median	Mean	Std Dev
NAVY	Flaming	Ion			88	64%	299%	483%
NAVY	Flaming	Photo			67	22%	103%	249%
NAVY	Smoldering	Ion	0.019 m^{-1}	Off	4	-40%	-41%	31%
NAVY	Smoldering	Ion	0.019 m^{-1}	On	1		-54%	
NAVY	Smoldering	Ion	0.023 m^{-1}	Off	14	-33%	-31%	25%
NAVY	Smoldering	Ion	0.023 m^{-1}	On	9	1%	4%	80%
NAVY	Smoldering	Photo		Off	20	-28%	-32%	26%
NAVY	Smoldering	Photo		On	33	-8%	12%	72%

Test Series	Fire Type	Detector Type	Nominal Sensitivity	Ventilation Status	80% Optical Density Threshold			
					Alarms Predicted	Error in Predicted Alarm Time		
						Median	Mean	Std Dev
NAVY	Flaming	Ion			66	613%	817%	800%
NAVY	Flaming	Photo			51	73%	192%	381%
NAVY	Smoldering	Ion	0.019 m^{-1}	Off	3	-13%	-32%	36%
NAVY	Smoldering	Ion	0.019 m^{-1}	On	1		-51%	
NAVY	Smoldering	Ion	0.023 m^{-1}	Off	11	-5%	-22%	28%
NAVY	Smoldering	Ion	0.023 m^{-1}	On	7	7%	-20%	42%
NAVY	Smoldering	Photo		Off	11	-24%	-30%	22%
NAVY	Smoldering	Photo		On	21	12%	40%	84%

Although the magnitude of the errors using the 20, 50, and 80 percent alarm thresholds to predicted detector responses are not as significant as with the previous thresholds, it is still worthwhile to examine the percentage of predictions within ±30 seconds and ±60 seconds. Figure 18 demonstrates that for flaming fires the predicted responses were within ±60 seconds of the experimental alarm 63 percent of the time for ionization

detectors and 49 percent of the time for photoelectric detectors. Approximately 40

percent of predicted ionization and photoelectric responses to flaming fires were within

±30 seconds using the 20 percent alarm threshold. In general, between 15 and 20 percent

of predicted alarms to smoldering fires were within ±30 seconds of the experimental

alarm time, with similar or slightly greater percentages within ±60 seconds of the 20

percent threshold. The predicted responses of photoelectric detectors to smoldering fires

with the ventilation system off had a greater percentage of predicted alarms within the

±30 second and ±60 second windows, as compared to the other smoldering alarm

predictions. Generally speaking, the percentages of predicted alarms within each window

of time decrease at the 50 percent and 80 percent thresholds. The exception to this trend

are the predicted responses of the $0.023m^{-1}$ nominal sensitivity ionization detector to

smoldering fires with the ventilation system operating, which had the greatest percentage

of predicted alarms within each window of time (36 percent for ±30 seconds and 55

percent for ±60 seconds) at the 80 percent alarm threshold. Finally, caution should be

exercised when basing any conclusions on Figure 18, realizing that some of the

percentages presented therein incorporate fewer than 10 predicted alarms (e.g. the 0

percent values for smoldering fires with the 0.019 m^{-1} nominal sensitivity ionization

detector for the 50 percent and 80 percent thresholds).
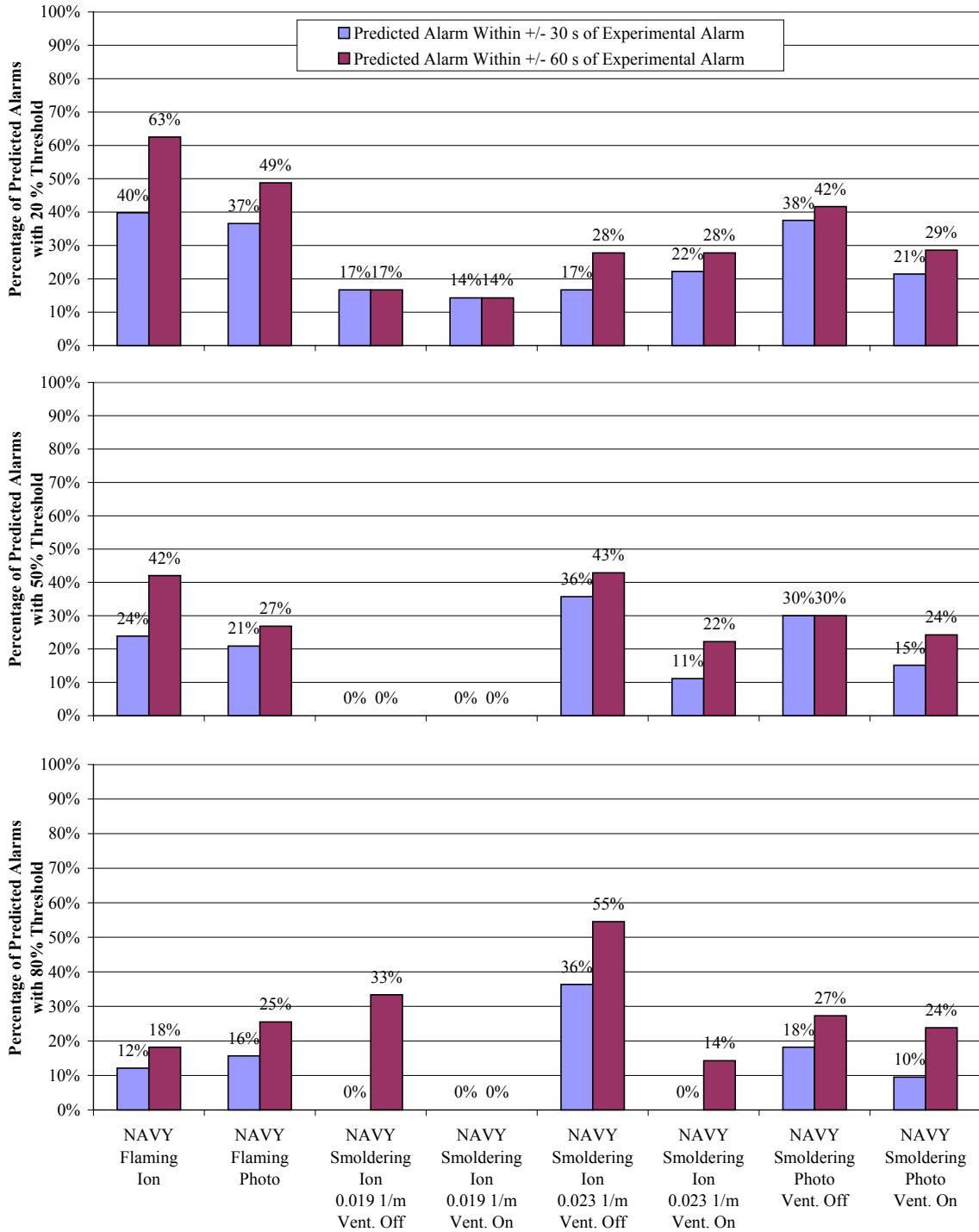
Figure 18 - Percentage of predicted alarms that occurred within ±30 and ±60 seconds of the experimental alarm for the Navy tests using the 20 percent (top), 50 percent (middle), and 80 percent (bottom) optical density alarm thresholds from Table 12.

An important feature of using 20, 50, and 80 percent thresholds is the ability to provide a range of likely alarm times and, hopefully in the majority of cases, provide bounding conditions with the 20 percent and 80 percent alarm thresholds. To investigate this hypothesis the alarm times from the 20 percent and 80 percent threshold were compared to the experimental alarm time to determine if experimental alarms fell within the bounds of the predicted alarm times.
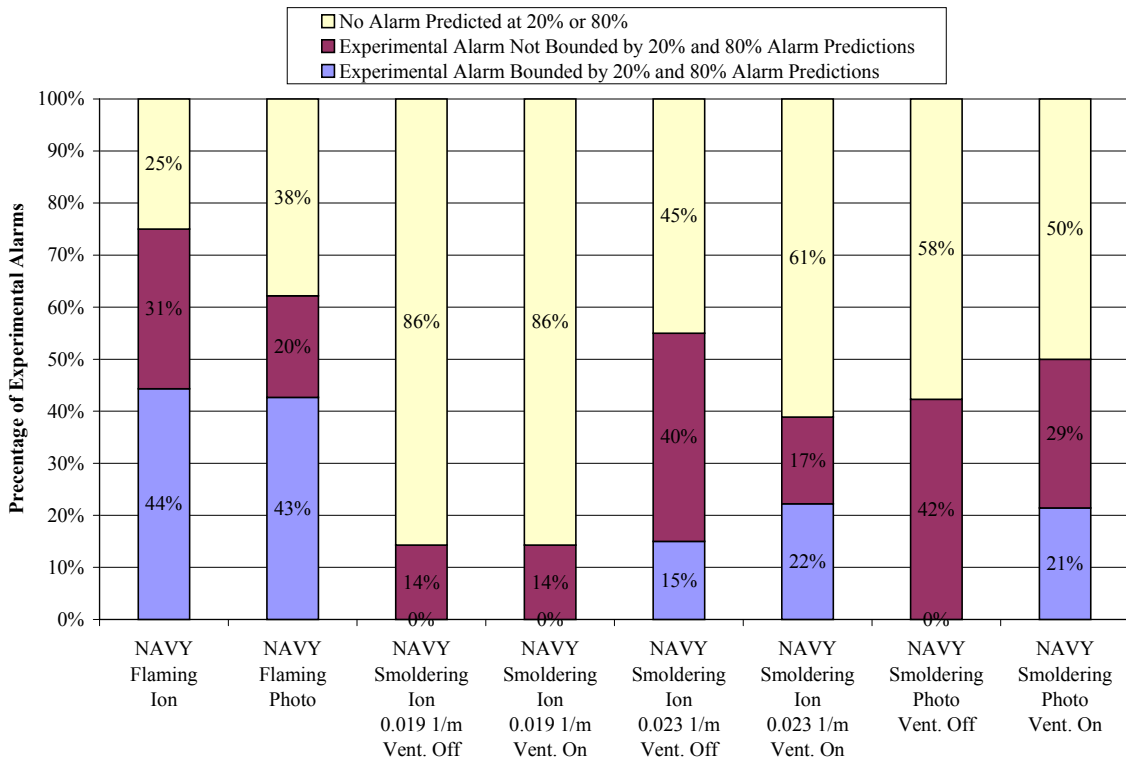
Figure 19 - Percentage of Navy experimental alarms bounded by the 20 percent and 80 percent optical density alarm thresholds from Table 12.

Disappointingly, only approximately 40 percent of experimental flaming alarms and less than 20 percent of experimental smoldering alarms were bounded by the alarm times predicted using the 20 percent and 80 percent optical density thresholds. However, a significant portion of the experimental alarms that did not fall within these bounds were

due to the optical density not increasing sufficiently to cause alarm predictions at one or both of the alarm thresholds.

Detector alarms from the Kemano test series were predicted in the same manner as the Navy tests, however using different thresholds from Table 12. As Figure 20 shows, 100 percent of experimental alarms were predicted for all cases and three threshold levels, except for the predicted responses of ionization detectors to smoldering fires of which 91 percent of alarms were predicted. Although Figure 20 demonstrates exceptional performance by the 20, 50 and 80 percent alarm thresholds, the outlook for these thresholds is diminished after reviewing the quantitative results in Table 21. For example, the median error in the predicted response of ionization detectors to flaming fires is roughly –100 percent for the 20, 50, and 80 percent thresholds. The predicted response of photoelectric detectors to flaming fires was quite similar with median errors between –74 to –95 percent. In both cases, these results indicate that a majority of the predicted alarms are occurring at or immediately following the transition to flaming and the experimental detector responses do not demonstrate corresponding behavior, or at least not to the same degree. Another observation from Table 21 is that the median prediction errors decrease from –44 to –26 percent for ionization detector and –19 to –7 percent for photoelectric detectors for smoldering fires from the 20 percent thresholds to the 80 percent thresholds. In constrast, the mean error in the predicted response of photoelectric detectors to smoldering fires increases from –12 to +58 percent from the 20 percent to 80 percent thresholds, with the standard deviation increasing likewise from 34 percent to 177 percent.
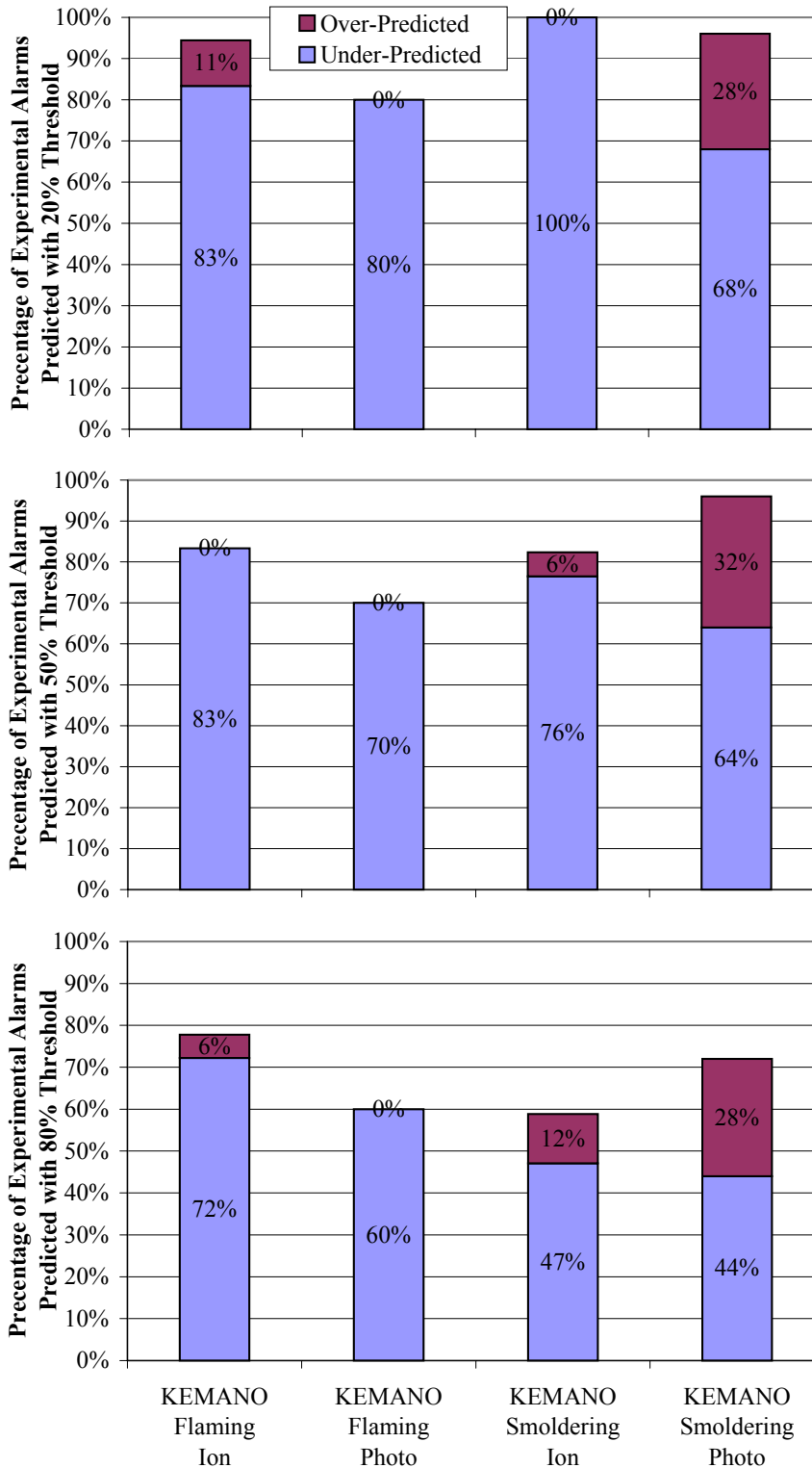
Figure 20 - Percentage of under-predicted and over-predicted alarms for the Kemano tests using the 20 percent (top), 50 percent (middle), and 80 percent (bottom) optical density alarm thresholds from Table 12.

Table 21 - Mean and median error in predicted alarm times for the Kemano tests using the 20 percent (top), 50 percent (middle), and 80 percent (bottom) optical density alarm thresholds from Table 12.

Test Series	Fire Type	Detector Type	20% Optical Density Threshold			
			Alarms Predicted	Error in Predicted Alarm Time		
				Median	Mean	Std Dev
KEMANO	Flaming	Ion	17	-100%	-27%	159%
KEMANO	Flaming	Photo	8	-91%	-61%	49%
KEMANO	Smoldering	Ion	17	-44%	-47%	21%
KEMANO	Smoldering	Photo	24	-19%	-12%	34%

Test Series	Fire Type	Detector Type	50% Optical Density Threshold			
			Alarms Predicted	Error in Predicted Alarm Time		
				Median	Mean	Std Dev
KEMANO	Flaming	Ion	15	-100%	-78%	40%
KEMANO	Flaming	Photo	7	-95%	-58%	51%
KEMANO	Smoldering	Ion	14	-31%	-30%	22%
KEMANO	Smoldering	Photo	24	-12%	26%	105%

Test Series	Fire Type	Detector Type	80% Optical Density Threshold			
			Alarms Predicted	Error in Predicted Alarm Time		
				Median	Mean	Std Dev
KEMANO	Flaming	Ion	14	-97%	-58%	71%
KEMANO	Flaming	Photo	6	-74%	-57%	44%
KEMANO	Smoldering	Ion	11	-26%	-18%	33%
KEMANO	Smoldering	Photo	18	-7%	58%	177%

Figure 21 presents the percentages of the predicted alarms that occurred within ± 30 seconds and ± 60 seconds of the experimental alarm times. Approximately 40 to 50 percent of predicted ionization and photoelectric responses are within ± 60 of the experimental alarms for the 20, 50 and 80 percent thresholds. A window of ± 30 seconds around the experimental alarm times includes approximately 20 percent of predicted ionization detector responses and 35 to 40 percent of photoelectric detector responses for

flaming fires. These figures are inflated due to the methodology used to predict the

detector response during the flaming portion of smoldering-to-flaming transitional fires.

Alarm predictions in these flaming scenarios are forced to occur after the time when

transition to flaming occurs. In combination with the observation that most of the

experimental alarms that occurred during the flaming period occurred soon after the

transition time, it comes as no surprise that so many of the predicted alarms occurred

within 60 seconds of the experimental alarm. The percentage of predicted ionization and

photoelectric alarms within the $\pm$ 30 second and $\pm$ 60 second windows increased to a

maximum of approximately 20 percent for $\pm$ 30 seconds and 30 percent for $\pm$ 60 seconds

at the 80 percent threshold.
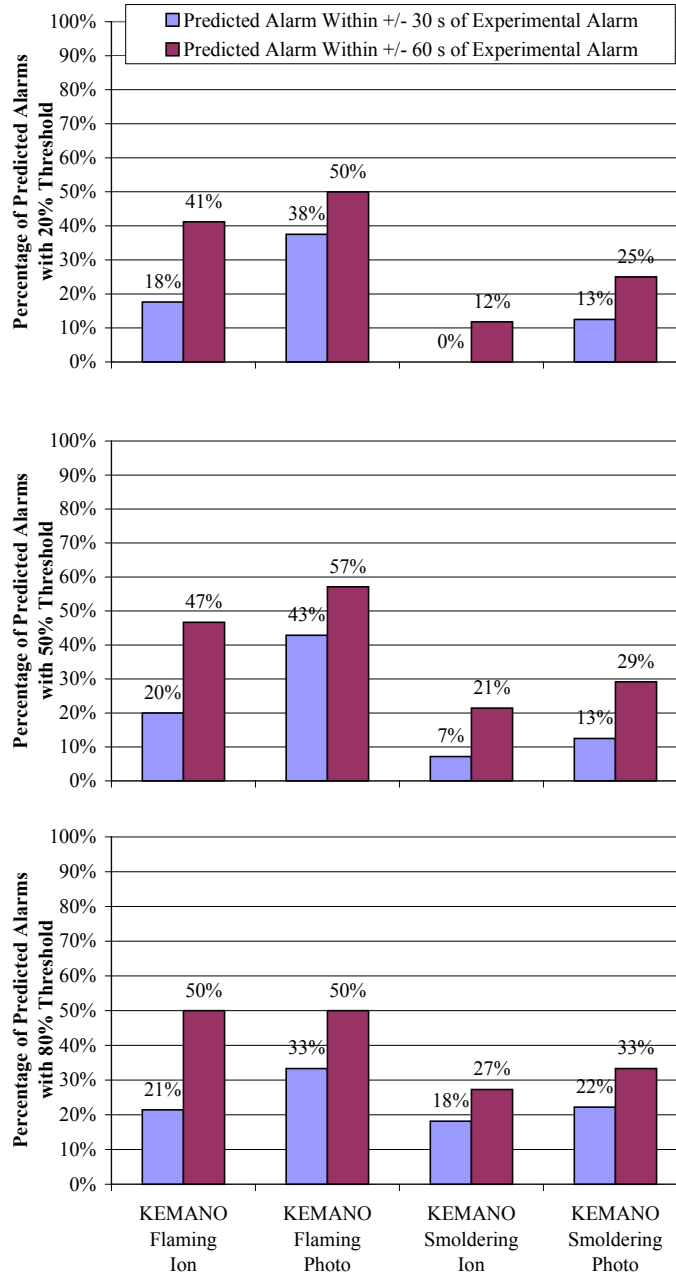
Figure 21 - Percentage of predicted alarms that occurred within ±30 and ±60 seconds of the experimental alarm for the Kemano tests using the 20 percent (top), 50 percent (middle), and 80 percent (bottom) optical density alarm thresholds from Table 12.

As with the Navy tests, the ability of the 20, 50, and 80 percent optical density thresholds to provide a range of likely alarm times and hopefully in the majority of cases provide bounding conditions with the 20 percent and 80 percent alarm thresholds is examined.

The alarm times from the 20 percent and 80 percent thresholds are compared to the experimental alarm times to determine if the experimental alarm fell within the bounds of the predicted alarm times. The results of this analysis are shown in Figure 22.
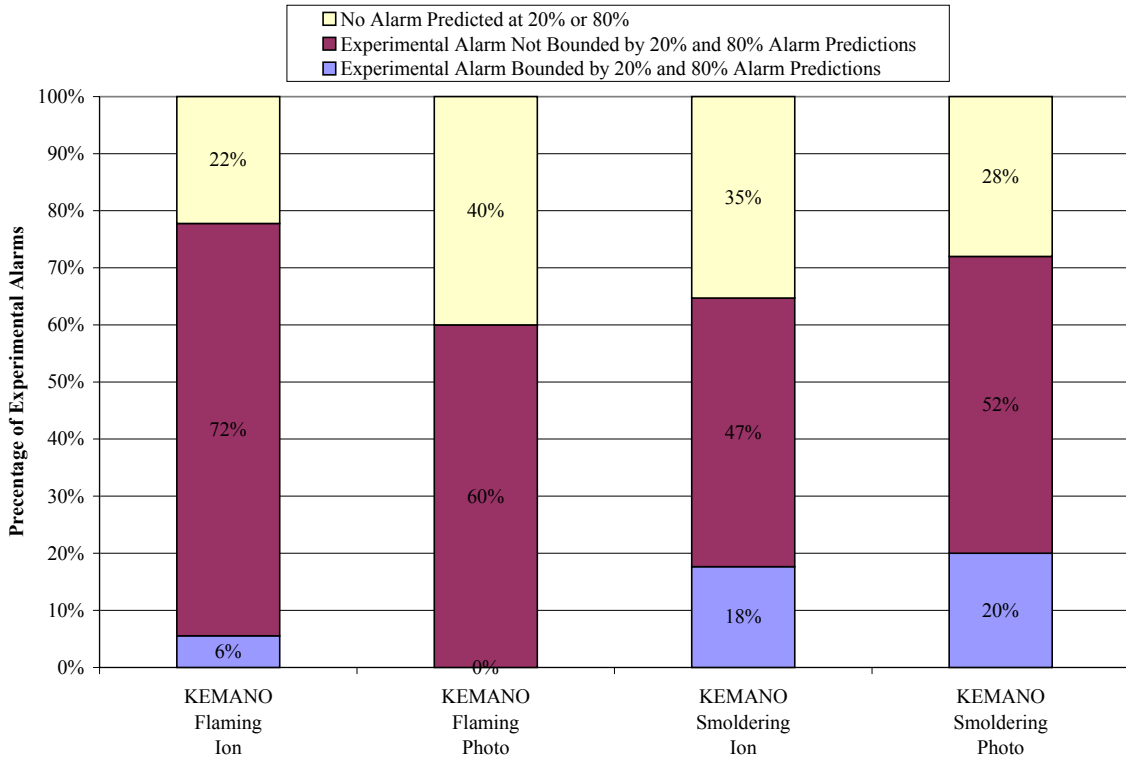
Figure 22 - Percentage of Kemano experimental alarms bounded by the 20 percent and 80 percent optical density alarm thresholds from Table 12.

As was seen in the Navy tests, less than 20 percent of experimental alarms from the Kemano tests were bounded by the alarm times predicted using the 20 percent and 80 percent optical density thresholds. In contrast though, a significant portion (47 to 72 percent) of the experimental alarms did not fall within the bounds of the 20 percent and 80 percent thresholds.

5.3 Uncertainty in Alarm Predictions using Temperature Rise Thresholds

The same approach to examine the uncertainty in the predicted alarm times used for the optical density thresholds is adopted for the temperature rise thresholds. The alarm predictions for each threshold will be examined for the percentages of alarms over- and under-predicted, the mean and median errors, and the percentage of predicted alarms that are within $\pm$ 30 and $\pm$ 60 seconds of the experimental alarm time.

As shown in Figure 23, a temperature rise threshold of 4 ºC predicts 100 percent of experimental detector alarms from flaming fires in the Navy test series with approximately a 4:1 ratio of over-predicted to under-predicted alarms for the ionization detectors and conversely a 1:3 ratio for photoelectric detectors. Less than 11 percent of all experimental detector alarms for smoldering fires from the Navy tests were predicted with this threshold. In addition, only 20 to 30 percent of the detector alarms that occurred during the flaming combustion in the Kemano tests were predicted. None of the experimental alarms that occurred during the smoldering period of the Kemano fires were predicted.
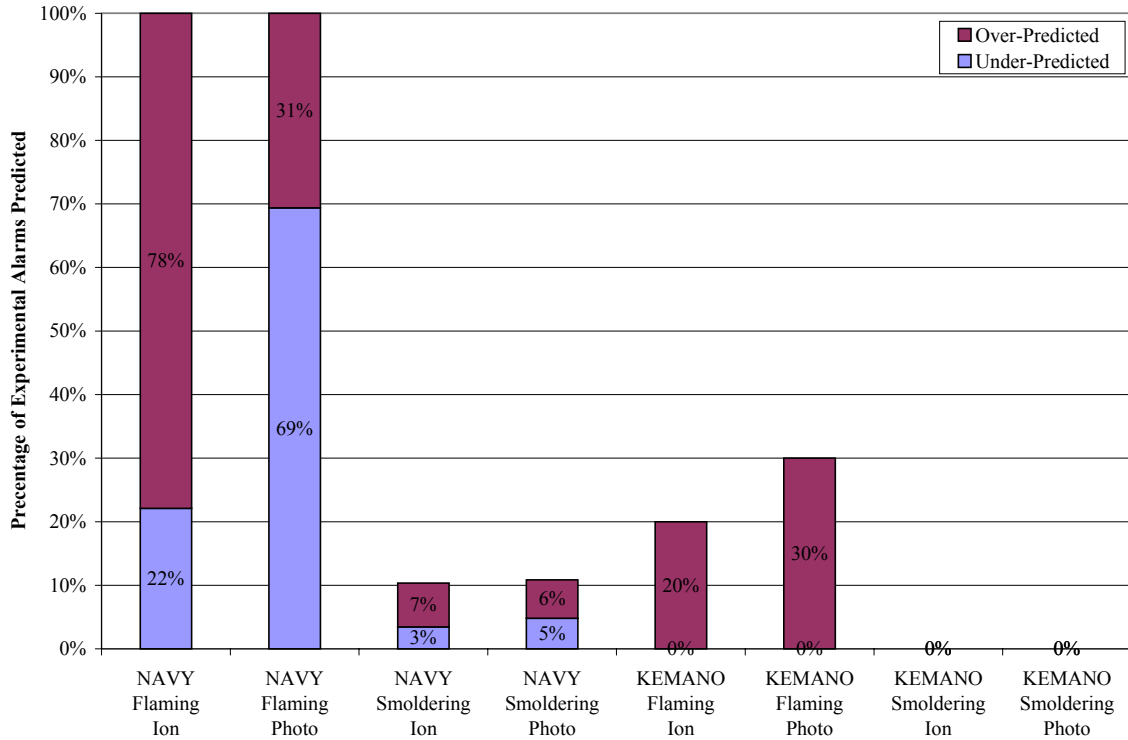
Figure 23 - Percentage of under-predicted and over-predicted alarms using a temperature rise of 4 °C as an alarm threshold.

Based on the limited percentages of experimental alarms predicted in Figure 23, a temperature rise threshold of even 4 ºC appears inadequate to predict smoldering or smoldering-to-flaming transition fires. However, the error in the alarms that are predicted for the Navy smoldering fires is in the range of 30 to 70 percent over-prediction for both the mean and median values, as shown in Table 22. The magnitude of the error in the predicted alarm times is 40 to 85 percent for flaming fires from the Navy test series. The error predicting photoelectric detector response to flaming fires has a median value of –60 percent, while the mean value is +5 percent. This indicates that the presence of large positive (over-prediction) errors are skewing the mean error value, based on the fact that almost 3 times as many under-predicted alarms occurred as over-predicted alarms (see Figure 23).

117

Table 22 - Mean and median error in predicted alarm times using a temperature rise of 4 °C as an alarm threshold.

Test Series	Fire Type	Detector Type	4 °C Temperature Rise Threshold			
			Alarms Predicted	Error in Predicted Alarm		
				Median	Mean	Std Dev
NAVY	Flaming	Ion	104	41%	85%	138%
NAVY	Flaming	Photo	98	-60%	5%	161%
NAVY	Smoldering	Ion	6	67%	70%	104%
NAVY	Smoldering	Photo	9	33%	41%	87%
KEMANO	Flaming	Ion	4	677%	574%	410%
KEMANO	Flaming	Photo	3	70%	476%	716%
KEMANO	Smoldering	Ion	0			
KEMANO	Smoldering	Photo	0			

Despite drastically different overall percentages of alarms predicted, the percentage of alarms that were predicted that occurred within ± 30 and ± 60 seconds was fairly consistent across the flaming and smoldering Navy tests. As Figure 24 shows, over 50 percent of all predicted alarms were within ± 60 seconds of the experimental alarm for ionization detectors responding to flaming fires in the Navy test series. The percentages presented in Figure 24 for smoldering fires from the Navy tests and for flaming fires from the Kemano tests are based on less than 10 predicted alarms for smoldering fires and are therefore inconclusive. The success of these same cases at predicting alarms within ± 30 seconds ranged from 20 to 35 percent. Interestingly, even though all experimental photoelectric detector responses to flaming fires were predicted with this threshold, Figure 24 only shows 30 percent of these predictions occurring within ± 60 seconds.
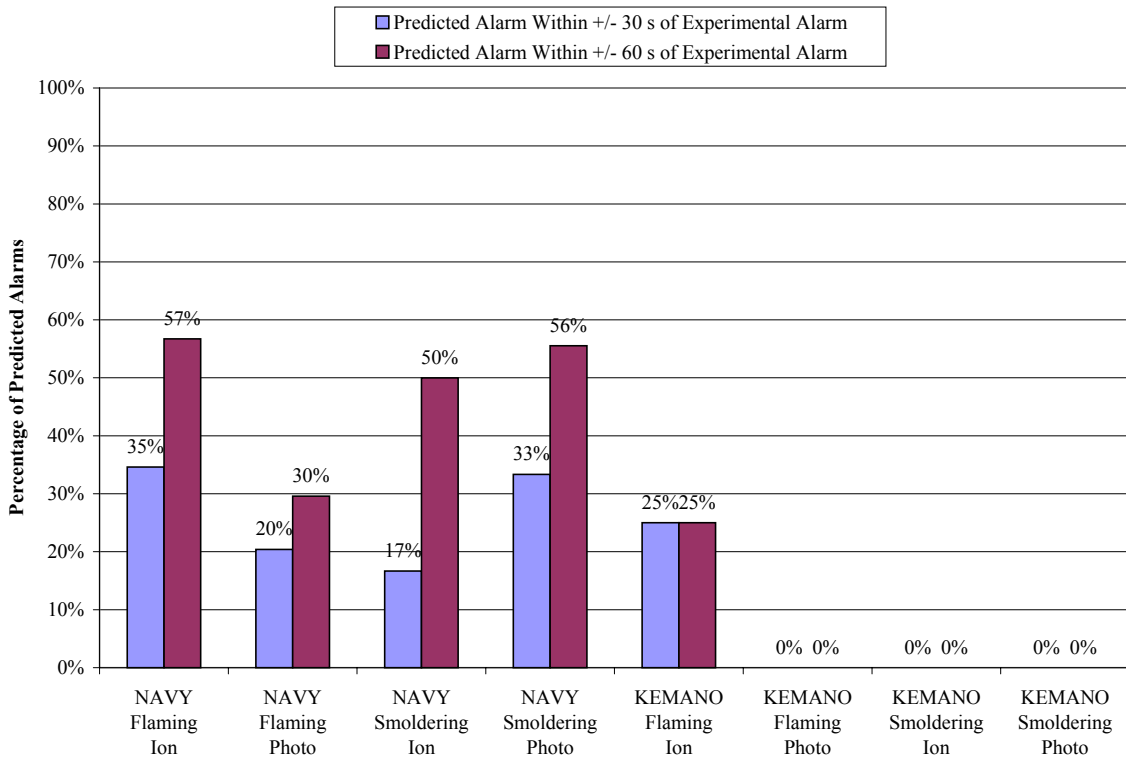
Figure 24 - Percentage of predicted alarms that occurred within ±30 and ±60 seconds of the experimental alarm with a temperature rise of 4 °C used as an alarm threshold.

As expected, the inadequacy of the 4 ºC temperature rise threshold at capturing the response of detectors to smoldering and smoldering-to-flaming transitional fires is only magnified when the 13 ºC temperature rise threshold is used. None of the smoke detector responses in the smoldering and smoldering-to-flaming transitional fires were predicted with the 13 ºC temperature rise threshold. Eighty-three percent of the experimental detector alarms were over-predicted, while only 6 percent were under-predicted, for ionization detectors responding to flaming fires in the Navy tests. In contrast, an almost one-to-one ratio of over-predicted to under-predicted alarms occurred for photoelectric detectors responding to flaming fires where 48 percent of experimental alarms were over-

predicted and 44 percent were under-predicted. Similar to the 4 ºC temperature rise

threshold, the 13 ºC temperature rise threshold predicted approximately 90 percent of

experimental ionization and photoelectric detector alarms that occurred in the flaming

fire experiments. However, in contrast, the mean and median errors in the alarm times

predicted with the 13 ºC temperature rise threshold for the flaming Navy fires are much

greater than with the 4 ºC temperature rise threshold. For example, the mean and median

errors associated with the 4 ºC temperature rise threshold alarm predictions are in the

range of 40 – 80 percent, whereas with the 13 ºC temperature rise threshold, the mean

and median error increases to approximately 200 – 400 percent over-prediction.

Table 23 - Mean and median error in predicted alarm times using a temperature rise of 13 °C as an alarm threshold.

Test Series	Fire Type	Detector Type	13 °C Temperature Rise Threshold			
			Alarms Predicted	Error in Predicted Alarm		
				Median	Mean	Std Dev
NAVY	Flaming	Ion	92	230%	390%	469%
NAVY	Flaming	Photo	90	16%	154%	375%
NAVY	Smoldering	Ion	0			
NAVY	Smoldering	Photo	0			
KEMANO	Flaming	Ion	0			
KEMANO	Flaming	Photo	0			
KEMANO	Smoldering	Ion	0			
KEMANO	Smoldering	Photo	0			

In spite of the near equality in the number of over-predicted and under-predicted alarms

for photoelectric detectors in the flaming Navy fires, the mean error in the predicted

alarm times is positive, which means that the over-prediction errors are greater in

magnitude than the under-prediction errors.

Examining the percentage of predicted alarms that occurred within ± 30 and ± 60 seconds with the 13 ºC temperature rise threshold does not shed a more positive light on this threshold. Only 4 percent of the predicted ionization alarms and 11 percent of the photoelectric alarms occurred within ± 60 seconds of the experimental alarms in the flaming Navy tests. Likewise, only 1 percent of ionization and 3 percent of photoelectric alarm predictions occurred within ± 30 seconds. Based on results presented in this section, the use of a 13 ºC temperature rise threshold is not recommended in most circumstances. For smoldering and smoldering-to-flaming transition fires there appears to be no basis for using this threshold at all. For flaming fires, the errors in the predicted alarm times were significant and almost none of the predicted alarms were within 60 seconds of the actual alarms.

Few of the fire sources examined in this study coincided with the fire sources for which material specific temperature rise thresholds are available from Heskestad and Delichatsios [1977]. The only truly similar fire source was the flaming wood crib fires from the Navy test series. The simulated upholstered furniture (polyurethane foam covered with cotton fabric) and cotton fabric fire sources used in the Kemano tests are similar to fire sources used by Heskestad and Delichatsios, but much smaller in scale and in this case these sources began as smoldering fires and only later transitioned to flaming. Regardless of this lack of complete correlation between these sources, they are examined for completeness. Other than the flaming wood fires, there are too few experimental and predicted detector alarms to draw any firm conclusions. For the flaming wood fires 70 percent of ionization alarms and 22 percent of photoelectric detectors were predicted (all

over-predictions). This result suggests that the 42 ºC temperature rise threshold

recommended for the photoelectric detector tested by Heskestad and Delichatsios may

not apply to modern photoelectric detectors. For flaming wood fires, the mean and

median errors in the predicted alarm times for both ionization and photoelectric detectors

were significantly large (on the order of 500 – 1000 percent over-predicted). Although

not shown in Table 24, none of the predicted alarm times were within ±60 seconds of the

experimental alarms.

Table 24 - Overview of results from using the material specific temperature rise thresholds from Heskestad & Delichatsios [1977] as detector alarm thresholds.

Fire Type	Source Classification	Detector Type	Experimental Alarms	Under- Predicted	Over- Predicted	Median	Mean	Std Dev
Flaming	Wood	Ion	67	0%	70%	460%	628%	544%
Flaming	Wood	Photo	60	0%	22%	949%	1299%	1267%
Flaming	Upholstered Furniture	Ion	8	0%	13%		48%	
Flaming	Upholstered Furniture	Photo	1	0%	0%			
Flaming	Cotton Fabric	Ion	3	0%	67%	172%	172%	71%
Flaming	Cotton Fabric	Photo	2	0%	0%			

5.4 Uncertainty in Alarm Predictions using Velocity Thresholds

The uncertainty in using a *critical velocity* of 0.15 m/s as an alarm threshold for the

estimation of smoke detector response is examined. To characterize the uncertainty in

the predicted alarms the percentages of alarms over- and under-predicted, the mean and

median errors, and the percentage of predicted alarms that are within ± 30 and ± 60

seconds of the experimental alarm time are all investigated. As expected, using 0.15 m/s

as an alarm threshold for smoldering fires predicted none of the 23 experimental detector

alarms that occurred. In absolute contrast, this same threshold predicted all 30

experimental detector alarms from flaming fires with 57 percent of predicted alarms

being under-predicted and 43 percent being over-predicted. The mean error in the

predicted alarm times with respect to the experimental alarm times was +40 percent with a standard deviation of 187 percent for flaming fires. Quite the opposite trend was observed for the median error in the predicted alarm times, which was –27 percent (under-prediction). The errors associated with an alarm threshold of 0.15 m/s are comparable to errors in using a 4 °C temperature rise or the 20 percent optical density alarm threshold for flaming fires, although the standard deviation in the error is larger than in most these cases. Likewise, 43 percent of alarms predicted for flaming fires using 0.15 m/s as an alarm threshold were within ±60 seconds of the experimental alarm, with 17 percent of the predicted alarms being within ±30 seconds. These percentages are approximately 50 percent less than the figures for the 4 °C temperature rise or the 20 percent optical density alarm thresholds.

CHAPTER 6: CONCLUSIONS

The goals of this project were to evaluate alarm thresholds commonly used to estimate the response of smoke detectors and then to quantify the uncertainty in alarm predictions made using these thresholds. Chapters 4 and 5 presented the results that addressed both of these goals. This chapter derives conclusions based on the results presented in the two previous sections. In addition, recommendations are provided to serve as guidance to those who would like to predict the response of smoke detectors with alarm thresholds. Finally, future work that extends and complements this project is identified.

Phase 1 provided numerous insights into the alarm thresholds examined. First of all, the values of optical density and temperature rise at the time of detector alarm do not appear to be normally distributed. However, the values of velocity magnitude at the time of detector alarm do appear to be normally distributed. Each measurement used as alarm thresholds appeared to be influenced by different variables. Optical density at alarm values were sensitive to the fire type, detector type, ventilation for smoldering fires, and the nominal sensitivity/detector design for ionization detectors during smoldering fires. In contrast, temperature rise at alarm values were only sensitive to fire type and detector type and velocity at alarm values were only affected by the fire type.

The dependence of the optical density at alarm values for ionization detectors responding to smoldering fires on the nominal sensitivity or detector design (it was unclear from this study exactly which of these is the cause) means that it is difficult to generalize the results for this case to other detector designs/nominal sensitivity values. Another

124

interesting observation derived from the Phase 1 results from the Navy tests was that the optical density at alarm for smoldering fires with no ventilation was two to three times greater than the optical density at alarm for smoldering fires with ventilation (approximately 12 air changes per hour). Comparing the results from the Navy tests from this study with the Navy test results presented by Geiman and Gottuk [2003] shows that the optical density alarm values from this study are, in general, less then the previously presented results. Reasons for this discrepancy are not initially obvious, but possible explanations include random variations between test series or differences between the white light optical density meters used by Geiman and Gottuk and the laser optical density meters used in this study.

In general, the trends in the optical density at alarm data are that alarms for ionization detectors responding to flaming fires occur at the lowest smoke optical densities and those for ionization detectors responding to smoldering fires occur at the greatest optical densities. The optical density at the time of photoelectric detector alarms for flaming and smoldering fires falls in between these two extremes, with significantly less variation among the two fire types.

Phase 1 results for the temperature rise at detector alarm are significantly lower than traditionally reported. There was no noticeable temperature rise at alarm (i.e. maximum values of 1 to 3 °C) for the smoldering or smoldering-to-flaming transition fires. In the smoldering-to-flaming transition fires, the detector alarms typically occurred either during the smoldering period or soon after the transition to flaming before significant

temperature rises could occur. These results are not unexpected for smoldering fires, however what was somewhat unexpected was that 80 percent of ionization detectors alarmed at temperature rises less than or equal to 3 ºC for flaming fires (cardboard boxes and wood cribs). Traditionally, much larger temperature rise values are associated with detector response to flaming fires. The scale of the fire sources, or the growth rate of the fire, may influence the temperature rise at alarm. This hypothesis is consistent with the results of Brammer [2002] who found that an alarm threshold of 20 ºC was most appropriate for the 600 kW and 1 MW fires examined in that study.

There were serious questions raised regarding the constancy of the optical density to temperature rise ratio upon which the temperature rise method of smoke detector response estimation is based. Values for this ratio ranged one to two orders of magnitude above the recommended value by Heskestad and Delichatsios [1977] for flaming wood crib fires. Loss of heat to the ceiling, smoke aging (reactions occurring in the smoke after leaving the fire source), or detector alarms not occurring during what Heskestad and Delichatsios refer to as the "active growth" period are all possible causes of the anomalies.

For smoldering fires, the Phase 1 results showed no consistently obvious increase in the velocity magnitude above ambient conditions attributable to the fire source at the time of detector alarms. For flaming fires, the velocity magnitude at detector alarm appeared normally distributed, with a mean value of 0.13 m/s and a standard deviation of 0.07 m/s.

These values are consistent with previously cited *critical velocity* values for flaming fires by other authors [Brozovski, 1991; Cleary, et al., 2000].

Phase 2 involved a simple, yet novel approach to further evaluating the various alarm thresholds considered in this study. Alarm responses of the detectors examined in this study were estimated using the time-dependent experimental data and the alarm thresholds identified in the literature. The uncertainty in the predicted alarm times is quantified with respect to the experimental alarm time.

A majority of predicted alarms are under-predicted for smoldering fires when the nominal sensitivity of the detector is used as an alarm threshold. For flaming fires, the nominal sensitivity of the detector results in approximately a 3:2 ratio of over-predicted to under-predicted alarms. Overall, the nominal sensitivity predicts a high percentage of detector alarms. Despite fairly large percentage errors for flaming fires, 30 to 40 percent of the predicted alarms were within ±60 seconds of the experimental alarms.

An optical density of $0.14\ m^{-1}$ predicted less than 50 percent of experimental alarms. Along with a low percentage of predicted alarms, the error in the predicted alarms was overwhelmingly in over-prediction (+1000 to +2000 percent error) for flaming fires. The results were more varied for smoldering fires, with the majority of alarms still being under-predicted for smoldering fires with the ventilation off. As anticipated from these conclusions, an alarm threshold of $0.14\ m^{-1}$ rarely predicts alarms within ±60 seconds of the experimental alarms.

A slightly different approach to using an optical density threshold is to consider a range of threshold values, in this study the 20-, 50-, and 80-percent optical density alarm thresholds based on the data of Geiman and Gottuk [2003]. The values used for the alarm threshold depended on the type of fire and type of detector whose response was being predicted, as well as which of the three threshold levels was desired. Detector responses from both the Navy and Kemano test series were evaluated with this approach. For the Navy test series, the overall percentage of alarms predicted decreased and the number of over-predicted alarms increased from the 20 percent threshold to the 80 percent threshold, as expected. Error was not minimized at the 50 percent threshold as was previously assumed, due to the generally lower optical density at alarm values (with respect to the values presented by Geiman and Gottuk [2003]) found in this study. At the 20 percent threshold, 49 and 63 percent of predicted alarms were within ±60 seconds of the experimental alarms for flaming fires being detected by photoelectric and ionization detectors respectively. These results make the 20 percent optical density alarm thresholds the most effective threshold at predicting ionization and photoelectric detector alarms reasonably close to the experimental alarms. The percentage of predicted detector responses within ±30 and ±60 seconds of the experimental alarms decreased from the 20 percent to the 80 percent optical density thresholds. Finally, approximately 40 percent of experimental alarm times were bounded between the alarm times predicted by the 20 percent and 80 percent alarm thresholds for flaming fires, with significantly less success for smoldering fires.

Attempts to predict the alarm responses from the Kemano test series proved difficult, particularly for those that occurred after the transition to flaming. Prediction of detector alarms that occurred during the smoldering period was straightforward and the results for this test series using the 20, 50 and 80 percent thresholds from Table 12 yielded comparable results to the Navy smoldering tests. However, the difficulties lied in the method used to predict detector alarms that occurred after the transition to a flaming fire. The approach taken in this study was to force the predicted alarms to occur during the same mode of combustion as was experienced by the detector in the experiments. Knowledge of the transition time from the experiments was required to successfully use this approach and the resulting alarm times were highly sensitive to this time. Most predicted alarms (regardless of threshold level) occurred almost instantaneously after the transition to flaming, due to the significant build-up of optically dense smoke in the smoldering portion of many of the tests.

Traditionally, temperature rise thresholds have been used to estimate the response of smoke detectors primarily due to the ability to model temperature measurements with reasonable accuracy. Temperature rise thresholds were still examined in Phase 2 despite evidence that questioned the validity of this approach in Phase 1. A temperature rise of 4 ºC predicted all detector responses from the Navy flaming fires and practically none of the detector responses from the Navy smoldering or Kemano smoldering-to-flaming transition fires. The uncertainty in the predicted alarms to flaming fires in terms of mean and median errors and percentages of predicted responses within ±30 and ±60 seconds

was slightly better than using the nominal sensitivity as a threshold, but not quite as good as the 20 percent optical density alarm thresholds.

A temperature rise of 13 ºC has unfortunately become the de facto standard method for engineers to predict smoke detector responses, despite a limited amount of research supporting this approach. Based on the results of Phase 2 of this study, a 13 ºC temperature rise alarm threshold is completely unacceptable to predict smoldering or smoldering-to-flaming transitional fires; none of the experimental alarms for these cases were predicted. For flaming fires, this threshold predicted approximately 90 percent of the experimental alarms (mostly over-predictions for ionization detectors) but the mean and median errors were large. In addition, less than 11 percent of predicted photoelectric alarms and 4 percent of ionization alarms were within ±60 seconds of the experimental alarms.

The use of material- and detector-specific temperature rises as alarm thresholds was the original intent of Heskestad and Delichatsios [2002]. Only the flaming wood crib fires provided a comparable fire source between this study and the original that produced a sufficient quantity of results for examination in Phase 2. The temperature rise threshold recommended for photoelectric detectors for this fire source seemed exceedingly high compared to the data in this study.

Finally, the use of a velocity magnitude of 0.15 m/s as an alarm threshold produced results with comparable uncertainty to the temperature rise threshold of 4 ºC. For

example, all of the experimental detector alarms that occurred during flaming fires were predicted with a threshold of 0.15 m/s, but none of the experimental alarms that occurred during the smoldering fires. The magnitude of the errors associated with the predicted alarm times for flaming fires was comparable to errors in using a 4 ºC temperature rise or the 20 percent optical density alarm threshold for flaming fires, however the percentage of predicted alarms within ±60 seconds was significantly less than either of these thresholds.

6.1 Recommendations

A characterization of the crude nature of the estimates of detector response from the various thresholds examined has been established. Overall, with few exceptions, the percentage of predicted alarm times within ±60 seconds of the experimental alarm time was less than 50 percent. This fact when taken in combination with the large variation in the errors of the predicted alarm times limits the usefulness of these approaches to predicting the response of smoke detectors in many applications. At best, errors of 20 to 60 percent (often in under-prediction) can be expected for smoldering fires using an optical density threshold. For flaming fires, errors on the order of 100 to 1000 percent in over-prediction are common.

The 20 percent optical density alarm threshold provided the best overall performance of the thresholds examined in this study in terms of the percentage of alarms predicted, the error associated with the predictions, and the percentage of predicted alarms reasonably close to the experimental alarms. In addition, the 20, 50 and 80 percent thresholds can be

used to provide a range of predicted alarm times, with the understanding that the 20

percent and 80 percent thresholds only provide bounding conditions in approximately 40

percent of the detectors responding to flaming fires and less than 20 percent of the

detectors responding to smoldering fires. In addition, often an alarm may not be

predicted by at least one of the threshold levels, which precludes the estimation of a range

of alarm times.

However, the 20, 50 and 80 percent optical density alarm thresholds are not necessarily

the optimum approach in all situations. For example, if primarily over-predicted detector

responses are desired for flaming fires, an optical density of 0.14 m^{-1} and a temperature

rise of 13 ºC generally provided a predicted alarm time that occurred after the

experimental alarm, often extremely so. For ionization detectors responding to flaming

fires, a temperature rise threshold of 4 ºC may prove most effective, since it predicted all

experimental alarms, had a mean error less than +100 percent, and greater than 50 percent

of the predicted alarms were within ±60 seconds. Despite the success of the temperature

rise thresholds in certain situations, caution needs to be exercised to ensure all the

assumptions inherent in this method are met. Likewise, temperature rise and velocity rise

thresholds should never be used for smoldering fires or fires that smolder initially for a

period of time.

For prediction of detector responses to smoldering fires, only the nominal sensitivity and

20, 50 and 80 percent optical density thresholds are appropriate. In either case, a

significant portion of the predicted alarms may be under-predicted with respect to the

experimental alarm time. This results from the difficulty in quantifying a practical, yet conservative upper bound for optical density in smoldering fires without significantly reducing the percentage of experimental alarms predicted. Ventilation in smoldering fires needs to be known in order to model the response of detectors properly. Prediction of detector responses in the flaming period following an initially smoldering fire is not recommended. Alarm predictions in this case are highly dependent on the time of the transition from smoldering to flaming, which is generally unknown a priori.

6.2 Future Work

During the course of this research project, as with most, numerous opportunities for future research present themselves. This section contains many of these possible topics along with brief explanations for the benefit future researchers to advance the state-of-the-art in the prediction of smoke detector response.

- Analyze false positive alarm responses predicted with these alarm thresholds – Prediction of an alarm response, when none occurred experimentally is highly undesirable. Alarms in this study were predicted only for those smoke detectors that alarmed during experiments. It would be instructive to perform a similar analysis for detectors that did not alarm and quantify the propensity of the thresholds to yield false positive responses; this may provide further guidance on the most appropriate modeling approach in a given scenario.

- Examine differences between optical density thresholds based on laser and white light optical density meters.

- Characterize smoke entry characteristics for various detectors. Refining the currently available models provides a means to reduce the error in the estimated alarm times from optical density thresholds.

- Investigate smoke detector alarms to larger fire sources. Lower values of optical density and temperature rise at alarm were reported in this study than have been previously reported. The small, challenging fire sources used in this study are a possible cause of this result.

- Address the impracticalities in the first-principles methods of detector response prediction that prevent their widespread use. Using threshold measurements does not provide satisfactory prediction of alarm responses in many cases and the first-principles methods offer the opportunity to address this problem, but additional research is required to make these methods useful.

  o Quantify uncertainty in predicted alarm responses using Newton's ionization chamber model.

  o Verify Meacham's model of photoelectric detector response experimentally and through modeling.

  o Conducted additional research on the optical properties of smoke (as required by Meacham's photoelectric smoke detector model).

APPENDIX A: PHASE 1 DATA – VALUES AT ALARM

Appendix A includes data used in Phase 1 of this report. The optical density, temperature rise, and velocity magnitude at the time of alarm are presented along with supplementary test information. Additional details on the tests and detectors used in this study were presented in Chapter 3.

Test Series	Test ID	Detector ID	Fire Type	Fire Source Description	Alarm Time (s)	Optical Density (m^{-1})	Temp. Rise (°C)	Velocity (m/s)	Ventilation Status
NAVY	1-37	5	Flaming	12 kW wood crib	45	0.006	0		Off
NAVY	1-37	3	Flaming	12 kW wood crib	177	0.008	9		Off
NAVY	1-37	1	Flaming	12 kW wood crib	61	0.009	2		Off
NAVY	1-37	7	Flaming	12 kW wood crib	174	0.004	4		Off
NAVY	1-37	6	Flaming	12 kW wood crib	816	0.021	11		Off
NAVY	1-37	2	Flaming	12 kW wood crib	901	0.028	14		Off
NAVY	1-37	8	Flaming	12 kW wood crib	990	0.032	11		Off
NAVY	1-37	4	Flaming	12 kW wood crib	1007	0.035	15		Off
NAVY	1-38	7	Flaming	12 kW wood crib	182	0.002	4		Off
NAVY	1-38	3	Flaming	12 kW wood crib	155	0.010	4	0.14	Off
NAVY	1-38	5	Flaming	12 kW wood crib	65	0.004	1		Off
NAVY	1-38	1	Flaming	12 kW wood crib	62	0.013	2	0.12	Off
NAVY	1-38	6	Flaming	12 kW wood crib	794	0.019	8		Off
NAVY	1-38	8	Flaming	12 kW wood crib	943	0.025	10		Off
NAVY	1-38	4	Flaming	12 kW wood crib	860	0.029	11	0.11	Off
NAVY	1-38	2	Flaming	12 kW wood crib	874	0.030	8	0.08	Off
NAVY	1-39	1	Flaming	50 kW wood crib	69	0.019	0	0.07	Off
NAVY	1-39	3	Flaming	50 kW wood crib	43	0.031	1	0.06	Off
NAVY	1-39	7	Flaming	50 kW wood crib	134	0.014	3		Off
NAVY	1-39	6	Flaming	50 kW wood crib	366	0.017	16		Off
NAVY	1-39	5	Flaming	50 kW wood crib	39	0.020	1		Off
NAVY	1-39	2	Flaming	50 kW wood crib	546	0.028	29		Off
NAVY	1-39	4	Flaming	50 kW wood crib	555	0.029	30	0.16	Off
NAVY	1-39	8	Flaming	50 kW wood crib	634	0.031	29		Off
NAVY	1-40	5	Flaming	50 kW wood crib	39	0.009	0		On
NAVY	1-40	7	Flaming	50 kW wood crib	57	0.007	1		On
NAVY	1-40	3	Flaming	50 kW wood crib	123	0.004	4	0.20	On
NAVY	1-40	1	Flaming	50 kW wood crib	43	0.012	3	0.18	On
NAVY	1-40	4	Flaming	50 kW wood crib	886	0.047	35		On
NAVY	1-40	2	Flaming	50 kW wood crib	1036	0.063	37		On
NAVY	1-40	6	Flaming	50 kW wood crib	956	0.066	38		On
NAVY	1-40	8	Flaming	50 kW wood crib	1023	0.075	38		On
NAVY	1-41	7	Flaming	50 kW wood crib	124	0.004	3		Off
NAVY	1-41	3	Flaming	50 kW wood crib	152	0.003	5		Off

Test Series	Test ID	Detector ID	Fire Type	Fire Source Description	Alarm Time (s)	Values at Alarm			Ventilation Status
						Optical Density (m^{-1})	Temp. Rise (°C)	Velocity (m/s)	
NAVY	1-41	1	Flaming	50 kW wood crib	69	0.004	1		Off
NAVY	1-41	5	Flaming	50 kW wood crib	46	0.011	1		Off
NAVY	1-41	6	Flaming	50 kW wood crib	484	0.014	16		Off
NAVY	1-41	4	Flaming	50 kW wood crib	494	0.015	24		Off
NAVY	1-41	2	Flaming	50 kW wood crib	529	0.017	24		Off
NAVY	1-41	8	Flaming	50 kW wood crib	553	0.020	17		Off
NAVY	1-50	19	Flaming	12 kW wood crib	128	0.001	3		Off
NAVY	1-50	21	Flaming	12 kW wood crib	112	0.003	2		Off
NAVY	1-50	23	Flaming	12 kW wood crib	161	0.003	2		Off
NAVY	1-50	17	Flaming	12 kW wood crib	75	0.004	2		Off
NAVY	1-50	13	Flaming	12 kW wood crib	48	0.006	2		Off
NAVY	1-50	15	Flaming	12 kW wood crib	65	0.006	3		Off
NAVY	1-50	9	Flaming	12 kW wood crib	24		3		Off
NAVY	1-50	11	Flaming	12 kW wood crib	25		3		Off
NAVY	1-50	12	Flaming	12 kW wood crib	1113		12		Off
NAVY	1-50	20	Flaming	12 kW wood crib	1194	0.047	3		Off
NAVY	1-50	24	Flaming	12 kW wood crib	1149	0.073	5		Off
NAVY	1-50	16	Flaming	12 kW wood crib	1149	0.083	3		Off
NAVY	1-51	9	Flaming	50 kW wood crib	22		1		Off
NAVY	1-51	10	Flaming	50 kW wood crib	28		1		Off
NAVY	1-51	11	Flaming	50 kW wood crib	22		1		Off
NAVY	1-51	12	Flaming	50 kW wood crib	17		0		Off
NAVY	1-51	23	Flaming	50 kW wood crib	89	0.010	1		Off
NAVY	1-51	16	Flaming	50 kW wood crib	53	0.033	0		Off
NAVY	1-51	21	Flaming	50 kW wood crib	99	0.011	1		Off
NAVY	1-51	15	Flaming	50 kW wood crib	90	0.013	1		Off
NAVY	1-51	19	Flaming	50 kW wood crib	182	0.013	5		Off
NAVY	1-51	20	Flaming	50 kW wood crib	82	0.020	3		Off
NAVY	1-51	17	Flaming	50 kW wood crib	79	0.021	1		Off
NAVY	1-51	22	Flaming	50 kW wood crib	518	0.021	13		Off
NAVY	1-51	13	Flaming	50 kW wood crib	44	0.027	3		Off
NAVY	1-51	14	Flaming	50 kW wood crib	54	0.031	2		Off
NAVY	1-51	18	Flaming	50 kW wood crib	612	0.032	23		Off
NAVY	1-52	9	Flaming	50 kW wood crib	21		2		On
NAVY	1-52	10	Flaming	50 kW wood crib	16		1		On
NAVY	1-52	11	Flaming	50 kW wood crib	25		1		On
NAVY	1-52	12	Flaming	50 kW wood crib	17		1		On
NAVY	1-52	13	Flaming	50 kW wood crib	38	0.025	0		On
NAVY	1-52	14	Flaming	50 kW wood crib	38	0.025	0		On
NAVY	1-52	16	Flaming	50 kW wood crib	35	0.040	0		On
NAVY	1-52	20	Flaming	50 kW wood crib	40	0.053	-1		On
NAVY	1-52	21	Flaming	50 kW wood crib	84	0.010	0		On
NAVY	1-52	23	Flaming	50 kW wood crib	177	0.004	-1		On
NAVY	1-52	19	Flaming	50 kW wood crib	73	0.020	3		On

136

Test Series	Test ID	Detector ID	Fire Type	Fire Source Description	Alarm Time (s)	Optical Density (m^{-1})	Temp. Rise (°C)	Velocity (m/s)	Ventilation Status
NAVY	1-52	15	Flaming	50 kW wood crib	65	0.033	1		On
NAVY	1-52	18	Flaming	50 kW wood crib	49	0.051	3		On
NAVY	1-53	13	Flaming	25 kW wood crib	42	0.007	1		Off
NAVY	1-53	15	Flaming	25 kW wood crib	101	0.008	2		Off
NAVY	1-53	10	Flaming	25 kW wood crib	790		20		Off
NAVY	1-53	11	Flaming	25 kW wood crib	16		1		Off
NAVY	1-53	12	Flaming	25 kW wood crib	908		20		Off
NAVY	1-53	17	Flaming	25 kW wood crib	123	0.007	0		Off
NAVY	1-53	19	Flaming	25 kW wood crib	126	0.007	0		Off
NAVY	1-53	21	Flaming	25 kW wood crib	95	0.006	0		Off
NAVY	1-53	23	Flaming	25 kW wood crib	164	0.002	0		Off
NAVY	1-53	14	Flaming	25 kW wood crib	662	0.017	11		Off
NAVY	1-53	22	Flaming	25 kW wood crib	680	0.017	7		Off
NAVY	1-53	20	Flaming	25 kW wood crib	689	0.019	11		Off
NAVY	1-53	16	Flaming	25 kW wood crib	768	0.021	11		Off
NAVY	1-53	18	Flaming	25 kW wood crib	841	0.023	12		Off
NAVY	1-53	24	Flaming	25 kW wood crib	906	0.025	6		Off
NAVY	1-54	9	Flaming	125 kW wood crib	27		2		Off
NAVY	1-54	10	Flaming	125 kW wood crib	51		5		Off
NAVY	1-54	16	Flaming	125 kW wood crib	45	0.130	0		Off
NAVY	1-54	20	Flaming	125 kW wood crib	49	0.064	0		Off
NAVY	1-54	19	Flaming	125 kW wood crib	116	0.021	1		Off
NAVY	1-54	18	Flaming	125 kW wood crib	96	0.039	1		Off
NAVY	1-54	17	Flaming	125 kW wood crib	75	0.071	1		Off
NAVY	1-54	15	Flaming	125 kW wood crib	66	0.078	1		Off
NAVY	1-54	13	Flaming	125 kW wood crib	50	0.147	2		Off
NAVY	1-54	14	Flaming	125 kW wood crib	51	0.147	1		Off
NAVY	1-55	10	Flaming	125 kW wood crib	40		0		On
NAVY	1-55	13	Flaming	125 kW wood crib	36	0.042	0		On
NAVY	1-55	16	Flaming	125 kW wood crib	35	0.034	-1		On
NAVY	1-55	17	Flaming	125 kW wood crib	53	0.070	0		On
NAVY	1-55	18	Flaming	125 kW wood crib	55	0.069	0		On
NAVY	1-55	19	Flaming	125 kW wood crib	43	0.091	0		On
NAVY	1-55	20	Flaming	125 kW wood crib	35	0.074	0		On
NAVY	1-55	15	Flaming	125 kW wood crib	68	0.062	3		On
NAVY	2-01	1	Smoldering	Cable Bundle	2029	0.226	2	0.05	Off
NAVY	2-01	4	Smoldering	Cable Bundle	2232	0.134	0		Off
NAVY	2-01	8	Smoldering	Cable Bundle	2232	0.148	0		Off
NAVY	2-01	5	Smoldering	Cable Bundle	2138	0.154	1		Off
NAVY	2-01	2	Smoldering	Cable Bundle	2034	0.227	0	0.05	Off
NAVY	2-02	6	Smoldering	Cable Bundle	656	0.018	0		On
NAVY	2-02	2	Smoldering	Cable Bundle	775	0.032	0	0.04	On
NAVY	2-02	4	Smoldering	Cable Bundle	2000	0.054	0	0.03	On
NAVY	2-04	2	Smoldering	Cable Bundle	1713	0.160	0		Off

137

Test Series	Test ID	Detector ID	Fire Type	Fire Source Description	Alarm Time (s)	Optical Density (m⁻¹)	Temp. Rise (°C)	Velocity (m/s)	Ventilation Status
						Values at Alarm			
NAVY	2-04	5	Smoldering	Cable Bundle	1057	0.504	-1	0.05	Off
NAVY	2-04	6	Smoldering	Cable Bundle	796	0.417	0	0.04	Off
NAVY	2-05	1	Smoldering	Cable Bundle	1695	0.047	-1		On
NAVY	2-05	2	Smoldering	Cable Bundle	559	0.021	0		On
NAVY	2-05	8	Smoldering	Cable Bundle	297	0.053	0	0.02	On
NAVY	2-05	4	Smoldering	Cable Bundle	639	0.033	0		On
NAVY	2-05	6	Smoldering	Cable Bundle	424	0.091	0	0.02	On
NAVY	2-05	5	Smoldering	Cable Bundle	643	0.330	1	0.02	On
NAVY	2-07	1	Smoldering	Cable Bundle	831	0.116	0		Off
NAVY	2-07	4	Smoldering	Cable Bundle	936	0.096	0		Off
NAVY	2-07	6	Smoldering	Cable Bundle	908	0.147	0	0.04	Off
NAVY	2-07	5	Smoldering	Cable Bundle	1365	0.240	0	0.02	Off
NAVY	2-08	1	Smoldering	Cable Bundle	1372	0.039	0		On
NAVY	2-08	2	Smoldering	Cable Bundle	728	0.017	0		On
NAVY	2-08	4	Smoldering	Cable Bundle	845	0.018	0		On
NAVY	2-08	6	Smoldering	Cable Bundle	539	0.050	0	0.03	On
NAVY	2-08	8	Smoldering	Cable Bundle	775	0.054	1	0.02	On
NAVY	2-08	5	Smoldering	Cable Bundle	1391	0.106	0	0.04	On
NAVY	2-09	5	Flaming	Cardboard Box Stack	86	0.004	2	0.22	Off
NAVY	2-09	7	Flaming	Cardboard Box Stack	100	0.007	3	0.24	Off
NAVY	2-09	4	Flaming	Cardboard Box Stack	169	0.014	3		Off
NAVY	2-09	1	Flaming	Cardboard Box Stack	162	0.013	2		Off
NAVY	2-09	3	Flaming	Cardboard Box Stack	165	0.013	2		Off
NAVY	2-09	8	Flaming	Cardboard Box Stack	124	0.020	6	0.25	Off
NAVY	2-09	6	Flaming	Cardboard Box Stack	129	0.021	6	0.25	Off
NAVY	2-09	2	Flaming	Cardboard Box Stack	480	0.028	16		Off
NAVY	2-10	7	Flaming	Cardboard Box Stack	228	0.010	12	0.21	On
NAVY	2-10	8	Flaming	Cardboard Box Stack	260	0.014	20	0.30	On
NAVY	2-10	4	Flaming	Cardboard Box Stack	281	0.015	9		On
NAVY	2-10	1	Flaming	Cardboard Box Stack	229	0.007	1		On
NAVY	2-10	5	Flaming	Cardboard Box Stack	166	0.003	0	0.22	On
NAVY	2-10	3	Flaming	Cardboard Box Stack	239	0.010	1		On
NAVY	2-10	2	Flaming	Cardboard Box Stack	643	0.054	11		On
NAVY	2-10	6	Flaming	Cardboard Box Stack	592	0.122	25	0.14	On

138

Test Series	Test ID	Detector ID	Fire Type	Fire Source Description	Alarm Time (s)	Values at Alarm			Ventilation Status
						Optical Density (m^{-1})	Temp. Rise (°C)	Velocity (m/s)	
NAVY	2-11	7	Flaming	Cardboard Box Stack	89	0.021	3		Off
NAVY	2-11	5	Flaming	Cardboard Box Stack	93	0.021	3		Off
NAVY	2-11	8	Flaming	Cardboard Box Stack	93	0.021	3		Off
NAVY	2-11	3	Flaming	Cardboard Box Stack	67	0.021	2	0.05	Off
NAVY	2-11	6	Flaming	Cardboard Box Stack	110	0.027	6		Off
NAVY	2-11	4	Flaming	Cardboard Box Stack	84	0.040	6	0.08	Off
NAVY	2-11	2	Flaming	Cardboard Box Stack	76	0.057	2	0.04	Off
NAVY	2-12	5	Flaming	Cardboard Box Stack	66	0.002	0		On
NAVY	2-12	7	Flaming	Cardboard Box Stack	63	0.002	0		On
NAVY	2-12	8	Flaming	Cardboard Box Stack	107	0.017	6		On
NAVY	2-12	6	Flaming	Cardboard Box Stack	115	0.017	7		On
NAVY	2-12	4	Flaming	Cardboard Box Stack	82	0.021	7	0.05	On
NAVY	2-12	3	Flaming	Cardboard Box Stack	57	0.000	0	0.07	On
NAVY	2-12	1	Flaming	Cardboard Box Stack	28	0.002	0	0.04	On
NAVY	2-13	5	Smoldering	Potassium Chlorate / Lactose	536	0.074	0	0.06	Off
NAVY	2-13	6	Smoldering	Potassium Chlorate / Lactose	524	0.059	-1	0.12	Off
NAVY	2-13	8	Smoldering	Potassium Chlorate / Lactose	710	0.028	0	0.09	Off
NAVY	2-13	4	Smoldering	Potassium Chlorate / Lactose	572	0.055	0		Off
NAVY	2-13	2	Smoldering	Potassium Chlorate / Lactose	578	0.062	0		Off
NAVY	2-14	4	Smoldering	Potassium Chlorate / Lactose	33	0.120	0	0.08	Off
NAVY	2-14	5	Smoldering	Potassium Chlorate / Lactose	98	0.054	0		Off
NAVY	2-14	1	Smoldering	Potassium Chlorate / Lactose	18	0.179	0	0.08	Off
NAVY	2-14	2	Smoldering	Potassium Chlorate / Lactose	20	0.183	3	0.10	Off
NAVY	2-15	2	Smoldering	Potassium Chlorate / Lactose	19	0.063	-1	0.09	On
NAVY	2-15	5	Smoldering	Potassium Chlorate / Lactose	70	0.035	0		On

Test Series	Test ID	Detector ID	Fire Type	Fire Source Description	Alarm Time (s)	Values at Alarm			Ventilation Status
						Optical Density (m^{-1})	Temp. Rise (°C)	Velocity (m/s)	
NAVY	2-15	8	Smoldering	Potassium Chlorate / Lactose	83	0.042	0		On
NAVY	2-15	4	Smoldering	Potassium Chlorate / Lactose	112	0.031	0	0.06	On
NAVY	2-15	6	Smoldering	Potassium Chlorate / Lactose	81	0.042	1		On
NAVY	2-15	1	Smoldering	Potassium Chlorate / Lactose	19	0.063	-1	0.09	On
NAVY	2-21	13	Flaming	Cardboard Box Stack	63	0.003	0	0.04	Off
NAVY	2-21	19	Flaming	Cardboard Box Stack	174	0.010	2		Off
NAVY	2-21	16	Flaming	Cardboard Box Stack	153	0.012	6	0.12	Off
NAVY	2-21	23	Flaming	Cardboard Box Stack	195	0.013	4		Off
NAVY	2-21	14	Flaming	Cardboard Box Stack	164	0.014	7	0.13	Off
NAVY	2-21	24	Flaming	Cardboard Box Stack	474	0.023	14		Off
NAVY	2-21	22	Flaming	Cardboard Box Stack	477	0.024	14		Off
NAVY	2-21	20	Flaming	Cardboard Box Stack	482	0.026	14		Off
NAVY	2-21	9	Flaming	Cardboard Box Stack	93		3		Off
NAVY	2-21	11	Flaming	Cardboard Box Stack	247		13		Off
NAVY	2-21	12	Flaming	Cardboard Box Stack	472		19		Off
NAVY	2-21	15	Flaming	Cardboard Box Stack	36	0.003	0	0.08	Off
NAVY	2-21	17	Flaming	Cardboard Box Stack	151	0.007	-2		Off
NAVY	2-21	21	Flaming	Cardboard Box Stack	143				Off
NAVY	2-21	18	Flaming	Cardboard Box Stack	498	0.028	14		Off
NAVY	2-22	13	Flaming	Cardboard Box Stack	43	0.002	1	0.09	On
NAVY	2-22	15	Flaming	Cardboard Box Stack	30	0.002	0	0.10	On
NAVY	2-22	16	Flaming	Cardboard Box Stack	414	0.024	22		On
NAVY	2-22	21	Flaming	Cardboard Box Stack	87	0.007	3		On
NAVY	2-22	14	Flaming	Cardboard Box Stack	83	0.029	4	0.11	On
NAVY	2-22	17	Flaming	Cardboard Box Stack	302	0.014	15		On
NAVY	2-22	24	Flaming	Cardboard Box Stack	443	0.022	15		On
NAVY	2-22	23	Flaming	Cardboard Box Stack	127	0.022	3		On

Test Series	Test ID	Detector ID	Fire Type	Fire Source Description	Alarm Time (s)	Values at Alarm			Ventilation Status
						Optical Density (m^{-1})	Temp. Rise (°C)	Velocity (m/s)	
NAVY	2-22	20	Flaming	Cardboard Box Stack	455	0.023	11		On
NAVY	2-22	18	Flaming	Cardboard Box Stack	479	0.024	11		On
NAVY	2-22	19	Flaming	Cardboard Box Stack	126	0.026	2		On
NAVY	2-22	22	Flaming	Cardboard Box Stack	118	0.028	3		On
NAVY	2-22	9	Flaming	Cardboard Box Stack	74		0		On
NAVY	2-22	11	Flaming	Cardboard Box Stack	129		4		On
NAVY	2-22	12	Flaming	Cardboard Box Stack	432		16		On
NAVY	2-23	17	Flaming	Cardboard Box Stack	54	0.004	1		Off
NAVY	2-23	13	Flaming	Cardboard Box Stack	119	0.005	0		Off
NAVY	2-23	16	Flaming	Cardboard Box Stack	139	0.014	1		Off
NAVY	2-23	20	Flaming	Cardboard Box Stack	310	0.015	31		Off
NAVY	2-23	18	Flaming	Cardboard Box Stack	97	0.026	1		Off
NAVY	2-23	22	Flaming	Cardboard Box Stack	173	0.027	2		Off
NAVY	2-23	21	Flaming	Cardboard Box Stack	125	0.028	1		Off
NAVY	2-23	23	Flaming	Cardboard Box Stack	144	0.031	1		Off
NAVY	2-23	24	Flaming	Cardboard Box Stack	139	0.031	1		Off
NAVY	2-23	10	Flaming	Cardboard Box Stack	89		1		Off
NAVY	2-23	11	Flaming	Cardboard Box Stack	120		0		Off
NAVY	2-23	12	Flaming	Cardboard Box Stack	349		16		Off
NAVY	2-23	14	Flaming	Cardboard Box Stack	151	0.020	0		Off
NAVY	2-23	15	Flaming	Cardboard Box Stack	143	0.014	0		Off
NAVY	2-23	19	Flaming	Cardboard Box Stack	122	0.032	1		Off
NAVY	2-24	21	Flaming	Cardboard Box Stack	58	0.003	0		On
NAVY	2-24	23	Flaming	Cardboard Box Stack	67	0.004	1		On
NAVY	2-24	17	Flaming	Cardboard Box Stack	62	0.009	1		On
NAVY	2-24	13	Flaming	Cardboard Box Stack	117	0.010	1		On
NAVY	2-24	15	Flaming	Cardboard Box Stack	142	0.016	1		On

Test Series	Test ID	Detector ID	Fire Type	Fire Source Description	Alarm Time (s)	Values at Alarm			Ventilation Status
						Optical Density (m^{-1})	Temp. Rise (°C)	Velocity (m/s)	
NAVY	2-24	14	Flaming	Cardboard Box Stack	139	0.016	1		On
NAVY	2-24	18	Flaming	Cardboard Box Stack	89	0.020	1		On
NAVY	2-24	19	Flaming	Cardboard Box Stack	100	0.022	5		On
NAVY	2-24	22	Flaming	Cardboard Box Stack	128	0.022	1		On
NAVY	2-24	24	Flaming	Cardboard Box Stack	413	0.022	14		On
NAVY	2-24	20	Flaming	Cardboard Box Stack	417	0.029	23		On
NAVY	2-24	10	Flaming	Cardboard Box Stack	95		0		On
NAVY	2-24	11	Flaming	Cardboard Box Stack	98		2		On
NAVY	2-24	12	Flaming	Cardboard Box Stack	423		15		On
NAVY	2-25	17	Smoldering	Potassium Chlorate / Lactose	126	0.003	1		Off
NAVY	2-25	21	Smoldering	Potassium Chlorate / Lactose	205	0.014	1		Off
NAVY	2-25	13	Smoldering	Potassium Chlorate / Lactose	100	0.028	0		Off
NAVY	2-25	16	Smoldering	Potassium Chlorate / Lactose	105	0.035	0		Off
NAVY	2-25	9	Smoldering	Potassium Chlorate / Lactose	146		0		Off
NAVY	2-25	12	Smoldering	Potassium Chlorate / Lactose	316		0		Off
NAVY	2-25	14	Smoldering	Potassium Chlorate / Lactose	94	0.021	-1		Off
NAVY	2-25	15	Smoldering	Potassium Chlorate / Lactose	222	0.016	0		Off
NAVY	2-25	18	Smoldering	Potassium Chlorate / Lactose	170	0.014	-2		Off
NAVY	2-25	19	Smoldering	Potassium Chlorate / Lactose	306	0.017	-1		Off
NAVY	2-25	20	Smoldering	Potassium Chlorate / Lactose	301	0.014	-1		Off
NAVY	2-25	24	Smoldering	Potassium Chlorate / Lactose	164	0.028	0		Off
NAVY	2-26	19	Smoldering	Potassium Chlorate / Lactose	234	0.022	2		On
NAVY	2-26	9	Smoldering	Potassium Chlorate / Lactose	334		0		On
NAVY	2-26	13	Smoldering	Potassium Chlorate / Lactose	64	0.041	0		On

| Test Series | Test ID | Detector ID | Fire Type | Fire Source Description | Alarm Time (s) | Values at Alarm | | | Ventilation Status |
						Optical Density (m^{-1})	Temp. Rise (°C)	Velocity (m/s)	
NAVY	2-26	14	Smoldering	Potassium Chlorate / Lactose	68	0.029	0		On
NAVY	2-26	15	Smoldering	Potassium Chlorate / Lactose	196	0.018	0		On
NAVY	2-26	16	Smoldering	Potassium Chlorate / Lactose	246	0.018	0		On
NAVY	2-26	18	Smoldering	Potassium Chlorate / Lactose	65	0.062	-2		On
NAVY	2-26	21	Smoldering	Potassium Chlorate / Lactose	145	0.070	1		On
NAVY	2-26	17	Smoldering	Potassium Chlorate / Lactose	53	0.073	1		On
NAVY	2-27	13	Smoldering	Potassium Chlorate / Lactose	257	0.010	1		Off
NAVY	2-27	24	Smoldering	Potassium Chlorate / Lactose	65	0.021	1		Off
NAVY	2-27	21	Smoldering	Potassium Chlorate / Lactose	66	0.029	1		Off
NAVY	2-27	18	Smoldering	Potassium Chlorate / Lactose	49	0.033	0		Off
NAVY	2-27	22	Smoldering	Potassium Chlorate / Lactose	67	0.033	1		Off
NAVY	2-27	23	Smoldering	Potassium Chlorate / Lactose	69	0.038	1		Off
NAVY	2-27	9	Smoldering	Potassium Chlorate / Lactose	161		1		Off
NAVY	2-27	19	Smoldering	Potassium Chlorate / Lactose	152	0.049	0		Off
NAVY	2-27	20	Smoldering	Potassium Chlorate / Lactose	68	0.066	0		Off
NAVY	2-27	17	Smoldering	Potassium Chlorate / Lactose	74	0.069	0		Off
NAVY	2-28	21	Smoldering	Potassium Chlorate / Lactose	38	0.000	1		On
NAVY	2-28	22	Smoldering	Potassium Chlorate / Lactose	34	0.000	1		On
NAVY	2-28	20	Smoldering	Potassium Chlorate / Lactose	348	0.007	0		On
NAVY	2-28	16	Smoldering	Potassium Chlorate / Lactose	331	0.008	1		On
NAVY	2-28	13	Smoldering	Potassium Chlorate / Lactose	192	0.029	1		On
NAVY	2-28	17	Smoldering	Potassium Chlorate / Lactose	122	0.032	1		On

Test Series	Test ID	Detector ID	Fire Type	Fire Source Description	Alarm Time (s)	Values at Alarm			Ventilation Status
						Optical Density (m^{-1})	Temp. Rise (°C)	Velocity (m/s)	
NAVY	2-28	18	Smoldering	Potassium Chlorate / Lactose	92	0.048	1		On
NAVY	2-28	9	Smoldering	Potassium Chlorate / Lactose	374		0		On
NAVY	2-28	19	Smoldering	Potassium Chlorate / Lactose	444	0.005	0		On
NAVY	2-28	23	Smoldering	Potassium Chlorate / Lactose	40	0.000	0		On
NAVY	2-28	24	Smoldering	Potassium Chlorate / Lactose	32	0.000	0		On
NAVY	2-34	19	Smoldering	Cable Bundle	840	0.020	2		Off
NAVY	2-34	12	Smoldering	Cable Bundle	892		1		Off
NAVY	2-34	20	Smoldering	Cable Bundle	648	0.074	1		Off
NAVY	2-34	18	Smoldering	Cable Bundle	297	0.038	-1		Off
NAVY	2-34	22	Smoldering	Cable Bundle	843	0.054	-3		Off
NAVY	2-34	24	Smoldering	Cable Bundle	732	0.054	-2		Off
NAVY	2-34	17	Smoldering	Cable Bundle	659	0.097	2		Off
NAVY	2-35	20	Smoldering	Cable Bundle	851	0.041	1		On
NAVY	2-35	21	Smoldering	Cable Bundle	1408	0.062	3		On
NAVY	2-35	18	Smoldering	Cable Bundle	423	0.008	-3		On
NAVY	2-35	17	Smoldering	Cable Bundle	922	0.092	1		On
NAVY	2-35	22	Smoldering	Cable Bundle	656	0.010	-1		On
NAVY	2-35	24	Smoldering	Cable Bundle	989	0.018	-1		On
NAVY	2-36	20	Smoldering	Cable Bundle	860	0.026	1		Off
NAVY	2-36	14	Smoldering	Cable Bundle	1611	0.038	0		Off
NAVY	2-36	17	Smoldering	Cable Bundle	1354	0.157	-2		Off
NAVY	2-36	18	Smoldering	Cable Bundle	756	0.018	-1		Off
NAVY	2-36	22	Smoldering	Cable Bundle	1356	0.039	0		Off
NAVY	2-36	24	Smoldering	Cable Bundle	915	0.011	0		Off
NAVY	2-36	19	Smoldering	Cable Bundle	1490	0.252	0		Off
NAVY	2-37	18	Smoldering	Cable Bundle	295	0.015	1		Off
NAVY	2-37	24	Smoldering	Cable Bundle	506	0.039	0		Off
NAVY	2-37	9	Smoldering	Cable Bundle	654		0		Off
NAVY	2-37	11	Smoldering	Cable Bundle	729		0		Off
NAVY	2-37	12	Smoldering	Cable Bundle	700		0		Off
NAVY	2-37	13	Smoldering	Cable Bundle	678	0.112	0		Off
NAVY	2-37	14	Smoldering	Cable Bundle	759	0.113	0		Off
NAVY	2-37	16	Smoldering	Cable Bundle	735	0.113	0		Off
NAVY	2-37	19	Smoldering	Cable Bundle	393	0.102	-1		Off
NAVY	2-37	20	Smoldering	Cable Bundle	331	0.124	-1		Off
NAVY	2-37	21	Smoldering	Cable Bundle	566	0.091	0		Off
NAVY	2-37	17	Smoldering	Cable Bundle	335	0.122	0		Off
NAVY	2-37	22	Smoldering	Cable Bundle	633	0.131	0		Off
NAVY	2-38	22	Smoldering	Cable Bundle	189	0.001	1		On

| Test Series | Test ID | Detector ID | Fire Type | Fire Source Description | Alarm Time (s) | Values at Alarm | | | Ventilation Status |
						Optical Density (m⁻¹)	Temp. Rise (°C)	Velocity (m/s)	
NAVY	2-38	24	Smoldering	Cable Bundle	418	0.004	2		On
NAVY	2-38	18	Smoldering	Cable Bundle	549	0.007	1		On
NAVY	2-38	20	Smoldering	Cable Bundle	709	0.022	0		On
NAVY	2-38	17	Smoldering	Cable Bundle	771	0.032	0		On
NAVY	2-38	13	Smoldering	Cable Bundle	767	0.033	0		On
NAVY	2-38	14	Smoldering	Cable Bundle	754	0.036	-1		On
NAVY	2-38	16	Smoldering	Cable Bundle	843	0.028	-1		On
NAVY	2-38	19	Smoldering	Cable Bundle	768	0.032	-1		On
NAVY	2-38	21	Smoldering	Cable Bundle	561	0.006	-2		On
NAVY	2-38	23	Smoldering	Cable Bundle	730	0.014	-1		On
NAVY	2-39	22	Smoldering	Cable Bundle	786	0.001	1		Off
NAVY	2-39	18	Smoldering	Cable Bundle	1362	0.013	0		Off
NAVY	2-39	16	Smoldering	Cable Bundle	856	0.361	0		Off
NAVY	2-39	24	Smoldering	Cable Bundle	689	0.001	-1		Off
NAVY	2-39	14	Smoldering	Cable Bundle	941	0.266	1		Off
NAVY	2-39	13	Smoldering	Cable Bundle	760	0.675	1		Off
NAVY	2-40	18	Smoldering	Cable Bundle	1201	0.014	1		On
NAVY	2-40	22	Smoldering	Cable Bundle	1542	0.034	0		On
NAVY	2-40	14	Smoldering	Cable Bundle	402	0.039	0		On
NAVY	2-40	15	Smoldering	Cable Bundle	983	0.108	0		On
NAVY	2-40	16	Smoldering	Cable Bundle	679	0.129	0		On
NAVY	2-40	13	Smoldering	Cable Bundle	448	0.041	0		On
NAVY	2-40	20	Smoldering	Cable Bundle	1387	0.020	0		On
KEMANO	01	6	Smoldering	5 Pine Sticks	313	0.279	0		Off
KEMANO	01	8	Smoldering	5 Pine Sticks	269	0.173	0		Off
KEMANO	01	14	Smoldering	5 Pine Sticks	422	0.266	0		Off
KEMANO	01	16	Smoldering	5 Pine Sticks	337	0.191	0		Off
KEMANO	01	26	Flaming	5 Pine Sticks	545	0.089	0		Off
KEMANO	01	28	Flaming	5 Pine Sticks	480	0.040	0		Off
KEMANO	02	6	Smoldering	5 Pine Sticks	223	0.187	0		Off
KEMANO	02	8	Smoldering	5 Pine Sticks	218	0.173	0		Off
KEMANO	02	14	Flaming	5 Pine Sticks	1359	0.093	-1		Off
KEMANO	02	16	Flaming	5 Pine Sticks	1377	0.253	1		Off
KEMANO	02	26	Flaming	5 Pine Sticks	1408	0.059	-1		Off
KEMANO	02	28	Flaming	5 Pine Sticks	1388	0.060	-1		Off
KEMANO	03	6	Flaming	Cotton Flannel	403	0.008	3		Off
KEMANO	03	8	Flaming	Cotton Flannel	122	0.002	0		Off
KEMANO	03	14	Flaming	Cotton Flannel	155	0.001	1		Off
KEMANO	03	16	Flaming	Cotton Flannel	368	0.004	3		Off
KEMANO	03	28	Flaming	Cotton Flannel	226	0.001	0		Off
KEMANO	04	6	Smoldering	20 Sheets Of Newspaper	521	0.212	0		Off
KEMANO	04	8	Smoldering	20 Sheets Of Newspaper	522	0.217	0		Off

Test Series	Test ID	Detector ID	Fire Type	Fire Source Description	Alarm Time (s)	Values at Alarm			Ventilation Status
						Optical Density (m^{-1})	Temp. Rise (°C)	Velocity (m/s)	
KEMANO	04	14	Smoldering	20 Sheets Of Newspaper	377	0.112	1		Off
KEMANO	04	16	Smoldering	20 Sheets Of Newspaper	373	0.099	0		Off
KEMANO	04	26	Flaming	20 Sheets Of Newspaper	787	0.074	0		Off
KEMANO	04	28	Smoldering	20 Sheets Of Newspaper	686	0.055	0		Off
KEMANO	05	6	Smoldering	Polyurethane Foam + Cotton Flannel	461	0.296	1		Off
KEMANO	05	8	Smoldering	Polyurethane Foam + Cotton Flannel	325	0.258	0		Off
KEMANO	05	14	Smoldering	Polyurethane Foam + Cotton Flannel	315	0.166	-1		Off
KEMANO	05	16	Smoldering	Polyurethane Foam + Cotton Flannel	356	0.270	0		Off
KEMANO	05	26	Flaming	Polyurethane Foam + Cotton Flannel	922	0.142	0		Off
KEMANO	05	28	Flaming	Polyurethane Foam + Cotton Flannel	875	0.176	0		Off
KEMANO	06	6	Flaming	5 Pine Sticks	1112	0.013	1		Off
KEMANO	06	8	Flaming	5 Pine Sticks	1111	0.019	0		Off
KEMANO	06	14	Flaming	5 Pine Sticks	389	0.056	0		Off
KEMANO	06	16	Smoldering	5 Pine Sticks	297	0.043	-1		Off
KEMANO	06	26	Flaming	5 Pine Sticks	265	0.132	0		Off
KEMANO	06	28	Flaming	5 Pine Sticks	277	0.086	0		Off
KEMANO	07	6	Flaming	5 Pine Sticks	1115	0.033	1		Off
KEMANO	07	8	Flaming	5 Pine Sticks	1107	0.075	0		Off
KEMANO	07	14	Smoldering	5 Pine Sticks	606	0.153	0		Off
KEMANO	07	16	Smoldering	5 Pine Sticks	342	0.041	-1		Off
KEMANO	07	26	Smoldering	5 Pine Sticks	374	0.226	-1		Off
KEMANO	07	28	Smoldering	5 Pine Sticks	383	0.210	-1		Off
KEMANO	08	6	Smoldering	Polyurethane Foam + Cotton Flannel	376	0.012	0		Off
KEMANO	08	8	Flaming	Polyurethane Foam + Cotton Flannel	760	0.073	0		Off
KEMANO	08	14	Flaming	Polyurethane Foam + Cotton Flannel	860	0.151	0		Off
KEMANO	08	16	Smoldering	Polyurethane Foam + Cotton Flannel	334	0.036	-1		Off
KEMANO	08	26	Smoldering	Polyurethane Foam + Cotton Flannel	254	0.146	0		Off
KEMANO	08	28	Smoldering	Polyurethane Foam + Cotton Flannel	715	0.303	1		Off

Test Series	Test ID	Detector ID	Fire Type	Fire Source Description	Alarm Time (s)	Values at Alarm			Ventilation Status
						Optical Density (m⁻¹)	Temp. Rise (°C)	Velocity (m/s)	
KEMANO	09	6	Smoldering	Chair Section Upholstered	755	0.061	0		Off
KEMANO	09	8	Smoldering	Chair Section Upholstered	924	0.079	1		Off
KEMANO	09	14	Flaming	Chair Section Upholstered	906	0.135	1		Off
KEMANO	09	16	Smoldering	Chair Section Upholstered	376	0.037	0		Off
KEMANO	09	26	Smoldering	Chair Section Upholstered	288	0.068	0		Off
KEMANO	09	28	Smoldering	Chair Section Upholstered	795	0.209	1		Off
KEMANO	10	1	Smoldering	10 Pine Sticks	681		-1		Off
KEMANO	10	3	Smoldering	10 Pine Sticks	418		-1		Off
KEMANO	10	4	Smoldering	10 Pine Sticks	1044	0.154	-1		Off
KEMANO	10	6	Smoldering	10 Pine Sticks	504	0.117	-1		Off
KEMANO	10	7	Smoldering	10 Pine Sticks	2017	0.097	0		Off
KEMANO	10	9	Smoldering	10 Pine Sticks	605	0.020	0		Off
KEMANO	10	10	Smoldering	10 Pine Sticks	2055	0.084	-1		Off
KEMANO	10	12	Smoldering	10 Pine Sticks	755	0.027	0		Off
KEMANO	10	13	Flaming	10 Pine Sticks	2851		0		Off
KEMANO	10	15	Smoldering	10 Pine Sticks	687		0		Off
KEMANO	11	1	Flaming	Polyurethane Foam + Cotton Flannel	1690		0		Off
KEMANO	11	3	Smoldering	Polyurethane Foam + Cotton Flannel	344		-1		Off
KEMANO	11	4	Flaming	Polyurethane Foam + Cotton Flannel	1723	0.111	0		Off
KEMANO	11	6	Smoldering	Polyurethane Foam + Cotton Flannel	371	0.131	-1		Off
KEMANO	11	7	Flaming	Polyurethane Foam + Cotton Flannel	1763	0.078	0		Off
KEMANO	11	9	Smoldering	Polyurethane Foam + Cotton Flannel	439	0.022	0		Off
KEMANO	11	10	Flaming	Polyurethane Foam + Cotton Flannel	1756	0.063	0		Off
KEMANO	11	12	Smoldering	Polyurethane Foam + Cotton Flannel	485	0.013	0		Off
KEMANO	11	15	Smoldering	Polyurethane Foam + Cotton Flannel	580		0		Off
KEMANO	13	1	Smoldering	20 Sheets Of Newspaper	3121		0		Off
KEMANO	13	3	Smoldering	20 Sheets Of Newspaper	420		0		Off

Test Series	Test ID	Detector ID	Fire Type	Fire Source Description	Alarm Time (s)	Values at Alarm			Ventilation Status
						Optical Density (m^{-1})	Temp. Rise (°C)	Velocity (m/s)	
KEMANO	13	4	Smoldering	20 Sheets Of Newspaper	3246	0.104	0		Off
KEMANO	13	6	Smoldering	20 Sheets Of Newspaper	479	0.074	0		Off
KEMANO	13	7	Smoldering	20 Sheets Of Newspaper	4001	0.093	0		Off
KEMANO	13	9	Smoldering	20 Sheets Of Newspaper	658	0.021	0		Off
KEMANO	13	10	Smoldering	20 Sheets Of Newspaper	4091	0.076	0		Off
KEMANO	13	12	Smoldering	20 Sheets Of Newspaper	764	0.018	0		Off
KEMANO	13	13	Flaming	20 Sheets Of Newspaper	4977		0		Off
KEMANO	13	15	Smoldering	20 Sheets Of Newspaper	725		0		Off

APPENDIX B: PHASE 2 DATA – PREDICTED ALARM TIMES

Appendix B contains the predicted alarm times for each threshold examined in Phase 2.

The predicted alarm times and the errors associated with these predictions are presented

in separate tables for each alarm threshold examined. Additional details on the tests and

detectors used in this study were presented in Chapter 3.

Optical Density Alarm Threshold: Nominal Sensitivity

Test Series	Test ID	Fire Type	Material	Detector		Alarm Times (s)		Percent Error
				ID	Type	Experiment	Predicted	
NAVY	1-37	Flaming	Wood	1	Ion	61	715	1072%
NAVY	1-37	Flaming	Wood	3	Ion	177	614	247%
NAVY	1-37	Flaming	Wood	5	Ion	45	796	1669%
NAVY	1-37	Flaming	Wood	7	Ion	174	720	314%
NAVY	1-38	Flaming	Wood	1	Ion	62	700	1029%
NAVY	1-38	Flaming	Wood	3	Ion	155	547	253%
NAVY	1-38	Flaming	Wood	5	Ion	65	851	1209%
NAVY	1-38	Flaming	Wood	7	Ion	182	793	336%
NAVY	1-39	Flaming	Wood	1	Ion	69	27	-61%
NAVY	1-39	Flaming	Wood	3	Ion	43	24	-44%
NAVY	1-39	Flaming	Wood	5	Ion	39	48	23%
NAVY	1-39	Flaming	Wood	7	Ion	134	39	-71%
NAVY	1-40	Flaming	Wood	1	Ion	43	609	1316%
NAVY	1-40	Flaming	Wood	3	Ion	123	503	309%
NAVY	1-40	Flaming	Wood	5	Ion	39	606	1454%
NAVY	1-40	Flaming	Wood	7	Ion	57	548	861%
NAVY	1-41	Flaming	Wood	1	Ion	69	592	758%
NAVY	1-41	Flaming	Wood	3	Ion	152	546	259%
NAVY	1-41	Flaming	Wood	5	Ion	46	573	1146%
NAVY	1-41	Flaming	Wood	7	Ion	124	530	327%
NAVY	1-50	Flaming	Wood	13	Ion	48	1108	2208%
NAVY	1-50	Flaming	Wood	15	Ion	65	1106	1602%
NAVY	1-50	Flaming	Wood	17	Ion	75	1097	1363%
NAVY	1-50	Flaming	Wood	19	Ion	128	1096	756%
NAVY	1-50	Flaming	Wood	21	Ion	112	1093	876%
NAVY	1-50	Flaming	Wood	23	Ion	161	1092	578%
NAVY	1-51	Flaming	Wood	13	Ion	44	43	-2%
NAVY	1-51	Flaming	Wood	15	Ion	90	42	-53%
NAVY	1-51	Flaming	Wood	17	Ion	79	59	-25%
NAVY	1-51	Flaming	Wood	19	Ion	182	50	-73%
NAVY	1-51	Flaming	Wood	21	Ion	99	33	-67%

Optical Density Alarm Threshold: Nominal Sensitivity

Test Series	Test ID	Fire Type	Material	Detector		Alarm Times (s)		Percent Error
				ID	Type	Experiment	Predicted	
NAVY	1-51	Flaming	Wood	23	Ion	89	29	-67%
NAVY	1-52	Flaming	Wood	13	Ion	38	30	-21%
NAVY	1-52	Flaming	Wood	15	Ion	65	30	-54%
NAVY	1-52	Flaming	Wood	19	Ion	73	28	-62%
NAVY	1-52	Flaming	Wood	21	Ion	84	21	-75%
NAVY	1-52	Flaming	Wood	23	Ion	177	20	-89%
NAVY	1-53	Flaming	Wood	13	Ion	42	826	1867%
NAVY	1-53	Flaming	Wood	15	Ion	101	738	631%
NAVY	1-53	Flaming	Wood	17	Ion	123	821	567%
NAVY	1-53	Flaming	Wood	19	Ion	126	733	482%
NAVY	1-53	Flaming	Wood	21	Ion	95	772	713%
NAVY	1-53	Flaming	Wood	23	Ion	164	672	310%
NAVY	1-54	Flaming	Wood	13	Ion	50	36	-28%
NAVY	1-54	Flaming	Wood	15	Ion	66	36	-45%
NAVY	1-54	Flaming	Wood	17	Ion	75	44	-41%
NAVY	1-54	Flaming	Wood	19	Ion	116	43	-63%
NAVY	1-55	Flaming	Wood	13	Ion	36	34	-6%
NAVY	1-55	Flaming	Wood	15	Ion	68	32	-53%
NAVY	1-55	Flaming	Wood	17	Ion	53	20	-62%
NAVY	1-55	Flaming	Wood	19	Ion	43	20	-53%
NAVY	2-09	Flaming	Cardboard	1	Ion	162	434	168%
NAVY	2-09	Flaming	Cardboard	3	Ion	165	416	152%
NAVY	2-09	Flaming	Cardboard	5	Ion	86	383	345%
NAVY	2-09	Flaming	Cardboard	7	Ion	100	124	24%
NAVY	2-10	Flaming	Cardboard	1	Ion	229	404	76%
NAVY	2-10	Flaming	Cardboard	3	Ion	239	390	63%
NAVY	2-10	Flaming	Cardboard	5	Ion	166	381	130%
NAVY	2-10	Flaming	Cardboard	7	Ion	228	165	-28%
NAVY	2-11	Flaming	Cardboard	3	Ion	67	66	-1%
NAVY	2-11	Flaming	Cardboard	5	Ion	93	102	10%
NAVY	2-11	Flaming	Cardboard	7	Ion	89	88	-1%
NAVY	2-12	Flaming	Cardboard	5	Ion	66	487	638%
NAVY	2-12	Flaming	Cardboard	7	Ion	63	371	489%
NAVY	2-21	Flaming	Cardboard	13	Ion	63	459	629%
NAVY	2-21	Flaming	Cardboard	15	Ion	36	428	1089%
NAVY	2-21	Flaming	Cardboard	17	Ion	151	467	209%
NAVY	2-21	Flaming	Cardboard	19	Ion	174	414	138%
NAVY	2-21	Flaming	Cardboard	21	Ion	143	468	227%
NAVY	2-21	Flaming	Cardboard	23	Ion	195	453	132%
NAVY	2-22	Flaming	Cardboard	13	Ion	43	77	79%
NAVY	2-22	Flaming	Cardboard	15	Ion	30	71	137%
NAVY	2-22	Flaming	Cardboard	17	Ion	302	122	-60%
NAVY	2-22	Flaming	Cardboard	19	Ion	126	116	-8%
NAVY	2-22	Flaming	Cardboard	21	Ion	87	107	23%
NAVY	2-22	Flaming	Cardboard	23	Ion	127	104	-18%

Optical Density Alarm Threshold: Nominal Sensitivity

Test Series	Test ID	Fire Type	Material	Detector		Alarm Times (s)		Percent Error
				ID	Type	Experiment	Predicted	
NAVY	2-23	Flaming	Cardboard	13	Ion	119	168	41%
NAVY	2-23	Flaming	Cardboard	15	Ion	143	151	6%
NAVY	2-23	Flaming	Cardboard	17	Ion	54	88	63%
NAVY	2-23	Flaming	Cardboard	19	Ion	122	87	-29%
NAVY	2-23	Flaming	Cardboard	21	Ion	125	114	-9%
NAVY	2-23	Flaming	Cardboard	23	Ion	144	110	-24%
NAVY	2-24	Flaming	Cardboard	13	Ion	117	457	291%
NAVY	2-24	Flaming	Cardboard	15	Ion	142	434	206%
NAVY	2-24	Flaming	Cardboard	17	Ion	62	102	65%
NAVY	2-24	Flaming	Cardboard	19	Ion	100	78	-22%
NAVY	2-24	Flaming	Cardboard	21	Ion	58	116	100%
NAVY	2-24	Flaming	Cardboard	23	Ion	67	102	52%
NAVY	1-37	Flaming	Wood	2	Photo	901	1200	33%
NAVY	1-37	Flaming	Wood	4	Photo	1007	995	-1%
NAVY	1-37	Flaming	Wood	6	Photo	816	1240	52%
NAVY	1-37	Flaming	Wood	8	Photo	990	1038	5%
NAVY	1-38	Flaming	Wood	2	Photo	874	1433	64%
NAVY	1-38	Flaming	Wood	4	Photo	860	1072	25%
NAVY	1-38	Flaming	Wood	6	Photo	794	1575	98%
NAVY	1-38	Flaming	Wood	8	Photo	943	1303	38%
NAVY	1-39	Flaming	Wood	2	Photo	546	769	41%
NAVY	1-39	Flaming	Wood	4	Photo	555	602	8%
NAVY	1-39	Flaming	Wood	6	Photo	366	825	125%
NAVY	1-39	Flaming	Wood	8	Photo	634	682	8%
NAVY	1-40	Flaming	Wood	2	Photo	1036	918	-11%
NAVY	1-40	Flaming	Wood	4	Photo	886	756	-15%
NAVY	1-40	Flaming	Wood	6	Photo	956	828	-13%
NAVY	1-40	Flaming	Wood	8	Photo	1023	699	-32%
NAVY	1-41	Flaming	Wood	2	Photo	529	879	66%
NAVY	1-41	Flaming	Wood	4	Photo	494	745	51%
NAVY	1-41	Flaming	Wood	6	Photo	484	871	80%
NAVY	1-41	Flaming	Wood	8	Photo	553	738	33%
NAVY	1-50	Flaming	Wood	16	Photo	1149	1139	-1%
NAVY	1-50	Flaming	Wood	20	Photo	1194	1128	-6%
NAVY	1-50	Flaming	Wood	24	Photo	1149	1094	-5%
NAVY	1-51	Flaming	Wood	14	Photo	54	804	1389%
NAVY	1-51	Flaming	Wood	16	Photo	53	662	1149%
NAVY	1-51	Flaming	Wood	18	Photo	612	778	27%
NAVY	1-51	Flaming	Wood	20	Photo	82	661	706%
NAVY	1-51	Flaming	Wood	22	Photo	518	782	51%
NAVY	1-52	Flaming	Wood	14	Photo	38	32	-16%
NAVY	1-52	Flaming	Wood	16	Photo	35	31	-11%
NAVY	1-52	Flaming	Wood	18	Photo	49	39	-20%
NAVY	1-52	Flaming	Wood	20	Photo	40	32	-20%
NAVY	1-53	Flaming	Wood	14	Photo	662	1534	132%

Optical Density Alarm Threshold: Nominal Sensitivity

Test Series	Test ID	Fire Type	Material	Detector ID	Detector Type	Alarm Times (s) Experiment	Alarm Times (s) Predicted	Percent Error
NAVY	1-53	Flaming	Wood	16	Photo	768	1208	57%
NAVY	1-53	Flaming	Wood	18	Photo	841	1530	82%
NAVY	1-53	Flaming	Wood	20	Photo	689	1198	74%
NAVY	1-53	Flaming	Wood	22	Photo	680	1460	115%
NAVY	1-53	Flaming	Wood	24	Photo	906	1115	23%
NAVY	1-54	Flaming	Wood	14	Photo	51	40	-22%
NAVY	1-54	Flaming	Wood	16	Photo	45	38	-16%
NAVY	1-54	Flaming	Wood	18	Photo	96	47	-51%
NAVY	1-54	Flaming	Wood	20	Photo	49	45	-8%
NAVY	1-55	Flaming	Wood	16	Photo	35	36	3%
NAVY	1-55	Flaming	Wood	18	Photo	55	28	-49%
NAVY	1-55	Flaming	Wood	20	Photo	35	22	-37%
NAVY	2-09	Flaming	Cardboard	2	Photo	480	640	33%
NAVY	2-09	Flaming	Cardboard	4	Photo	169	505	199%
NAVY	2-09	Flaming	Cardboard	6	Photo	129	589	357%
NAVY	2-09	Flaming	Cardboard	8	Photo	124	484	290%
NAVY	2-10	Flaming	Cardboard	2	Photo	643	470	-27%
NAVY	2-10	Flaming	Cardboard	4	Photo	281	462	64%
NAVY	2-10	Flaming	Cardboard	6	Photo	592	447	-24%
NAVY	2-10	Flaming	Cardboard	8	Photo	260	445	71%
NAVY	2-11	Flaming	Cardboard	2	Photo	76	73	-4%
NAVY	2-11	Flaming	Cardboard	4	Photo	84	71	-15%
NAVY	2-11	Flaming	Cardboard	6	Photo	110	472	329%
NAVY	2-11	Flaming	Cardboard	8	Photo	93	389	318%
NAVY	2-12	Flaming	Cardboard	6	Photo	115	DNA (0.025 @ 519 s)	
NAVY	2-12	Flaming	Cardboard	8	Photo	107	DNA (0.025 @ 519 s)	
NAVY	2-21	Flaming	Cardboard	14	Photo	164	556	239%
NAVY	2-21	Flaming	Cardboard	16	Photo	153	512	235%
NAVY	2-21	Flaming	Cardboard	18	Photo	498	765	54%
NAVY	2-21	Flaming	Cardboard	20	Photo	482	548	14%
NAVY	2-21	Flaming	Cardboard	22	Photo	477	DNA (0.049 @ 755 s)	
NAVY	2-21	Flaming	Cardboard	24	Photo	474	546	15%
NAVY	2-22	Flaming	Cardboard	14	Photo	83	DNA (0.049 @ 95 s)	
NAVY	2-22	Flaming	Cardboard	16	Photo	414	87	-79%
NAVY	2-22	Flaming	Cardboard	18	Photo	479	DNA (0.027 @ 132 s)	
NAVY	2-22	Flaming	Cardboard	20	Photo	455	DNA (0.027 @ 132 s)	
NAVY	2-22	Flaming	Cardboard	22	Photo	118	DNA (0.028 @ 117 s)	
NAVY	2-22	Flaming	Cardboard	24	Photo	443	DNA (0.028 @ 117 s)	

Optical Density Alarm Threshold: Nominal Sensitivity

Test Series	Test ID	Fire Type	Material	Detector		Alarm Times (s)		Percent Error
				ID	Type	Experiment	Predicted	
NAVY	2-23	Flaming	Cardboard	14	Photo	151	DNA (0.036 @ 684 s)	
NAVY	2-23	Flaming	Cardboard	16	Photo	139	DNA (0.036 @ 684 s)	
NAVY	2-23	Flaming	Cardboard	18	Photo	97	DNA (0.045 @ 715 s)	
NAVY	2-23	Flaming	Cardboard	20	Photo	310	516	66%
NAVY	2-23	Flaming	Cardboard	22	Photo	173	DNA (0.040 @ 727 s)	
NAVY	2-23	Flaming	Cardboard	24	Photo	139	605	335%
NAVY	2-24	Flaming	Cardboard	14	Photo	139	DNA (0.024 @ 497 s)	
NAVY	2-24	Flaming	Cardboard	18	Photo	89	DNA (0.032 @ 458 s)	
NAVY	2-24	Flaming	Cardboard	20	Photo	417	DNA (0.032 @ 458 s)	
NAVY	2-24	Flaming	Cardboard	22	Photo	128	DNA (0.028 @ 470 s)	
NAVY	2-24	Flaming	Cardboard	24	Photo	413	DNA (0.028 @ 470 s)	
NAVY	2-25	Smoldering	Potassium Chlorate / Lactose	15	Ion	222	92	-59%
NAVY	2-25	Smoldering	Potassium Chlorate / Lactose	19	Ion	306	94	-69%
NAVY	2-27	Smoldering	Potassium Chlorate / Lactose	19	Ion	152	27	-82%
NAVY	2-27	Smoldering	Potassium Chlorate / Lactose	23	Ion	69	65	-6%
NAVY	2-34	Smoldering	Electrical Cable	19	Ion	840	168	-80%
NAVY	2-36	Smoldering	Electrical Cable	19	Ion	1490	667	-55%
NAVY	2-37	Smoldering	Electrical Cable	19	Ion	393	236	-40%
NAVY	2-26	Smoldering	Potassium Chlorate / Lactose	15	Ion	196	48	-76%
NAVY	2-26	Smoldering	Potassium Chlorate / Lactose	19	Ion	234	32	-86%
NAVY	2-28	Smoldering	Potassium Chlorate / Lactose	19	Ion	444	59	-87%
NAVY	2-28	Smoldering	Potassium Chlorate / Lactose	23	Ion	40	93	133%
NAVY	2-38	Smoldering	Electrical Cable	19	Ion	768	597	-22%
NAVY	2-38	Smoldering	Electrical Cable	23	Ion	730	741	2%
NAVY	2-40	Smoldering	Electrical Cable	15	Ion	983	313	-68%
NAVY	2-01	Smoldering	Electrical Cable	1	Ion	2029	1156	-43%
NAVY	2-01	Smoldering	Electrical Cable	5	Ion	2138	663	-69%
NAVY	2-04	Smoldering	Electrical Cable	5	Ion	1057	366	-65%
NAVY	2-07	Smoldering	Electrical Cable	1	Ion	831	437	-47%
NAVY	2-07	Smoldering	Electrical Cable	5	Ion	1365	521	-62%

Optical Density Alarm Threshold: Nominal Sensitivity

Test Series	Test ID	Fire Type	Material	Detector ID	Type	Experiment	Predicted	Percent Error
NAVY	2-13	Smoldering	Potassium Chlorate / Lactose	5	Ion	536	502	-6%
NAVY	2-14	Smoldering	Potassium Chlorate / Lactose	1	Ion	18	6	-67%
NAVY	2-14	Smoldering	Potassium Chlorate / Lactose	5	Ion	98	30	-69%
NAVY	2-25	Smoldering	Potassium Chlorate / Lactose	13	Ion	100	95	-5%
NAVY	2-25	Smoldering	Potassium Chlorate / Lactose	17	Ion	126	217	72%
NAVY	2-25	Smoldering	Potassium Chlorate / Lactose	21	Ion	205	21	-90%
NAVY	2-27	Smoldering	Potassium Chlorate / Lactose	13	Ion	257	DNA (0.011 @ 99 s)	
NAVY	2-27	Smoldering	Potassium Chlorate / Lactose	17	Ion	74	28	-62%
NAVY	2-27	Smoldering	Potassium Chlorate / Lactose	21	Ion	66	66	0%
NAVY	2-34	Smoldering	Electrical Cable	17	Ion	659	168	-75%
NAVY	2-36	Smoldering	Electrical Cable	17	Ion	1354	668	-51%
NAVY	2-37	Smoldering	Electrical Cable	13	Ion	678	585	-14%
NAVY	2-37	Smoldering	Electrical Cable	17	Ion	335	236	-30%
NAVY	2-37	Smoldering	Electrical Cable	21	Ion	566	377	-33%
NAVY	2-39	Smoldering	Electrical Cable	13	Ion	760	278	-63%
NAVY	2-05	Smoldering	Electrical Cable	1	Ion	1695	579	-66%
NAVY	2-05	Smoldering	Electrical Cable	5	Ion	643	209	-67%
NAVY	2-08	Smoldering	Electrical Cable	1	Ion	1372	1027	-25%
NAVY	2-08	Smoldering	Electrical Cable	5	Ion	1391	417	-70%
NAVY	2-15	Smoldering	Potassium Chlorate / Lactose	1	Ion	19	5	-74%
NAVY	2-15	Smoldering	Potassium Chlorate / Lactose	5	Ion	70	50	-29%
NAVY	2-26	Smoldering	Potassium Chlorate / Lactose	13	Ion	64	49	-23%
NAVY	2-26	Smoldering	Potassium Chlorate / Lactose	17	Ion	53	32	-40%
NAVY	2-26	Smoldering	Potassium Chlorate / Lactose	21	Ion	145	15	-90%
NAVY	2-28	Smoldering	Potassium Chlorate / Lactose	13	Ion	192	94	-51%
NAVY	2-28	Smoldering	Potassium Chlorate / Lactose	17	Ion	122	73	-40%
NAVY	2-28	Smoldering	Potassium Chlorate / Lactose	21	Ion	38	109	187%
NAVY	2-35	Smoldering	Electrical Cable	17	Ion	922	199	-78%
NAVY	2-35	Smoldering	Electrical Cable	21	Ion	1408	1228	-13%
NAVY	2-38	Smoldering	Electrical Cable	13	Ion	767	603	-21%
NAVY	2-38	Smoldering	Electrical Cable	17	Ion	771	704	-9%
NAVY	2-38	Smoldering	Electrical Cable	21	Ion	561	746	33%

Optical Density Alarm Threshold: Nominal Sensitivity

Test Series	Test ID	Fire Type	Material	Detector		Alarm Times (s)		Percent Error
				ID	Type	Experiment	Predicted	
NAVY	2-40	Smoldering	Electrical Cable	13	Ion	448	332	-26%
NAVY	2-01	Smoldering	Electrical Cable	2	Photo	2034	1356	-33%
NAVY	2-01	Smoldering	Electrical Cable	4	Photo	2232	1247	-44%
NAVY	2-01	Smoldering	Electrical Cable	8	Photo	2232	835	-63%
NAVY	2-04	Smoldering	Electrical Cable	2	Photo	1713	640	-63%
NAVY	2-04	Smoldering	Electrical Cable	6	Photo	796	423	-47%
NAVY	2-07	Smoldering	Electrical Cable	4	Photo	936	448	-52%
NAVY	2-07	Smoldering	Electrical Cable	6	Photo	908	612	-33%
NAVY	2-13	Smoldering	Potassium Chlorate / Lactose	2	Photo	578	504	-13%
NAVY	2-13	Smoldering	Potassium Chlorate / Lactose	4	Photo	572	499	-13%
NAVY	2-13	Smoldering	Potassium Chlorate / Lactose	6	Photo	524	518	-1%
NAVY	2-13	Smoldering	Potassium Chlorate / Lactose	8	Photo	710	510	-28%
NAVY	2-14	Smoldering	Potassium Chlorate / Lactose	2	Photo	20	9	-55%
NAVY	2-14	Smoldering	Potassium Chlorate / Lactose	4	Photo	33	7	-79%
NAVY	2-25	Smoldering	Potassium Chlorate / Lactose	14	Photo	94	DNA (0.037 @ 124 s)	
NAVY	2-25	Smoldering	Potassium Chlorate / Lactose	16	Photo	105	109	4%
NAVY	2-25	Smoldering	Potassium Chlorate / Lactose	18	Photo	170	DNA (0.023 @ 217 s)	
NAVY	2-25	Smoldering	Potassium Chlorate / Lactose	20	Photo	301	DNA (0.023 @ 217 s)	
NAVY	2-25	Smoldering	Potassium Chlorate / Lactose	24	Photo	164	25	-85%
NAVY	2-27	Smoldering	Potassium Chlorate / Lactose	18	Photo	49	53	8%
NAVY	2-27	Smoldering	Potassium Chlorate / Lactose	20	Photo	68	34	-50%
NAVY	2-27	Smoldering	Potassium Chlorate / Lactose	22	Photo	67	112	67%
NAVY	2-27	Smoldering	Potassium Chlorate / Lactose	24	Photo	65	68	5%
NAVY	2-34	Smoldering	Electrical Cable	18	Photo	297	169	-43%
NAVY	2-34	Smoldering	Electrical Cable	20	Photo	648	169	-74%
NAVY	2-34	Smoldering	Electrical Cable	22	Photo	843	714	-15%
NAVY	2-34	Smoldering	Electrical Cable	24	Photo	732	710	-3%
NAVY	2-36	Smoldering	Electrical Cable	14	Photo	1611	1786	11%
NAVY	2-36	Smoldering	Electrical Cable	18	Photo	756	841	11%
NAVY	2-36	Smoldering	Electrical Cable	20	Photo	860	839	-2%
NAVY	2-36	Smoldering	Electrical Cable	22	Photo	1356	1142	-16%
NAVY	2-36	Smoldering	Electrical Cable	24	Photo	915	837	-9%
NAVY	2-37	Smoldering	Electrical Cable	14	Photo	759	651	-14%

Optical Density Alarm Threshold: Nominal Sensitivity

Test Series	Test ID	Fire Type	Material	Detector		Alarm Times (s)		Percent Error
				ID	Type	Experiment	Predicted	
NAVY	2-37	Smoldering	Electrical Cable	16	Photo	735	635	-14%
NAVY	2-37	Smoldering	Electrical Cable	18	Photo	295	240	-19%
NAVY	2-37	Smoldering	Electrical Cable	20	Photo	331	236	-29%
NAVY	2-37	Smoldering	Electrical Cable	22	Photo	633	468	-26%
NAVY	2-37	Smoldering	Electrical Cable	24	Photo	506	387	-24%
NAVY	2-39	Smoldering	Electrical Cable	14	Photo	941	278	-70%
NAVY	2-39	Smoldering	Electrical Cable	16	Photo	856	278	-68%
NAVY	2-39	Smoldering	Electrical Cable	18	Photo	1362	DNA (0.046 @ 1518 s)	
NAVY	2-39	Smoldering	Electrical Cable	22	Photo	786	1072	36%
NAVY	2-39	Smoldering	Electrical Cable	24	Photo	689	1041	51%
NAVY	2-02	Smoldering	Electrical Cable	2	Photo	775	1921	148%
NAVY	2-02	Smoldering	Electrical Cable	4	Photo	2000	781	-61%
NAVY	2-02	Smoldering	Electrical Cable	6	Photo	656	DNA (0.039 @ 618 s)	
NAVY	2-05	Smoldering	Electrical Cable	2	Photo	559	1701	204%
NAVY	2-05	Smoldering	Electrical Cable	4	Photo	639	692	8%
NAVY	2-05	Smoldering	Electrical Cable	6	Photo	424	273	-36%
NAVY	2-05	Smoldering	Electrical Cable	8	Photo	297	217	-27%
NAVY	2-08	Smoldering	Electrical Cable	2	Photo	728	1419	95%
NAVY	2-08	Smoldering	Electrical Cable	4	Photo	845	1316	56%
NAVY	2-08	Smoldering	Electrical Cable	6	Photo	539	481	-11%
NAVY	2-08	Smoldering	Electrical Cable	8	Photo	775	445	-43%
NAVY	2-15	Smoldering	Potassium Chlorate / Lactose	2	Photo	19	10	-47%
NAVY	2-15	Smoldering	Potassium Chlorate / Lactose	4	Photo	112	8	-93%
NAVY	2-15	Smoldering	Potassium Chlorate / Lactose	6	Photo	81	DNA (0.047 @ 99 s)	
NAVY	2-15	Smoldering	Potassium Chlorate / Lactose	8	Photo	83	74	-11%
NAVY	2-26	Smoldering	Potassium Chlorate / Lactose	14	Photo	68	DNA (0.044 @ 82 s)	
NAVY	2-26	Smoldering	Potassium Chlorate / Lactose	16	Photo	246	53	-78%
NAVY	2-26	Smoldering	Potassium Chlorate / Lactose	18	Photo	65	38	-42%
NAVY	2-28	Smoldering	Potassium Chlorate / Lactose	16	Photo	331	116	-65%
NAVY	2-28	Smoldering	Potassium Chlorate / Lactose	18	Photo	92	77	-16%
NAVY	2-28	Smoldering	Potassium Chlorate / Lactose	20	Photo	348	75	-78%
NAVY	2-28	Smoldering	Potassium Chlorate / Lactose	22	Photo	34	DNA (0.033 @ 160 s)	
NAVY	2-28	Smoldering	Potassium Chlorate / Lactose	24	Photo	32	DNA (0.033 @ 160 s)	

Optical Density Alarm Threshold: Nominal Sensitivity

Test Series	Test ID	Fire Type	Material	Detector ID	Type	Experiment	Predicted	Percent Error
NAVY	2-35	Smoldering	Electrical Cable	18	Photo	423	351	-17%
NAVY	2-35	Smoldering	Electrical Cable	20	Photo	851	231	-73%
NAVY	2-35	Smoldering	Electrical Cable	22	Photo	656	1323	102%
NAVY	2-35	Smoldering	Electrical Cable	24	Photo	989	1284	30%
NAVY	2-38	Smoldering	Electrical Cable	14	Photo	754	DNA (0.039 @ 745 s)	
NAVY	2-38	Smoldering	Electrical Cable	16	Photo	843	741	-12%
NAVY	2-38	Smoldering	Electrical Cable	18	Photo	549	DNA (0.048 @ 704 s)	
NAVY	2-38	Smoldering	Electrical Cable	20	Photo	709	704	-1%
NAVY	2-38	Smoldering	Electrical Cable	22	Photo	189	DNA (0.031 @ 791 s)	
NAVY	2-38	Smoldering	Electrical Cable	24	Photo	418	DNA (0.031 @ 791 s)	
NAVY	2-40	Smoldering	Electrical Cable	14	Photo	402	358	-11%
NAVY	2-40	Smoldering	Electrical Cable	16	Photo	679	356	-48%
NAVY	2-40	Smoldering	Electrical Cable	18	Photo	1201	DNA (0.037 @ 1503 s)	
NAVY	2-40	Smoldering	Electrical Cable	20	Photo	1387	1503	8%
NAVY	2-40	Smoldering	Electrical Cable	22	Photo	1542	1626	5%

Optical Density Alarm Threshold: 0.14 m^{-1}

Test Series	Test ID	Fire Type	Material	Detector ID	Detector Type	Experiment	Predicted	Percent Error
NAVY	1-37	Flaming	Wood	1	Ion	61	1555	2449%
NAVY	1-37	Flaming	Wood	3	Ion	177	1555	779%
NAVY	1-37	Flaming	Wood	5	Ion	45	1558	3362%
NAVY	1-37	Flaming	Wood	7	Ion	174	1558	795%
NAVY	1-38	Flaming	Wood	1	Ion	62	DNA (0.133 @ 1584 s)	
NAVY	1-38	Flaming	Wood	3	Ion	155	DNA (0.133 @ 1584 s)	
NAVY	1-38	Flaming	Wood	5	Ion	65	DNA (0.078 @ 1611 s)	
NAVY	1-38	Flaming	Wood	7	Ion	182	DNA (0.078 @ 1611 s)	
NAVY	1-39	Flaming	Wood	1	Ion	69	1468	2028%
NAVY	1-39	Flaming	Wood	3	Ion	43	1468	3314%
NAVY	1-39	Flaming	Wood	5	Ion	39	1509	3769%
NAVY	1-39	Flaming	Wood	7	Ion	134	1509	1026%
NAVY	1-40	Flaming	Wood	1	Ion	43	1665	3772%
NAVY	1-40	Flaming	Wood	3	Ion	123	1665	1254%
NAVY	1-40	Flaming	Wood	5	Ion	39	1675	4195%
NAVY	1-40	Flaming	Wood	7	Ion	57	1675	2839%
NAVY	1-41	Flaming	Wood	1	Ion	69	1285	1762%
NAVY	1-41	Flaming	Wood	3	Ion	152	1285	745%
NAVY	1-41	Flaming	Wood	5	Ion	46	1277	2676%
NAVY	1-41	Flaming	Wood	7	Ion	124	1277	930%
NAVY	1-50	Flaming	Wood	13	Ion	48	DNA (0.120 @ 1155 s)	
NAVY	1-50	Flaming	Wood	15	Ion	65	DNA (0.120 @ 1155 s)	
NAVY	1-50	Flaming	Wood	17	Ion	75	DNA (0.070 @ 1143 s)	
NAVY	1-50	Flaming	Wood	19	Ion	128	DNA (0.070 @ 1143 s)	
NAVY	1-50	Flaming	Wood	21	Ion	112	DNA (0.086 @ 1158 s)	
NAVY	1-50	Flaming	Wood	23	Ion	161	DNA (0.086 @ 1158 s)	
NAVY	1-51	Flaming	Wood	13	Ion	44	1717	3802%
NAVY	1-51	Flaming	Wood	15	Ion	90	1717	1808%
NAVY	1-51	Flaming	Wood	17	Ion	79	DNA (0.137 @ 1771 s)	
NAVY	1-51	Flaming	Wood	19	Ion	182	DNA (0.137 @ 1771 s)	
NAVY	1-51	Flaming	Wood	21	Ion	99	1720	1637%
NAVY	1-51	Flaming	Wood	23	Ion	89	1720	1833%
NAVY	1-52	Flaming	Wood	13	Ion	38	DNA (0.054 @ 32 s)	

Optical Density Alarm Threshold: 0.14 m⁻¹

Test Series	Test ID	Fire Type	Material	Detector ID	Detector Type	Alarm Times (s) Experiment	Alarm Times (s) Predicted	Percent Error
NAVY	1-52	Flaming	Wood	15	Ion	65	DNA (0.054 @ 32 s)	
NAVY	1-52	Flaming	Wood	19	Ion	73	DNA (0.062 @ 1469 s)	
NAVY	1-52	Flaming	Wood	21	Ion	84	DNA (0.085 @ 31 s)	
NAVY	1-52	Flaming	Wood	23	Ion	177	DNA (0.085 @ 31 s)	
NAVY	1-53	Flaming	Wood	13	Ion	42	DNA (0.111 @ 2218 s)	
NAVY	1-53	Flaming	Wood	15	Ion	101	DNA (0.111 @ 2218 s)	
NAVY	1-53	Flaming	Wood	17	Ion	123	DNA (0.112 @ 2216 s)	
NAVY	1-53	Flaming	Wood	19	Ion	126	DNA (0.112 @ 2216 s)	
NAVY	1-53	Flaming	Wood	21	Ion	95	DNA (0.122 @ 2204 s)	
NAVY	1-53	Flaming	Wood	23	Ion	164	DNA (0.122 @ 2204 s)	
NAVY	1-54	Flaming	Wood	13	Ion	50	46	-8%
NAVY	1-54	Flaming	Wood	15	Ion	66	46	-30%
NAVY	1-54	Flaming	Wood	17	Ion	75	1437	1816%
NAVY	1-54	Flaming	Wood	19	Ion	116	1437	1139%
NAVY	1-55	Flaming	Wood	13	Ion	36	1329	3592%
NAVY	1-55	Flaming	Wood	15	Ion	68	1329	1854%
NAVY	1-55	Flaming	Wood	17	Ion	53	1319	2389%
NAVY	1-55	Flaming	Wood	19	Ion	43	1319	2967%
NAVY	2-09	Flaming	Cardboard	1	Ion	162	DNA (0.052 @ 647 s)	
NAVY	2-09	Flaming	Cardboard	3	Ion	165	DNA (0.052 @ 647 s)	
NAVY	2-09	Flaming	Cardboard	5	Ion	86	DNA (0.078 @ 680 s)	
NAVY	2-09	Flaming	Cardboard	7	Ion	100	DNA (0.078 @ 680 s)	
NAVY	2-10	Flaming	Cardboard	1	Ion	229	DNA (0.075 @ 483 s)	
NAVY	2-10	Flaming	Cardboard	3	Ion	239	DNA (0.075 @ 483 s)	
NAVY	2-10	Flaming	Cardboard	5	Ion	166	DNA (0.122 @ 457 s)	
NAVY	2-10	Flaming	Cardboard	7	Ion	228	DNA (0.122 @ 457 s)	
NAVY	2-11	Flaming	Cardboard	3	Ion	67	DNA (0.086 @ 546 s)	
NAVY	2-11	Flaming	Cardboard	5	Ion	93	DNA (0.074 @ 702 s)	
NAVY	2-11	Flaming	Cardboard	7	Ion	89	DNA (0.074 @ 702 s)	

Optical Density Alarm Threshold: 0.14 m⁻¹

Test Series	Test ID	Fire Type	Material	Detector		Alarm Times (s)		Percent Error
				ID	Type	Experiment	Predicted	
NAVY	2-12	Flaming	Cardboard	5	Ion	66	DNA (0.025 @ 519 s)	
NAVY	2-12	Flaming	Cardboard	7	Ion	63	DNA (0.025 @ 519 s)	
NAVY	2-21	Flaming	Cardboard	13	Ion	63	DNA (0.055 @ 567 s)	
NAVY	2-21	Flaming	Cardboard	15	Ion	36	DNA (0.055 @ 567 s)	
NAVY	2-21	Flaming	Cardboard	17	Ion	151	DNA (0.051 @ 765 s)	
NAVY	2-21	Flaming	Cardboard	19	Ion	174	DNA (0.051 @ 765 s)	
NAVY	2-21	Flaming	Cardboard	21	Ion	143	DNA (0.049 @ 755 s)	
NAVY	2-21	Flaming	Cardboard	23	Ion	195	DNA (0.049 @ 755 s)	
NAVY	2-22	Flaming	Cardboard	13	Ion	43	DNA (0.049 @ 95 s)	
NAVY	2-22	Flaming	Cardboard	15	Ion	30	DNA (0.049 @ 95 s)	
NAVY	2-22	Flaming	Cardboard	17	Ion	302	DNA (0.027 @ 132 s)	
NAVY	2-22	Flaming	Cardboard	19	Ion	126	DNA (0.027 @ 132 s)	
NAVY	2-22	Flaming	Cardboard	21	Ion	87	DNA (0.028 @ 117 s)	
NAVY	2-22	Flaming	Cardboard	23	Ion	127	DNA (0.028 @ 117 s)	
NAVY	2-23	Flaming	Cardboard	13	Ion	119	DNA (0.036 @ 684 s)	
NAVY	2-23	Flaming	Cardboard	15	Ion	143	DNA (0.036 @ 684 s)	
NAVY	2-23	Flaming	Cardboard	17	Ion	54	DNA (0.045 @ 715 s)	
NAVY	2-23	Flaming	Cardboard	19	Ion	122	DNA (0.045 @ 715 s)	
NAVY	2-23	Flaming	Cardboard	21	Ion	125	DNA (0.040 @ 727 s)	
NAVY	2-23	Flaming	Cardboard	23	Ion	144	DNA (0.040 @ 727 s)	
NAVY	2-24	Flaming	Cardboard	13	Ion	117	DNA (0.024 @ 497 s)	
NAVY	2-24	Flaming	Cardboard	15	Ion	142	DNA (0.024 @ 497 s)	
NAVY	2-24	Flaming	Cardboard	17	Ion	62	DNA (0.032 @ 458 s)	
NAVY	2-24	Flaming	Cardboard	19	Ion	100	DNA (0.032 @ 458 s)	
NAVY	2-24	Flaming	Cardboard	21	Ion	58	DNA (0.028 @ 470 s)	

Optical Density Alarm Threshold: 0.14 m⁻¹

Test Series	Test ID	Fire Type	Material	Detector		Alarm Times (s)		Percent Error
				ID	Type	Experiment	Predicted	
NAVY	2-24	Flaming	Cardboard	23	Ion	67	DNA (0.028 @ 470 s)	
NAVY	1-37	Flaming	Wood	2	Photo	901	1555	73%
NAVY	1-37	Flaming	Wood	4	Photo	1007	1555	54%
NAVY	1-37	Flaming	Wood	6	Photo	816	1558	91%
NAVY	1-37	Flaming	Wood	8	Photo	990	1558	57%
NAVY	1-38	Flaming	Wood	2	Photo	874	DNA (0.133 @ 1584 s)	
NAVY	1-38	Flaming	Wood	4	Photo	860	DNA (0.133 @ 1584 s)	
NAVY	1-38	Flaming	Wood	6	Photo	794	DNA (0.078 @ 1611 s)	
NAVY	1-38	Flaming	Wood	8	Photo	943	DNA (0.078 @ 1611 s)	
NAVY	1-39	Flaming	Wood	2	Photo	546	1468	169%
NAVY	1-39	Flaming	Wood	4	Photo	555	1468	165%
NAVY	1-39	Flaming	Wood	6	Photo	366	1509	312%
NAVY	1-39	Flaming	Wood	8	Photo	634	1509	138%
NAVY	1-40	Flaming	Wood	2	Photo	1036	1665	61%
NAVY	1-40	Flaming	Wood	4	Photo	886	1665	88%
NAVY	1-40	Flaming	Wood	6	Photo	956	1675	75%
NAVY	1-40	Flaming	Wood	8	Photo	1023	1675	64%
NAVY	1-41	Flaming	Wood	2	Photo	529	1285	143%
NAVY	1-41	Flaming	Wood	4	Photo	494	1285	160%
NAVY	1-41	Flaming	Wood	6	Photo	484	1277	164%
NAVY	1-41	Flaming	Wood	8	Photo	553	1277	131%
NAVY	1-50	Flaming	Wood	16	Photo	1149	DNA (0.120 @ 1155 s)	
NAVY	1-50	Flaming	Wood	20	Photo	1194	DNA (0.070 @ 1143 s)	
NAVY	1-50	Flaming	Wood	24	Photo	1149	DNA (0.086 @ 1158 s)	
NAVY	1-51	Flaming	Wood	14	Photo	54	1717	3080%
NAVY	1-51	Flaming	Wood	16	Photo	53	1717	3140%
NAVY	1-51	Flaming	Wood	18	Photo	612	DNA (0.137 @ 1771 s)	
NAVY	1-51	Flaming	Wood	20	Photo	82	DNA (0.137 @ 1771 s)	
NAVY	1-51	Flaming	Wood	22	Photo	518	1720	232%
NAVY	1-52	Flaming	Wood	14	Photo	38	DNA (0.054 @ 32 s)	
NAVY	1-52	Flaming	Wood	16	Photo	35	DNA (0.054 @ 32 s)	
NAVY	1-52	Flaming	Wood	18	Photo	49	DNA (0.062 @ 1469 s)	
NAVY	1-52	Flaming	Wood	20	Photo	40	DNA (0.062 @ 1469 s)	
NAVY	1-53	Flaming	Wood	14	Photo	662	DNA (0.111 @ 2218 s)	

Optical Density Alarm Threshold: 0.14 m⁻¹

Test Series	Test ID	Fire Type	Material	Detector		Alarm Times (s)		Percent Error
				ID	Type	Experiment	Predicted	
NAVY	1-53	Flaming	Wood	16	Photo	768	DNA (0.111 @ 2218 s)	
NAVY	1-53	Flaming	Wood	18	Photo	841	DNA (0.112 @ 2216 s)	
NAVY	1-53	Flaming	Wood	20	Photo	689	DNA (0.112 @ 2216 s)	
NAVY	1-53	Flaming	Wood	22	Photo	680	DNA (0.122 @ 2204 s)	
NAVY	1-53	Flaming	Wood	24	Photo	906	DNA (0.122 @ 2204 s)	
NAVY	1-54	Flaming	Wood	14	Photo	51	46	-10%
NAVY	1-54	Flaming	Wood	16	Photo	45	46	2%
NAVY	1-54	Flaming	Wood	18	Photo	96	1437	1397%
NAVY	1-54	Flaming	Wood	20	Photo	49	1437	2833%
NAVY	1-55	Flaming	Wood	16	Photo	35	1329	3697%
NAVY	1-55	Flaming	Wood	18	Photo	55	1319	2298%
NAVY	1-55	Flaming	Wood	20	Photo	35	1319	3669%
NAVY	2-09	Flaming	Cardboard	2	Photo	480	DNA (0.052 @ 647 s)	
NAVY	2-09	Flaming	Cardboard	4	Photo	169	DNA (0.052 @ 647 s)	
NAVY	2-09	Flaming	Cardboard	6	Photo	129	DNA (0.078 @ 680 s)	
NAVY	2-09	Flaming	Cardboard	8	Photo	124	DNA (0.078 @ 680 s)	
NAVY	2-10	Flaming	Cardboard	2	Photo	643	DNA (0.075 @ 483 s)	
NAVY	2-10	Flaming	Cardboard	4	Photo	281	DNA (0.075 @ 483 s)	
NAVY	2-10	Flaming	Cardboard	6	Photo	592	DNA (0.122 @ 457 s)	
NAVY	2-10	Flaming	Cardboard	8	Photo	260	DNA (0.122 @ 457 s)	
NAVY	2-11	Flaming	Cardboard	2	Photo	76	DNA (0.086 @ 546 s)	
NAVY	2-11	Flaming	Cardboard	4	Photo	84	DNA (0.086 @ 546 s)	
NAVY	2-11	Flaming	Cardboard	6	Photo	110	DNA (0.074 @ 702 s)	
NAVY	2-11	Flaming	Cardboard	8	Photo	93	DNA (0.074 @ 702 s)	
NAVY	2-12	Flaming	Cardboard	6	Photo	115	DNA (0.025 @ 519 s)	
NAVY	2-12	Flaming	Cardboard	8	Photo	107	DNA (0.025 @ 519 s)	
NAVY	2-21	Flaming	Cardboard	14	Photo	164	DNA (0.055 @ 567 s)	
NAVY	2-21	Flaming	Cardboard	16	Photo	153	DNA (0.055 @ 567 s)	

Optical Density Alarm Threshold: 0.14 m⁻¹ — wait, use LaTeX.

Optical Density Alarm Threshold: 0.14 m^{-1}

Test Series	Test ID	Fire Type	Material	Detector ID	Detector Type	Alarm Times (s) Experiment	Alarm Times (s) Predicted	Percent Error
NAVY	2-21	Flaming	Cardboard	18	Photo	498	DNA (0.051 @ 765 s)	
NAVY	2-21	Flaming	Cardboard	20	Photo	482	DNA (0.051 @ 765 s)	
NAVY	2-21	Flaming	Cardboard	22	Photo	477	DNA (0.049 @ 755 s)	
NAVY	2-21	Flaming	Cardboard	24	Photo	474	DNA (0.049 @ 755 s)	
NAVY	2-22	Flaming	Cardboard	14	Photo	83	DNA (0.049 @ 95 s)	
NAVY	2-22	Flaming	Cardboard	16	Photo	414	DNA (0.049 @ 95 s)	
NAVY	2-22	Flaming	Cardboard	18	Photo	479	DNA (0.027 @ 132 s)	
NAVY	2-22	Flaming	Cardboard	20	Photo	455	DNA (0.027 @ 132 s)	
NAVY	2-22	Flaming	Cardboard	22	Photo	118	DNA (0.028 @ 117 s)	
NAVY	2-22	Flaming	Cardboard	24	Photo	443	DNA (0.028 @ 117 s)	
NAVY	2-23	Flaming	Cardboard	14	Photo	151	DNA (0.036 @ 684 s)	
NAVY	2-23	Flaming	Cardboard	16	Photo	139	DNA (0.036 @ 684 s)	
NAVY	2-23	Flaming	Cardboard	18	Photo	97	DNA (0.045 @ 715 s)	
NAVY	2-23	Flaming	Cardboard	20	Photo	310	DNA (0.045 @ 715 s)	
NAVY	2-23	Flaming	Cardboard	22	Photo	173	DNA (0.040 @ 727 s)	
NAVY	2-23	Flaming	Cardboard	24	Photo	139	DNA (0.040 @ 727 s)	
NAVY	2-24	Flaming	Cardboard	14	Photo	139	DNA (0.024 @ 497 s)	
NAVY	2-24	Flaming	Cardboard	18	Photo	89	DNA (0.032 @ 458 s)	
NAVY	2-24	Flaming	Cardboard	20	Photo	417	DNA (0.032 @ 458 s)	
NAVY	2-24	Flaming	Cardboard	22	Photo	128	DNA (0.028 @ 470 s)	
NAVY	2-24	Flaming	Cardboard	24	Photo	413	DNA (0.028 @ 470 s)	
NAVY	2-25	Smoldering	Potassium Chlorate / Lactose	15	Ion	222	DNA (0.037 @ 124 s)	
NAVY	2-25	Smoldering	Potassium Chlorate / Lactose	19	Ion	306	DNA (0.023 @ 217 s)	
NAVY	2-27	Smoldering	Potassium Chlorate / Lactose	19	Ion	152	DNA (0.112 @ 62 s)	
NAVY	2-27	Smoldering	Potassium Chlorate / Lactose	23	Ion	69	DNA (0.055 @ 125 s)	
NAVY	2-34	Smoldering	Electrical Cable	19	Ion	840	227	-73%

Optical Density Alarm Threshold: 0.14 m^{-1}

Test Series	Test ID	Fire Type	Material	Detector ID	Detector Type	Alarm Times (s) Experiment	Alarm Times (s) Predicted	Percent Error
NAVY	2-36	Smoldering	Electrical Cable	19	Ion	1490	1342	-10%
NAVY	2-37	Smoldering	Electrical Cable	19	Ion	393	348	-11%
NAVY	2-26	Smoldering	Potassium Chlorate / Lactose	15	Ion	196	DNA (0.044 @ 82 s)	
NAVY	2-26	Smoldering	Potassium Chlorate / Lactose	19	Ion	234	DNA (0.086 @ 51 s)	
NAVY	2-28	Smoldering	Potassium Chlorate / Lactose	19	Ion	444	DNA (0.089 @ 80 s)	
NAVY	2-28	Smoldering	Potassium Chlorate / Lactose	23	Ion	40	DNA (0.033 @ 160 s)	
NAVY	2-38	Smoldering	Electrical Cable	19	Ion	768	DNA (0.048 @ 704 s)	
NAVY	2-38	Smoldering	Electrical Cable	23	Ion	730	DNA (0.031 @ 791 s)	
NAVY	2-40	Smoldering	Electrical Cable	15	Ion	983	481	-51%
NAVY	2-01	Smoldering	Electrical Cable	1	Ion	2029	1987	-2%
NAVY	2-01	Smoldering	Electrical Cable	5	Ion	2138	2050	-4%
NAVY	2-04	Smoldering	Electrical Cable	5	Ion	1057	486	-54%
NAVY	2-07	Smoldering	Electrical Cable	1	Ion	831	1275	53%
NAVY	2-07	Smoldering	Electrical Cable	5	Ion	1365	897	-34%
NAVY	2-13	Smoldering	Potassium Chlorate / Lactose	5	Ion	536	DNA (0.077 @ 527 s)	
NAVY	2-14	Smoldering	Potassium Chlorate / Lactose	1	Ion	18	13	-28%
NAVY	2-14	Smoldering	Potassium Chlorate / Lactose	5	Ion	98	DNA (0.059 @ 53 s)	
NAVY	2-25	Smoldering	Potassium Chlorate / Lactose	13	Ion	100	DNA (0.037 @ 124 s)	
NAVY	2-25	Smoldering	Potassium Chlorate / Lactose	17	Ion	126	DNA (0.023 @ 217 s)	
NAVY	2-25	Smoldering	Potassium Chlorate / Lactose	21	Ion	205	DNA (0.091 @ 78 s)	
NAVY	2-27	Smoldering	Potassium Chlorate / Lactose	13	Ion	257	DNA (0.011 @ 99 s)	
NAVY	2-27	Smoldering	Potassium Chlorate / Lactose	17	Ion	74	DNA (0.112 @ 62 s)	
NAVY	2-27	Smoldering	Potassium Chlorate / Lactose	21	Ion	66	DNA (0.055 @ 125 s)	
NAVY	2-34	Smoldering	Electrical Cable	17	Ion	659	227	-66%
NAVY	2-36	Smoldering	Electrical Cable	17	Ion	1354	1342	-1%
NAVY	2-37	Smoldering	Electrical Cable	13	Ion	678	DNA (0.121 @ 708 s)	
NAVY	2-37	Smoldering	Electrical Cable	17	Ion	335	348	4%
NAVY	2-37	Smoldering	Electrical Cable	21	Ion	566	575	2%
NAVY	2-39	Smoldering	Electrical Cable	13	Ion	760	279	-63%
NAVY	2-05	Smoldering	Electrical Cable	1	Ion	1695	1947	15%
NAVY	2-05	Smoldering	Electrical Cable	5	Ion	643	397	-38%
NAVY	2-08	Smoldering	Electrical Cable	1	Ion	1372	DNA (0.117 @ 1616 s)	

Optical Density Alarm Threshold: 0.14 m⁻¹

Test Series	Test ID	Fire Type	Material	Detector ID	Detector Type	Alarm Times (s) Experiment	Alarm Times (s) Predicted	Percent Error
NAVY	2-08	Smoldering	Electrical Cable	5	Ion	1391	1603	15%
NAVY	2-15	Smoldering	Potassium Chlorate / Lactose	1	Ion	19	DNA (0.109 @ 57 s)	
NAVY	2-15	Smoldering	Potassium Chlorate / Lactose	5	Ion	70	DNA (0.047 @ 99 s)	
NAVY	2-26	Smoldering	Potassium Chlorate / Lactose	13	Ion	64	DNA (0.044 @ 82 s)	
NAVY	2-26	Smoldering	Potassium Chlorate / Lactose	17	Ion	53	DNA (0.086 @ 51 s)	
NAVY	2-26	Smoldering	Potassium Chlorate / Lactose	21	Ion	145	19	-87%
NAVY	2-28	Smoldering	Potassium Chlorate / Lactose	13	Ion	192	DNA (0.039 @ 134 s)	
NAVY	2-28	Smoldering	Potassium Chlorate / Lactose	17	Ion	122	DNA (0.089 @ 80 s)	
NAVY	2-28	Smoldering	Potassium Chlorate / Lactose	21	Ion	38	DNA (0.033 @ 160 s)	
NAVY	2-35	Smoldering	Electrical Cable	17	Ion	922	363	-61%
NAVY	2-35	Smoldering	Electrical Cable	21	Ion	1408	1532	9%
NAVY	2-38	Smoldering	Electrical Cable	13	Ion	767	DNA (0.039 @ 745 s)	
NAVY	2-38	Smoldering	Electrical Cable	17	Ion	771	DNA (0.048 @ 704 s)	
NAVY	2-38	Smoldering	Electrical Cable	21	Ion	561	DNA (0.031 @ 791 s)	
NAVY	2-40	Smoldering	Electrical Cable	13	Ion	448	481	7%
NAVY	2-01	Smoldering	Electrical Cable	2	Photo	2034	1987	-2%
NAVY	2-01	Smoldering	Electrical Cable	4	Photo	2232	1987	-11%
NAVY	2-01	Smoldering	Electrical Cable	8	Photo	2232	2050	-8%
NAVY	2-04	Smoldering	Electrical Cable	2	Photo	1713	1017	-41%
NAVY	2-04	Smoldering	Electrical Cable	6	Photo	796	486	-39%
NAVY	2-07	Smoldering	Electrical Cable	4	Photo	936	1275	36%
NAVY	2-07	Smoldering	Electrical Cable	6	Photo	908	897	-1%
NAVY	2-13	Smoldering	Potassium Chlorate / Lactose	2	Photo	578	DNA (0.078 @ 527 s)	
NAVY	2-13	Smoldering	Potassium Chlorate / Lactose	4	Photo	572	DNA (0.078 @ 527 s)	
NAVY	2-13	Smoldering	Potassium Chlorate / Lactose	6	Photo	524	DNA (0.077 @ 527 s)	
NAVY	2-13	Smoldering	Potassium Chlorate / Lactose	8	Photo	710	DNA (0.077 @ 527 s)	
NAVY	2-14	Smoldering	Potassium Chlorate / Lactose	2	Photo	20	13	-35%
NAVY	2-14	Smoldering	Potassium Chlorate / Lactose	4	Photo	33	13	-61%
NAVY	2-25	Smoldering	Potassium Chlorate / Lactose	14	Photo	94	DNA (0.037 @ 124 s)	
NAVY	2-25	Smoldering	Potassium Chlorate / Lactose	16	Photo	105	DNA (0.037 @ 124 s)	

Optical Density Alarm Threshold: 0.14 m^{-1}

Test Series	Test ID	Fire Type	Material	Detector		Alarm Times (s)		Percent Error
				ID	Type	Experiment	Predicted	
NAVY	2-25	Smoldering	Potassium Chlorate / Lactose	18	Photo	170	DNA (0.023 @ 217 s)	
NAVY	2-25	Smoldering	Potassium Chlorate / Lactose	20	Photo	301	DNA (0.023 @ 217 s)	
NAVY	2-25	Smoldering	Potassium Chlorate / Lactose	24	Photo	164	DNA (0.091 @ 78 s)	
NAVY	2-27	Smoldering	Potassium Chlorate / Lactose	18	Photo	49	DNA (0.112 @ 62 s)	
NAVY	2-27	Smoldering	Potassium Chlorate / Lactose	20	Photo	68	DNA (0.112 @ 62 s)	
NAVY	2-27	Smoldering	Potassium Chlorate / Lactose	22	Photo	67	DNA (0.055 @ 125 s)	
NAVY	2-27	Smoldering	Potassium Chlorate / Lactose	24	Photo	65	DNA (0.055 @ 125 s)	
NAVY	2-34	Smoldering	Electrical Cable	18	Photo	297	227	-24%
NAVY	2-34	Smoldering	Electrical Cable	20	Photo	648	227	-65%
NAVY	2-34	Smoldering	Electrical Cable	22	Photo	843	DNA (0.074 @ 720 s)	
NAVY	2-34	Smoldering	Electrical Cable	24	Photo	732	DNA (0.074 @ 720 s)	
NAVY	2-36	Smoldering	Electrical Cable	14	Photo	1611	DNA (0.091 @ 1794 s)	
NAVY	2-36	Smoldering	Electrical Cable	18	Photo	756	1342	78%
NAVY	2-36	Smoldering	Electrical Cable	20	Photo	860	1342	56%
NAVY	2-36	Smoldering	Electrical Cable	22	Photo	1356	1574	16%
NAVY	2-36	Smoldering	Electrical Cable	24	Photo	915	1574	72%
NAVY	2-37	Smoldering	Electrical Cable	14	Photo	759	DNA (0.121 @ 708 s)	
NAVY	2-37	Smoldering	Electrical Cable	16	Photo	735	DNA (0.121 @ 708 s)	
NAVY	2-37	Smoldering	Electrical Cable	18	Photo	295	348	18%
NAVY	2-37	Smoldering	Electrical Cable	20	Photo	331	348	5%
NAVY	2-37	Smoldering	Electrical Cable	22	Photo	633	575	-9%
NAVY	2-37	Smoldering	Electrical Cable	24	Photo	506	575	14%
NAVY	2-39	Smoldering	Electrical Cable	14	Photo	941	279	-70%
NAVY	2-39	Smoldering	Electrical Cable	16	Photo	856	279	-67%
NAVY	2-39	Smoldering	Electrical Cable	18	Photo	1362	DNA (0.046 @ 1518 s)	
NAVY	2-39	Smoldering	Electrical Cable	22	Photo	786	DNA (0.078 @ 1542 s)	
NAVY	2-39	Smoldering	Electrical Cable	24	Photo	689	DNA (0.078 @ 1542 s)	
NAVY	2-02	Smoldering	Electrical Cable	2	Photo	775	DNA (0.074 @ 2081 s)	
NAVY	2-02	Smoldering	Electrical Cable	4	Photo	2000	DNA (0.074 @ 2081 s)	
NAVY	2-02	Smoldering	Electrical Cable	6	Photo	656	DNA (0.039 @ 618 s)	
NAVY	2-05	Smoldering	Electrical Cable	2	Photo	559	1947	248%

Optical Density Alarm Threshold: 0.14 m⁻¹

Test Series	Test ID	Fire Type	Material	Detector ID	Detector Type	Alarm Times (s) Experiment	Alarm Times (s) Predicted	Percent Error
NAVY	2-05	Smoldering	Electrical Cable	4	Photo	639	1947	205%
NAVY	2-05	Smoldering	Electrical Cable	6	Photo	424	397	-6%
NAVY	2-05	Smoldering	Electrical Cable	8	Photo	297	397	34%
NAVY	2-08	Smoldering	Electrical Cable	2	Photo	728	DNA (0.117 @ 1616 s)	
NAVY	2-08	Smoldering	Electrical Cable	4	Photo	845	DNA (0.117 @ 1616 s)	
NAVY	2-08	Smoldering	Electrical Cable	6	Photo	539	1603	197%
NAVY	2-08	Smoldering	Electrical Cable	8	Photo	775	1603	107%
NAVY	2-15	Smoldering	Potassium Chlorate / Lactose	2	Photo	19	DNA (0.109 @ 57 s)	
NAVY	2-15	Smoldering	Potassium Chlorate / Lactose	4	Photo	112	DNA (0.109 @ 57 s)	
NAVY	2-15	Smoldering	Potassium Chlorate / Lactose	6	Photo	81	DNA (0.047 @ 99 s)	
NAVY	2-15	Smoldering	Potassium Chlorate / Lactose	8	Photo	83	DNA (0.047 @ 99 s)	
NAVY	2-26	Smoldering	Potassium Chlorate / Lactose	14	Photo	68	DNA (0.044 @ 82 s)	
NAVY	2-26	Smoldering	Potassium Chlorate / Lactose	16	Photo	246	DNA (0.044 @ 82 s)	
NAVY	2-26	Smoldering	Potassium Chlorate / Lactose	18	Photo	65	DNA (0.086 @ 51 s)	
NAVY	2-28	Smoldering	Potassium Chlorate / Lactose	16	Photo	331	DNA (0.039 @ 134 s)	
NAVY	2-28	Smoldering	Potassium Chlorate / Lactose	18	Photo	92	DNA (0.089 @ 80 s)	
NAVY	2-28	Smoldering	Potassium Chlorate / Lactose	20	Photo	348	DNA (0.089 @ 80 s)	
NAVY	2-28	Smoldering	Potassium Chlorate / Lactose	22	Photo	34	DNA (0.033 @ 160 s)	
NAVY	2-28	Smoldering	Potassium Chlorate / Lactose	24	Photo	32	DNA (0.033 @ 160 s)	
NAVY	2-35	Smoldering	Electrical Cable	18	Photo	423	363	-14%
NAVY	2-35	Smoldering	Electrical Cable	20	Photo	851	363	-57%
NAVY	2-35	Smoldering	Electrical Cable	22	Photo	656	1532	134%
NAVY	2-35	Smoldering	Electrical Cable	24	Photo	989	1532	55%
NAVY	2-38	Smoldering	Electrical Cable	14	Photo	754	DNA (0.039 @ 745 s)	
NAVY	2-38	Smoldering	Electrical Cable	16	Photo	843	DNA (0.039 @ 745 s)	
NAVY	2-38	Smoldering	Electrical Cable	18	Photo	549	DNA (0.048 @ 704 s)	
NAVY	2-38	Smoldering	Electrical Cable	20	Photo	709	DNA (0.048 @ 704 s)	
NAVY	2-38	Smoldering	Electrical Cable	22	Photo	189	DNA (0.031 @ 791 s)	
NAVY	2-38	Smoldering	Electrical Cable	24	Photo	418	DNA (0.031 @ 791 s)	
NAVY	2-40	Smoldering	Electrical Cable	14	Photo	402	481	20%

Optical Density Alarm Threshold: 0.14 m⁻¹

Test Series	Test ID	Fire Type	Material	Detector		Alarm Times (s)		Percent Error
				ID	Type	Experiment	Predicted	
NAVY	2-40	Smoldering	Electrical Cable	16	Photo	679	481	-29%
NAVY	2-40	Smoldering	Electrical Cable	18	Photo	1201	DNA (0.037 @ 1503 s)	
NAVY	2-40	Smoldering	Electrical Cable	20	Photo	1387	DNA (0.037 @ 1503 s)	
NAVY	2-40	Smoldering	Electrical Cable	22	Photo	1542	DNA (0.058 @ 1632 s)	
KEMANO	01	Flaming	Wood	28	Ion	480	468	-13%
KEMANO	02	Flaming	Wood	14	Ion	1359	1362	0%
KEMANO	02	Flaming	Wood	28	Ion	1388	1424	4%
KEMANO	03	Flaming	Cotton Fabric	8	Ion	122	DNA (0.012 @ 462 s)	
KEMANO	03	Flaming	Cotton Fabric	14	Ion	155	DNA (0.011 @ 509 s)	
KEMANO	03	Flaming	Cotton Fabric	28	Ion	226	DNA (0.006 @ 550 s)	
KEMANO	05	Flaming	Upholstered Furniture	28	Ion	875	771	-88%
KEMANO	06	Flaming	Wood	8	Ion	1111	DNA (0.042 @ 1181 s)	
KEMANO	06	Flaming	Wood	14	Ion	389	DNA (0.113 @ 705 s)	
KEMANO	06	Flaming	Wood	28	Ion	277	234	-100%
KEMANO	07	Flaming	Wood	8	Ion	1107	DNA (0.092 @ 1190 s)	
KEMANO	08	Flaming	Upholstered Furniture	8	Ion	760	DNA (0.136 @ 833 s)	
KEMANO	08	Flaming	Upholstered Furniture	14	Ion	860	726	-100%
KEMANO	09	Flaming	Upholstered Furniture	14	Ion	906	854	-100%
KEMANO	10	Flaming	Wood	13	Ion	2851	DNA (0.100 @ 2799 s)	
KEMANO	11	Flaming	Upholstered Furniture	4	Ion	1723	1719	-8%
KEMANO	11	Flaming	Upholstered Furniture	7	Ion	1763	DNA (0.084 @ 1748 s)	
KEMANO	13	Flaming	Paper	13	Ion	4977	DNA (0.082 @ 4951 s)	
KEMANO	01	Flaming	Wood	26	Photo	545	468	-49%
KEMANO	02	Flaming	Wood	16	Photo	1377	1362	-2%
KEMANO	02	Flaming	Wood	26	Photo	1408	1424	2%
KEMANO	03	Flaming	Cotton Fabric	6	Photo	403	DNA (0.012 @ 462 s)	
KEMANO	03	Flaming	Cotton Fabric	16	Photo	368	DNA (0.011 @ 509 s)	
KEMANO	04	Flaming	Paper	26	Photo	787	644	-73%
KEMANO	05	Flaming	Upholstered Furniture	26	Photo	922	771	-92%
KEMANO	06	Flaming	Wood	6	Photo	1112	DNA (0.042 @ 1181 s)	
KEMANO	06	Flaming	Wood	26	Photo	265	234	-100%
KEMANO	07	Flaming	Wood	6	Photo	1115	DNA (0.092 @ 1190 s)	

Optical Density Alarm Threshold: 0.14 m⁻¹

Test Series	Test ID	Fire Type	Material	Detector ID	Detector Type	Experiment	Predicted	Percent Error
KEMANO	01	Smoldering	Wood	8	Ion	269	211	-22%
KEMANO	01	Smoldering	Wood	14	Ion	422	269	-36%
KEMANO	02	Smoldering	Wood	8	Ion	218	186	-15%
KEMANO	04	Smoldering	Paper	8	Ion	522	318	-39%
KEMANO	04	Smoldering	Paper	14	Ion	377	376	0%
KEMANO	04	Smoldering	Paper	28	Ion	686	DNA (0.089 @ 526 s)	
KEMANO	05	Smoldering	Upholstered Furniture	8	Ion	325	239	-26%
KEMANO	05	Smoldering	Upholstered Furniture	14	Ion	315	286	-9%
KEMANO	07	Smoldering	Wood	14	Ion	606	560	-8%
KEMANO	07	Smoldering	Wood	28	Ion	383	246	-36%
KEMANO	08	Smoldering	Upholstered Furniture	28	Ion	715	206	-71%
KEMANO	09	Smoldering	Upholstered Furniture	8	Ion	924	DNA (0.107 @ 774 s)	
KEMANO	09	Smoldering	Upholstered Furniture	28	Ion	795	322	-59%
KEMANO	10	Smoldering	Wood	4	Ion	1044	622	-40%
KEMANO	10	Smoldering	Wood	7	Ion	2017	DNA (0.130 @ 2184 s)	
KEMANO	13	Smoldering	Paper	4	Ion	3246	3441	6%
KEMANO	13	Smoldering	Paper	7	Ion	4001	DNA (0.112 @ 3630 s)	
KEMANO	01	Smoldering	Wood	6	Photo	313	211	-33%
KEMANO	01	Smoldering	Wood	16	Photo	337	269	-20%
KEMANO	02	Smoldering	Wood	6	Photo	223	186	-17%
KEMANO	04	Smoldering	Paper	6	Photo	521	318	-39%
KEMANO	04	Smoldering	Paper	16	Photo	373	376	1%
KEMANO	05	Smoldering	Upholstered Furniture	6	Photo	461	239	-48%
KEMANO	05	Smoldering	Upholstered Furniture	16	Photo	356	286	-20%
KEMANO	06	Smoldering	Wood	16	Photo	297	DNA (0.006 @ 234 s)	
KEMANO	07	Smoldering	Wood	16	Photo	342	560	64%
KEMANO	07	Smoldering	Wood	26	Photo	374	246	-34%
KEMANO	08	Smoldering	Upholstered Furniture	6	Photo	376	DNA (0.105 @ 713 s)	
KEMANO	08	Smoldering	Upholstered Furniture	16	Photo	334	618	85%
KEMANO	08	Smoldering	Upholstered Furniture	26	Photo	254	206	-19%
KEMANO	09	Smoldering	Upholstered Furniture	6	Photo	755	DNA (0.107 @ 774 s)	
KEMANO	09	Smoldering	Upholstered Furniture	16	Photo	376	591	57%
KEMANO	09	Smoldering	Upholstered Furniture	26	Photo	288	322	12%
KEMANO	10	Smoldering	Wood	6	Photo	504	622	23%
KEMANO	10	Smoldering	Wood	9	Photo	605	DNA (0.130 @ 2184 s)	
KEMANO	10	Smoldering	Wood	15	Photo	687	DNA (0.099 @ 2473 s)	
KEMANO	11	Smoldering	Upholstered Furniture	6	Photo	371	385	4%
KEMANO	11	Smoldering	Upholstered Furniture	9	Photo	439	DNA (0.093 @ 1122 s)	

Optical Density Alarm Threshold: 0.14 m^{-1}

Test Series	Test ID	Fire Type	Material	Detector		Alarm Times (s)		Percent Error
				ID	Type	Experiment	Predicted	
KEMANO	11	Smoldering	Upholstered Furniture	15	Photo	580	DNA (0.068 @ 1152 s)	
KEMANO	13	Smoldering	Paper	6	Photo	479	3441	618%
KEMANO	13	Smoldering	Paper	9	Photo	658	DNA (0.112 @ 3630 s)	
KEMANO	13	Smoldering	Paper	15	Photo	725	DNA (0.087 @ 4497 s)	

Optical Density Alarm Threshold: 20% Threshold; Navy tests (see Table 12)

Test ID	Fire Type	Material	Detector		Alarm Times (s)		Percent Error
			ID	Type	Experiment	Predicted	
1-37	Flaming	Wood	1	Ion	61	25	-59%
1-37	Flaming	Wood	3	Ion	177	25	-86%
1-37	Flaming	Wood	5	Ion	45	417	827%
1-37	Flaming	Wood	7	Ion	174	417	140%
1-38	Flaming	Wood	1	Ion	62	25	-60%
1-38	Flaming	Wood	3	Ion	155	25	-84%
1-38	Flaming	Wood	5	Ion	65	481	640%
1-38	Flaming	Wood	7	Ion	182	481	164%
1-39	Flaming	Wood	1	Ion	69	12	-83%
1-39	Flaming	Wood	3	Ion	43	12	-72%
1-39	Flaming	Wood	5	Ion	39	21	-46%
1-39	Flaming	Wood	7	Ion	134	21	-84%
1-40	Flaming	Wood	1	Ion	43	28	-35%
1-40	Flaming	Wood	3	Ion	123	28	-77%
1-40	Flaming	Wood	5	Ion	39	19	-51%
1-40	Flaming	Wood	7	Ion	57	19	-67%
1-41	Flaming	Wood	1	Ion	69	33	-52%
1-41	Flaming	Wood	3	Ion	152	33	-78%
1-41	Flaming	Wood	5	Ion	46	30	-35%
1-41	Flaming	Wood	7	Ion	124	30	-76%
1-50	Flaming	Wood	13	Ion	48	708	1375%
1-50	Flaming	Wood	15	Ion	65	708	989%
1-50	Flaming	Wood	17	Ion	75	774	932%
1-50	Flaming	Wood	19	Ion	128	774	505%
1-50	Flaming	Wood	21	Ion	112	571	410%
1-50	Flaming	Wood	23	Ion	161	571	255%
1-51	Flaming	Wood	13	Ion	44	31	-30%
1-51	Flaming	Wood	15	Ion	90	31	-66%
1-51	Flaming	Wood	17	Ion	79	37	-53%
1-51	Flaming	Wood	19	Ion	182	37	-80%
1-51	Flaming	Wood	21	Ion	99	25	-75%
1-51	Flaming	Wood	23	Ion	89	25	-72%
1-52	Flaming	Wood	13	Ion	38	28	-26%
1-52	Flaming	Wood	15	Ion	65	28	-57%
1-52	Flaming	Wood	19	Ion	73	25	-66%
1-52	Flaming	Wood	21	Ion	84	17	-80%
1-52	Flaming	Wood	23	Ion	177	17	-90%
1-53	Flaming	Wood	13	Ion	42	32	-24%
1-53	Flaming	Wood	15	Ion	101	32	-68%
1-53	Flaming	Wood	17	Ion	123	48	-61%
1-53	Flaming	Wood	19	Ion	126	48	-62%

Optical Density Alarm Threshold: 20% Threshold; Navy tests (see Table 12)

Test ID	Fire Type	Material	Detector ID	Type	Experiment	Predicted	Percent Error
1-53	Flaming	Wood	21	Ion	95	23	-76%
1-53	Flaming	Wood	23	Ion	164	23	-86%
1-54	Flaming	Wood	13	Ion	50	34	-32%
1-54	Flaming	Wood	15	Ion	66	34	-48%
1-54	Flaming	Wood	17	Ion	75	40	-47%
1-54	Flaming	Wood	19	Ion	116	40	-66%
1-55	Flaming	Wood	13	Ion	36	28	-22%
1-55	Flaming	Wood	15	Ion	68	28	-59%
1-55	Flaming	Wood	17	Ion	53	17	-68%
1-55	Flaming	Wood	19	Ion	43	17	-60%
2-09	Flaming	Cardboard	1	Ion	162	152	-6%
2-09	Flaming	Cardboard	3	Ion	165	152	-8%
2-09	Flaming	Cardboard	5	Ion	86	104	21%
2-09	Flaming	Cardboard	7	Ion	100	104	4%
2-10	Flaming	Cardboard	1	Ion	229	96	-58%
2-10	Flaming	Cardboard	3	Ion	239	96	-60%
2-10	Flaming	Cardboard	5	Ion	166	68	-59%
2-10	Flaming	Cardboard	7	Ion	228	68	-70%
2-11	Flaming	Cardboard	3	Ion	67	52	-22%
2-11	Flaming	Cardboard	5	Ion	93	81	-13%
2-11	Flaming	Cardboard	7	Ion	89	81	-9%
2-12	Flaming	Cardboard	5	Ion	66	87	32%
2-12	Flaming	Cardboard	7	Ion	63	87	38%
2-21	Flaming	Cardboard	13	Ion	63	118	87%
2-21	Flaming	Cardboard	15	Ion	36	118	228%
2-21	Flaming	Cardboard	17	Ion	151	160	6%
2-21	Flaming	Cardboard	19	Ion	174	160	-8%
2-21	Flaming	Cardboard	21	Ion	143	172	20%
2-21	Flaming	Cardboard	23	Ion	195	172	-12%
2-22	Flaming	Cardboard	13	Ion	43	59	37%
2-22	Flaming	Cardboard	15	Ion	30	59	97%
2-22	Flaming	Cardboard	17	Ion	302	101	-67%
2-22	Flaming	Cardboard	19	Ion	126	101	-20%
2-22	Flaming	Cardboard	21	Ion	87	89	2%
2-22	Flaming	Cardboard	23	Ion	127	89	-30%
2-23	Flaming	Cardboard	13	Ion	119	126	6%
2-23	Flaming	Cardboard	15	Ion	143	126	-12%
2-23	Flaming	Cardboard	17	Ion	54	71	31%
2-23	Flaming	Cardboard	19	Ion	122	71	-42%
2-23	Flaming	Cardboard	21	Ion	125	93	-26%
2-23	Flaming	Cardboard	23	Ion	144	93	-35%
2-24	Flaming	Cardboard	13	Ion	117	115	-2%
2-24	Flaming	Cardboard	15	Ion	142	115	-19%

Optical Density Alarm Threshold: 20% Threshold; Navy tests (see Table 12)

Test ID	Fire Type	Material	Detector ID	Type	Alarm Times (s) Experiment	Predicted	Percent Error
2-24	Flaming	Cardboard	17	Ion	62	61	-2%
2-24	Flaming	Cardboard	19	Ion	100	61	-39%
2-24	Flaming	Cardboard	21	Ion	58	81	40%
2-24	Flaming	Cardboard	23	Ion	67	81	21%
1-37	Flaming	Wood	2	Photo	901	588	-35%
1-37	Flaming	Wood	4	Photo	1007	588	-42%
1-37	Flaming	Wood	6	Photo	816	706	-13%
1-37	Flaming	Wood	8	Photo	990	706	-29%
1-38	Flaming	Wood	2	Photo	874	535	-39%
1-38	Flaming	Wood	4	Photo	860	535	-38%
1-38	Flaming	Wood	6	Photo	794	775	-2%
1-38	Flaming	Wood	8	Photo	943	775	-18%
1-39	Flaming	Wood	2	Photo	546	24	-96%
1-39	Flaming	Wood	4	Photo	555	24	-96%
1-39	Flaming	Wood	6	Photo	366	37	-90%
1-39	Flaming	Wood	8	Photo	634	37	-94%
1-40	Flaming	Wood	2	Photo	1036	503	-51%
1-40	Flaming	Wood	4	Photo	886	503	-43%
1-40	Flaming	Wood	6	Photo	956	526	-45%
1-40	Flaming	Wood	8	Photo	1023	526	-49%
1-41	Flaming	Wood	2	Photo	529	539	2%
1-41	Flaming	Wood	4	Photo	494	539	9%
1-41	Flaming	Wood	6	Photo	484	525	8%
1-41	Flaming	Wood	8	Photo	553	525	-5%
1-50	Flaming	Wood	16	Photo	1149	1106	-4%
1-50	Flaming	Wood	20	Photo	1194	1096	-8%
1-50	Flaming	Wood	24	Photo	1149	1092	-5%
1-51	Flaming	Wood	14	Photo	54	42	-22%
1-51	Flaming	Wood	16	Photo	53	42	-21%
1-51	Flaming	Wood	18	Photo	612	50	-92%
1-51	Flaming	Wood	20	Photo	82	50	-39%
1-51	Flaming	Wood	22	Photo	518	29	-94%
1-52	Flaming	Wood	14	Photo	38	30	-21%
1-52	Flaming	Wood	16	Photo	35	30	-14%
1-52	Flaming	Wood	18	Photo	49	28	-43%
1-52	Flaming	Wood	20	Photo	40	28	-30%
1-53	Flaming	Wood	14	Photo	662	692	5%
1-53	Flaming	Wood	16	Photo	768	692	-10%
1-53	Flaming	Wood	18	Photo	841	683	-19%
1-53	Flaming	Wood	20	Photo	689	683	-1%
1-53	Flaming	Wood	22	Photo	680	672	-1%
1-53	Flaming	Wood	24	Photo	906	672	-26%
1-54	Flaming	Wood	14	Photo	51	36	-29%

Optical Density Alarm Threshold: 20% Threshold; Navy tests (see Table 12)

Test ID	Fire Type	Material	Detector		Alarm Times (s)		Percent Error
			ID	Type	Experiment	Predicted	
1-54	Flaming	Wood	16	Photo	45	36	-20%
1-54	Flaming	Wood	18	Photo	96	42	-56%
1-54	Flaming	Wood	20	Photo	49	42	-14%
1-55	Flaming	Wood	16	Photo	35	32	-9%
1-55	Flaming	Wood	18	Photo	55	20	-64%
1-55	Flaming	Wood	20	Photo	35	20	-43%
2-09	Flaming	Cardboard	2	Photo	480	406	-15%
2-09	Flaming	Cardboard	4	Photo	169	406	140%
2-09	Flaming	Cardboard	6	Photo	129	122	-5%
2-09	Flaming	Cardboard	8	Photo	124	122	-2%
2-10	Flaming	Cardboard	2	Photo	643	388	-40%
2-10	Flaming	Cardboard	4	Photo	281	388	38%
2-10	Flaming	Cardboard	6	Photo	592	165	-72%
2-10	Flaming	Cardboard	8	Photo	260	165	-37%
2-11	Flaming	Cardboard	2	Photo	76	66	-13%
2-11	Flaming	Cardboard	4	Photo	84	66	-21%
2-11	Flaming	Cardboard	6	Photo	110	87	-21%
2-11	Flaming	Cardboard	8	Photo	93	87	-6%
2-12	Flaming	Cardboard	6	Photo	115	353	207%
2-12	Flaming	Cardboard	8	Photo	107	353	230%
2-21	Flaming	Cardboard	14	Photo	164	395	141%
2-21	Flaming	Cardboard	16	Photo	153	395	158%
2-21	Flaming	Cardboard	18	Photo	498	402	-19%
2-21	Flaming	Cardboard	20	Photo	482	402	-17%
2-21	Flaming	Cardboard	22	Photo	477	446	-6%
2-21	Flaming	Cardboard	24	Photo	474	446	-6%
2-22	Flaming	Cardboard	14	Photo	83	70	-16%
2-22	Flaming	Cardboard	16	Photo	414	70	-83%
2-22	Flaming	Cardboard	18	Photo	479	114	-76%
2-22	Flaming	Cardboard	20	Photo	455	114	-75%
2-22	Flaming	Cardboard	22	Photo	118	103	-13%
2-22	Flaming	Cardboard	24	Photo	443	103	-77%
2-23	Flaming	Cardboard	14	Photo	151	149	-1%
2-23	Flaming	Cardboard	16	Photo	139	149	7%
2-23	Flaming	Cardboard	18	Photo	97	87	-10%
2-23	Flaming	Cardboard	20	Photo	310	87	-72%
2-23	Flaming	Cardboard	22	Photo	173	107	-38%
2-23	Flaming	Cardboard	24	Photo	139	107	-23%
2-24	Flaming	Cardboard	14	Photo	139	431	210%
2-24	Flaming	Cardboard	18	Photo	89	77	-13%
2-24	Flaming	Cardboard	20	Photo	417	77	-82%
2-24	Flaming	Cardboard	22	Photo	128	100	-22%
2-24	Flaming	Cardboard	24	Photo	413	100	-76%

Optical Density Alarm Threshold: 20% Threshold; Navy tests (see Table 12)

Test ID	Fire Type	Material	Detector ID	Detector Type	Alarm Times (s) Experiment	Alarm Times (s) Predicted	Percent Error
2-25	Smoldering	Potassium Chlorate / Lactose	15	Ion	222	98	-56%
2-25	Smoldering	Potassium Chlorate / Lactose	19	Ion	306	DNA (0.023 @ 217 s)	
2-27	Smoldering	Potassium Chlorate / Lactose	19	Ion	152	30	-80%
2-27	Smoldering	Potassium Chlorate / Lactose	23	Ion	69	66	-4%
2-34	Smoldering	Electrical Cable	19	Ion	840	169	-80%
2-36	Smoldering	Electrical Cable	19	Ion	1490	738	-50%
2-37	Smoldering	Electrical Cable	19	Ion	393	236	-40%
2-26	Smoldering	Potassium Chlorate / Lactose	15	Ion	196	50	-74%
2-26	Smoldering	Potassium Chlorate / Lactose	19	Ion	234	32	-86%
2-28	Smoldering	Potassium Chlorate / Lactose	19	Ion	444	74	-83%
2-28	Smoldering	Potassium Chlorate / Lactose	23	Ion	40	111	178%
2-38	Smoldering	Electrical Cable	19	Ion	768	704	-8%
2-38	Smoldering	Electrical Cable	23	Ion	730	752	3%
2-40	Smoldering	Electrical Cable	15	Ion	983	333	-66%
2-01	Smoldering	Electrical Cable	1	Ion	2029	1207	-41%
2-01	Smoldering	Electrical Cable	5	Ion	2138	751	-65%
2-04	Smoldering	Electrical Cable	5	Ion	1057	369	-65%
2-07	Smoldering	Electrical Cable	1	Ion	831	438	-47%
2-07	Smoldering	Electrical Cable	5	Ion	1365	560	-59%
2-13	Smoldering	Potassium Chlorate / Lactose	5	Ion	536	506	-6%
2-14	Smoldering	Potassium Chlorate / Lactose	1	Ion	18	7	-61%
2-14	Smoldering	Potassium Chlorate / Lactose	5	Ion	98	31	-68%
2-25	Smoldering	Potassium Chlorate / Lactose	13	Ion	100	98	-2%
2-25	Smoldering	Potassium Chlorate / Lactose	17	Ion	126	DNA (0.023 @ 217 s)	
2-25	Smoldering	Potassium Chlorate / Lactose	21	Ion	205	23	-89%
2-27	Smoldering	Potassium Chlorate / Lactose	13	Ion	257	DNA (0.011 @ 99 s)	
2-27	Smoldering	Potassium Chlorate / Lactose	17	Ion	74	30	-59%
2-27	Smoldering	Potassium Chlorate / Lactose	21	Ion	66	66	0%
2-34	Smoldering	Electrical Cable	17	Ion	659	169	-74%
2-36	Smoldering	Electrical Cable	17	Ion	1354	738	-45%
2-37	Smoldering	Electrical Cable	13	Ion	678	604	-11%
2-37	Smoldering	Electrical Cable	17	Ion	335	236	-30%
2-37	Smoldering	Electrical Cable	21	Ion	566	378	-33%
2-39	Smoldering	Electrical Cable	13	Ion	760	278	-63%
2-05	Smoldering	Electrical Cable	1	Ion	1695	615	-64%
2-05	Smoldering	Electrical Cable	5	Ion	643	211	-67%
2-08	Smoldering	Electrical Cable	1	Ion	1372	1300	-5%
2-08	Smoldering	Electrical Cable	5	Ion	1391	432	-69%
2-15	Smoldering	Potassium Chlorate / Lactose	1	Ion	19	5	-74%
2-15	Smoldering	Potassium Chlorate / Lactose	5	Ion	70	58	-17%
2-26	Smoldering	Potassium Chlorate / Lactose	13	Ion	64	50	-22%

Optical Density Alarm Threshold: 20% Threshold; Navy tests (see Table 12)

Test ID	Fire Type	Material	Detector		Alarm Times (s)		Percent Error
			ID	Type	Experiment	Predicted	
2-26	Smoldering	Potassium Chlorate / Lactose	17	Ion	53	32	-40%
2-26	Smoldering	Potassium Chlorate / Lactose	21	Ion	145	16	-89%
2-28	Smoldering	Potassium Chlorate / Lactose	13	Ion	192	97	-49%
2-28	Smoldering	Potassium Chlorate / Lactose	17	Ion	122	74	-39%
2-28	Smoldering	Potassium Chlorate / Lactose	21	Ion	38	111	192%
2-35	Smoldering	Electrical Cable	17	Ion	922	214	-77%
2-35	Smoldering	Electrical Cable	21	Ion	1408	1242	-12%
2-38	Smoldering	Electrical Cable	13	Ion	767	648	-16%
2-38	Smoldering	Electrical Cable	17	Ion	771	704	-9%
2-38	Smoldering	Electrical Cable	21	Ion	561	752	34%
2-40	Smoldering	Electrical Cable	13	Ion	448	333	-26%
2-01	Smoldering	Electrical Cable	2	Photo	2034	1224	-40%
2-01	Smoldering	Electrical Cable	4	Photo	2232	1224	-45%
2-01	Smoldering	Electrical Cable	8	Photo	2232	763	-66%
2-04	Smoldering	Electrical Cable	2	Photo	1713	584	-66%
2-04	Smoldering	Electrical Cable	6	Photo	796	370	-54%
2-07	Smoldering	Electrical Cable	4	Photo	936	439	-53%
2-07	Smoldering	Electrical Cable	6	Photo	908	568	-37%
2-13	Smoldering	Potassium Chlorate / Lactose	2	Photo	578	485	-16%
2-13	Smoldering	Potassium Chlorate / Lactose	4	Photo	572	485	-15%
2-13	Smoldering	Potassium Chlorate / Lactose	6	Photo	524	507	-3%
2-13	Smoldering	Potassium Chlorate / Lactose	8	Photo	710	507	-29%
2-14	Smoldering	Potassium Chlorate / Lactose	2	Photo	20	7	-65%
2-14	Smoldering	Potassium Chlorate / Lactose	4	Photo	33	7	-79%
2-25	Smoldering	Potassium Chlorate / Lactose	14	Photo	94	102	9%
2-25	Smoldering	Potassium Chlorate / Lactose	16	Photo	105	102	-3%
2-25	Smoldering	Potassium Chlorate / Lactose	18	Photo	170	DNA (0.023 @ 217 s)	
2-25	Smoldering	Potassium Chlorate / Lactose	20	Photo	301	DNA (0.023 @ 217 s)	
2-25	Smoldering	Potassium Chlorate / Lactose	24	Photo	164	23	-86%
2-27	Smoldering	Potassium Chlorate / Lactose	18	Photo	49	31	-37%
2-27	Smoldering	Potassium Chlorate / Lactose	20	Photo	68	31	-54%
2-27	Smoldering	Potassium Chlorate / Lactose	22	Photo	67	67	0%
2-27	Smoldering	Potassium Chlorate / Lactose	24	Photo	65	67	3%
2-34	Smoldering	Electrical Cable	18	Photo	297	169	-43%
2-34	Smoldering	Electrical Cable	20	Photo	648	169	-74%
2-34	Smoldering	Electrical Cable	22	Photo	843	710	-16%
2-34	Smoldering	Electrical Cable	24	Photo	732	710	-3%
2-36	Smoldering	Electrical Cable	14	Photo	1611	1593	-1%
2-36	Smoldering	Electrical Cable	18	Photo	756	839	11%
2-36	Smoldering	Electrical Cable	20	Photo	860	839	-2%
2-36	Smoldering	Electrical Cable	22	Photo	1356	837	-38%

Optical Density Alarm Threshold: 20% Threshold; Navy tests (see Table 12)

Test ID	Fire Type	Material	Detector ID	Type	Experiment	Predicted	Percent Error
2-36	Smoldering	Electrical Cable	24	Photo	915	837	-9%
2-37	Smoldering	Electrical Cable	14	Photo	759	622	-18%
2-37	Smoldering	Electrical Cable	16	Photo	735	622	-15%
2-37	Smoldering	Electrical Cable	18	Photo	295	236	-20%
2-37	Smoldering	Electrical Cable	20	Photo	331	236	-29%
2-37	Smoldering	Electrical Cable	22	Photo	633	378	-40%
2-37	Smoldering	Electrical Cable	24	Photo	506	378	-25%
2-39	Smoldering	Electrical Cable	14	Photo	941	278	-70%
2-39	Smoldering	Electrical Cable	16	Photo	856	278	-68%
2-39	Smoldering	Electrical Cable	18	Photo	1362	1494	10%
2-39	Smoldering	Electrical Cable	22	Photo	786	1041	32%
2-39	Smoldering	Electrical Cable	24	Photo	689	1041	51%
2-02	Smoldering	Electrical Cable	2	Photo	775	765	-1%
2-02	Smoldering	Electrical Cable	4	Photo	2000	765	-62%
2-02	Smoldering	Electrical Cable	6	Photo	656	618	-6%
2-05	Smoldering	Electrical Cable	2	Photo	559	627	12%
2-05	Smoldering	Electrical Cable	4	Photo	639	627	-2%
2-05	Smoldering	Electrical Cable	6	Photo	424	211	-50%
2-05	Smoldering	Electrical Cable	8	Photo	297	211	-29%
2-08	Smoldering	Electrical Cable	2	Photo	728	1307	80%
2-08	Smoldering	Electrical Cable	4	Photo	845	1307	55%
2-08	Smoldering	Electrical Cable	6	Photo	539	435	-19%
2-08	Smoldering	Electrical Cable	8	Photo	775	435	-44%
2-15	Smoldering	Potassium Chlorate / Lactose	2	Photo	19	6	-68%
2-15	Smoldering	Potassium Chlorate / Lactose	4	Photo	112	6	-95%
2-15	Smoldering	Potassium Chlorate / Lactose	6	Photo	81	66	-19%
2-15	Smoldering	Potassium Chlorate / Lactose	8	Photo	83	66	-20%
2-26	Smoldering	Potassium Chlorate / Lactose	14	Photo	68	51	-25%
2-26	Smoldering	Potassium Chlorate / Lactose	16	Photo	246	51	-79%
2-26	Smoldering	Potassium Chlorate / Lactose	18	Photo	65	33	-49%
2-28	Smoldering	Potassium Chlorate / Lactose	16	Photo	331	100	-70%
2-28	Smoldering	Potassium Chlorate / Lactose	18	Photo	92	75	-18%
2-28	Smoldering	Potassium Chlorate / Lactose	20	Photo	348	75	-78%
2-28	Smoldering	Potassium Chlorate / Lactose	22	Photo	34	117	244%
2-28	Smoldering	Potassium Chlorate / Lactose	24	Photo	32	117	266%
2-35	Smoldering	Electrical Cable	18	Photo	423	224	-47%
2-35	Smoldering	Electrical Cable	20	Photo	851	224	-74%
2-35	Smoldering	Electrical Cable	22	Photo	656	1279	95%
2-35	Smoldering	Electrical Cable	24	Photo	989	1279	29%
2-38	Smoldering	Electrical Cable	14	Photo	754	738	-2%
2-38	Smoldering	Electrical Cable	16	Photo	843	738	-12%
2-38	Smoldering	Electrical Cable	18	Photo	549	704	28%
2-38	Smoldering	Electrical Cable	20	Photo	709	704	-1%

Optical Density Alarm Threshold: 20% Threshold; Navy tests (see Table 12)

| Test ID | Fire Type | Material | Detector | | Alarm Times (s) | | Percent Error |
			ID	Type	Experiment	Predicted	
2-38	Smoldering	Electrical Cable	22	Photo	189	765	305%
2-38	Smoldering	Electrical Cable	24	Photo	418	765	83%
2-40	Smoldering	Electrical Cable	14	Photo	402	334	-17%
2-40	Smoldering	Electrical Cable	16	Photo	679	334	-51%
2-40	Smoldering	Electrical Cable	18	Photo	1201	1488	24%
2-40	Smoldering	Electrical Cable	20	Photo	1387	1488	7%
2-40	Smoldering	Electrical Cable	22	Photo	1542	1182	-23%

Optical Density Alarm Threshold: 50% Threshold; Navy tests (see Table 12)

Test ID	Fire Type	Material	Detector ID	Detector Type	Alarm Times (s) Experiment	Alarm Times (s) Predicted	Percent Error
1-37	Flaming	Wood	1	Ion	61	614	907%
1-37	Flaming	Wood	3	Ion	177	614	247%
1-37	Flaming	Wood	5	Ion	45	720	1500%
1-37	Flaming	Wood	7	Ion	174	720	314%
1-38	Flaming	Wood	1	Ion	62	547	782%
1-38	Flaming	Wood	3	Ion	155	547	253%
1-38	Flaming	Wood	5	Ion	65	793	1120%
1-38	Flaming	Wood	7	Ion	182	793	336%
1-39	Flaming	Wood	1	Ion	69	24	-65%
1-39	Flaming	Wood	3	Ion	43	24	-44%
1-39	Flaming	Wood	5	Ion	39	39	0%
1-39	Flaming	Wood	7	Ion	134	39	-71%
1-40	Flaming	Wood	1	Ion	43	503	1070%
1-40	Flaming	Wood	3	Ion	123	503	309%
1-40	Flaming	Wood	5	Ion	39	548	1305%
1-40	Flaming	Wood	7	Ion	57	548	861%
1-41	Flaming	Wood	1	Ion	69	546	691%
1-41	Flaming	Wood	3	Ion	152	546	259%
1-41	Flaming	Wood	5	Ion	46	530	1052%
1-41	Flaming	Wood	7	Ion	124	530	327%
1-50	Flaming	Wood	13	Ion	48	1106	2204%
1-50	Flaming	Wood	15	Ion	65	1106	1602%
1-50	Flaming	Wood	17	Ion	75	1096	1361%
1-50	Flaming	Wood	19	Ion	128	1096	756%
1-50	Flaming	Wood	21	Ion	112	1092	875%
1-50	Flaming	Wood	23	Ion	161	1092	578%
1-51	Flaming	Wood	13	Ion	44	42	-5%
1-51	Flaming	Wood	15	Ion	90	42	-53%
1-51	Flaming	Wood	17	Ion	79	50	-37%
1-51	Flaming	Wood	19	Ion	182	50	-73%
1-51	Flaming	Wood	21	Ion	99	29	-71%
1-51	Flaming	Wood	23	Ion	89	29	-67%
1-52	Flaming	Wood	13	Ion	38	30	-21%
1-52	Flaming	Wood	15	Ion	65	30	-54%
1-52	Flaming	Wood	19	Ion	73	28	-62%
1-52	Flaming	Wood	21	Ion	84	20	-76%
1-52	Flaming	Wood	23	Ion	177	20	-89%
1-53	Flaming	Wood	13	Ion	42	738	1657%
1-53	Flaming	Wood	15	Ion	101	738	631%
1-53	Flaming	Wood	17	Ion	123	733	496%
1-53	Flaming	Wood	19	Ion	126	733	482%
1-53	Flaming	Wood	21	Ion	95	672	607%

Optical Density Alarm Threshold: 50% Threshold; Navy tests (see Table 12)

Test ID	Fire Type	Material	Detector ID	Type	Experiment	Predicted	Percent Error
1-53	Flaming	Wood	23	Ion	164	672	310%
1-54	Flaming	Wood	13	Ion	50	36	-28%
1-54	Flaming	Wood	15	Ion	66	36	-45%
1-54	Flaming	Wood	17	Ion	75	43	-43%
1-54	Flaming	Wood	19	Ion	116	43	-63%
1-55	Flaming	Wood	13	Ion	36	32	-11%
1-55	Flaming	Wood	15	Ion	68	32	-53%
1-55	Flaming	Wood	17	Ion	53	20	-62%
1-55	Flaming	Wood	19	Ion	43	20	-53%
2-09	Flaming	Cardboard	1	Ion	162	416	157%
2-09	Flaming	Cardboard	3	Ion	165	416	152%
2-09	Flaming	Cardboard	5	Ion	86	124	44%
2-09	Flaming	Cardboard	7	Ion	100	124	24%
2-10	Flaming	Cardboard	1	Ion	229	390	70%
2-10	Flaming	Cardboard	3	Ion	239	390	63%
2-10	Flaming	Cardboard	5	Ion	166	165	-1%
2-10	Flaming	Cardboard	7	Ion	228	165	-28%
2-11	Flaming	Cardboard	3	Ion	67	66	-1%
2-11	Flaming	Cardboard	5	Ion	93	88	-5%
2-11	Flaming	Cardboard	7	Ion	89	88	-1%
2-12	Flaming	Cardboard	5	Ion	66	371	462%
2-12	Flaming	Cardboard	7	Ion	63	371	489%
2-21	Flaming	Cardboard	13	Ion	63	428	579%
2-21	Flaming	Cardboard	15	Ion	36	428	1089%
2-21	Flaming	Cardboard	17	Ion	151	414	174%
2-21	Flaming	Cardboard	19	Ion	174	414	138%
2-21	Flaming	Cardboard	21	Ion	143	453	217%
2-21	Flaming	Cardboard	23	Ion	195	453	132%
2-22	Flaming	Cardboard	13	Ion	43	71	65%
2-22	Flaming	Cardboard	15	Ion	30	71	137%
2-22	Flaming	Cardboard	17	Ion	302	116	-62%
2-22	Flaming	Cardboard	19	Ion	126	116	-8%
2-22	Flaming	Cardboard	21	Ion	87	104	20%
2-22	Flaming	Cardboard	23	Ion	127	104	-18%
2-23	Flaming	Cardboard	13	Ion	119	151	27%
2-23	Flaming	Cardboard	15	Ion	143	151	6%
2-23	Flaming	Cardboard	17	Ion	54	87	61%
2-23	Flaming	Cardboard	19	Ion	122	87	-29%
2-23	Flaming	Cardboard	21	Ion	125	110	-12%
2-23	Flaming	Cardboard	23	Ion	144	110	-24%
2-24	Flaming	Cardboard	13	Ion	117	434	271%
2-24	Flaming	Cardboard	15	Ion	142	434	206%
2-24	Flaming	Cardboard	17	Ion	62	78	26%
2-24	Flaming	Cardboard	19	Ion	100	78	-22%

Optical Density Alarm Threshold: 50% Threshold; Navy tests (see Table 12)

Test ID	Fire Type	Material	Detector ID	Detector Type	Experiment	Predicted	Percent Error
2-24	Flaming	Cardboard	21	Ion	58	102	76%
2-24	Flaming	Cardboard	23	Ion	67	102	52%
1-37	Flaming	Wood	2	Photo	901	1076	19%
1-37	Flaming	Wood	4	Photo	1007	1076	7%
1-37	Flaming	Wood	6	Photo	816	1152	41%
1-37	Flaming	Wood	8	Photo	990	1152	16%
1-38	Flaming	Wood	2	Photo	874	1293	48%
1-38	Flaming	Wood	4	Photo	860	1293	50%
1-38	Flaming	Wood	6	Photo	794	1437	81%
1-38	Flaming	Wood	8	Photo	943	1437	52%
1-39	Flaming	Wood	2	Photo	546	725	33%
1-39	Flaming	Wood	4	Photo	555	725	31%
1-39	Flaming	Wood	6	Photo	366	759	107%
1-39	Flaming	Wood	8	Photo	634	759	20%
1-40	Flaming	Wood	2	Photo	1036	860	-17%
1-40	Flaming	Wood	4	Photo	886	860	-3%
1-40	Flaming	Wood	6	Photo	956	772	-19%
1-40	Flaming	Wood	8	Photo	1023	772	-25%
1-41	Flaming	Wood	2	Photo	529	810	53%
1-41	Flaming	Wood	4	Photo	494	810	64%
1-41	Flaming	Wood	6	Photo	484	818	69%
1-41	Flaming	Wood	8	Photo	553	818	48%
1-50	Flaming	Wood	16	Photo	1149	1140	-1%
1-50	Flaming	Wood	20	Photo	1194	1134	-5%
1-50	Flaming	Wood	24	Photo	1149	1094	-5%
1-51	Flaming	Wood	14	Photo	54	727	1246%
1-51	Flaming	Wood	16	Photo	53	727	1272%
1-51	Flaming	Wood	18	Photo	612	726	19%
1-51	Flaming	Wood	20	Photo	82	726	785%
1-51	Flaming	Wood	22	Photo	518	723	40%
1-52	Flaming	Wood	14	Photo	38	31	-18%
1-52	Flaming	Wood	16	Photo	35	31	-11%
1-52	Flaming	Wood	18	Photo	49	36	-27%
1-52	Flaming	Wood	20	Photo	40	36	-10%
1-53	Flaming	Wood	14	Photo	662	1338	102%
1-53	Flaming	Wood	16	Photo	768	1338	74%
1-53	Flaming	Wood	18	Photo	841	1310	56%
1-53	Flaming	Wood	20	Photo	689	1310	90%
1-53	Flaming	Wood	22	Photo	680	1271	87%
1-53	Flaming	Wood	24	Photo	906	1271	40%
1-54	Flaming	Wood	14	Photo	51	38	-25%
1-54	Flaming	Wood	16	Photo	45	38	-16%
1-54	Flaming	Wood	18	Photo	96	46	-52%
1-54	Flaming	Wood	20	Photo	49	46	-6%

Optical Density Alarm Threshold: 50% Threshold; Navy tests (see Table 12)

Test ID	Fire Type	Material	Detector		Alarm Times (s)		Percent Error
			ID	Type	Experiment	Predicted	
1-55	Flaming	Wood	16	Photo	35	37	6%
1-55	Flaming	Wood	18	Photo	55	22	-60%
1-55	Flaming	Wood	20	Photo	35	22	-37%
2-09	Flaming	Cardboard	2	Photo	480	520	8%
2-09	Flaming	Cardboard	4	Photo	169	520	208%
2-09	Flaming	Cardboard	6	Photo	129	487	278%
2-09	Flaming	Cardboard	8	Photo	124	487	293%
2-10	Flaming	Cardboard	2	Photo	643	468	-27%
2-10	Flaming	Cardboard	4	Photo	281	468	67%
2-10	Flaming	Cardboard	6	Photo	592	447	-24%
2-10	Flaming	Cardboard	8	Photo	260	447	72%
2-11	Flaming	Cardboard	2	Photo	76	73	-4%
2-11	Flaming	Cardboard	4	Photo	84	73	-13%
2-11	Flaming	Cardboard	6	Photo	110	416	278%
2-11	Flaming	Cardboard	8	Photo	93	416	347%
2-12	Flaming	Cardboard	6	Photo	115	DNA (0.025 @ 519 s)	
2-12	Flaming	Cardboard	8	Photo	107	DNA (0.025 @ 519 s)	
2-21	Flaming	Cardboard	14	Photo	164	516	215%
2-21	Flaming	Cardboard	16	Photo	153	516	237%
2-21	Flaming	Cardboard	18	Photo	498	585	17%
2-21	Flaming	Cardboard	20	Photo	482	585	21%
2-21	Flaming	Cardboard	22	Photo	477	579	21%
2-21	Flaming	Cardboard	24	Photo	474	579	22%
2-22	Flaming	Cardboard	14	Photo	83	94	13%
2-22	Flaming	Cardboard	16	Photo	414	94	-77%
2-22	Flaming	Cardboard	18	Photo	479	DNA (0.027 @ 132 s)	
2-22	Flaming	Cardboard	20	Photo	455	DNA (0.027 @ 132 s)	
2-22	Flaming	Cardboard	22	Photo	118	DNA (0.028 @ 117 s)	
2-22	Flaming	Cardboard	24	Photo	443	DNA (0.028 @ 117 s)	
2-23	Flaming	Cardboard	14	Photo	151	DNA (0.036 @ 684 s)	
2-23	Flaming	Cardboard	16	Photo	139	DNA (0.036 @ 684 s)	
2-23	Flaming	Cardboard	18	Photo	97	711	633%
2-23	Flaming	Cardboard	20	Photo	310	711	129%
2-23	Flaming	Cardboard	22	Photo	173	DNA (0.040 @ 727 s)	
2-23	Flaming	Cardboard	24	Photo	139	DNA (0.040 @ 727 s)	
2-24	Flaming	Cardboard	14	Photo	139	DNA (0.024 @ 497 s)	

Optical Density Alarm Threshold: 50% Threshold; Navy tests (see Table 12)

Test ID	Fire Type	Material	Detector ID	Type	Experiment	Predicted	Percent Error
2-24	Flaming	Cardboard	18	Photo	89	DNA (0.032 @ 458 s)	
2-24	Flaming	Cardboard	20	Photo	417	DNA (0.032 @ 458 s)	
2-24	Flaming	Cardboard	22	Photo	128	DNA (0.028 @ 470 s)	
2-24	Flaming	Cardboard	24	Photo	413	DNA (0.028 @ 470 s)	
2-25	Smoldering	Potassium Chlorate / Lactose	15	Ion	222	DNA (0.037 @ 124 s)	
2-25	Smoldering	Potassium Chlorate / Lactose	19	Ion	306	DNA (0.023 @ 217 s)	
2-27	Smoldering	Potassium Chlorate / Lactose	19	Ion	152	59	-61%
2-27	Smoldering	Potassium Chlorate / Lactose	23	Ion	69	DNA (0.055 @ 125 s)	
2-34	Smoldering	Electrical Cable	19	Ion	840	225	-73%
2-36	Smoldering	Electrical Cable	19	Ion	1490	1321	-11%
2-37	Smoldering	Electrical Cable	19	Ion	393	319	-19%
2-26	Smoldering	Potassium Chlorate / Lactose	15	Ion	196	DNA (0.044 @ 82 s)	
2-26	Smoldering	Potassium Chlorate / Lactose	19	Ion	234	DNA (0.086 @ 51 s)	
2-28	Smoldering	Potassium Chlorate / Lactose	19	Ion	444	DNA (0.089 @ 80 s)	
2-28	Smoldering	Potassium Chlorate / Lactose	23	Ion	40	DNA (0.033 @ 160 s)	
2-38	Smoldering	Electrical Cable	19	Ion	768	DNA (0.048 @ 704 s)	
2-38	Smoldering	Electrical Cable	23	Ion	730	DNA (0.031 @ 791 s)	
2-40	Smoldering	Electrical Cable	15	Ion	983	454	-54%
2-01	Smoldering	Electrical Cable	1	Ion	2029	1946	-4%
2-01	Smoldering	Electrical Cable	5	Ion	2138	1528	-29%
2-04	Smoldering	Electrical Cable	5	Ion	1057	473	-55%
2-07	Smoldering	Electrical Cable	1	Ion	831	531	-36%
2-07	Smoldering	Electrical Cable	5	Ion	1365	702	-49%
2-13	Smoldering	Potassium Chlorate / Lactose	5	Ion	536	DNA (0.077 @ 527 s)	
2-14	Smoldering	Potassium Chlorate / Lactose	1	Ion	18	11	-39%
2-14	Smoldering	Potassium Chlorate / Lactose	5	Ion	98	DNA (0.059 @ 53 s)	
2-25	Smoldering	Potassium Chlorate / Lactose	13	Ion	100	DNA (0.037 @ 124 s)	
2-25	Smoldering	Potassium Chlorate / Lactose	17	Ion	126	DNA (0.023 @ 217 s)	
2-25	Smoldering	Potassium Chlorate / Lactose	21	Ion	205	78	-62%
2-27	Smoldering	Potassium Chlorate / Lactose	13	Ion	257	DNA (0.011 @ 99 s)	
2-27	Smoldering	Potassium Chlorate / Lactose	17	Ion	74	59	-20%

Optical Density Alarm Threshold: 50% Threshold; Navy tests (see Table 12)

Test ID	Fire Type	Material	Detector ID	Type	Alarm Times (s) Experiment	Predicted	Percent Error
2-27	Smoldering	Potassium Chlorate / Lactose	21	Ion	66	DNA (0.055 @ 125 s)	
2-34	Smoldering	Electrical Cable	17	Ion	659	225	-66%
2-36	Smoldering	Electrical Cable	17	Ion	1354	1321	-2%
2-37	Smoldering	Electrical Cable	13	Ion	678	665	-2%
2-37	Smoldering	Electrical Cable	17	Ion	335	319	-5%
2-37	Smoldering	Electrical Cable	21	Ion	566	566	0%
2-39	Smoldering	Electrical Cable	13	Ion	760	278	-63%
2-05	Smoldering	Electrical Cable	1	Ion	1695	1865	10%
2-05	Smoldering	Electrical Cable	5	Ion	643	385	-40%
2-08	Smoldering	Electrical Cable	1	Ion	1372	1602	17%
2-08	Smoldering	Electrical Cable	5	Ion	1391	1325	-5%
2-15	Smoldering	Potassium Chlorate / Lactose	1	Ion	19	56	195%
2-15	Smoldering	Potassium Chlorate / Lactose	5	Ion	70	DNA (0.047 @ 99 s)	
2-26	Smoldering	Potassium Chlorate / Lactose	13	Ion	64	DNA (0.044 @ 82 s)	
2-26	Smoldering	Potassium Chlorate / Lactose	17	Ion	53	DNA (0.086 @ 51 s)	
2-26	Smoldering	Potassium Chlorate / Lactose	21	Ion	145	18	-88%
2-28	Smoldering	Potassium Chlorate / Lactose	13	Ion	192	DNA (0.039 @ 134 s)	
2-28	Smoldering	Potassium Chlorate / Lactose	17	Ion	122	DNA (0.089 @ 80 s)	
2-28	Smoldering	Potassium Chlorate / Lactose	21	Ion	38	DNA (0.033 @ 160 s)	
2-35	Smoldering	Electrical Cable	17	Ion	922	358	-61%
2-35	Smoldering	Electrical Cable	21	Ion	1408	1496	6%
2-38	Smoldering	Electrical Cable	13	Ion	767	DNA (0.039 @ 745 s)	
2-38	Smoldering	Electrical Cable	17	Ion	771	DNA (0.048 @ 704 s)	
2-38	Smoldering	Electrical Cable	21	Ion	561	DNA (0.031 @ 791 s)	
2-40	Smoldering	Electrical Cable	13	Ion	448	454	1%
2-01	Smoldering	Electrical Cable	2	Photo	2034	1711	-16%
2-01	Smoldering	Electrical Cable	4	Photo	2232	1711	-23%
2-01	Smoldering	Electrical Cable	8	Photo	2232	1119	-50%
2-04	Smoldering	Electrical Cable	2	Photo	1713	680	-60%
2-04	Smoldering	Electrical Cable	6	Photo	796	429	-46%
2-07	Smoldering	Electrical Cable	4	Photo	936	523	-44%
2-07	Smoldering	Electrical Cable	6	Photo	908	639	-30%
2-13	Smoldering	Potassium Chlorate / Lactose	2	Photo	578	508	-12%
2-13	Smoldering	Potassium Chlorate / Lactose	4	Photo	572	508	-11%
2-13	Smoldering	Potassium Chlorate / Lactose	6	Photo	524	525	0%
2-13	Smoldering	Potassium Chlorate / Lactose	8	Photo	710	525	-26%
2-14	Smoldering	Potassium Chlorate / Lactose	2	Photo	20	9	-55%

Optical Density Alarm Threshold: 50% Threshold; Navy tests (see Table 12)

Test ID	Fire Type	Material	ID	Type	Experiment	Predicted	Percent Error
			Detector		Alarm Times (s)		
2-14	Smoldering	Potassium Chlorate / Lactose	4	Photo	33	9	-73%
2-25	Smoldering	Potassium Chlorate / Lactose	14	Photo	94	DNA (0.037 @ 124 s)	
2-25	Smoldering	Potassium Chlorate / Lactose	16	Photo	105	DNA (0.037 @ 124 s)	
2-25	Smoldering	Potassium Chlorate / Lactose	18	Photo	170	DNA (0.023 @ 217 s)	
2-25	Smoldering	Potassium Chlorate / Lactose	20	Photo	301	DNA (0.023 @ 217 s)	
2-25	Smoldering	Potassium Chlorate / Lactose	24	Photo	164	36	-78%
2-27	Smoldering	Potassium Chlorate / Lactose	18	Photo	49	56	14%
2-27	Smoldering	Potassium Chlorate / Lactose	20	Photo	68	56	-18%
2-27	Smoldering	Potassium Chlorate / Lactose	22	Photo	67	DNA (0.055 @ 125 s)	
2-27	Smoldering	Potassium Chlorate / Lactose	24	Photo	65	DNA (0.055 @ 125 s)	
2-34	Smoldering	Electrical Cable	18	Photo	297	198	-33%
2-34	Smoldering	Electrical Cable	20	Photo	648	198	-69%
2-34	Smoldering	Electrical Cable	22	Photo	843	714	-15%
2-34	Smoldering	Electrical Cable	24	Photo	732	714	-2%
2-36	Smoldering	Electrical Cable	14	Photo	1611	1788	11%
2-36	Smoldering	Electrical Cable	18	Photo	756	1117	48%
2-36	Smoldering	Electrical Cable	20	Photo	860	1117	30%
2-36	Smoldering	Electrical Cable	22	Photo	1356	1409	4%
2-36	Smoldering	Electrical Cable	24	Photo	915	1409	54%
2-37	Smoldering	Electrical Cable	14	Photo	759	656	-14%
2-37	Smoldering	Electrical Cable	16	Photo	735	656	-11%
2-37	Smoldering	Electrical Cable	18	Photo	295	240	-19%
2-37	Smoldering	Electrical Cable	20	Photo	331	240	-27%
2-37	Smoldering	Electrical Cable	22	Photo	633	468	-26%
2-37	Smoldering	Electrical Cable	24	Photo	506	468	-8%
2-39	Smoldering	Electrical Cable	14	Photo	941	278	-70%
2-39	Smoldering	Electrical Cable	16	Photo	856	278	-68%
2-39	Smoldering	Electrical Cable	18	Photo	1362	DNA (0.046 @ 1518 s)	
2-39	Smoldering	Electrical Cable	22	Photo	786	1073	37%
2-39	Smoldering	Electrical Cable	24	Photo	689	1073	56%
2-02	Smoldering	Electrical Cable	2	Photo	775	1940	150%
2-02	Smoldering	Electrical Cable	4	Photo	2000	1940	-3%
2-02	Smoldering	Electrical Cable	6	Photo	656	DNA (0.039 @ 618 s)	
2-05	Smoldering	Electrical Cable	2	Photo	559	1719	208%
2-05	Smoldering	Electrical Cable	4	Photo	639	1719	169%
2-05	Smoldering	Electrical Cable	6	Photo	424	316	-25%
2-05	Smoldering	Electrical Cable	8	Photo	297	316	6%
2-08	Smoldering	Electrical Cable	2	Photo	728	1514	108%

185

Optical Density Alarm Threshold: 50% Threshold; Navy tests (see Table 12)

Test ID	Fire Type	Material	Detector ID	Type	Alarm Times (s) Experiment	Predicted	Percent Error
2-08	Smoldering	Electrical Cable	4	Photo	845	1514	79%
2-08	Smoldering	Electrical Cable	6	Photo	539	516	-4%
2-08	Smoldering	Electrical Cable	8	Photo	775	516	-33%
2-15	Smoldering	Potassium Chlorate / Lactose	2	Photo	19	10	-47%
2-15	Smoldering	Potassium Chlorate / Lactose	4	Photo	112	10	-91%
2-15	Smoldering	Potassium Chlorate / Lactose	6	Photo	81	DNA (0.047 @ 99 s)	
2-15	Smoldering	Potassium Chlorate / Lactose	8	Photo	83	DNA (0.047 @ 99 s)	
2-26	Smoldering	Potassium Chlorate / Lactose	14	Photo	68	DNA (0.044 @ 82 s)	
2-26	Smoldering	Potassium Chlorate / Lactose	16	Photo	246	DNA (0.044 @ 82 s)	
2-26	Smoldering	Potassium Chlorate / Lactose	18	Photo	65	41	-37%
2-28	Smoldering	Potassium Chlorate / Lactose	16	Photo	331	DNA (0.039 @ 134 s)	
2-28	Smoldering	Potassium Chlorate / Lactose	18	Photo	92	77	-16%
2-28	Smoldering	Potassium Chlorate / Lactose	20	Photo	348	77	-78%
2-28	Smoldering	Potassium Chlorate / Lactose	22	Photo	34	DNA (0.033 @ 160 s)	
2-28	Smoldering	Potassium Chlorate / Lactose	24	Photo	32	DNA (0.033 @ 160 s)	
2-35	Smoldering	Electrical Cable	18	Photo	423	352	-17%
2-35	Smoldering	Electrical Cable	20	Photo	851	352	-59%
2-35	Smoldering	Electrical Cable	22	Photo	656	1331	103%
2-35	Smoldering	Electrical Cable	24	Photo	989	1331	35%
2-38	Smoldering	Electrical Cable	14	Photo	754	DNA (0.039 @ 745 s)	
2-38	Smoldering	Electrical Cable	16	Photo	843	DNA (0.039 @ 745 s)	
2-38	Smoldering	Electrical Cable	18	Photo	549	DNA (0.048 @ 704 s)	
2-38	Smoldering	Electrical Cable	20	Photo	709	DNA (0.048 @ 704 s)	
2-38	Smoldering	Electrical Cable	22	Photo	189	DNA (0.031 @ 791 s)	
2-38	Smoldering	Electrical Cable	24	Photo	418	DNA (0.031 @ 791 s)	
2-40	Smoldering	Electrical Cable	14	Photo	402	366	-9%
2-40	Smoldering	Electrical Cable	16	Photo	679	366	-46%
2-40	Smoldering	Electrical Cable	18	Photo	1201	DNA (0.037 @ 1503 s)	
2-40	Smoldering	Electrical Cable	20	Photo	1387	DNA (0.037 @ 1503 s)	
2-40	Smoldering	Electrical Cable	22	Photo	1542	DNA (0.058 @ 1632 s)	

Optical Density Alarm Threshold: 80% Threshold; Navy tests (see Table 12)

Test ID	Fire Type	Material	Detector		Alarm Times (s)		Percent Error
			ID	Type	Experiment	Predicted	
1-37	Flaming	Wood	1	Ion	61	1182	1838%
1-37	Flaming	Wood	3	Ion	177	1182	568%
1-37	Flaming	Wood	5	Ion	45	1224	2620%
1-37	Flaming	Wood	7	Ion	174	1224	603%
1-38	Flaming	Wood	1	Ion	62	1412	2177%
1-38	Flaming	Wood	3	Ion	155	1412	811%
1-38	Flaming	Wood	5	Ion	65	1561	2302%
1-38	Flaming	Wood	7	Ion	182	1561	758%
1-39	Flaming	Wood	1	Ion	69	769	1014%
1-39	Flaming	Wood	3	Ion	43	769	1688%
1-39	Flaming	Wood	5	Ion	39	821	2005%
1-39	Flaming	Wood	7	Ion	134	821	513%
1-40	Flaming	Wood	1	Ion	43	889	1967%
1-40	Flaming	Wood	3	Ion	123	889	623%
1-40	Flaming	Wood	5	Ion	39	810	1977%
1-40	Flaming	Wood	7	Ion	57	810	1321%
1-41	Flaming	Wood	1	Ion	69	857	1142%
1-41	Flaming	Wood	3	Ion	152	857	464%
1-41	Flaming	Wood	5	Ion	46	862	1774%
1-41	Flaming	Wood	7	Ion	124	862	595%
1-50	Flaming	Wood	13	Ion	48	1141	2277%
1-50	Flaming	Wood	15	Ion	65	1141	1655%
1-50	Flaming	Wood	17	Ion	75	1134	1412%
1-50	Flaming	Wood	19	Ion	128	1134	786%
1-50	Flaming	Wood	21	Ion	112	1094	877%
1-50	Flaming	Wood	23	Ion	161	1094	580%
1-51	Flaming	Wood	13	Ion	44	784	1682%
1-51	Flaming	Wood	15	Ion	90	784	771%
1-51	Flaming	Wood	17	Ion	79	761	863%
1-51	Flaming	Wood	19	Ion	182	761	318%
1-51	Flaming	Wood	21	Ion	99	765	673%
1-51	Flaming	Wood	23	Ion	89	765	760%
1-52	Flaming	Wood	13	Ion	38	31	-18%
1-52	Flaming	Wood	15	Ion	65	31	-52%
1-52	Flaming	Wood	19	Ion	73	39	-47%
1-52	Flaming	Wood	21	Ion	84	25	-70%
1-52	Flaming	Wood	23	Ion	177	25	-86%
1-53	Flaming	Wood	13	Ion	42	1518	3514%
1-53	Flaming	Wood	15	Ion	101	1518	1403%
1-53	Flaming	Wood	17	Ion	123	1510	1128%
1-53	Flaming	Wood	19	Ion	126	1510	1098%
1-53	Flaming	Wood	21	Ion	95	1460	1437%

Optical Density Alarm Threshold: 80% Threshold; Navy tests (see Table 12)

Test ID	Fire Type	Material	Detector ID	Detector Type	Experiment	Predicted	Percent Error
1-53	Flaming	Wood	23	Ion	164	1460	790%
1-54	Flaming	Wood	13	Ion	50	40	-20%
1-54	Flaming	Wood	15	Ion	66	40	-39%
1-54	Flaming	Wood	17	Ion	75	47	-37%
1-54	Flaming	Wood	19	Ion	116	47	-59%
1-55	Flaming	Wood	13	Ion	36	37	3%
1-55	Flaming	Wood	15	Ion	68	37	-46%
1-55	Flaming	Wood	17	Ion	53	26	-51%
1-55	Flaming	Wood	19	Ion	43	26	-40%
2-09	Flaming	Cardboard	1	Ion	162	630	289%
2-09	Flaming	Cardboard	3	Ion	165	630	282%
2-09	Flaming	Cardboard	5	Ion	86	582	577%
2-09	Flaming	Cardboard	7	Ion	100	582	482%
2-10	Flaming	Cardboard	1	Ion	229	469	105%
2-10	Flaming	Cardboard	3	Ion	239	469	96%
2-10	Flaming	Cardboard	5	Ion	166	447	169%
2-10	Flaming	Cardboard	7	Ion	228	447	96%
2-11	Flaming	Cardboard	3	Ion	67	73	9%
2-11	Flaming	Cardboard	5	Ion	93	466	401%
2-11	Flaming	Cardboard	7	Ion	89	466	424%
2-12	Flaming	Cardboard	5	Ion	66	DNA (0.025 @ 519 s)	
2-12	Flaming	Cardboard	7	Ion	63	DNA (0.025 @ 519 s)	
2-21	Flaming	Cardboard	13	Ion	63	554	779%
2-21	Flaming	Cardboard	15	Ion	36	554	1439%
2-21	Flaming	Cardboard	17	Ion	151	607	302%
2-21	Flaming	Cardboard	19	Ion	174	607	249%
2-21	Flaming	Cardboard	21	Ion	143	DNA (0.049 @ 755 s)	
2-21	Flaming	Cardboard	23	Ion	195	DNA (0.049 @ 755 s)	
2-22	Flaming	Cardboard	13	Ion	43	DNA (0.049 @ 95 s)	
2-22	Flaming	Cardboard	15	Ion	30	DNA (0.049 @ 95 s)	
2-22	Flaming	Cardboard	17	Ion	302	DNA (0.027 @ 132 s)	
2-22	Flaming	Cardboard	19	Ion	126	DNA (0.027 @ 132 s)	
2-22	Flaming	Cardboard	21	Ion	87	DNA (0.028 @ 117 s)	
2-22	Flaming	Cardboard	23	Ion	127	DNA (0.028 @ 117 s)	
2-23	Flaming	Cardboard	13	Ion	119	DNA (0.036 @ 684 s)	

Optical Density Alarm Threshold: 80% Threshold; Navy tests (see Table 12)

Test ID	Fire Type	Material	Detector ID	Detector Type	Alarm Times (s) Experiment	Alarm Times (s) Predicted	Percent Error
2-23	Flaming	Cardboard	15	Ion	143	DNA (0.036 @ 684 s)	
2-23	Flaming	Cardboard	17	Ion	54	DNA (0.045 @ 715 s)	
2-23	Flaming	Cardboard	19	Ion	122	DNA (0.045 @ 715 s)	
2-23	Flaming	Cardboard	21	Ion	125	DNA (0.040 @ 727 s)	
2-23	Flaming	Cardboard	23	Ion	144	DNA (0.040 @ 727 s)	
2-24	Flaming	Cardboard	13	Ion	117	DNA (0.024 @ 497 s)	
2-24	Flaming	Cardboard	15	Ion	142	DNA (0.024 @ 497 s)	
2-24	Flaming	Cardboard	17	Ion	62	DNA (0.032 @ 458 s)	
2-24	Flaming	Cardboard	19	Ion	100	DNA (0.032 @ 458 s)	
2-24	Flaming	Cardboard	21	Ion	58	DNA (0.028 @ 470 s)	
2-24	Flaming	Cardboard	23	Ion	67	DNA (0.028 @ 470 s)	
1-37	Flaming	Wood	2	Photo	901	1362	51%
1-37	Flaming	Wood	4	Photo	1007	1362	35%
1-37	Flaming	Wood	6	Photo	816	1421	74%
1-37	Flaming	Wood	8	Photo	990	1421	44%
1-38	Flaming	Wood	2	Photo	874	1575	80%
1-38	Flaming	Wood	4	Photo	860	1575	83%
1-38	Flaming	Wood	6	Photo	794	1591	100%
1-38	Flaming	Wood	8	Photo	943	1591	69%
1-39	Flaming	Wood	2	Photo	546	919	68%
1-39	Flaming	Wood	4	Photo	555	919	66%
1-39	Flaming	Wood	6	Photo	366	956	161%
1-39	Flaming	Wood	8	Photo	634	956	51%
1-40	Flaming	Wood	2	Photo	1036	1076	4%
1-40	Flaming	Wood	4	Photo	886	1076	21%
1-40	Flaming	Wood	6	Photo	956	990	4%
1-40	Flaming	Wood	8	Photo	1023	990	-3%
1-41	Flaming	Wood	2	Photo	529	982	86%
1-41	Flaming	Wood	4	Photo	494	982	99%
1-41	Flaming	Wood	6	Photo	484	988	104%
1-41	Flaming	Wood	8	Photo	553	988	79%
1-50	Flaming	Wood	16	Photo	1149	1147	0%
1-50	Flaming	Wood	20	Photo	1194	1143	-4%
1-50	Flaming	Wood	24	Photo	1149	1143	-1%
1-51	Flaming	Wood	14	Photo	54	1000	1752%
1-51	Flaming	Wood	16	Photo	53	1000	1787%

Optical Density Alarm Threshold: 80% Threshold; Navy tests (see Table 12)

Test ID	Fire Type	Material	Detector		Alarm Times (s)		Percent Error
			ID	Type	Experiment	Predicted	
1-51	Flaming	Wood	18	Photo	612	985	61%
1-51	Flaming	Wood	20	Photo	82	985	1101%
1-51	Flaming	Wood	22	Photo	518	985	90%
1-52	Flaming	Wood	14	Photo	38	DNA (0.054 @ 32 s)	
1-52	Flaming	Wood	16	Photo	35	DNA (0.054 @ 32 s)	
1-52	Flaming	Wood	18	Photo	49	DNA (0.062 @ 1469 s)	
1-52	Flaming	Wood	20	Photo	40	DNA (0.062 @ 1469 s)	
1-53	Flaming	Wood	14	Photo	662	1859	181%
1-53	Flaming	Wood	16	Photo	768	1859	142%
1-53	Flaming	Wood	18	Photo	841	1831	118%
1-53	Flaming	Wood	20	Photo	689	1831	166%
1-53	Flaming	Wood	22	Photo	680	1807	166%
1-53	Flaming	Wood	24	Photo	906	1807	99%
1-54	Flaming	Wood	14	Photo	51	41	-20%
1-54	Flaming	Wood	16	Photo	45	41	-9%
1-54	Flaming	Wood	18	Photo	96	50	-48%
1-54	Flaming	Wood	20	Photo	49	50	2%
1-55	Flaming	Wood	16	Photo	35	40	14%
1-55	Flaming	Wood	18	Photo	55	35	-36%
1-55	Flaming	Wood	20	Photo	35	35	0%
2-09	Flaming	Cardboard	2	Photo	480	DNA (0.052 @ 647 s)	
2-09	Flaming	Cardboard	4	Photo	169	DNA (0.052 @ 647 s)	
2-09	Flaming	Cardboard	6	Photo	129	672	421%
2-09	Flaming	Cardboard	8	Photo	124	672	442%
2-10	Flaming	Cardboard	2	Photo	643	478	-26%
2-10	Flaming	Cardboard	4	Photo	281	478	70%
2-10	Flaming	Cardboard	6	Photo	592	449	-24%
2-10	Flaming	Cardboard	8	Photo	260	449	73%
2-11	Flaming	Cardboard	2	Photo	76	526	592%
2-11	Flaming	Cardboard	4	Photo	84	526	526%
2-11	Flaming	Cardboard	6	Photo	110	555	405%
2-11	Flaming	Cardboard	8	Photo	93	555	497%
2-12	Flaming	Cardboard	6	Photo	115	DNA (0.025 @ 519 s)	
2-12	Flaming	Cardboard	8	Photo	107	DNA (0.025 @ 519 s)	
2-21	Flaming	Cardboard	14	Photo	164	DNA (0.055 @ 567 s)	
2-21	Flaming	Cardboard	16	Photo	153	DNA (0.055 @ 567 s)	

Optical Density Alarm Threshold: 80% Threshold; Navy tests (see Table 12)

Test ID	Fire Type	Material	Detector		Alarm Times (s)		Percent Error
			ID	Type	Experiment	Predicted	
2-21	Flaming	Cardboard	18	Photo	498	DNA (0.051 @ 765 s)	
2-21	Flaming	Cardboard	20	Photo	482	DNA (0.051 @ 765 s)	
2-21	Flaming	Cardboard	22	Photo	477	DNA (0.049 @ 755 s)	
2-21	Flaming	Cardboard	24	Photo	474	DNA (0.049 @ 755 s)	
2-22	Flaming	Cardboard	14	Photo	83	DNA (0.049 @ 95 s)	
2-22	Flaming	Cardboard	16	Photo	414	DNA (0.049 @ 95 s)	
2-22	Flaming	Cardboard	18	Photo	479	DNA (0.027 @ 132 s)	
2-22	Flaming	Cardboard	20	Photo	455	DNA (0.027 @ 132 s)	
2-22	Flaming	Cardboard	22	Photo	118	DNA (0.028 @ 117 s)	
2-22	Flaming	Cardboard	24	Photo	443	DNA (0.028 @ 117 s)	
2-23	Flaming	Cardboard	14	Photo	151	DNA (0.036 @ 684 s)	
2-23	Flaming	Cardboard	16	Photo	139	DNA (0.036 @ 684 s)	
2-23	Flaming	Cardboard	18	Photo	97	DNA (0.045 @ 715 s)	
2-23	Flaming	Cardboard	20	Photo	310	DNA (0.045 @ 715 s)	
2-23	Flaming	Cardboard	22	Photo	173	DNA (0.040 @ 727 s)	
2-23	Flaming	Cardboard	24	Photo	139	DNA (0.040 @ 727 s)	
2-24	Flaming	Cardboard	14	Photo	139	DNA (0.024 @ 497 s)	
2-24	Flaming	Cardboard	18	Photo	89	DNA (0.032 @ 458 s)	
2-24	Flaming	Cardboard	20	Photo	417	DNA (0.032 @ 458 s)	
2-24	Flaming	Cardboard	22	Photo	128	DNA (0.028 @ 470 s)	
2-24	Flaming	Cardboard	24	Photo	413	DNA (0.028 @ 470 s)	
2-25	Smoldering	Potassium Chlorate / Lactose	15	Ion	222	DNA (0.037 @ 124 s)	
2-25	Smoldering	Potassium Chlorate / Lactose	19	Ion	306	DNA (0.023 @ 217 s)	
2-27	Smoldering	Potassium Chlorate / Lactose	19	Ion	152	DNA (0.112 @ 62 s)	
2-27	Smoldering	Potassium Chlorate / Lactose	23	Ion	69	DNA (0.055 @ 125 s)	

Optical Density Alarm Threshold: 80% Threshold; Navy tests (see Table 12)

Test ID	Fire Type	Material	Detector		Alarm Times (s)		Percent Error
			ID	Type	Experiment	Predicted	
2-34	Smoldering	Electrical Cable	19	Ion	840	227	-73%
2-36	Smoldering	Electrical Cable	19	Ion	1490	1342	-10%
2-37	Smoldering	Electrical Cable	19	Ion	393	341	-13%
2-26	Smoldering	Potassium Chlorate / Lactose	15	Ion	196	DNA (0.044 @ 82 s)	
2-26	Smoldering	Potassium Chlorate / Lactose	19	Ion	234	DNA (0.086 @ 51 s)	
2-28	Smoldering	Potassium Chlorate / Lactose	19	Ion	444	DNA (0.089 @ 80 s)	
2-28	Smoldering	Potassium Chlorate / Lactose	23	Ion	40	DNA (0.033 @ 160 s)	
2-38	Smoldering	Electrical Cable	19	Ion	768	DNA (0.048 @ 704 s)	
2-38	Smoldering	Electrical Cable	23	Ion	730	DNA (0.031 @ 791 s)	
2-40	Smoldering	Electrical Cable	15	Ion	983	480	-51%
2-01	Smoldering	Electrical Cable	1	Ion	2029	1985	-2%
2-01	Smoldering	Electrical Cable	5	Ion	2138	2038	-5%
2-04	Smoldering	Electrical Cable	5	Ion	1057	486	-54%
2-07	Smoldering	Electrical Cable	1	Ion	831	887	7%
2-07	Smoldering	Electrical Cable	5	Ion	1365	856	-37%
2-13	Smoldering	Potassium Chlorate / Lactose	5	Ion	536	DNA (0.077 @ 527 s)	
2-14	Smoldering	Potassium Chlorate / Lactose	1	Ion	18	13	-28%
2-14	Smoldering	Potassium Chlorate / Lactose	5	Ion	98	DNA (0.059 @ 53 s)	
2-25	Smoldering	Potassium Chlorate / Lactose	13	Ion	100	DNA (0.037 @ 124 s)	
2-25	Smoldering	Potassium Chlorate / Lactose	17	Ion	126	DNA (0.023 @ 217 s)	
2-25	Smoldering	Potassium Chlorate / Lactose	21	Ion	205	DNA (0.091 @ 78 s)	
2-27	Smoldering	Potassium Chlorate / Lactose	13	Ion	257	DNA (0.011 @ 99 s)	
2-27	Smoldering	Potassium Chlorate / Lactose	17	Ion	74	DNA (0.112 @ 62 s)	
2-27	Smoldering	Potassium Chlorate / Lactose	21	Ion	66	DNA (0.055 @ 125 s)	
2-34	Smoldering	Electrical Cable	17	Ion	659	227	-66%
2-36	Smoldering	Electrical Cable	17	Ion	1354	1342	-1%
2-37	Smoldering	Electrical Cable	13	Ion	678	DNA (0.121 @ 708 s)	
2-37	Smoldering	Electrical Cable	17	Ion	335	341	2%
2-37	Smoldering	Electrical Cable	21	Ion	566	575	2%
2-39	Smoldering	Electrical Cable	13	Ion	760	279	-63%
2-05	Smoldering	Electrical Cable	1	Ion	1695	1944	15%
2-05	Smoldering	Electrical Cable	5	Ion	643	397	-38%

Optical Density Alarm Threshold: 80% Threshold; Navy tests (see Table 12)

Test ID	Fire Type	Material	Detector ID	Type	Experiment	Predicted	Percent Error
2-08	Smoldering	Electrical Cable	1	Ion	1372	DNA (0.117 @ 1616 s)	
2-08	Smoldering	Electrical Cable	5	Ion	1391	1592	14%
2-15	Smoldering	Potassium Chlorate / Lactose	1	Ion	19	DNA (0.109 @ 57 s)	
2-15	Smoldering	Potassium Chlorate / Lactose	5	Ion	70	DNA (0.047 @ 99 s)	
2-26	Smoldering	Potassium Chlorate / Lactose	13	Ion	64	DNA (0.044 @ 82 s)	
2-26	Smoldering	Potassium Chlorate / Lactose	17	Ion	53	DNA (0.086 @ 51 s)	
2-26	Smoldering	Potassium Chlorate / Lactose	21	Ion	145	19	-87%
2-28	Smoldering	Potassium Chlorate / Lactose	13	Ion	192	DNA (0.039 @ 134 s)	
2-28	Smoldering	Potassium Chlorate / Lactose	17	Ion	122	DNA (0.089 @ 80 s)	
2-28	Smoldering	Potassium Chlorate / Lactose	21	Ion	38	DNA (0.033 @ 160 s)	
2-35	Smoldering	Electrical Cable	17	Ion	922	363	-61%
2-35	Smoldering	Electrical Cable	21	Ion	1408	1532	9%
2-38	Smoldering	Electrical Cable	13	Ion	767	DNA (0.039 @ 745 s)	
2-38	Smoldering	Electrical Cable	17	Ion	771	DNA (0.048 @ 704 s)	
2-38	Smoldering	Electrical Cable	21	Ion	561	DNA (0.031 @ 791 s)	
2-40	Smoldering	Electrical Cable	13	Ion	448	480	7%
2-01	Smoldering	Electrical Cable	2	Photo	2034	1978	-3%
2-01	Smoldering	Electrical Cable	4	Photo	2232	1978	-11%
2-01	Smoldering	Electrical Cable	8	Photo	2232	2016	-10%
2-04	Smoldering	Electrical Cable	2	Photo	1713	974	-43%
2-04	Smoldering	Electrical Cable	6	Photo	796	484	-39%
2-07	Smoldering	Electrical Cable	4	Photo	936	827	-12%
2-07	Smoldering	Electrical Cable	6	Photo	908	781	-14%
2-13	Smoldering	Potassium Chlorate / Lactose	2	Photo	578	DNA (0.078 @ 527 s)	
2-13	Smoldering	Potassium Chlorate / Lactose	4	Photo	572	DNA (0.078 @ 527 s)	
2-13	Smoldering	Potassium Chlorate / Lactose	6	Photo	524	DNA (0.077 @ 527 s)	
2-13	Smoldering	Potassium Chlorate / Lactose	8	Photo	710	DNA (0.077 @ 527 s)	
2-14	Smoldering	Potassium Chlorate / Lactose	2	Photo	20	12	-40%
2-14	Smoldering	Potassium Chlorate / Lactose	4	Photo	33	12	-64%
2-25	Smoldering	Potassium Chlorate / Lactose	14	Photo	94	DNA (0.037 @ 124 s)	

Optical Density Alarm Threshold: 80% Threshold; Navy tests (see Table 12)

Test ID	Fire Type	Material	Detector ID	Type	Alarm Times (s) Experiment	Predicted	Percent Error
2-25	Smoldering	Potassium Chlorate / Lactose	16	Photo	105	DNA (0.037 @ 124 s)	
2-25	Smoldering	Potassium Chlorate / Lactose	18	Photo	170	DNA (0.023 @ 217 s)	
2-25	Smoldering	Potassium Chlorate / Lactose	20	Photo	301	DNA (0.023 @ 217 s)	
2-25	Smoldering	Potassium Chlorate / Lactose	24	Photo	164	DNA (0.091 @ 78 s)	
2-27	Smoldering	Potassium Chlorate / Lactose	18	Photo	49	DNA (0.112 @ 62 s)	
2-27	Smoldering	Potassium Chlorate / Lactose	20	Photo	68	DNA (0.112 @ 62 s)	
2-27	Smoldering	Potassium Chlorate / Lactose	22	Photo	67	DNA (0.055 @ 125 s)	
2-27	Smoldering	Potassium Chlorate / Lactose	24	Photo	65	DNA (0.055 @ 125 s)	
2-34	Smoldering	Electrical Cable	18	Photo	297	227	-24%
2-34	Smoldering	Electrical Cable	20	Photo	648	227	-65%
2-34	Smoldering	Electrical Cable	22	Photo	843	DNA (0.074 @ 720 s)	
2-34	Smoldering	Electrical Cable	24	Photo	732	DNA (0.074 @ 720 s)	
2-36	Smoldering	Electrical Cable	14	Photo	1611	DNA (0.091 @ 1794 s)	
2-36	Smoldering	Electrical Cable	18	Photo	756	1334	76%
2-36	Smoldering	Electrical Cable	20	Photo	860	1334	55%
2-36	Smoldering	Electrical Cable	22	Photo	1356	1480	9%
2-36	Smoldering	Electrical Cable	24	Photo	915	1480	62%
2-37	Smoldering	Electrical Cable	14	Photo	759	695	-8%
2-37	Smoldering	Electrical Cable	16	Photo	735	695	-5%
2-37	Smoldering	Electrical Cable	18	Photo	295	329	12%
2-37	Smoldering	Electrical Cable	20	Photo	331	329	-1%
2-37	Smoldering	Electrical Cable	22	Photo	633	575	-9%
2-37	Smoldering	Electrical Cable	24	Photo	506	575	14%
2-39	Smoldering	Electrical Cable	14	Photo	941	279	-70%
2-39	Smoldering	Electrical Cable	16	Photo	856	279	-67%
2-39	Smoldering	Electrical Cable	18	Photo	1362	DNA (0.046 @ 1518 s)	
2-39	Smoldering	Electrical Cable	22	Photo	786	DNA (0.078 @ 1542 s)	
2-39	Smoldering	Electrical Cable	24	Photo	689	DNA (0.078 @ 1542 s)	
2-02	Smoldering	Electrical Cable	2	Photo	775	DNA (0.074 @ 2081 s)	
2-02	Smoldering	Electrical Cable	4	Photo	2000	DNA (0.074 @ 2081 s)	
2-02	Smoldering	Electrical Cable	6	Photo	656	DNA (0.039 @ 618 s)	
2-05	Smoldering	Electrical Cable	2	Photo	559	1931	245%

Optical Density Alarm Threshold: 80% Threshold; Navy tests (see Table 12)

Test ID	Fire Type	Material	Detector		Alarm Times (s)		Percent Error
			ID	Type	Experiment	Predicted	
2-05	Smoldering	Electrical Cable	4	Photo	639	1931	202%
2-05	Smoldering	Electrical Cable	6	Photo	424	397	-6%
2-05	Smoldering	Electrical Cable	8	Photo	297	397	34%
2-08	Smoldering	Electrical Cable	2	Photo	728	DNA (0.117 @ 1616 s)	
2-08	Smoldering	Electrical Cable	4	Photo	845	DNA (0.117 @ 1616 s)	
2-08	Smoldering	Electrical Cable	6	Photo	539	1377	155%
2-08	Smoldering	Electrical Cable	8	Photo	775	1377	78%
2-15	Smoldering	Potassium Chlorate / Lactose	2	Photo	19	DNA (0.109 @ 57 s)	
2-15	Smoldering	Potassium Chlorate / Lactose	4	Photo	112	DNA (0.109 @ 57 s)	
2-15	Smoldering	Potassium Chlorate / Lactose	6	Photo	81	DNA (0.047 @ 99 s)	
2-15	Smoldering	Potassium Chlorate / Lactose	8	Photo	83	DNA (0.047 @ 99 s)	
2-26	Smoldering	Potassium Chlorate / Lactose	14	Photo	68	DNA (0.044 @ 82 s)	
2-26	Smoldering	Potassium Chlorate / Lactose	16	Photo	246	DNA (0.044 @ 82 s)	
2-26	Smoldering	Potassium Chlorate / Lactose	18	Photo	65	DNA (0.086 @ 51 s)	
2-28	Smoldering	Potassium Chlorate / Lactose	16	Photo	331	DNA (0.039 @ 134 s)	
2-28	Smoldering	Potassium Chlorate / Lactose	18	Photo	92	DNA (0.089 @ 80 s)	
2-28	Smoldering	Potassium Chlorate / Lactose	20	Photo	348	DNA (0.089 @ 80 s)	
2-28	Smoldering	Potassium Chlorate / Lactose	22	Photo	34	DNA (0.033 @ 160 s)	
2-28	Smoldering	Potassium Chlorate / Lactose	24	Photo	32	DNA (0.033 @ 160 s)	
2-35	Smoldering	Electrical Cable	18	Photo	423	362	-14%
2-35	Smoldering	Electrical Cable	20	Photo	851	362	-57%
2-35	Smoldering	Electrical Cable	22	Photo	656	1532	134%
2-35	Smoldering	Electrical Cable	24	Photo	989	1532	55%
2-38	Smoldering	Electrical Cable	14	Photo	754	DNA (0.039 @ 745 s)	
2-38	Smoldering	Electrical Cable	16	Photo	843	DNA (0.039 @ 745 s)	
2-38	Smoldering	Electrical Cable	18	Photo	549	DNA (0.048 @ 704 s)	
2-38	Smoldering	Electrical Cable	20	Photo	709	DNA (0.048 @ 704 s)	
2-38	Smoldering	Electrical Cable	22	Photo	189	DNA (0.031 @ 791 s)	
2-38	Smoldering	Electrical Cable	24	Photo	418	DNA (0.031 @ 791 s)	

Optical Density Alarm Threshold: 80% Threshold; Navy tests (see Table 12)

Test ID	Fire Type	Material	Detector		Alarm Times (s)		Percent Error
			ID	Type	Experiment	Predicted	
2-40	Smoldering	Electrical Cable	14	Photo	402	479	19%
2-40	Smoldering	Electrical Cable	16	Photo	679	479	-29%
2-40	Smoldering	Electrical Cable	18	Photo	1201	DNA (0.037 @ 1503 s)	
2-40	Smoldering	Electrical Cable	20	Photo	1387	DNA (0.037 @ 1503 s)	
2-40	Smoldering	Electrical Cable	22	Photo	1542	DNA (0.058 @ 1632 s)	

Optical Density Alarm Threshold: 20% Threshold; Kemano tests (see Table 12)

Test ID	Fire Type	Material	Detector ID	Detector Type	Experiment	Predicted	Percent Error
01	Flaming	Wood	28	Ion	480	388	-100%
02	Flaming	Wood	14	Ion	1359	390	-100%
02	Flaming	Wood	28	Ion	1388	1379	-1%
03	Flaming	Cotton Fabric	8	Ion	122	377	472%
03	Flaming	Cotton Fabric	14	Ion	155	390	270%
03	Flaming	Cotton Fabric	28	Ion	226	DNA (0.006 @ 550 s)	
05	Flaming	Upholstered Furniture	28	Ion	875	757	-100%
06	Flaming	Wood	8	Ion	1111	1095	-2%
06	Flaming	Wood	14	Ion	389	245	-93%
06	Flaming	Wood	28	Ion	277	234	-100%
07	Flaming	Wood	8	Ion	1107	1093	-3%
08	Flaming	Upholstered Furniture	8	Ion	760	726	-100%
08	Flaming	Upholstered Furniture	14	Ion	860	726	-100%
09	Flaming	Upholstered Furniture	14	Ion	906	854	-100%
10	Flaming	Wood	13	Ion	2851	2744	-100%
11	Flaming	Upholstered Furniture	4	Ion	1723	1674	-100%
11	Flaming	Upholstered Furniture	7	Ion	1763	1674	-100%
13	Flaming	Paper	13	Ion	4977	4794	-100%
01	Flaming	Wood	26	Photo	545	388	-100%
02	Flaming	Wood	16	Photo	1377	575	-81%
02	Flaming	Wood	26	Photo	1408	1379	-3%
03	Flaming	Cotton Fabric	6	Photo	403	DNA (0.012 @ 462 s)	
03	Flaming	Cotton Fabric	16	Photo	368	DNA (0.011 @ 509 s)	
04	Flaming	Paper	26	Photo	787	591	-100%
05	Flaming	Upholstered Furniture	26	Photo	922	757	-100%
06	Flaming	Wood	6	Photo	1112	1100	-1%
06	Flaming	Wood	26	Photo	265	234	-100%
07	Flaming	Wood	6	Photo	1115	1094	-4%
01	Smoldering	Wood	8	Ion	269	171	-36%
01	Smoldering	Wood	14	Ion	422	213	-50%
02	Smoldering	Wood	8	Ion	218	142	-35%
04	Smoldering	Paper	8	Ion	522	293	-44%
04	Smoldering	Paper	14	Ion	377	325	-14%
04	Smoldering	Paper	28	Ion	686	474	-31%
05	Smoldering	Upholstered Furniture	8	Ion	325	231	-29%
05	Smoldering	Upholstered Furniture	14	Ion	315	262	-17%
07	Smoldering	Wood	14	Ion	606	334	-45%
07	Smoldering	Wood	28	Ion	383	236	-38%
08	Smoldering	Upholstered Furniture	28	Ion	715	193	-73%
09	Smoldering	Upholstered Furniture	8	Ion	924	534	-42%

Optical Density Alarm Threshold: 20% Threshold; Kemano tests (see Table 12)

Test ID	Fire Type	Material	Detector ID	Type	Experiment	Predicted	Percent Error
09	Smoldering	Upholstered Furniture	28	Ion	795	138	-83%
10	Smoldering	Wood	4	Ion	1044	446	-57%
10	Smoldering	Wood	7	Ion	2017	735	-64%
13	Smoldering	Paper	4	Ion	3246	432	-87%
13	Smoldering	Paper	7	Ion	4001	2152	-46%
01	Smoldering	Wood	6	Photo	313	170	-46%
01	Smoldering	Wood	16	Photo	337	209	-38%
02	Smoldering	Wood	6	Photo	223	142	-36%
04	Smoldering	Paper	6	Photo	521	292	-44%
04	Smoldering	Paper	16	Photo	373	298	-20%
05	Smoldering	Upholstered Furniture	6	Photo	461	230	-50%
05	Smoldering	Upholstered Furniture	16	Photo	356	257	-28%
06	Smoldering	Wood	16	Photo	297	DNA (0.006 @ 234 s)	
07	Smoldering	Wood	16	Photo	342	331	-3%
07	Smoldering	Wood	26	Photo	374	233	-38%
08	Smoldering	Upholstered Furniture	6	Photo	376	438	16%
08	Smoldering	Upholstered Furniture	16	Photo	334	301	-10%
08	Smoldering	Upholstered Furniture	26	Photo	254	193	-24%
09	Smoldering	Upholstered Furniture	6	Photo	755	460	-39%
09	Smoldering	Upholstered Furniture	16	Photo	376	318	-15%
09	Smoldering	Upholstered Furniture	26	Photo	288	128	-56%
10	Smoldering	Wood	6	Photo	504	385	-24%
10	Smoldering	Wood	9	Photo	605	688	14%
10	Smoldering	Wood	15	Photo	687	828	21%
11	Smoldering	Upholstered Furniture	6	Photo	371	309	-17%
11	Smoldering	Upholstered Furniture	9	Photo	439	465	6%
11	Smoldering	Upholstered Furniture	15	Photo	580	605	4%
13	Smoldering	Paper	6	Photo	479	431	-10%
13	Smoldering	Paper	9	Photo	658	948	44%
13	Smoldering	Paper	15	Photo	725	1404	94%

Optical Density Alarm Threshold: 50% Threshold; Kemano tests (see Table 12)

Test ID	Fire Type	Material	Detector		Alarm Times (s)		Percent Error
			ID	Type	Experiment	Predicted	
01	Flaming	Wood	28	Ion	480	388	-100%
02	Flaming	Wood	14	Ion	1359	496	-89%
02	Flaming	Wood	28	Ion	1388	1379	-1%
03	Flaming	Cotton Fabric	8	Ion	122	DNA (0.012 @ 462 s)	
03	Flaming	Cotton Fabric	14	Ion	155	DNA (0.011 @ 509 s)	
03	Flaming	Cotton Fabric	28	Ion	226	DNA (0.006 @ 550 s)	
05	Flaming	Upholstered Furniture	28	Ion	875	757	-100%
06	Flaming	Wood	8	Ion	1111	1096	-2%
06	Flaming	Wood	14	Ion	389	278	-72%
06	Flaming	Wood	28	Ion	277	234	-100%
07	Flaming	Wood	8	Ion	1107	1094	-3%
08	Flaming	Upholstered Furniture	8	Ion	760	726	-100%
08	Flaming	Upholstered Furniture	14	Ion	860	726	-100%
09	Flaming	Upholstered Furniture	14	Ion	906	854	-100%
10	Flaming	Wood	13	Ion	2851	2744	-100%
11	Flaming	Upholstered Furniture	4	Ion	1723	1674	-100%
11	Flaming	Upholstered Furniture	7	Ion	1763	1674	-100%
13	Flaming	Paper	13	Ion	4977	4794	-100%
01	Flaming	Wood	26	Photo	545	396	-95%
02	Flaming	Wood	16	Photo	1377	1357	-2%
02	Flaming	Wood	26	Photo	1408	1380	-3%
03	Flaming	Cotton Fabric	6	Photo	403	DNA (0.012 @ 462 s)	
03	Flaming	Cotton Fabric	16	Photo	368	DNA (0.011 @ 509 s)	
04	Flaming	Paper	26	Photo	787	591	-100%
05	Flaming	Upholstered Furniture	26	Photo	922	757	-100%
06	Flaming	Wood	6	Photo	1112	DNA (0.042 @ 1181 s)	
06	Flaming	Wood	26	Photo	265	234	-100%
07	Flaming	Wood	6	Photo	1115	1099	-3%
01	Smoldering	Wood	8	Ion	269	182	-32%
01	Smoldering	Wood	14	Ion	422	261	-38%
02	Smoldering	Wood	8	Ion	218	152	-30%
04	Smoldering	Paper	8	Ion	522	317	-39%
04	Smoldering	Paper	14	Ion	377	345	-8%
04	Smoldering	Paper	28	Ion	686	DNA (0.089 @ 526 s)	
05	Smoldering	Upholstered Furniture	8	Ion	325	239	-26%
05	Smoldering	Upholstered Furniture	14	Ion	315	286	-9%
07	Smoldering	Wood	14	Ion	606	500	-17%

Optical Density Alarm Threshold: 50% Threshold; Kemano tests (see Table 12)

Test ID	Fire Type	Material	Detector		Alarm Times (s)		Percent Error
			ID	Type	Experiment	Predicted	
07	Smoldering	Wood	28	Ion	383	246	-36%
08	Smoldering	Upholstered Furniture	28	Ion	715	197	-72%
09	Smoldering	Upholstered Furniture	8	Ion	924	DNA (0.107 @ 774 s)	
09	Smoldering	Upholstered Furniture	28	Ion	795	312	-61%
10	Smoldering	Wood	4	Ion	1044	479	-54%
10	Smoldering	Wood	7	Ion	2017	1948	-3%
13	Smoldering	Paper	4	Ion	3246	3302	2%
13	Smoldering	Paper	7	Ion	4001	DNA (0.112 @ 3630 s)	
01	Smoldering	Wood	6	Photo	313	175	-44%
01	Smoldering	Wood	16	Photo	337	223	-34%
02	Smoldering	Wood	6	Photo	223	144	-35%
04	Smoldering	Paper	6	Photo	521	297	-43%
04	Smoldering	Paper	16	Photo	373	325	-13%
05	Smoldering	Upholstered Furniture	6	Photo	461	231	-50%
05	Smoldering	Upholstered Furniture	16	Photo	356	263	-26%
06	Smoldering	Wood	16	Photo	297	DNA (0.006 @ 234 s)	
07	Smoldering	Wood	16	Photo	342	335	-2%
07	Smoldering	Wood	26	Photo	374	240	-36%
08	Smoldering	Upholstered Furniture	6	Photo	376	534	42%
08	Smoldering	Upholstered Furniture	16	Photo	334	306	-8%
08	Smoldering	Upholstered Furniture	26	Photo	254	196	-23%
09	Smoldering	Upholstered Furniture	6	Photo	755	575	-24%
09	Smoldering	Upholstered Furniture	16	Photo	376	392	4%
09	Smoldering	Upholstered Furniture	26	Photo	288	164	-43%
10	Smoldering	Wood	6	Photo	504	449	-11%
10	Smoldering	Wood	9	Photo	605	998	65%
10	Smoldering	Wood	15	Photo	687	1467	114%
11	Smoldering	Upholstered Furniture	6	Photo	371	310	-16%
11	Smoldering	Upholstered Furniture	9	Photo	439	795	81%
11	Smoldering	Upholstered Furniture	15	Photo	580	995	72%
13	Smoldering	Paper	6	Photo	479	448	-6%
13	Smoldering	Paper	9	Photo	658	2704	311%
13	Smoldering	Paper	15	Photo	725	3333	360%

Optical Density Alarm Threshold: 80% Threshold; Kemano tests (see Table 12)

| Test ID | Fire Type | Material | Detector | | Alarm Times (s) | | Percent Error |
			ID	Type	Experiment	Predicted	
01	Flaming	Wood	28	Ion	480	396	-91%
02	Flaming	Wood	14	Ion	1359	1358	0%
02	Flaming	Wood	28	Ion	1388	1381	-1%
03	Flaming	Cotton Fabric	8	Ion	122	DNA (0.012 @ 462 s)	
03	Flaming	Cotton Fabric	14	Ion	155	DNA (0.011 @ 509 s)	
03	Flaming	Cotton Fabric	28	Ion	226	DNA (0.006 @ 550 s)	
05	Flaming	Upholstered Furniture	28	Ion	875	757	-100%
06	Flaming	Wood	8	Ion	1111	DNA (0.042 @ 1181 s)	
06	Flaming	Wood	14	Ion	389	610	143%
06	Flaming	Wood	28	Ion	277	234	-100%
07	Flaming	Wood	8	Ion	1107	1099	-2%
08	Flaming	Upholstered Furniture	8	Ion	760	728	-94%
08	Flaming	Upholstered Furniture	14	Ion	860	726	-100%
09	Flaming	Upholstered Furniture	14	Ion	906	854	-100%
10	Flaming	Wood	13	Ion	2851	2744	-100%
11	Flaming	Upholstered Furniture	4	Ion	1723	1674	-100%
11	Flaming	Upholstered Furniture	7	Ion	1763	1698	-73%
13	Flaming	Paper	13	Ion	4977	4794	-100%
01	Flaming	Wood	26	Photo	545	428	-75%
02	Flaming	Wood	16	Photo	1377	1361	-2%
02	Flaming	Wood	26	Photo	1408	1387	-2%
03	Flaming	Cotton Fabric	6	Photo	403	DNA (0.012 @ 462 s)	
03	Flaming	Cotton Fabric	16	Photo	368	DNA (0.011 @ 509 s)	
04	Flaming	Paper	26	Photo	787	642	-74%
05	Flaming	Upholstered Furniture	26	Photo	922	769	-93%
06	Flaming	Wood	6	Photo	1112	DNA (0.042 @ 1181 s)	
06	Flaming	Wood	26	Photo	265	234	-100%
07	Flaming	Wood	6	Photo	1115	DNA (0.092 @ 1190 s)	
01	Smoldering	Wood	8	Ion	269	229	-15%
01	Smoldering	Wood	14	Ion	422	305	-28%
02	Smoldering	Wood	8	Ion	218	219	0%
04	Smoldering	Paper	8	Ion	522	350	-33%
04	Smoldering	Paper	14	Ion	377	448	19%
04	Smoldering	Paper	28	Ion	686	DNA (0.089 @ 526 s)	
05	Smoldering	Upholstered Furniture	8	Ion	325	240	-26%
05	Smoldering	Upholstered Furniture	14	Ion	315	292	-7%

201

Optical Density Alarm Threshold: 80% Threshold; Kemano tests (see Table 12)

Test ID	Fire Type	Material	Detector		Alarm Times (s)		Percent Error
			ID	Type	Experiment	Predicted	
07	Smoldering	Wood	14	Ion	606	DNA (0.158 @ 583 s)	
07	Smoldering	Wood	28	Ion	383	247	-36%
08	Smoldering	Upholstered Furniture	28	Ion	715	236	-67%
09	Smoldering	Upholstered Furniture	8	Ion	924	DNA (0.107 @ 774 s)	
09	Smoldering	Upholstered Furniture	28	Ion	795	330	-58%
10	Smoldering	Wood	4	Ion	1044	1541	48%
10	Smoldering	Wood	7	Ion	2017	DNA (0.130 @ 2184 s)	
13	Smoldering	Paper	4	Ion	3246	DNA (0.152 @ 3626 s)	
13	Smoldering	Paper	7	Ion	4001	DNA (0.112 @ 3630 s)	
01	Smoldering	Wood	6	Photo	313	182	-42%
01	Smoldering	Wood	16	Photo	337	247	-27%
02	Smoldering	Wood	6	Photo	223	149	-33%
04	Smoldering	Paper	6	Photo	521	317	-39%
04	Smoldering	Paper	16	Photo	373	345	-8%
05	Smoldering	Upholstered Furniture	6	Photo	461	239	-48%
05	Smoldering	Upholstered Furniture	16	Photo	356	284	-20%
06	Smoldering	Wood	16	Photo	297	DNA (0.006 @ 234 s)	
07	Smoldering	Wood	16	Photo	342	500	46%
07	Smoldering	Wood	26	Photo	374	246	-34%
08	Smoldering	Upholstered Furniture	6	Photo	376	DNA (0.105 @ 713 s)	
08	Smoldering	Upholstered Furniture	16	Photo	334	381	14%
08	Smoldering	Upholstered Furniture	26	Photo	254	197	-22%
09	Smoldering	Upholstered Furniture	6	Photo	755	DNA (0.107 @ 774 s)	
09	Smoldering	Upholstered Furniture	16	Photo	376	528	40%
09	Smoldering	Upholstered Furniture	26	Photo	288	311	8%
10	Smoldering	Wood	6	Photo	504	479	-5%
10	Smoldering	Wood	9	Photo	605	1696	180%
10	Smoldering	Wood	15	Photo	687	DNA (0.099 @ 2473 s)	
11	Smoldering	Upholstered Furniture	6	Photo	371	354	-5%
11	Smoldering	Upholstered Furniture	9	Photo	439	DNA (0.093 @ 1122 s)	
11	Smoldering	Upholstered Furniture	15	Photo	580	DNA (0.068 @ 1152 s)	
13	Smoldering	Paper	6	Photo	479	3272	583%
13	Smoldering	Paper	9	Photo	658	3630	452%
13	Smoldering	Paper	15	Photo	725	DNA (0.087 @ 4497 s)	

Temperature Rise Alarm Threshold: 4 °C

Test Series	Test ID	Fire Type	Material	Detector ID	Type	Alarm Times (s) Experiment	Predicted	Percent Error
NAVY	1-37	Flaming	Wood	1	Ion	61	104	70%
NAVY	1-37	Flaming	Wood	3	Ion	177	104	-41%
NAVY	1-37	Flaming	Wood	5	Ion	45	151	236%
NAVY	1-37	Flaming	Wood	7	Ion	174	151	-13%
NAVY	1-38	Flaming	Wood	1	Ion	62	95	53%
NAVY	1-38	Flaming	Wood	3	Ion	155	95	-39%
NAVY	1-38	Flaming	Wood	5	Ion	65	190	192%
NAVY	1-38	Flaming	Wood	7	Ion	182	190	4%
NAVY	1-39	Flaming	Wood	1	Ion	69	99	43%
NAVY	1-39	Flaming	Wood	3	Ion	43	99	130%
NAVY	1-39	Flaming	Wood	5	Ion	39	173	344%
NAVY	1-39	Flaming	Wood	7	Ion	134	173	29%
NAVY	1-40	Flaming	Wood	1	Ion	43	139	223%
NAVY	1-40	Flaming	Wood	3	Ion	123	139	13%
NAVY	1-40	Flaming	Wood	5	Ion	39	119	205%
NAVY	1-40	Flaming	Wood	7	Ion	57	119	109%
NAVY	1-41	Flaming	Wood	1	Ion	69	36	-48%
NAVY	1-41	Flaming	Wood	3	Ion	152	36	-76%
NAVY	1-41	Flaming	Wood	5	Ion	46	106	130%
NAVY	1-41	Flaming	Wood	7	Ion	124	106	-15%
NAVY	1-50	Flaming	Wood	9	Ion	24	34	42%
NAVY	1-50	Flaming	Wood	11	Ion	25	34	36%
NAVY	1-50	Flaming	Wood	13	Ion	48	148	208%
NAVY	1-50	Flaming	Wood	15	Ion	65	148	128%
NAVY	1-50	Flaming	Wood	17	Ion	75	126	68%
NAVY	1-50	Flaming	Wood	19	Ion	128	126	-2%
NAVY	1-50	Flaming	Wood	21	Ion	112	149	33%
NAVY	1-50	Flaming	Wood	23	Ion	161	149	-7%
NAVY	1-51	Flaming	Wood	9	Ion	22	100	355%
NAVY	1-51	Flaming	Wood	11	Ion	22	100	355%
NAVY	1-51	Flaming	Wood	13	Ion	44	206	368%
NAVY	1-51	Flaming	Wood	15	Ion	90	206	129%
NAVY	1-51	Flaming	Wood	17	Ion	79	166	110%
NAVY	1-51	Flaming	Wood	19	Ion	182	166	-9%
NAVY	1-51	Flaming	Wood	21	Ion	99	224	126%
NAVY	1-51	Flaming	Wood	23	Ion	89	224	152%
NAVY	1-52	Flaming	Wood	9	Ion	21	151	619%
NAVY	1-52	Flaming	Wood	11	Ion	25	151	504%
NAVY	1-52	Flaming	Wood	13	Ion	38	152	300%
NAVY	1-52	Flaming	Wood	15	Ion	65	152	134%
NAVY	1-52	Flaming	Wood	19	Ion	73	88	21%
NAVY	1-52	Flaming	Wood	21	Ion	84	430	412%
NAVY	1-52	Flaming	Wood	23	Ion	177	430	143%
NAVY	1-53	Flaming	Wood	11	Ion	16	127	694%

Temperature Rise Alarm Threshold: 4 °C

Test Series	Test ID	Fire Type	Material	Detector		Alarm Times (s)		Percent Error
				ID	Type	Experiment	Predicted	
NAVY	1-53	Flaming	Wood	13	Ion	42	208	395%
NAVY	1-53	Flaming	Wood	15	Ion	101	208	106%
NAVY	1-53	Flaming	Wood	17	Ion	123	212	72%
NAVY	1-53	Flaming	Wood	19	Ion	126	212	68%
NAVY	1-53	Flaming	Wood	21	Ion	95	277	192%
NAVY	1-53	Flaming	Wood	23	Ion	164	277	69%
NAVY	1-54	Flaming	Wood	9	Ion	27	46	70%
NAVY	1-54	Flaming	Wood	13	Ion	50	55	10%
NAVY	1-54	Flaming	Wood	15	Ion	66	55	-17%
NAVY	1-54	Flaming	Wood	17	Ion	75	151	101%
NAVY	1-54	Flaming	Wood	19	Ion	116	151	30%
NAVY	1-55	Flaming	Wood	13	Ion	36	69	92%
NAVY	1-55	Flaming	Wood	15	Ion	68	69	1%
NAVY	1-55	Flaming	Wood	17	Ion	53	62	17%
NAVY	1-55	Flaming	Wood	19	Ion	43	62	44%
NAVY	2-09	Flaming	Cardboard	1	Ion	162	184	14%
NAVY	2-09	Flaming	Cardboard	3	Ion	165	184	12%
NAVY	2-09	Flaming	Cardboard	5	Ion	86	104	21%
NAVY	2-09	Flaming	Cardboard	7	Ion	100	104	4%
NAVY	2-10	Flaming	Cardboard	1	Ion	229	122	-47%
NAVY	2-10	Flaming	Cardboard	3	Ion	239	122	-49%
NAVY	2-10	Flaming	Cardboard	5	Ion	166	47	-72%
NAVY	2-10	Flaming	Cardboard	7	Ion	228	47	-79%
NAVY	2-11	Flaming	Cardboard	3	Ion	67	83	24%
NAVY	2-11	Flaming	Cardboard	5	Ion	93	100	8%
NAVY	2-11	Flaming	Cardboard	7	Ion	89	100	12%
NAVY	2-12	Flaming	Cardboard	1	Ion	28	79	182%
NAVY	2-12	Flaming	Cardboard	3	Ion	57	79	39%
NAVY	2-12	Flaming	Cardboard	5	Ion	66	77	17%
NAVY	2-12	Flaming	Cardboard	7	Ion	63	77	22%
NAVY	2-21	Flaming	Cardboard	9	Ion	93	161	73%
NAVY	2-21	Flaming	Cardboard	11	Ion	247	161	-35%
NAVY	2-21	Flaming	Cardboard	13	Ion	63	61	-3%
NAVY	2-21	Flaming	Cardboard	15	Ion	36	61	69%
NAVY	2-21	Flaming	Cardboard	17	Ion	151	206	36%
NAVY	2-21	Flaming	Cardboard	19	Ion	174	206	18%
NAVY	2-21	Flaming	Cardboard	21	Ion	143	162	13%
NAVY	2-21	Flaming	Cardboard	23	Ion	195	162	-17%
NAVY	2-22	Flaming	Cardboard	9	Ion	74	117	58%
NAVY	2-22	Flaming	Cardboard	11	Ion	129	117	-9%
NAVY	2-22	Flaming	Cardboard	13	Ion	43	74	72%
NAVY	2-22	Flaming	Cardboard	15	Ion	30	74	147%
NAVY	2-22	Flaming	Cardboard	17	Ion	302	114	-62%
NAVY	2-22	Flaming	Cardboard	19	Ion	126	114	-10%

Temperature Rise Alarm Threshold: 4 °C

Test Series	Test ID	Fire Type	Material	Detector		Alarm Times (s)		Percent Error
				ID	Type	Experiment	Predicted	
NAVY	2-22	Flaming	Cardboard	21	Ion	87	95	9%
NAVY	2-22	Flaming	Cardboard	23	Ion	127	95	-25%
NAVY	2-23	Flaming	Cardboard	11	Ion	120	177	48%
NAVY	2-23	Flaming	Cardboard	13	Ion	119	205	72%
NAVY	2-23	Flaming	Cardboard	15	Ion	143	205	43%
NAVY	2-23	Flaming	Cardboard	17	Ion	54	112	107%
NAVY	2-23	Flaming	Cardboard	19	Ion	122	112	-8%
NAVY	2-23	Flaming	Cardboard	21	Ion	125	194	55%
NAVY	2-23	Flaming	Cardboard	23	Ion	144	194	35%
NAVY	2-24	Flaming	Cardboard	11	Ion	98	129	32%
NAVY	2-24	Flaming	Cardboard	13	Ion	117	161	38%
NAVY	2-24	Flaming	Cardboard	15	Ion	142	161	13%
NAVY	2-24	Flaming	Cardboard	17	Ion	62	79	27%
NAVY	2-24	Flaming	Cardboard	19	Ion	100	79	-21%
NAVY	2-24	Flaming	Cardboard	21	Ion	58	127	119%
NAVY	2-24	Flaming	Cardboard	23	Ion	67	127	90%
NAVY	1-37	Flaming	Wood	2	Photo	901	104	-88%
NAVY	1-37	Flaming	Wood	4	Photo	1007	104	-90%
NAVY	1-37	Flaming	Wood	6	Photo	816	151	-81%
NAVY	1-37	Flaming	Wood	8	Photo	990	151	-85%
NAVY	1-38	Flaming	Wood	2	Photo	874	95	-89%
NAVY	1-38	Flaming	Wood	4	Photo	860	95	-89%
NAVY	1-38	Flaming	Wood	6	Photo	794	190	-76%
NAVY	1-38	Flaming	Wood	8	Photo	943	190	-80%
NAVY	1-39	Flaming	Wood	2	Photo	546	99	-82%
NAVY	1-39	Flaming	Wood	4	Photo	555	99	-82%
NAVY	1-39	Flaming	Wood	6	Photo	366	173	-53%
NAVY	1-39	Flaming	Wood	8	Photo	634	173	-73%
NAVY	1-40	Flaming	Wood	2	Photo	1036	139	-87%
NAVY	1-40	Flaming	Wood	4	Photo	886	139	-84%
NAVY	1-40	Flaming	Wood	6	Photo	956	119	-88%
NAVY	1-40	Flaming	Wood	8	Photo	1023	119	-88%
NAVY	1-41	Flaming	Wood	2	Photo	529	36	-93%
NAVY	1-41	Flaming	Wood	4	Photo	494	36	-93%
NAVY	1-41	Flaming	Wood	6	Photo	484	106	-78%
NAVY	1-41	Flaming	Wood	8	Photo	553	106	-81%
NAVY	1-50	Flaming	Wood	12	Photo	1113	34	-97%
NAVY	1-50	Flaming	Wood	16	Photo	1149	148	-87%
NAVY	1-50	Flaming	Wood	20	Photo	1194	126	-89%
NAVY	1-50	Flaming	Wood	24	Photo	1149	149	-87%
NAVY	1-51	Flaming	Wood	10	Photo	28	100	257%
NAVY	1-51	Flaming	Wood	12	Photo	17	100	488%
NAVY	1-51	Flaming	Wood	14	Photo	54	206	281%
NAVY	1-51	Flaming	Wood	16	Photo	53	206	289%

Temperature Rise Alarm Threshold: 4 °C

Test Series	Test ID	Fire Type	Material	Detector ID	Detector Type	Alarm Times (s) Experiment	Alarm Times (s) Predicted	Percent Error
NAVY	1-51	Flaming	Wood	18	Photo	612	166	-73%
NAVY	1-51	Flaming	Wood	20	Photo	82	166	102%
NAVY	1-51	Flaming	Wood	22	Photo	518	224	-57%
NAVY	1-52	Flaming	Wood	10	Photo	16	151	844%
NAVY	1-52	Flaming	Wood	12	Photo	17	151	788%
NAVY	1-52	Flaming	Wood	14	Photo	38	152	300%
NAVY	1-52	Flaming	Wood	16	Photo	35	152	334%
NAVY	1-52	Flaming	Wood	18	Photo	49	88	80%
NAVY	1-52	Flaming	Wood	20	Photo	40	88	120%
NAVY	1-53	Flaming	Wood	10	Photo	790	127	-84%
NAVY	1-53	Flaming	Wood	12	Photo	908	127	-86%
NAVY	1-53	Flaming	Wood	14	Photo	662	208	-69%
NAVY	1-53	Flaming	Wood	16	Photo	768	208	-73%
NAVY	1-53	Flaming	Wood	18	Photo	841	212	-75%
NAVY	1-53	Flaming	Wood	20	Photo	689	212	-69%
NAVY	1-53	Flaming	Wood	22	Photo	680	277	-59%
NAVY	1-53	Flaming	Wood	24	Photo	906	277	-69%
NAVY	1-54	Flaming	Wood	10	Photo	51	46	-10%
NAVY	1-54	Flaming	Wood	14	Photo	51	55	8%
NAVY	1-54	Flaming	Wood	16	Photo	45	55	22%
NAVY	1-54	Flaming	Wood	18	Photo	96	151	57%
NAVY	1-54	Flaming	Wood	20	Photo	49	151	208%
NAVY	1-55	Flaming	Wood	10	Photo	40	145	263%
NAVY	1-55	Flaming	Wood	16	Photo	35	69	97%
NAVY	1-55	Flaming	Wood	18	Photo	55	62	13%
NAVY	1-55	Flaming	Wood	20	Photo	35	62	77%
NAVY	2-09	Flaming	Cardboard	2	Photo	480	184	-62%
NAVY	2-09	Flaming	Cardboard	4	Photo	169	184	9%
NAVY	2-09	Flaming	Cardboard	6	Photo	129	104	-19%
NAVY	2-09	Flaming	Cardboard	8	Photo	124	104	-16%
NAVY	2-10	Flaming	Cardboard	2	Photo	643	122	-81%
NAVY	2-10	Flaming	Cardboard	4	Photo	281	122	-57%
NAVY	2-10	Flaming	Cardboard	6	Photo	592	47	-92%
NAVY	2-10	Flaming	Cardboard	8	Photo	260	47	-82%
NAVY	2-11	Flaming	Cardboard	2	Photo	76	83	9%
NAVY	2-11	Flaming	Cardboard	4	Photo	84	83	-1%
NAVY	2-11	Flaming	Cardboard	6	Photo	110	100	-9%
NAVY	2-11	Flaming	Cardboard	8	Photo	93	100	8%
NAVY	2-12	Flaming	Cardboard	4	Photo	82	79	-4%
NAVY	2-12	Flaming	Cardboard	6	Photo	115	77	-33%
NAVY	2-12	Flaming	Cardboard	8	Photo	107	77	-28%
NAVY	2-21	Flaming	Cardboard	12	Photo	472	161	-66%
NAVY	2-21	Flaming	Cardboard	14	Photo	164	61	-63%
NAVY	2-21	Flaming	Cardboard	16	Photo	153	61	-60%

Temperature Rise Alarm Threshold: 4 °C

Test Series	Test ID	Fire Type	Material	Detector ID	Detector Type	Alarm Times (s) Experiment	Alarm Times (s) Predicted	Percent Error
NAVY	2-21	Flaming	Cardboard	18	Photo	498	206	-59%
NAVY	2-21	Flaming	Cardboard	20	Photo	482	206	-57%
NAVY	2-21	Flaming	Cardboard	22	Photo	477	162	-66%
NAVY	2-21	Flaming	Cardboard	24	Photo	474	162	-66%
NAVY	2-22	Flaming	Cardboard	12	Photo	432	117	-73%
NAVY	2-22	Flaming	Cardboard	14	Photo	83	74	-11%
NAVY	2-22	Flaming	Cardboard	16	Photo	414	74	-82%
NAVY	2-22	Flaming	Cardboard	18	Photo	479	114	-76%
NAVY	2-22	Flaming	Cardboard	20	Photo	455	114	-75%
NAVY	2-22	Flaming	Cardboard	22	Photo	118	95	-19%
NAVY	2-22	Flaming	Cardboard	24	Photo	443	95	-79%
NAVY	2-23	Flaming	Cardboard	10	Photo	89	177	99%
NAVY	2-23	Flaming	Cardboard	12	Photo	349	177	-49%
NAVY	2-23	Flaming	Cardboard	14	Photo	151	205	36%
NAVY	2-23	Flaming	Cardboard	16	Photo	139	205	47%
NAVY	2-23	Flaming	Cardboard	18	Photo	97	112	15%
NAVY	2-23	Flaming	Cardboard	20	Photo	310	112	-64%
NAVY	2-23	Flaming	Cardboard	22	Photo	173	194	12%
NAVY	2-23	Flaming	Cardboard	24	Photo	139	194	40%
NAVY	2-24	Flaming	Cardboard	10	Photo	95	129	36%
NAVY	2-24	Flaming	Cardboard	12	Photo	423	129	-70%
NAVY	2-24	Flaming	Cardboard	14	Photo	139	161	16%
NAVY	2-24	Flaming	Cardboard	18	Photo	89	79	-11%
NAVY	2-24	Flaming	Cardboard	20	Photo	417	79	-81%
NAVY	2-24	Flaming	Cardboard	22	Photo	128	127	-1%
NAVY	2-24	Flaming	Cardboard	24	Photo	413	127	-69%
NAVY	2-01	Smoldering	Electrical Cable	1	Ion	2029	DNA (3 @ 692 s)	
NAVY	2-01	Smoldering	Electrical Cable	5	Ion	2138	DNA (2 @ 1706 s)	
NAVY	2-04	Smoldering	Electrical Cable	5	Ion	1057	DNA (2 @ 1790 s)	
NAVY	2-05	Smoldering	Electrical Cable	1	Ion	1695	DNA (1 @ 83 s)	
NAVY	2-05	Smoldering	Electrical Cable	5	Ion	643	DNA (2 @ 504 s)	
NAVY	2-07	Smoldering	Electrical Cable	1	Ion	831	DNA (2 @ 1378 s)	
NAVY	2-07	Smoldering	Electrical Cable	5	Ion	1365	1569	15%
NAVY	2-08	Smoldering	Electrical Cable	1	Ion	1372	DNA (2 @ 1140 s)	
NAVY	2-08	Smoldering	Electrical Cable	5	Ion	1391	DNA (3 @ 1628 s)	
NAVY	2-13	Smoldering	Potassium Chlorate / Lactose	5	Ion	536	DNA (2 @ 403 s)	
NAVY	2-14	Smoldering	Potassium Chlorate / Lactose	1	Ion	18	44	144%

Temperature Rise Alarm Threshold: 4 °C

Test Series	Test ID	Fire Type	Material	Detector		Alarm Times (s)		Percent Error
				ID	Type	Experiment	Predicted	
NAVY	2-14	Smoldering	Potassium Chlorate / Lactose	5	Ion	98	DNA (4 @ 125 s)	
NAVY	2-15	Smoldering	Potassium Chlorate / Lactose	1	Ion	19	59	211%
NAVY	2-15	Smoldering	Potassium Chlorate / Lactose	5	Ion	70	DNA (3 @ 134 s)	
NAVY	2-25	Smoldering	Potassium Chlorate / Lactose	9	Ion	146	DNA (1 @ 21 s)	
NAVY	2-25	Smoldering	Potassium Chlorate / Lactose	13	Ion	100	DNA (1 @ 215 s)	
NAVY	2-25	Smoldering	Potassium Chlorate / Lactose	15	Ion	222	DNA (1 @ 215 s)	
NAVY	2-25	Smoldering	Potassium Chlorate / Lactose	17	Ion	126	275	118%
NAVY	2-25	Smoldering	Potassium Chlorate / Lactose	19	Ion	306	275	-10%
NAVY	2-25	Smoldering	Potassium Chlorate / Lactose	21	Ion	205	DNA (2 @ 225 s)	
NAVY	2-26	Smoldering	Potassium Chlorate / Lactose	9	Ion	334	DNA (1 @ 381 s)	
NAVY	2-26	Smoldering	Potassium Chlorate / Lactose	13	Ion	64	DNA (1 @ 0 s)	
NAVY	2-26	Smoldering	Potassium Chlorate / Lactose	15	Ion	196	DNA (1 @ 0 s)	
NAVY	2-26	Smoldering	Potassium Chlorate / Lactose	17	Ion	53	DNA (3 @ 200 s)	
NAVY	2-26	Smoldering	Potassium Chlorate / Lactose	19	Ion	234	DNA (3 @ 200 s)	
NAVY	2-26	Smoldering	Potassium Chlorate / Lactose	21	Ion	145	DNA (2 @ 243 s)	
NAVY	2-27	Smoldering	Potassium Chlorate / Lactose	9	Ion	161	DNA (1 @ 161 s)	
NAVY	2-27	Smoldering	Potassium Chlorate / Lactose	13	Ion	257	DNA (1 @ 18 s)	
NAVY	2-27	Smoldering	Potassium Chlorate / Lactose	17	Ion	74	DNA (3 @ 1 s)	
NAVY	2-27	Smoldering	Potassium Chlorate / Lactose	19	Ion	152	DNA (3 @ 1 s)	
NAVY	2-27	Smoldering	Potassium Chlorate / Lactose	21	Ion	66	DNA (2 @ 83 s)	
NAVY	2-27	Smoldering	Potassium Chlorate / Lactose	23	Ion	69	DNA (2 @ 83 s)	
NAVY	2-28	Smoldering	Potassium Chlorate / Lactose	9	Ion	374	DNA (1 @ 201 s)	
NAVY	2-28	Smoldering	Potassium Chlorate / Lactose	13	Ion	192	DNA (2 @ 11 s)	
NAVY	2-28	Smoldering	Potassium Chlorate / Lactose	17	Ion	122	DNA (2 @ 240 s)	
NAVY	2-28	Smoldering	Potassium Chlorate / Lactose	19	Ion	444	DNA (2 @ 240 s)	

Temperature Rise Alarm Threshold: 4 °C

Test Series	Test ID	Fire Type	Material	Detector ID	Type	Alarm Times (s) Experiment	Predicted	Percent Error
NAVY	2-28	Smoldering	Potassium Chlorate / Lactose	21	Ion	38	DNA (3 @ 75 s)	
NAVY	2-28	Smoldering	Potassium Chlorate / Lactose	23	Ion	40	DNA (3 @ 75 s)	
NAVY	2-34	Smoldering	Electrical Cable	17	Ion	659	DNA (3 @ 828 s)	
NAVY	2-34	Smoldering	Electrical Cable	19	Ion	840	DNA (3 @ 828 s)	
NAVY	2-35	Smoldering	Electrical Cable	17	Ion	922	355	-61%
NAVY	2-35	Smoldering	Electrical Cable	21	Ion	1408	DNA (4 @ 1022 s)	
NAVY	2-36	Smoldering	Electrical Cable	17	Ion	1354	DNA (3 @ 1787 s)	
NAVY	2-36	Smoldering	Electrical Cable	19	Ion	1490	DNA (3 @ 1787 s)	
NAVY	2-37	Smoldering	Electrical Cable	9	Ion	654	DNA (1 @ 744 s)	
NAVY	2-37	Smoldering	Electrical Cable	11	Ion	729	DNA (1 @ 744 s)	
NAVY	2-37	Smoldering	Electrical Cable	13	Ion	678	DNA (2 @ 474 s)	
NAVY	2-37	Smoldering	Electrical Cable	17	Ion	335	DNA (4 @ 732 s)	
NAVY	2-37	Smoldering	Electrical Cable	19	Ion	393	DNA (4 @ 732 s)	
NAVY	2-37	Smoldering	Electrical Cable	21	Ion	566	DNA (2 @ 758 s)	
NAVY	2-38	Smoldering	Electrical Cable	13	Ion	767	DNA (1 @ 893 s)	
NAVY	2-38	Smoldering	Electrical Cable	17	Ion	771	DNA (3 @ 348 s)	
NAVY	2-38	Smoldering	Electrical Cable	19	Ion	768	DNA (3 @ 348 s)	
NAVY	2-38	Smoldering	Electrical Cable	21	Ion	561	DNA (2 @ 914 s)	
NAVY	2-38	Smoldering	Electrical Cable	23	Ion	730	DNA (2 @ 914 s)	
NAVY	2-39	Smoldering	Electrical Cable	13	Ion	760	DNA (2 @ 623 s)	
NAVY	2-40	Smoldering	Electrical Cable	13	Ion	448	DNA (1 @ 930 s)	
NAVY	2-40	Smoldering	Electrical Cable	15	Ion	983	DNA (1 @ 930 s)	
NAVY	2-01	Smoldering	Electrical Cable	2	Photo	2034	DNA (3 @ 692 s)	
NAVY	2-01	Smoldering	Electrical Cable	4	Photo	2232	DNA (3 @ 692 s)	
NAVY	2-01	Smoldering	Electrical Cable	8	Photo	2232	DNA (2 @ 1706 s)	
NAVY	2-02	Smoldering	Electrical Cable	2	Photo	775	DNA (2 @

Temperature Rise Alarm Threshold: 4 °C

Test Series	Test ID	Fire Type	Material	Detector ID	Type	Alarm Times (s) Experiment	Predicted	Percent Error
							588 s)	
NAVY	2-02	Smoldering	Electrical Cable	4	Photo	2000	DNA (2 @ 588 s)	
NAVY	2-02	Smoldering	Electrical Cable	6	Photo	656	DNA (1 @ 1949 s)	
NAVY	2-04	Smoldering	Electrical Cable	2	Photo	1713	DNA (2 @ 822 s)	
NAVY	2-04	Smoldering	Electrical Cable	6	Photo	796	DNA (2 @ 1790 s)	
NAVY	2-05	Smoldering	Electrical Cable	2	Photo	559	DNA (1 @ 83 s)	
NAVY	2-05	Smoldering	Electrical Cable	4	Photo	639	DNA (1 @ 83 s)	
NAVY	2-05	Smoldering	Electrical Cable	6	Photo	424	DNA (2 @ 504 s)	
NAVY	2-05	Smoldering	Electrical Cable	8	Photo	297	DNA (2 @ 504 s)	
NAVY	2-07	Smoldering	Electrical Cable	4	Photo	936	DNA (2 @ 1378 s)	
NAVY	2-07	Smoldering	Electrical Cable	6	Photo	908	1569	73%
NAVY	2-08	Smoldering	Electrical Cable	2	Photo	728	DNA (2 @ 1140 s)	
NAVY	2-08	Smoldering	Electrical Cable	4	Photo	845	DNA (2 @ 1140 s)	
NAVY	2-08	Smoldering	Electrical Cable	6	Photo	539	DNA (3 @ 1628 s)	
NAVY	2-08	Smoldering	Electrical Cable	8	Photo	775	DNA (3 @ 1628 s)	
NAVY	2-13	Smoldering	Potassium Chlorate / Lactose	2	Photo	578	DNA (1 @ 481 s)	
NAVY	2-13	Smoldering	Potassium Chlorate / Lactose	4	Photo	572	DNA (1 @ 481 s)	
NAVY	2-13	Smoldering	Potassium Chlorate / Lactose	6	Photo	524	DNA (2 @ 403 s)	
NAVY	2-13	Smoldering	Potassium Chlorate / Lactose	8	Photo	710	DNA (2 @ 403 s)	
NAVY	2-14	Smoldering	Potassium Chlorate / Lactose	2	Photo	20	44	120%
NAVY	2-14	Smoldering	Potassium Chlorate / Lactose	4	Photo	33	44	33%
NAVY	2-15	Smoldering	Potassium Chlorate / Lactose	2	Photo	19	59	211%
NAVY	2-15	Smoldering	Potassium Chlorate / Lactose	4	Photo	112	59	-47%
NAVY	2-15	Smoldering	Potassium Chlorate / Lactose	6	Photo	81	DNA (3 @ 134 s)	
NAVY	2-15	Smoldering	Potassium Chlorate / Lactose	8	Photo	83	DNA (3 @ 134 s)	
NAVY	2-25	Smoldering	Potassium Chlorate / Lactose	12	Photo	316	DNA (1 @ 21 s)	

Temperature Rise Alarm Threshold: 4 °C

Test Series	Test ID	Fire Type	Material	Detector ID	Detector Type	Alarm Times (s) Experiment	Alarm Times (s) Predicted	Percent Error
NAVY	2-25	Smoldering	Potassium Chlorate / Lactose	14	Photo	94	DNA (1 @ 215 s)	
NAVY	2-25	Smoldering	Potassium Chlorate / Lactose	16	Photo	105	DNA (1 @ 215 s)	
NAVY	2-25	Smoldering	Potassium Chlorate / Lactose	18	Photo	170	275	62%
NAVY	2-25	Smoldering	Potassium Chlorate / Lactose	20	Photo	301	275	-9%
NAVY	2-25	Smoldering	Potassium Chlorate / Lactose	24	Photo	164	DNA (2 @ 225 s)	
NAVY	2-26	Smoldering	Potassium Chlorate / Lactose	14	Photo	68	DNA (1 @ 0 s)	
NAVY	2-26	Smoldering	Potassium Chlorate / Lactose	16	Photo	246	DNA (1 @ 0 s)	
NAVY	2-26	Smoldering	Potassium Chlorate / Lactose	18	Photo	65	DNA (3 @ 200 s)	
NAVY	2-27	Smoldering	Potassium Chlorate / Lactose	18	Photo	49	DNA (3 @ 1 s)	
NAVY	2-27	Smoldering	Potassium Chlorate / Lactose	20	Photo	68	DNA (3 @ 1 s)	
NAVY	2-27	Smoldering	Potassium Chlorate / Lactose	22	Photo	67	DNA (2 @ 83 s)	
NAVY	2-27	Smoldering	Potassium Chlorate / Lactose	24	Photo	65	DNA (2 @ 83 s)	
NAVY	2-28	Smoldering	Potassium Chlorate / Lactose	16	Photo	331	DNA (2 @ 11 s)	
NAVY	2-28	Smoldering	Potassium Chlorate / Lactose	18	Photo	92	DNA (2 @ 240 s)	
NAVY	2-28	Smoldering	Potassium Chlorate / Lactose	20	Photo	348	DNA (2 @ 240 s)	
NAVY	2-28	Smoldering	Potassium Chlorate / Lactose	22	Photo	34	DNA (3 @ 75 s)	
NAVY	2-28	Smoldering	Potassium Chlorate / Lactose	24	Photo	32	DNA (3 @ 75 s)	
NAVY	2-34	Smoldering	Electrical Cable	12	Photo	892	DNA (2 @ 7 s)	
NAVY	2-34	Smoldering	Electrical Cable	18	Photo	297	DNA (3 @ 828 s)	
NAVY	2-34	Smoldering	Electrical Cable	20	Photo	648	DNA (3 @ 828 s)	
NAVY	2-34	Smoldering	Electrical Cable	22	Photo	843	DNA (3 @ 31 s)	
NAVY	2-34	Smoldering	Electrical Cable	24	Photo	732	DNA (3 @ 31 s)	
NAVY	2-35	Smoldering	Electrical Cable	18	Photo	423	355	-16%
NAVY	2-35	Smoldering	Electrical Cable	20	Photo	851	355	-58%
NAVY	2-35	Smoldering	Electrical Cable	22	Photo	656	DNA (4 @ 1022 s)	
NAVY	2-35	Smoldering	Electrical Cable	24	Photo	989	DNA (4 @ 1022 s)	

Temperature Rise Alarm Threshold: 4 °C

Test Series	Test ID	Fire Type	Material	Detector		Alarm Times (s)		Percent Error
				ID	Type	Experiment	Predicted	
NAVY	2-36	Smoldering	Electrical Cable	14	Photo	1611	DNA (3 @ 963 s)	
NAVY	2-36	Smoldering	Electrical Cable	18	Photo	756	DNA (3 @ 1787 s)	
NAVY	2-36	Smoldering	Electrical Cable	20	Photo	860	DNA (3 @ 1787 s)	
NAVY	2-36	Smoldering	Electrical Cable	22	Photo	1356	DNA (2 @ 2 s)	
NAVY	2-36	Smoldering	Electrical Cable	24	Photo	915	DNA (2 @ 2 s)	
NAVY	2-37	Smoldering	Electrical Cable	12	Photo	700	DNA (1 @ 744 s)	
NAVY	2-37	Smoldering	Electrical Cable	14	Photo	759	DNA (2 @ 474 s)	
NAVY	2-37	Smoldering	Electrical Cable	16	Photo	735	DNA (2 @ 474 s)	
NAVY	2-37	Smoldering	Electrical Cable	18	Photo	295	DNA (4 @ 732 s)	
NAVY	2-37	Smoldering	Electrical Cable	20	Photo	331	DNA (4 @ 732 s)	
NAVY	2-37	Smoldering	Electrical Cable	22	Photo	633	DNA (2 @ 758 s)	
NAVY	2-37	Smoldering	Electrical Cable	24	Photo	506	DNA (2 @ 758 s)	
NAVY	2-38	Smoldering	Electrical Cable	14	Photo	754	DNA (1 @ 893 s)	
NAVY	2-38	Smoldering	Electrical Cable	16	Photo	843	DNA (1 @ 893 s)	
NAVY	2-38	Smoldering	Electrical Cable	18	Photo	549	DNA (3 @ 348 s)	
NAVY	2-38	Smoldering	Electrical Cable	20	Photo	709	DNA (3 @ 348 s)	
NAVY	2-38	Smoldering	Electrical Cable	22	Photo	189	DNA (2 @ 914 s)	
NAVY	2-38	Smoldering	Electrical Cable	24	Photo	418	DNA (2 @ 914 s)	
NAVY	2-39	Smoldering	Electrical Cable	14	Photo	941	DNA (2 @ 623 s)	
NAVY	2-39	Smoldering	Electrical Cable	16	Photo	856	DNA (2 @ 623 s)	
NAVY	2-39	Smoldering	Electrical Cable	18	Photo	1362	DNA (2 @ 312 s)	
NAVY	2-39	Smoldering	Electrical Cable	22	Photo	786	DNA (2 @ 270 s)	
NAVY	2-39	Smoldering	Electrical Cable	24	Photo	689	DNA (2 @ 270 s)	
NAVY	2-40	Smoldering	Electrical Cable	14	Photo	402	DNA (1 @ 930 s)	
NAVY	2-40	Smoldering	Electrical Cable	16	Photo	679	DNA (1 @ 930 s)	

Temperature Rise Alarm Threshold: 4 °C

Test Series	Test ID	Fire Type	Material	Detector		Alarm Times (s)		Percent Error
				ID	Type	Experiment	Predicted	
NAVY	2-40	Smoldering	Electrical Cable	18	Photo	1201	DNA (2 @ 1069 s)	
NAVY	2-40	Smoldering	Electrical Cable	20	Photo	1387	DNA (2 @ 1069 s)	
NAVY	2-40	Smoldering	Electrical Cable	22	Photo	1542	DNA (3 @ 1534 s)	
KEMANO	01	Flaming	Wood	28	Ion	480	DNA (1 @ 795 s)	
KEMANO	02	Flaming	Wood	14	Ion	1359	DNA (3 @ 1464 s)	
KEMANO	02	Flaming	Wood	28	Ion	1388	DNA (0 @ 1507 s)	
KEMANO	03	Flaming	Cotton Fabric	8	Ion	122	590	867%
KEMANO	03	Flaming	Cotton Fabric	14	Ion	155	579	487%
KEMANO	03	Flaming	Cotton Fabric	28	Ion	226	DNA (1 @ 836 s)	
KEMANO	05	Flaming	Upholstered Furniture	28	Ion	875	DNA (1 @ 1062 s)	
KEMANO	06	Flaming	Wood	8	Ion	1111	DNA (1 @ 1184 s)	
KEMANO	06	Flaming	Wood	14	Ion	389	DNA (2 @ 771 s)	
KEMANO	06	Flaming	Wood	28	Ion	277	669	912%
KEMANO	07	Flaming	Wood	8	Ion	1107	DNA (1 @ 1203 s)	
KEMANO	08	Flaming	Upholstered Furniture	8	Ion	760	DNA (0 @ 931 s)	
KEMANO	08	Flaming	Upholstered Furniture	14	Ion	860	DNA (2 @ 968 s)	
KEMANO	09	Flaming	Upholstered Furniture	14	Ion	906	921	29%
KEMANO	10	Flaming	Wood	13	Ion	2851	DNA (2 @ 2867 s)	
KEMANO	11	Flaming	Upholstered Furniture	1	Ion	1690	DNA (3 @ 1724 s)	
KEMANO	11	Flaming	Upholstered Furniture	4	Ion	1723	DNA (2 @ 1760 s)	
KEMANO	11	Flaming	Upholstered Furniture	7	Ion	1763	DNA (1 @ 1765 s)	
KEMANO	11	Flaming	Upholstered Furniture	10	Ion	1756	DNA (0 @ 1787 s)	
KEMANO	13	Flaming	Paper	13	Ion	4977	DNA (0 @ 5045 s)	
KEMANO	01	Flaming	Wood	26	Photo	545	DNA (1 @ 795 s)	
KEMANO	02	Flaming	Wood	16	Photo	1377	DNA (3 @ 1464 s)	
KEMANO	02	Flaming	Wood	26	Photo	1408	DNA (0 @ 1507 s)	
KEMANO	03	Flaming	Cotton Fabric	6	Photo	403	590	56%

Temperature Rise Alarm Threshold: 4 °C

Test Series	Test ID	Fire Type	Material	Detector ID	Detector Type	Alarm Times (s) Experiment	Alarm Times (s) Predicted	Percent Error
KEMANO	03	Flaming	Cotton Fabric	16	Photo	368	579	70%
KEMANO	04	Flaming	Paper	26	Photo	787	DNA (0 @ 867 s)	
KEMANO	05	Flaming	Upholstered Furniture	26	Photo	922	DNA (1 @ 1062 s)	
KEMANO	06	Flaming	Wood	6	Photo	1112	DNA (1 @ 1184 s)	
KEMANO	06	Flaming	Wood	26	Photo	265	669	1303%
KEMANO	07	Flaming	Wood	6	Photo	1115	DNA (1 @ 1203 s)	
KEMANO	01	Smoldering	Wood	8	Ion	269	DNA (1 @ 383 s)	
KEMANO	01	Smoldering	Wood	14	Ion	422	DNA (0 @ 12 s)	
KEMANO	02	Smoldering	Wood	8	Ion	218	DNA (1 @ 385 s)	
KEMANO	04	Smoldering	Paper	8	Ion	522	DNA (0 @ 584 s)	
KEMANO	04	Smoldering	Paper	14	Ion	377	DNA (1 @ 580 s)	
KEMANO	04	Smoldering	Paper	28	Ion	686	DNA (0 @ 0 s)	
KEMANO	05	Smoldering	Upholstered Furniture	8	Ion	325	DNA (2 @ 746 s)	
KEMANO	05	Smoldering	Upholstered Furniture	14	Ion	315	DNA (2 @ 718 s)	
KEMANO	07	Smoldering	Wood	14	Ion	606	DNA (1 @ 23 s)	
KEMANO	07	Smoldering	Wood	28	Ion	383	DNA (0 @ 2 s)	
KEMANO	08	Smoldering	Upholstered Furniture	28	Ion	715	DNA (1 @ 720 s)	
KEMANO	09	Smoldering	Upholstered Furniture	8	Ion	924	DNA (0 @ 672 s)	
KEMANO	09	Smoldering	Upholstered Furniture	28	Ion	795	DNA (1 @ 851 s)	
KEMANO	10	Smoldering	Wood	1	Ion	681	DNA (0 @ 1 s)	
KEMANO	10	Smoldering	Wood	4	Ion	1044	DNA (0 @ 30 s)	
KEMANO	10	Smoldering	Wood	7	Ion	2017	DNA (0 @ 18 s)	
KEMANO	10	Smoldering	Wood	10	Ion	2055	DNA (0 @ 18 s)	
KEMANO	13	Smoldering	Paper	1	Ion	3121	DNA (1 @ 3781 s)	
KEMANO	13	Smoldering	Paper	4	Ion	3246	DNA (1 @ 3934 s)	
KEMANO	13	Smoldering	Paper	7	Ion	4001	DNA (0 @ 15 s)	

Temperature Rise Alarm Threshold: 4 °C

Test Series	Test ID	Fire Type	Material	Detector		Alarm Times (s)		Percent Error
				ID	Type	Experiment	Predicted	
KEMANO	13	Smoldering	Paper	10	Ion	4091	DNA (0 @ 17 s)	
KEMANO	01	Smoldering	Wood	6	Photo	313	DNA (1 @ 383 s)	
KEMANO	01	Smoldering	Wood	16	Photo	337	DNA (0 @ 12 s)	
KEMANO	02	Smoldering	Wood	6	Photo	223	DNA (1 @ 385 s)	
KEMANO	04	Smoldering	Paper	6	Photo	521	DNA (0 @ 584 s)	
KEMANO	04	Smoldering	Paper	16	Photo	373	DNA (1 @ 580 s)	
KEMANO	05	Smoldering	Upholstered Furniture	6	Photo	461	DNA (2 @ 746 s)	
KEMANO	05	Smoldering	Upholstered Furniture	16	Photo	356	DNA (2 @ 718 s)	
KEMANO	06	Smoldering	Wood	16	Photo	297	DNA (1 @ 63 s)	
KEMANO	07	Smoldering	Wood	16	Photo	342	DNA (1 @ 23 s)	
KEMANO	07	Smoldering	Wood	26	Photo	374	DNA (0 @ 2 s)	
KEMANO	08	Smoldering	Upholstered Furniture	6	Photo	376	DNA (0 @ 0 s)	
KEMANO	08	Smoldering	Upholstered Furniture	16	Photo	334	DNA (1 @ 706 s)	
KEMANO	08	Smoldering	Upholstered Furniture	26	Photo	254	DNA (1 @ 720 s)	
KEMANO	09	Smoldering	Upholstered Furniture	6	Photo	755	DNA (0 @ 672 s)	
KEMANO	09	Smoldering	Upholstered Furniture	16	Photo	376	DNA (1 @ 701 s)	
KEMANO	09	Smoldering	Upholstered Furniture	26	Photo	288	DNA (1 @ 851 s)	
KEMANO	10	Smoldering	Wood	3	Photo	418	DNA (0 @ 1 s)	
KEMANO	10	Smoldering	Wood	6	Photo	504	DNA (0 @ 30 s)	
KEMANO	10	Smoldering	Wood	9	Photo	605	DNA (0 @ 18 s)	
KEMANO	10	Smoldering	Wood	12	Photo	755	DNA (0 @ 18 s)	
KEMANO	10	Smoldering	Wood	15	Photo	687	DNA (0 @ 18 s)	
KEMANO	11	Smoldering	Upholstered Furniture	3	Photo	344	DNA (0 @ 22 s)	
KEMANO	11	Smoldering	Upholstered Furniture	6	Photo	371	DNA (0 @ 117 s)	
KEMANO	11	Smoldering	Upholstered Furniture	9	Photo	439	DNA (0 @ 20 s)	

Temperature Rise Alarm Threshold: 4 °C

Test Series	Test ID	Fire Type	Material	Detector		Alarm Times (s)		Percent Error
				ID	Type	Experiment	Predicted	
KEMANO	11	Smoldering	Upholstered Furniture	12	Photo	485	DNA (0 @ 24 s)	
KEMANO	11	Smoldering	Upholstered Furniture	15	Photo	580	DNA (0 @ 24 s)	
KEMANO	13	Smoldering	Paper	3	Photo	420	DNA (1 @ 3781 s)	
KEMANO	13	Smoldering	Paper	6	Photo	479	DNA (1 @ 3934 s)	
KEMANO	13	Smoldering	Paper	9	Photo	658	DNA (0 @ 15 s)	
KEMANO	13	Smoldering	Paper	12	Photo	764	DNA (0 @ 17 s)	
KEMANO	13	Smoldering	Paper	15	Photo	725	DNA (0 @ 15 s)	

Temperature Rise Alarm Threshold: 13 °C

Test Series	Test ID	Fire Type	Material	Detector		Alarm Times (s)		Percent Error
				ID	Type	Experiment	Predicted	
NAVY	1-37	Flaming	Wood	1	Ion	61	277	354%
NAVY	1-37	Flaming	Wood	3	Ion	177	277	56%
NAVY	1-37	Flaming	Wood	5	Ion	45	455	911%
NAVY	1-37	Flaming	Wood	7	Ion	174	455	161%
NAVY	1-38	Flaming	Wood	1	Ion	62	360	481%
NAVY	1-38	Flaming	Wood	3	Ion	155	360	132%
NAVY	1-38	Flaming	Wood	5	Ion	65	1339	1960%
NAVY	1-38	Flaming	Wood	7	Ion	182	1339	636%
NAVY	1-39	Flaming	Wood	1	Ion	69	251	264%
NAVY	1-39	Flaming	Wood	3	Ion	43	251	484%
NAVY	1-39	Flaming	Wood	5	Ion	39	345	785%
NAVY	1-39	Flaming	Wood	7	Ion	134	345	157%
NAVY	1-40	Flaming	Wood	1	Ion	43	263	512%
NAVY	1-40	Flaming	Wood	3	Ion	123	263	114%
NAVY	1-40	Flaming	Wood	5	Ion	39	271	595%
NAVY	1-40	Flaming	Wood	7	Ion	57	271	375%
NAVY	1-41	Flaming	Wood	1	Ion	69	226	228%
NAVY	1-41	Flaming	Wood	3	Ion	152	226	49%
NAVY	1-41	Flaming	Wood	5	Ion	46	291	533%
NAVY	1-41	Flaming	Wood	7	Ion	124	291	135%
NAVY	1-50	Flaming	Wood	9	Ion	24	249	938%
NAVY	1-50	Flaming	Wood	11	Ion	25	249	896%
NAVY	1-50	Flaming	Wood	13	Ion	48	DNA (11 @ 487 s)	
NAVY	1-50	Flaming	Wood	15	Ion	65	DNA (11 @ 487 s)	
NAVY	1-50	Flaming	Wood	17	Ion	75	DNA (12 @ 531 s)	
NAVY	1-50	Flaming	Wood	19	Ion	128	DNA (12 @ 531 s)	
NAVY	1-50	Flaming	Wood	21	Ion	112	DNA (8 @ 531 s)	
NAVY	1-50	Flaming	Wood	23	Ion	161	DNA (8 @ 531 s)	
NAVY	1-51	Flaming	Wood	9	Ion	22	236	973%
NAVY	1-51	Flaming	Wood	11	Ion	22	236	973%
NAVY	1-51	Flaming	Wood	13	Ion	44	338	668%
NAVY	1-51	Flaming	Wood	15	Ion	90	338	276%
NAVY	1-51	Flaming	Wood	17	Ion	79	336	325%
NAVY	1-51	Flaming	Wood	19	Ion	182	336	85%
NAVY	1-51	Flaming	Wood	21	Ion	99	432	336%
NAVY	1-51	Flaming	Wood	23	Ion	89	432	385%
NAVY	1-52	Flaming	Wood	9	Ion	21	321	1429%

Temperature Rise Alarm Threshold: 13 °C

Test Series	Test ID	Fire Type	Material	Detector		Alarm Times (s)		Percent Error
				ID	Type	Experiment	Predicted	
NAVY	1-52	Flaming	Wood	11	Ion	25	321	1184%
NAVY	1-52	Flaming	Wood	13	Ion	38	392	932%
NAVY	1-52	Flaming	Wood	15	Ion	65	392	503%
NAVY	1-52	Flaming	Wood	19	Ion	73	377	416%
NAVY	1-52	Flaming	Wood	21	Ion	84	835	894%
NAVY	1-52	Flaming	Wood	23	Ion	177	835	372%
NAVY	1-53	Flaming	Wood	11	Ion	16	293	1731%
NAVY	1-53	Flaming	Wood	13	Ion	42	1281	2950%
NAVY	1-53	Flaming	Wood	15	Ion	101	1281	1168%
NAVY	1-53	Flaming	Wood	17	Ion	123	909	639%
NAVY	1-53	Flaming	Wood	19	Ion	126	909	621%
NAVY	1-53	Flaming	Wood	21	Ion	95	DNA (11 @ 1171 s)	
NAVY	1-53	Flaming	Wood	23	Ion	164	DNA (11 @ 1171 s)	
NAVY	1-54	Flaming	Wood	9	Ion	27	186	589%
NAVY	1-54	Flaming	Wood	13	Ion	50	260	420%
NAVY	1-54	Flaming	Wood	15	Ion	66	260	294%
NAVY	1-54	Flaming	Wood	17	Ion	75	233	211%
NAVY	1-54	Flaming	Wood	19	Ion	116	233	101%
NAVY	1-55	Flaming	Wood	13	Ion	36	225	525%
NAVY	1-55	Flaming	Wood	15	Ion	68	225	231%
NAVY	1-55	Flaming	Wood	17	Ion	53	231	336%
NAVY	1-55	Flaming	Wood	19	Ion	43	231	437%
NAVY	2-09	Flaming	Cardboard	1	Ion	162	304	88%
NAVY	2-09	Flaming	Cardboard	3	Ion	165	304	84%
NAVY	2-09	Flaming	Cardboard	5	Ion	86	162	88%
NAVY	2-09	Flaming	Cardboard	7	Ion	100	162	62%
NAVY	2-10	Flaming	Cardboard	1	Ion	229	192	-16%
NAVY	2-10	Flaming	Cardboard	3	Ion	239	192	-20%
NAVY	2-10	Flaming	Cardboard	5	Ion	166	99	-40%
NAVY	2-10	Flaming	Cardboard	7	Ion	228	99	-57%
NAVY	2-11	Flaming	Cardboard	3	Ion	67	147	119%
NAVY	2-11	Flaming	Cardboard	5	Ion	93	163	75%
NAVY	2-11	Flaming	Cardboard	7	Ion	89	163	83%
NAVY	2-12	Flaming	Cardboard	1	Ion	28	125	346%
NAVY	2-12	Flaming	Cardboard	3	Ion	57	125	119%
NAVY	2-12	Flaming	Cardboard	5	Ion	66	141	114%
NAVY	2-12	Flaming	Cardboard	7	Ion	63	141	124%
NAVY	2-21	Flaming	Cardboard	9	Ion	93	232	149%
NAVY	2-21	Flaming	Cardboard	11	Ion	247	232	-6%
NAVY	2-21	Flaming	Cardboard	13	Ion	63	183	190%
NAVY	2-21	Flaming	Cardboard	15	Ion	36	183	408%
NAVY	2-21	Flaming	Cardboard	17	Ion	151	322	113%
NAVY	2-21	Flaming	Cardboard	19	Ion	174	322	85%

Temperature Rise Alarm Threshold: 13 °C

Test Series	Test ID	Fire Type	Material	Detector ID	Type	Experiment	Predicted	Percent Error
NAVY	2-21	Flaming	Cardboard	21	Ion	143	312	118%
NAVY	2-21	Flaming	Cardboard	23	Ion	195	312	60%
NAVY	2-22	Flaming	Cardboard	9	Ion	74	195	164%
NAVY	2-22	Flaming	Cardboard	11	Ion	129	195	51%
NAVY	2-22	Flaming	Cardboard	13	Ion	43	121	181%
NAVY	2-22	Flaming	Cardboard	15	Ion	30	121	303%
NAVY	2-22	Flaming	Cardboard	17	Ion	302	242	-20%
NAVY	2-22	Flaming	Cardboard	19	Ion	126	242	92%
NAVY	2-22	Flaming	Cardboard	21	Ion	87	206	137%
NAVY	2-22	Flaming	Cardboard	23	Ion	127	206	62%
NAVY	2-23	Flaming	Cardboard	11	Ion	120	281	134%
NAVY	2-23	Flaming	Cardboard	13	Ion	119	DNA (12 @ 376 s)	
NAVY	2-23	Flaming	Cardboard	15	Ion	143	DNA (12 @ 376 s)	
NAVY	2-23	Flaming	Cardboard	17	Ion	54	193	257%
NAVY	2-23	Flaming	Cardboard	19	Ion	122	193	58%
NAVY	2-23	Flaming	Cardboard	21	Ion	125	320	156%
NAVY	2-23	Flaming	Cardboard	23	Ion	144	320	122%
NAVY	2-24	Flaming	Cardboard	11	Ion	98	307	213%
NAVY	2-24	Flaming	Cardboard	13	Ion	117	DNA (11 @ 414 s)	
NAVY	2-24	Flaming	Cardboard	15	Ion	142	DNA (11 @ 414 s)	
NAVY	2-24	Flaming	Cardboard	17	Ion	62	150	142%
NAVY	2-24	Flaming	Cardboard	19	Ion	100	150	50%
NAVY	2-24	Flaming	Cardboard	21	Ion	58	283	388%
NAVY	2-24	Flaming	Cardboard	23	Ion	67	283	322%
NAVY	1-37	Flaming	Wood	2	Photo	901	277	-69%
NAVY	1-37	Flaming	Wood	4	Photo	1007	277	-72%
NAVY	1-37	Flaming	Wood	6	Photo	816	455	-44%
NAVY	1-37	Flaming	Wood	8	Photo	990	455	-54%
NAVY	1-38	Flaming	Wood	2	Photo	874	360	-59%
NAVY	1-38	Flaming	Wood	4	Photo	860	360	-58%
NAVY	1-38	Flaming	Wood	6	Photo	794	1339	69%
NAVY	1-38	Flaming	Wood	8	Photo	943	1339	42%
NAVY	1-39	Flaming	Wood	2	Photo	546	251	-54%
NAVY	1-39	Flaming	Wood	4	Photo	555	251	-55%
NAVY	1-39	Flaming	Wood	6	Photo	366	345	-6%
NAVY	1-39	Flaming	Wood	8	Photo	634	345	-46%
NAVY	1-40	Flaming	Wood	2	Photo	1036	263	-75%
NAVY	1-40	Flaming	Wood	4	Photo	886	263	-70%
NAVY	1-40	Flaming	Wood	6	Photo	956	271	-72%
NAVY	1-40	Flaming	Wood	8	Photo	1023	271	-74%
NAVY	1-41	Flaming	Wood	2	Photo	529	226	-57%

Temperature Rise Alarm Threshold: 13 °C

Test Series	Test ID	Fire Type	Material	Detector ID	Detector Type	Experiment	Predicted	Percent Error
NAVY	1-41	Flaming	Wood	4	Photo	494	226	-54%
NAVY	1-41	Flaming	Wood	6	Photo	484	291	-40%
NAVY	1-41	Flaming	Wood	8	Photo	553	291	-47%
NAVY	1-50	Flaming	Wood	12	Photo	1113	249	-78%
NAVY	1-50	Flaming	Wood	16	Photo	1149	DNA (11 @ 487 s)	
NAVY	1-50	Flaming	Wood	20	Photo	1194	DNA (12 @ 531 s)	
NAVY	1-50	Flaming	Wood	24	Photo	1149	DNA (8 @ 531 s)	
NAVY	1-51	Flaming	Wood	10	Photo	28	236	743%
NAVY	1-51	Flaming	Wood	12	Photo	17	236	1288%
NAVY	1-51	Flaming	Wood	14	Photo	54	338	526%
NAVY	1-51	Flaming	Wood	16	Photo	53	338	538%
NAVY	1-51	Flaming	Wood	18	Photo	612	336	-45%
NAVY	1-51	Flaming	Wood	20	Photo	82	336	310%
NAVY	1-51	Flaming	Wood	22	Photo	518	432	-17%
NAVY	1-52	Flaming	Wood	10	Photo	16	321	1906%
NAVY	1-52	Flaming	Wood	12	Photo	17	321	1788%
NAVY	1-52	Flaming	Wood	14	Photo	38	392	932%
NAVY	1-52	Flaming	Wood	16	Photo	35	392	1020%
NAVY	1-52	Flaming	Wood	18	Photo	49	377	669%
NAVY	1-52	Flaming	Wood	20	Photo	40	377	843%
NAVY	1-53	Flaming	Wood	10	Photo	790	293	-63%
NAVY	1-53	Flaming	Wood	12	Photo	908	293	-68%
NAVY	1-53	Flaming	Wood	14	Photo	662	1281	94%
NAVY	1-53	Flaming	Wood	16	Photo	768	1281	67%
NAVY	1-53	Flaming	Wood	18	Photo	841	909	8%
NAVY	1-53	Flaming	Wood	20	Photo	689	909	32%
NAVY	1-53	Flaming	Wood	22	Photo	680	DNA (11 @ 1171 s)	
NAVY	1-53	Flaming	Wood	24	Photo	906	DNA (11 @ 1171 s)	
NAVY	1-54	Flaming	Wood	10	Photo	51	186	265%
NAVY	1-54	Flaming	Wood	14	Photo	51	260	410%
NAVY	1-54	Flaming	Wood	16	Photo	45	260	478%
NAVY	1-54	Flaming	Wood	18	Photo	96	233	143%
NAVY	1-54	Flaming	Wood	20	Photo	49	233	376%
NAVY	1-55	Flaming	Wood	10	Photo	40	209	423%
NAVY	1-55	Flaming	Wood	16	Photo	35	225	543%
NAVY	1-55	Flaming	Wood	18	Photo	55	231	320%
NAVY	1-55	Flaming	Wood	20	Photo	35	231	560%
NAVY	2-09	Flaming	Cardboard	2	Photo	480	304	-37%
NAVY	2-09	Flaming	Cardboard	4	Photo	169	304	80%
NAVY	2-09	Flaming	Cardboard	6	Photo	129	162	26%
NAVY	2-09	Flaming	Cardboard	8	Photo	124	162	31%

Temperature Rise Alarm Threshold: 13 °C

Test Series	Test ID	Fire Type	Material	Detector ID	Detector Type	Experiment	Predicted	Percent Error
NAVY	2-10	Flaming	Cardboard	2	Photo	643	192	-70%
NAVY	2-10	Flaming	Cardboard	4	Photo	281	192	-32%
NAVY	2-10	Flaming	Cardboard	6	Photo	592	99	-83%
NAVY	2-10	Flaming	Cardboard	8	Photo	260	99	-62%
NAVY	2-11	Flaming	Cardboard	2	Photo	76	147	93%
NAVY	2-11	Flaming	Cardboard	4	Photo	84	147	75%
NAVY	2-11	Flaming	Cardboard	6	Photo	110	163	48%
NAVY	2-11	Flaming	Cardboard	8	Photo	93	163	75%
NAVY	2-12	Flaming	Cardboard	4	Photo	82	125	52%
NAVY	2-12	Flaming	Cardboard	6	Photo	115	141	23%
NAVY	2-12	Flaming	Cardboard	8	Photo	107	141	32%
NAVY	2-21	Flaming	Cardboard	12	Photo	472	232	-51%
NAVY	2-21	Flaming	Cardboard	14	Photo	164	183	12%
NAVY	2-21	Flaming	Cardboard	16	Photo	153	183	20%
NAVY	2-21	Flaming	Cardboard	18	Photo	498	322	-35%
NAVY	2-21	Flaming	Cardboard	20	Photo	482	322	-33%
NAVY	2-21	Flaming	Cardboard	22	Photo	477	312	-35%
NAVY	2-21	Flaming	Cardboard	24	Photo	474	312	-34%
NAVY	2-22	Flaming	Cardboard	12	Photo	432	195	-55%
NAVY	2-22	Flaming	Cardboard	14	Photo	83	121	46%
NAVY	2-22	Flaming	Cardboard	16	Photo	414	121	-71%
NAVY	2-22	Flaming	Cardboard	18	Photo	479	242	-49%
NAVY	2-22	Flaming	Cardboard	20	Photo	455	242	-47%
NAVY	2-22	Flaming	Cardboard	22	Photo	118	206	75%
NAVY	2-22	Flaming	Cardboard	24	Photo	443	206	-53%
NAVY	2-23	Flaming	Cardboard	10	Photo	89	281	216%
NAVY	2-23	Flaming	Cardboard	12	Photo	349	281	-19%
NAVY	2-23	Flaming	Cardboard	14	Photo	151	DNA (12 @ 376 s)	
NAVY	2-23	Flaming	Cardboard	16	Photo	139	DNA (12 @ 376 s)	
NAVY	2-23	Flaming	Cardboard	18	Photo	97	193	99%
NAVY	2-23	Flaming	Cardboard	20	Photo	310	193	-38%
NAVY	2-23	Flaming	Cardboard	22	Photo	173	320	85%
NAVY	2-23	Flaming	Cardboard	24	Photo	139	320	130%
NAVY	2-24	Flaming	Cardboard	10	Photo	95	307	223%
NAVY	2-24	Flaming	Cardboard	12	Photo	423	307	-27%
NAVY	2-24	Flaming	Cardboard	14	Photo	139	DNA (11 @ 414 s)	
NAVY	2-24	Flaming	Cardboard	18	Photo	89	150	69%
NAVY	2-24	Flaming	Cardboard	20	Photo	417	150	-64%
NAVY	2-24	Flaming	Cardboard	22	Photo	128	283	121%
NAVY	2-24	Flaming	Cardboard	24	Photo	413	283	-31%
NAVY	2-01	Smoldering	Electrical Cable	1	Ion	2029	DNA (3 @ 692 s)	

Temperature Rise Alarm Threshold: 13 °C

Test Series	Test ID	Fire Type	Material	Detector ID	Type	Alarm Times (s) Experiment	Predicted	Percent Error
NAVY	2-01	Smoldering	Electrical Cable	5	Ion	2138	DNA (2 @ 1706 s)	
NAVY	2-04	Smoldering	Electrical Cable	5	Ion	1057	DNA (2 @ 1790 s)	
NAVY	2-05	Smoldering	Electrical Cable	1	Ion	1695	DNA (1 @ 83 s)	
NAVY	2-05	Smoldering	Electrical Cable	5	Ion	643	DNA (2 @ 504 s)	
NAVY	2-07	Smoldering	Electrical Cable	1	Ion	831	DNA (2 @ 1378 s)	
NAVY	2-07	Smoldering	Electrical Cable	5	Ion	1365	DNA (4 @ 1569 s)	
NAVY	2-08	Smoldering	Electrical Cable	1	Ion	1372	DNA (2 @ 1140 s)	
NAVY	2-08	Smoldering	Electrical Cable	5	Ion	1391	DNA (3 @ 1628 s)	
NAVY	2-13	Smoldering	Potassium Chlorate / Lactose	5	Ion	536	DNA (2 @ 403 s)	
NAVY	2-14	Smoldering	Potassium Chlorate / Lactose	1	Ion	18	DNA (4 @ 46 s)	
NAVY	2-14	Smoldering	Potassium Chlorate / Lactose	5	Ion	98	DNA (4 @ 125 s)	
NAVY	2-15	Smoldering	Potassium Chlorate / Lactose	1	Ion	19	DNA (4 @ 107 s)	
NAVY	2-15	Smoldering	Potassium Chlorate / Lactose	5	Ion	70	DNA (3 @ 134 s)	
NAVY	2-25	Smoldering	Potassium Chlorate / Lactose	9	Ion	146	DNA (1 @ 21 s)	
NAVY	2-25	Smoldering	Potassium Chlorate / Lactose	13	Ion	100	DNA (1 @ 215 s)	
NAVY	2-25	Smoldering	Potassium Chlorate / Lactose	15	Ion	222	DNA (1 @ 215 s)	
NAVY	2-25	Smoldering	Potassium Chlorate / Lactose	17	Ion	126	DNA (4 @ 284 s)	
NAVY	2-25	Smoldering	Potassium Chlorate / Lactose	19	Ion	306	DNA (4 @ 284 s)	
NAVY	2-25	Smoldering	Potassium Chlorate / Lactose	21	Ion	205	DNA (2 @ 225 s)	
NAVY	2-26	Smoldering	Potassium Chlorate / Lactose	9	Ion	334	DNA (1 @ 381 s)	
NAVY	2-26	Smoldering	Potassium Chlorate / Lactose	13	Ion	64	DNA (1 @ 0 s)	
NAVY	2-26	Smoldering	Potassium Chlorate / Lactose	15	Ion	196	DNA (1 @ 0 s)	
NAVY	2-26	Smoldering	Potassium Chlorate / Lactose	17	Ion	53	DNA (3 @ 200 s)	
NAVY	2-26	Smoldering	Potassium Chlorate / Lactose	19	Ion	234	DNA (3 @ 200 s)	
NAVY	2-26	Smoldering	Potassium Chlorate / Lactose	21	Ion	145	DNA (2 @ 243 s)	

Temperature Rise Alarm Threshold: 13 °C

Test Series	Test ID	Fire Type	Material	Detector		Alarm Times (s)		Percent Error
				ID	Type	Experiment	Predicted	
NAVY	2-27	Smoldering	Potassium Chlorate / Lactose	9	Ion	161	DNA (1 @ 161 s)	
NAVY	2-27	Smoldering	Potassium Chlorate / Lactose	13	Ion	257	DNA (1 @ 18 s)	
NAVY	2-27	Smoldering	Potassium Chlorate / Lactose	17	Ion	74	DNA (3 @ 1 s)	
NAVY	2-27	Smoldering	Potassium Chlorate / Lactose	19	Ion	152	DNA (3 @ 1 s)	
NAVY	2-27	Smoldering	Potassium Chlorate / Lactose	21	Ion	66	DNA (2 @ 83 s)	
NAVY	2-27	Smoldering	Potassium Chlorate / Lactose	23	Ion	69	DNA (2 @ 83 s)	
NAVY	2-28	Smoldering	Potassium Chlorate / Lactose	9	Ion	374	DNA (1 @ 201 s)	
NAVY	2-28	Smoldering	Potassium Chlorate / Lactose	13	Ion	192	DNA (2 @ 11 s)	
NAVY	2-28	Smoldering	Potassium Chlorate / Lactose	17	Ion	122	DNA (2 @ 240 s)	
NAVY	2-28	Smoldering	Potassium Chlorate / Lactose	19	Ion	444	DNA (2 @ 240 s)	
NAVY	2-28	Smoldering	Potassium Chlorate / Lactose	21	Ion	38	DNA (3 @ 75 s)	
NAVY	2-28	Smoldering	Potassium Chlorate / Lactose	23	Ion	40	DNA (3 @ 75 s)	
NAVY	2-34	Smoldering	Electrical Cable	17	Ion	659	DNA (3 @ 828 s)	
NAVY	2-34	Smoldering	Electrical Cable	19	Ion	840	DNA (3 @ 828 s)	
NAVY	2-35	Smoldering	Electrical Cable	17	Ion	922	DNA (4 @ 1529 s)	
NAVY	2-35	Smoldering	Electrical Cable	21	Ion	1408	DNA (4 @ 1022 s)	
NAVY	2-36	Smoldering	Electrical Cable	17	Ion	1354	DNA (3 @ 1787 s)	
NAVY	2-36	Smoldering	Electrical Cable	19	Ion	1490	DNA (3 @ 1787 s)	
NAVY	2-37	Smoldering	Electrical Cable	9	Ion	654	DNA (1 @ 744 s)	
NAVY	2-37	Smoldering	Electrical Cable	11	Ion	729	DNA (1 @ 744 s)	
NAVY	2-37	Smoldering	Electrical Cable	13	Ion	678	DNA (2 @ 474 s)	
NAVY	2-37	Smoldering	Electrical Cable	17	Ion	335	DNA (4 @ 732 s)	
NAVY	2-37	Smoldering	Electrical Cable	19	Ion	393	DNA (4 @ 732 s)	
NAVY	2-37	Smoldering	Electrical Cable	21	Ion	566	DNA (2 @ 758 s)	
NAVY	2-38	Smoldering	Electrical Cable	13	Ion	767	DNA (1 @ 893 s)	

Temperature Rise Alarm Threshold: 13 °C

Test Series	Test ID	Fire Type	Material	Detector		Alarm Times (s)		Percent Error
				ID	Type	Experiment	Predicted	
NAVY	2-38	Smoldering	Electrical Cable	17	Ion	771	DNA (3 @ 348 s)	
NAVY	2-38	Smoldering	Electrical Cable	19	Ion	768	DNA (3 @ 348 s)	
NAVY	2-38	Smoldering	Electrical Cable	21	Ion	561	DNA (2 @ 914 s)	
NAVY	2-38	Smoldering	Electrical Cable	23	Ion	730	DNA (2 @ 914 s)	
NAVY	2-39	Smoldering	Electrical Cable	13	Ion	760	DNA (2 @ 623 s)	
NAVY	2-40	Smoldering	Electrical Cable	13	Ion	448	DNA (1 @ 930 s)	
NAVY	2-40	Smoldering	Electrical Cable	15	Ion	983	DNA (1 @ 930 s)	
NAVY	2-01	Smoldering	Electrical Cable	2	Photo	2034	DNA (3 @ 692 s)	
NAVY	2-01	Smoldering	Electrical Cable	4	Photo	2232	DNA (3 @ 692 s)	
NAVY	2-01	Smoldering	Electrical Cable	8	Photo	2232	DNA (2 @ 1706 s)	
NAVY	2-02	Smoldering	Electrical Cable	2	Photo	775	DNA (2 @ 588 s)	
NAVY	2-02	Smoldering	Electrical Cable	4	Photo	2000	DNA (2 @ 588 s)	
NAVY	2-02	Smoldering	Electrical Cable	6	Photo	656	DNA (1 @ 1949 s)	
NAVY	2-04	Smoldering	Electrical Cable	2	Photo	1713	DNA (2 @ 822 s)	
NAVY	2-04	Smoldering	Electrical Cable	6	Photo	796	DNA (2 @ 1790 s)	
NAVY	2-05	Smoldering	Electrical Cable	2	Photo	559	DNA (1 @ 83 s)	
NAVY	2-05	Smoldering	Electrical Cable	4	Photo	639	DNA (1 @ 83 s)	
NAVY	2-05	Smoldering	Electrical Cable	6	Photo	424	DNA (2 @ 504 s)	
NAVY	2-05	Smoldering	Electrical Cable	8	Photo	297	DNA (2 @ 504 s)	
NAVY	2-07	Smoldering	Electrical Cable	4	Photo	936	DNA (2 @ 1378 s)	
NAVY	2-07	Smoldering	Electrical Cable	6	Photo	908	DNA (4 @ 1569 s)	
NAVY	2-08	Smoldering	Electrical Cable	2	Photo	728	DNA (2 @ 1140 s)	
NAVY	2-08	Smoldering	Electrical Cable	4	Photo	845	DNA (2 @ 1140 s)	
NAVY	2-08	Smoldering	Electrical Cable	6	Photo	539	DNA (3 @ 1628 s)	
NAVY	2-08	Smoldering	Electrical Cable	8	Photo	775	DNA (3 @ 1628 s)	

Temperature Rise Alarm Threshold: 13 °C

Test Series	Test ID	Fire Type	Material	Detector		Alarm Times (s)		Percent Error
				ID	Type	Experiment	Predicted	
NAVY	2-13	Smoldering	Potassium Chlorate / Lactose	2	Photo	578	DNA (1 @ 481 s)	
NAVY	2-13	Smoldering	Potassium Chlorate / Lactose	4	Photo	572	DNA (1 @ 481 s)	
NAVY	2-13	Smoldering	Potassium Chlorate / Lactose	6	Photo	524	DNA (2 @ 403 s)	
NAVY	2-13	Smoldering	Potassium Chlorate / Lactose	8	Photo	710	DNA (2 @ 403 s)	
NAVY	2-14	Smoldering	Potassium Chlorate / Lactose	2	Photo	20	DNA (4 @ 46 s)	
NAVY	2-14	Smoldering	Potassium Chlorate / Lactose	4	Photo	33	DNA (4 @ 46 s)	
NAVY	2-15	Smoldering	Potassium Chlorate / Lactose	2	Photo	19	DNA (4 @ 107 s)	
NAVY	2-15	Smoldering	Potassium Chlorate / Lactose	4	Photo	112	DNA (4 @ 107 s)	
NAVY	2-15	Smoldering	Potassium Chlorate / Lactose	6	Photo	81	DNA (3 @ 134 s)	
NAVY	2-15	Smoldering	Potassium Chlorate / Lactose	8	Photo	83	DNA (3 @ 134 s)	
NAVY	2-25	Smoldering	Potassium Chlorate / Lactose	12	Photo	316	DNA (1 @ 21 s)	
NAVY	2-25	Smoldering	Potassium Chlorate / Lactose	14	Photo	94	DNA (1 @ 215 s)	
NAVY	2-25	Smoldering	Potassium Chlorate / Lactose	16	Photo	105	DNA (1 @ 215 s)	
NAVY	2-25	Smoldering	Potassium Chlorate / Lactose	18	Photo	170	DNA (4 @ 284 s)	
NAVY	2-25	Smoldering	Potassium Chlorate / Lactose	20	Photo	301	DNA (4 @ 284 s)	
NAVY	2-25	Smoldering	Potassium Chlorate / Lactose	24	Photo	164	DNA (2 @ 225 s)	
NAVY	2-26	Smoldering	Potassium Chlorate / Lactose	14	Photo	68	DNA (1 @ 0 s)	
NAVY	2-26	Smoldering	Potassium Chlorate / Lactose	16	Photo	246	DNA (1 @ 0 s)	
NAVY	2-26	Smoldering	Potassium Chlorate / Lactose	18	Photo	65	DNA (3 @ 200 s)	
NAVY	2-27	Smoldering	Potassium Chlorate / Lactose	18	Photo	49	DNA (3 @ 1 s)	
NAVY	2-27	Smoldering	Potassium Chlorate / Lactose	20	Photo	68	DNA (3 @ 1 s)	
NAVY	2-27	Smoldering	Potassium Chlorate / Lactose	22	Photo	67	DNA (2 @ 83 s)	
NAVY	2-27	Smoldering	Potassium Chlorate / Lactose	24	Photo	65	DNA (2 @ 83 s)	
NAVY	2-28	Smoldering	Potassium Chlorate / Lactose	16	Photo	331	DNA (2 @ 11 s)	
NAVY	2-28	Smoldering	Potassium Chlorate / Lactose	18	Photo	92	DNA (2 @ 240 s)	

Temperature Rise Alarm Threshold: 13 °C

Test Series	Test ID	Fire Type	Material	Detector ID	Detector Type	Alarm Times (s) Experiment	Alarm Times (s) Predicted	Percent Error
NAVY	2-28	Smoldering	Potassium Chlorate / Lactose	20	Photo	348	DNA (2 @ 240 s)	
NAVY	2-28	Smoldering	Potassium Chlorate / Lactose	22	Photo	34	DNA (3 @ 75 s)	
NAVY	2-28	Smoldering	Potassium Chlorate / Lactose	24	Photo	32	DNA (3 @ 75 s)	
NAVY	2-34	Smoldering	Electrical Cable	12	Photo	892	DNA (2 @ 7 s)	
NAVY	2-34	Smoldering	Electrical Cable	18	Photo	297	DNA (3 @ 828 s)	
NAVY	2-34	Smoldering	Electrical Cable	20	Photo	648	DNA (3 @ 828 s)	
NAVY	2-34	Smoldering	Electrical Cable	22	Photo	843	DNA (3 @ 31 s)	
NAVY	2-34	Smoldering	Electrical Cable	24	Photo	732	DNA (3 @ 31 s)	
NAVY	2-35	Smoldering	Electrical Cable	18	Photo	423	DNA (4 @ 1529 s)	
NAVY	2-35	Smoldering	Electrical Cable	20	Photo	851	DNA (4 @ 1529 s)	
NAVY	2-35	Smoldering	Electrical Cable	22	Photo	656	DNA (4 @ 1022 s)	
NAVY	2-35	Smoldering	Electrical Cable	24	Photo	989	DNA (4 @ 1022 s)	
NAVY	2-36	Smoldering	Electrical Cable	14	Photo	1611	DNA (3 @ 963 s)	
NAVY	2-36	Smoldering	Electrical Cable	18	Photo	756	DNA (3 @ 1787 s)	
NAVY	2-36	Smoldering	Electrical Cable	20	Photo	860	DNA (3 @ 1787 s)	
NAVY	2-36	Smoldering	Electrical Cable	22	Photo	1356	DNA (2 @ 2 s)	
NAVY	2-36	Smoldering	Electrical Cable	24	Photo	915	DNA (2 @ 2 s)	
NAVY	2-37	Smoldering	Electrical Cable	12	Photo	700	DNA (1 @ 744 s)	
NAVY	2-37	Smoldering	Electrical Cable	14	Photo	759	DNA (2 @ 474 s)	
NAVY	2-37	Smoldering	Electrical Cable	16	Photo	735	DNA (2 @ 474 s)	
NAVY	2-37	Smoldering	Electrical Cable	18	Photo	295	DNA (4 @ 732 s)	
NAVY	2-37	Smoldering	Electrical Cable	20	Photo	331	DNA (4 @ 732 s)	
NAVY	2-37	Smoldering	Electrical Cable	22	Photo	633	DNA (2 @ 758 s)	
NAVY	2-37	Smoldering	Electrical Cable	24	Photo	506	DNA (2 @ 758 s)	
NAVY	2-38	Smoldering	Electrical Cable	14	Photo	754	DNA (1 @ 893 s)	

Temperature Rise Alarm Threshold: 13 °C

Test Series	Test ID	Fire Type	Material	Detector ID	Detector Type	Experiment	Predicted	Percent Error
NAVY	2-38	Smoldering	Electrical Cable	16	Photo	843	DNA (1 @ 893 s)	
NAVY	2-38	Smoldering	Electrical Cable	18	Photo	549	DNA (3 @ 348 s)	
NAVY	2-38	Smoldering	Electrical Cable	20	Photo	709	DNA (3 @ 348 s)	
NAVY	2-38	Smoldering	Electrical Cable	22	Photo	189	DNA (2 @ 914 s)	
NAVY	2-38	Smoldering	Electrical Cable	24	Photo	418	DNA (2 @ 914 s)	
NAVY	2-39	Smoldering	Electrical Cable	14	Photo	941	DNA (2 @ 623 s)	
NAVY	2-39	Smoldering	Electrical Cable	16	Photo	856	DNA (2 @ 623 s)	
NAVY	2-39	Smoldering	Electrical Cable	18	Photo	1362	DNA (2 @ 312 s)	
NAVY	2-39	Smoldering	Electrical Cable	22	Photo	786	DNA (2 @ 270 s)	
NAVY	2-39	Smoldering	Electrical Cable	24	Photo	689	DNA (2 @ 270 s)	
NAVY	2-40	Smoldering	Electrical Cable	14	Photo	402	DNA (1 @ 930 s)	
NAVY	2-40	Smoldering	Electrical Cable	16	Photo	679	DNA (1 @ 930 s)	
NAVY	2-40	Smoldering	Electrical Cable	18	Photo	1201	DNA (2 @ 1069 s)	
NAVY	2-40	Smoldering	Electrical Cable	20	Photo	1387	DNA (2 @ 1069 s)	
NAVY	2-40	Smoldering	Electrical Cable	22	Photo	1542	DNA (3 @ 1534 s)	
KEMANO	01	Flaming	Wood	28	Ion	480	DNA (1 @ 795 s)	
KEMANO	02	Flaming	Wood	14	Ion	1359	DNA (3 @ 1464 s)	
KEMANO	02	Flaming	Wood	28	Ion	1388	DNA (0 @ 1507 s)	
KEMANO	03	Flaming	Cotton Fabric	8	Ion	122	DNA (4 @ 590 s)	
KEMANO	03	Flaming	Cotton Fabric	14	Ion	155	DNA (4 @ 579 s)	
KEMANO	03	Flaming	Cotton Fabric	28	Ion	226	DNA (1 @ 836 s)	
KEMANO	05	Flaming	Upholstered Furniture	28	Ion	875	DNA (1 @ 1062 s)	
KEMANO	06	Flaming	Wood	8	Ion	1111	DNA (1 @ 1184 s)	
KEMANO	06	Flaming	Wood	14	Ion	389	DNA (2 @ 771 s)	
KEMANO	06	Flaming	Wood	28	Ion	277	DNA (4 @ 723 s)	

Temperature Rise Alarm Threshold: 13 °C

Test Series	Test ID	Fire Type	Material	Detector ID	Detector Type	Alarm Times (s) Experiment	Alarm Times (s) Predicted	Percent Error
KEMANO	07	Flaming	Wood	8	Ion	1107	DNA (1 @ 1203 s)	
KEMANO	08	Flaming	Upholstered Furniture	8	Ion	760	DNA (0 @ 931 s)	
KEMANO	08	Flaming	Upholstered Furniture	14	Ion	860	DNA (2 @ 968 s)	
KEMANO	09	Flaming	Upholstered Furniture	14	Ion	906	DNA (10 @ 966 s)	
KEMANO	10	Flaming	Wood	13	Ion	2851	DNA (2 @ 2867 s)	
KEMANO	11	Flaming	Upholstered Furniture	1	Ion	1690	DNA (3 @ 1724 s)	
KEMANO	11	Flaming	Upholstered Furniture	4	Ion	1723	DNA (2 @ 1760 s)	
KEMANO	11	Flaming	Upholstered Furniture	7	Ion	1763	DNA (1 @ 1765 s)	
KEMANO	11	Flaming	Upholstered Furniture	10	Ion	1756	DNA (0 @ 1787 s)	
KEMANO	13	Flaming	Paper	13	Ion	4977	DNA (0 @ 5045 s)	
KEMANO	01	Flaming	Wood	26	Photo	545	DNA (1 @ 795 s)	
KEMANO	02	Flaming	Wood	16	Photo	1377	DNA (3 @ 1464 s)	
KEMANO	02	Flaming	Wood	26	Photo	1408	DNA (0 @ 1507 s)	
KEMANO	03	Flaming	Cotton Fabric	6	Photo	403	DNA (4 @ 590 s)	
KEMANO	03	Flaming	Cotton Fabric	16	Photo	368	DNA (4 @ 579 s)	
KEMANO	04	Flaming	Paper	26	Photo	787	DNA (0 @ 867 s)	
KEMANO	05	Flaming	Upholstered Furniture	26	Photo	922	DNA (1 @ 1062 s)	
KEMANO	06	Flaming	Wood	6	Photo	1112	DNA (1 @ 1184 s)	
KEMANO	06	Flaming	Wood	26	Photo	265	DNA (4 @ 723 s)	
KEMANO	07	Flaming	Wood	6	Photo	1115	DNA (1 @ 1203 s)	
KEMANO	01	Smoldering	Wood	8	Ion	269	DNA (1 @ 383 s)	
KEMANO	01	Smoldering	Wood	14	Ion	422	DNA (0 @ 12 s)	
KEMANO	02	Smoldering	Wood	8	Ion	218	DNA (1 @ 385 s)	
KEMANO	04	Smoldering	Paper	8	Ion	522	DNA (0 @ 584 s)	
KEMANO	04	Smoldering	Paper	14	Ion	377	DNA (1 @ 580 s)	

Temperature Rise Alarm Threshold: 13 °C

Test Series	Test ID	Fire Type	Material	Detector ID	Detector Type	Alarm Times (s) Experiment	Alarm Times (s) Predicted	Percent Error
KEMANO	04	Smoldering	Paper	28	Ion	686	DNA (0 @ 0 s)	
KEMANO	05	Smoldering	Upholstered Furniture	8	Ion	325	DNA (2 @ 746 s)	
KEMANO	05	Smoldering	Upholstered Furniture	14	Ion	315	DNA (2 @ 718 s)	
KEMANO	07	Smoldering	Wood	14	Ion	606	DNA (1 @ 23 s)	
KEMANO	07	Smoldering	Wood	28	Ion	383	DNA (0 @ 2 s)	
KEMANO	08	Smoldering	Upholstered Furniture	28	Ion	715	DNA (1 @ 720 s)	
KEMANO	09	Smoldering	Upholstered Furniture	8	Ion	924	DNA (0 @ 672 s)	
KEMANO	09	Smoldering	Upholstered Furniture	28	Ion	795	DNA (1 @ 851 s)	
KEMANO	10	Smoldering	Wood	1	Ion	681	DNA (0 @ 1 s)	
KEMANO	10	Smoldering	Wood	4	Ion	1044	DNA (0 @ 30 s)	
KEMANO	10	Smoldering	Wood	7	Ion	2017	DNA (0 @ 18 s)	
KEMANO	10	Smoldering	Wood	10	Ion	2055	DNA (0 @ 18 s)	
KEMANO	13	Smoldering	Paper	1	Ion	3121	DNA (1 @ 3781 s)	
KEMANO	13	Smoldering	Paper	4	Ion	3246	DNA (1 @ 3934 s)	
KEMANO	13	Smoldering	Paper	7	Ion	4001	DNA (0 @ 15 s)	
KEMANO	13	Smoldering	Paper	10	Ion	4091	DNA (0 @ 17 s)	
KEMANO	01	Smoldering	Wood	6	Photo	313	DNA (1 @ 383 s)	
KEMANO	01	Smoldering	Wood	16	Photo	337	DNA (0 @ 12 s)	
KEMANO	02	Smoldering	Wood	6	Photo	223	DNA (1 @ 385 s)	
KEMANO	04	Smoldering	Paper	6	Photo	521	DNA (0 @ 584 s)	
KEMANO	04	Smoldering	Paper	16	Photo	373	DNA (1 @ 580 s)	
KEMANO	05	Smoldering	Upholstered Furniture	6	Photo	461	DNA (2 @ 746 s)	
KEMANO	05	Smoldering	Upholstered Furniture	16	Photo	356	DNA (2 @ 718 s)	
KEMANO	06	Smoldering	Wood	16	Photo	297	DNA (1 @ 63 s)	
KEMANO	07	Smoldering	Wood	16	Photo	342	DNA (1 @ 23 s)	

Temperature Rise Alarm Threshold: 13 °C

Test Series	Test ID	Fire Type	Material	Detector ID	Detector Type	Alarm Times (s) Experiment	Alarm Times (s) Predicted	Percent Error
KEMANO	07	Smoldering	Wood	26	Photo	374	DNA (0 @ 2 s)	
KEMANO	08	Smoldering	Upholstered Furniture	6	Photo	376	DNA (0 @ 0 s)	
KEMANO	08	Smoldering	Upholstered Furniture	16	Photo	334	DNA (1 @ 706 s)	
KEMANO	08	Smoldering	Upholstered Furniture	26	Photo	254	DNA (1 @ 720 s)	
KEMANO	09	Smoldering	Upholstered Furniture	6	Photo	755	DNA (0 @ 672 s)	
KEMANO	09	Smoldering	Upholstered Furniture	16	Photo	376	DNA (1 @ 701 s)	
KEMANO	09	Smoldering	Upholstered Furniture	26	Photo	288	DNA (1 @ 851 s)	
KEMANO	10	Smoldering	Wood	3	Photo	418	DNA (0 @ 1 s)	
KEMANO	10	Smoldering	Wood	6	Photo	504	DNA (0 @ 30 s)	
KEMANO	10	Smoldering	Wood	9	Photo	605	DNA (0 @ 18 s)	
KEMANO	10	Smoldering	Wood	12	Photo	755	DNA (0 @ 18 s)	
KEMANO	10	Smoldering	Wood	15	Photo	687	DNA (0 @ 18 s)	
KEMANO	11	Smoldering	Upholstered Furniture	3	Photo	344	DNA (0 @ 22 s)	
KEMANO	11	Smoldering	Upholstered Furniture	6	Photo	371	DNA (0 @ 117 s)	
KEMANO	11	Smoldering	Upholstered Furniture	9	Photo	439	DNA (0 @ 20 s)	
KEMANO	11	Smoldering	Upholstered Furniture	12	Photo	485	DNA (0 @ 24 s)	
KEMANO	11	Smoldering	Upholstered Furniture	15	Photo	580	DNA (0 @ 24 s)	
KEMANO	13	Smoldering	Paper	3	Photo	420	DNA (1 @ 3781 s)	
KEMANO	13	Smoldering	Paper	6	Photo	479	DNA (1 @ 3934 s)	
KEMANO	13	Smoldering	Paper	9	Photo	658	DNA (0 @ 15 s)	
KEMANO	13	Smoldering	Paper	12	Photo	764	DNA (0 @ 17 s)	
KEMANO	13	Smoldering	Paper	15	Photo	725	DNA (0 @ 15 s)	

Velocity Alarm Threshold: 0.15 m/s

Test Series	Test ID	Fire Type	Material	Detector ID	Detector Type	Alarm Times (s) Experiment	Alarm Times (s) Predicted	Percent Error
NAVY	1-38	Flaming	Wood	1	Ion	62	40	-35%
NAVY	1-38	Flaming	Wood	2	Photo	874	40	-95%
NAVY	1-38	Flaming	Wood	3	Ion	155	40	-74%
NAVY	1-38	Flaming	Wood	4	Photo	860	40	-95%
NAVY	1-39	Flaming	Wood	1	Ion	69	9	-87%
NAVY	1-39	Flaming	Wood	3	Ion	43	9	-79%
NAVY	1-39	Flaming	Wood	4	Photo	555	9	-98%
NAVY	1-40	Flaming	Wood	1	Ion	43	6	-86%
NAVY	1-40	Flaming	Wood	3	Ion	123	6	-95%
NAVY	2-09	Flaming	Cardboard	5	Ion	86	81	-6%
NAVY	2-09	Flaming	Cardboard	6	Photo	129	81	-37%
NAVY	2-09	Flaming	Cardboard	7	Ion	100	81	-19%
NAVY	2-09	Flaming	Cardboard	8	Photo	124	81	-35%
NAVY	2-10	Flaming	Cardboard	5	Ion	166	4	-98%
NAVY	2-10	Flaming	Cardboard	6	Photo	592	4	-99%
NAVY	2-10	Flaming	Cardboard	7	Ion	228	4	-98%
NAVY	2-10	Flaming	Cardboard	8	Photo	260	4	-98%
NAVY	2-11	Flaming	Cardboard	2	Photo	76	106	39%
NAVY	2-11	Flaming	Cardboard	3	Ion	67	106	58%
NAVY	2-11	Flaming	Cardboard	4	Photo	84	106	26%
NAVY	2-12	Flaming	Cardboard	1	Ion	28	219	682%
NAVY	2-12	Flaming	Cardboard	3	Ion	57	219	284%
NAVY	2-12	Flaming	Cardboard	4	Photo	82	219	167%
NAVY	2-21	Flaming	Cardboard	13	Ion	63	213	238%
NAVY	2-21	Flaming	Cardboard	14	Photo	164	213	30%
NAVY	2-21	Flaming	Cardboard	15	Ion	36	213	492%
NAVY	2-21	Flaming	Cardboard	16	Photo	153	213	39%
NAVY	2-22	Flaming	Cardboard	13	Ion	43	99	130%
NAVY	2-22	Flaming	Cardboard	14	Photo	83	99	19%
NAVY	2-22	Flaming	Cardboard	15	Ion	30	99	230%

REFERENCES

Alpert, R.L., "Fire Induced Turbulent Ceiling Jet," Technical Report, FMRC 19722-2, Factory Mutual Research Corporation, Norwood, MA, May 1971.

Benjamin, I., Heskestad, G., Bright, R., and Hayes, T., "An Analysis of the Report on Environments of Fire Detectors," Fire Detection Institute, 1979.

Beyler, C., and DiNenno, P., "Letters to the Editor", *Fire Technology*, Vol. 27, No. 2, pp. 160-169, May 1991.

Bjorkman, J., Kokkala, M.A., and Ahola, H., "Measurements of the Characteristic Lengths of Smoke Detectors," *Fire Technology*, Vol. 28, No. 2, 1992, pp. 99-106.

Brammer, D.R., "A comparison between predicted and actual behavior of domestic smoke detectors in a realistic house fire," Master of Engineering Thesis, University of Canterbury, Christchurch, New Zealand, 2002.

Brozovski, E., "A Preliminary Approach to Siting Smoke Detectors Based on Design Fire Size and Detector Aerosol Entry Lag Time, Master of Science Thesis, Worcester Polytechnic Institute, Worcester, MA, 1991.

Bukowski, R.W., "Comments on Measurements of the Characteristic Lengths of Smoke Detectors," *Fire Technology*, Vol. 28, No. 2,1992, pp. 107-108.

Bukowski, R.W., and Averill, J.D., "Methods for Predicting Detector Activation," *Proceedings of 14th Joint Panel Meeting of the UJNR Panel on Fire Research and Safety*, May 28 – June 3, 1998, Tsukuba, Japan, U.S./Japan Government Cooperative Program on Natural Resources (UJNR), Fire Research and Safety, 1998, pp. 213-221.

Bukowski, R.W. and Mulholland, G.W., "Smoke Detector Design and Smoke Properties. Final Report," NBS Technical Note 973, National Bureau of Standards, Gaithersburg, MD, November 1978.

Bukowski, R.W., Waterman, T.E., and Christian, W.J., "Detector Sensitivity and Siting Requirements for Dwellings", Final Technical Report, IITRI Project J6340, Contract No. 4-36092, NBS-GCR-75-51, National Bureau of Standards, Gaithersburg, MD, 1975.

CAN/ULC-S531-M87, "Standard for Smoke Alarms," Underwriter's Laboratories of Canadam Toronto, ON, Canada, 1995 Ed., pp. 1-86.

Carhart, H.W., Toomey, T.A., and Williams, F.W., "The ex-USS SHADWELL Full-scale Fire Research and Test Ship," Naval Research Laboratory, NRL Memorandum Report 6074, Revised January 20, 1988, Reissued 1992.

Cholin, J.M., and Marrion, C., "Performance Metrics for Fire Detection," *Fire Protection Engineering*, pp. 21-30, No. 11, Summer 2001.

Collier, P.C.R., "Fire In a Residential Building: Comparisons Between Experimental Data and a Fire Zone Model," Fire Technology, Vol. 32, No. 3, August 1996, pp. 195 – 219.

Cleary, T., Chernovsky, A., Grosshandler, W., and M. Anderson, "Particulate Entry Lag in Spot-Type Smoke Detectors," *Fire Safety Science – Proceedings of the 6th International Symposium*, July 5-9, 1999, Poitiers, France, International Association for Fire Safety Science, Boston, MA, Curtat, M., Editor, 2000, pp. 779 – 790.

Davis, W.D., and Notarianni, K.A., "NASA Fire Detector Study," NISTIR 5798, National Institute of Standards and Technology, 1996.

Devore, J.L., *Probability and Statistics for Engineering and the Sciences*, 5th Edition, Duxbury, Pacific Grove, CA, 2000, pp. 40 – 44.

Evans, D., and Stroup, D., "Methods to Calculate the Response Time of Heat and Smoke Detectors Installed Below Large Unobstructed Ceilings," NBSIR 85-3167, National Bureau of Standards, Gaithersburg, MD, February 1985.

Foster, W.W., "Attenuation of Light by Wood Smoke," *British Journal of Applied Physics*, Vol. 10, Sept. 1959, pp. 416-420.

Geiman, J.A., and Gottuk, D.T., "Alarm Thresholds for Smoke Detector Modeling," *Fire Safety Science – Proceedings of the 7th International Symposium*, June 16-21, 2002, Worcester, MA, International Association for Fire Safety Science, Boston, MA, Evans, D.D., Editor, 2003, pp. 197 – 208.

Gottuk, D.T., Harrison, M.A., Rose-Pehrsson, S.L., Owrutsky, J.C., Williams, F.W., and Farley, J.P., "Shipboard Evaluation of Fire Detection Technologies for Volume Sensor Development," Naval Research Laboratory, Memorandum Report, 6180-0282, 2003.

Gottuk, D.T., Hill, S.A., Schemel, C.F., Strehlen, B.D., Rose-Phersson, S.L., Shaffer, R.E., Tatem, P.A., and Williams, F.W., "Identification of Fire Signatures for Shipboard Multi-criteria Fire Detection Systems," Naval Research Laboratory, Memorandum Report, 6180-99-8386, Washington, D.C., June 18, 1999.

Harrison, M.A., Gottuk, D.T., Rose-Pehrsson, S.L., Owrutsky, J.C., Williams, F.W., and Farley, J.P., "Video Image Detection (VID) Systems and Fire Detection Technologies: Preliminary Results from the Magazine Detection System Response Tests," Naval Research Laboratory, Memorandum Report, 6180-0262, 2003.

Helsper, C., Fissan, H.J., Muggli, J., and Scheidweiler, A., "Verification of Ionization Chamber Theory," *Fire Technology*, Vol. 19, No. 1, February 1983, pp. 14-21.

Heskestad, G., "Escape Potentials From Apartments Protected by Fire Detectors in High-Rise Buildings," Final Technical Report, Contract No. H-2034R, Department of Housing and Urban Development, FMRC Serial No. 21017, Factory Mutual Research Corp., Norwood, MA, June 1974.

Heskestad, G., "Generalized Characterization of Smoke Entry and Response for Products-of-Combustion Detectors," Proceedings, Fire Detection for Life Safety, March 31-April 1, 1975, National Research Council, pp. 93-127, 1975.

Heskestad, G., and Delichatsios, M.A., "Environments of Fire Detectors – Phase I: Effect of Fire Size, Ceiling Height, and Material," Volume I: "Measurements" (NBS-GCR-77-86), (1977), Volume II: "Analysis" (NBS-GCR-77-95), National Bureau of Standards, Gaithersburg, MD, 1977.

Hosemann, J.P., "Methods to Determine Particle Size Distribution of Highly Concentrated Polydispersions of Mie-Particles," Dissertation, Rheinisch-Westfalisch Technical University, Aachen, Germany, 1970.

Lee, T.G.K., and Mulholland, G. "Physical Properties of Smokes Pertinent to Smoke Detector Technology," NBSIR 77-1312, National Bureau of Standards, Gaithersburg, MD, Nov. 1977.

Litton, C.D., "Mathematical Model for Ionization-Type Smoke Detectors and the Reduced Source Approximation," *Fire Technology*, Vol. 13, No. 4, November 1977, pp. 266-281.

Loepfe, M., Ryser, P., Tompkin, C., and Wieser, D.,"Optical Properties of Fire and Non-fire Aerosols," *Fire Safety Journal*, Vol. 29, No. 2-3, September 1997, pp. 185-194.

Luck, H. and Sievert, U., "Does an Over-All Modeling Make Any Sense in Automatic Fire Detection?," *AUBE '99 Proceedings of the 11th International Conference on Automatic Fire Detection*, Gerhard Mercator Universität Duisburg, pp. 1-21, 1999.

Marrion, C., "Lag Time Modeling and the Effects of Ceiling Jet Velocity on the Placement of Optical Smoke Detectors," Master's Thesis, Worcester Polytechnic Institute, Worcester, MA, 1989.

McAvoy, T.J., Milke, J., and Kunt, T.A., "Using Multivariate Statistical Methods to Detect Fires," *Fire Technology*, Vol. 32, No. 1, Jan./Feb. 1996, pp. 6-24.

Meacham, B.J., "Characterization of Smoke from Burning Materials for the Evaluation of Light Scattering Type Smoke Detector Response," Master of Science Thesis, Worcester Polytechnic Institute, Worcester, MA, 1992.

Milke, J.A., "Application of Neural Networks for Discriminating Fire Detectors," International Conference on Automatic Fire Detection, AUBE '95, April 1995, pp. 213-222.

Milke, J., "Smoke Management for Covered Malls and Atria," Fire Technology, Vol. 26, No. 3, 1990, pp. 223 – 243.

Milke, J.A., and McAvoy, T.J., "Analysis of Fire and Non-fire Signatures for Discriminating Fire Detection," Fire Safety Science – Proceedings of the 5th International Symposium, March 3-7 1997, Melbourne, Australia, International Association for Fire Safety Science, Boston, MA, Hasemi, Y., ed., 1997, pp. 819-828.

Milke, J.A., and McAvoy, T.J., "Neural Networks for Smart Fire Detection," NIST-GCR-96-699, National Institute of Standards and Technology, Gaithersburg, MD, Dec. 1996.

Mowrer , F.W., and Friedman, J., "Experimental Investigation of Heat and Smoke Detector Response," *Proceedings of Fire Suppression and Detection Research Application Symposium*, Orlando, FL, February 24-26, 1998, pp. 256-264.

Mulholland, G.W., "How well are we measuring smoke?" *Fire and Materials*, Vol. 6, No. 2, June 1982, pp. 65-67.

Mulholland, G.W., "Smoke Production and Properties," *SFPE Handbook of Fire Protection Engineering*, Chapter 2-13, 3rd Edition, DiNenno, P.J., Ed., National Fire Protection Association, Quincy, MA, 2002.

Mulholland, G.W., and Croarkin, C., "Specific Extinction Coefficient of Flame Generated Smoke," *Fire and Materials*, Vol. 24, 2000, pp. 227-230.

Mulholland, G.W., Johnsson, E.L., Fernandez, M.G., and Shear, D.A., "Design and Testing of a New Smoke Concentration Meter," *Fire and Materials*, Vol. 24, No. 5, September/October 2000, pp. 231-243.

Mulholland, G.W., and Liu, B.Y.H., "Response of Smoke Detectors to Monodisperse Aerosols," *Journal of Research of the National Bureau of Standards*, Vol. 85, No. 3, May – June 1980, pp. 223 – 237.

Newman, J.S., "Modified Theory for the Characterization of Ionization Smoke Detectors," *Fire Safety Science – Proceedings of the 4th International Symposium*, July 13-17, 1994, Ottawa, Ontario, Canada, International Association for Fire Safety Science, Boston, MA, Kashiwagi, T., Editor, 1994, pp. 785-792.

NFPA 72, *National Fire Alarm Code,* National Fire Protection Association, Quincy, MA, 2002.

NFPA 92B, *Guide for Smoke Management Systems in Malls, Atria, and Large Areas*, National Fire Protection Association, Quincy, MA, 1990.

Oldweiler, A., "Investigation of the Smoke Detector L Number in the UL Smoke Box," Master of Science Thesis, Worcester Polytechnic Institute, Worcester, MA, 1995.

Putorti, A.D., "Design Parameters for Stack-Mounted Light Extinction Measurement Devices," NISTIR 6215, National Institute of Standards and Technology, Gaithersburg, MD, July 1998.

Quintiere, J.G., "Smoke Measurements: An Assessment of Correlations between Laboratory and Full-scale Experiments," *Fire and Materials*, Vol. 6, Nos. 3 and 4, 1982, pp. 145-148.

Rose-Pehrsson, S.L., Shaffer, R.E., Hart, S.J., Williams, F.W., Gottuk, D.T., Strehlen, B.D., and Hill, S.A., "Multi-Criteria Fire Detection Systems Using a Probalistic Neural Network," *Sensors and Acuators* B 69, 2000 pp. 325-335.

Scheidweiler, A., "Ionization Chamber as Smoke Dependent Resistance," *Fire Technology*, Vol. 12, No. 2, May 1976, pp. 113-123.

Schifiliti, R.P., Meacham, B.J., and Custer, R.L.P., "Design of Detection Systems," *SFPE Handbook of Fire Protection Engineering*, Chapter 4-1, 2nd Edition, DiNenno, P.J., Ed., National Fire Protection Association, Quincy, MA, 1995.

Schifiliti, R.P., Meacham, B.J., and Custer, R.L.P., "Design of Detection Systems," *SFPE Handbook of Fire Protection Engineering*, Chapter 4-1, 3rd Edition, DiNenno, P.J., Ed., National Fire Protection Association, Quincy, MA, 2002.

Schifiliti, R.P., and Pucci, W.E., "Fire Detection Modeling: State of the Art", Fire Detection Institute, Bloomfield, CT, 1996.

Seader, J.D. and Chien, W.P., "Physical Aspects of Smoke Development in an NBS Smoke-Density Chamber," *Journal of Fire and Flammability*, Vol. 6, 1975.

Seader, J.D., and Einhorn, I.N., "Some Physical, Chemical, Toxicological, and Physiological Aspects of Fire Smokes," Proceedings, 16th Symposium (International) on Combustion, The Combustion Institute, 1977, pp. 1423 – 1445.

Spearpoint, M.J., and Smithies, J.N., "Practical Comparison of Domestic Smoke Alarm Sensitivity Standards," Fire Research Station, Home Office Fire Research and Development Group, FRDG Publication No. 4/97, 1997.

Su, J.Z., Crampton, G.P., Carpenter, D.W., McCartney, C., and Leroux, P., "KEMANO FIRE STUDIES – Part 1: Response of Residential Smoke Alarms," Research Report 108, National Research Council of Canada, Ottawa, Canada, April 2003.

UL 217, "Standard for Single and Multiple Station Smoke Alarms," Fifth Edition dated February 21, 1997 with revisions through October 12, 2001, Underwriters Laboratories Inc., Northbrook, IL, 2001.

UL 268, "Standard for Smoke Detectors for Fire Protective Signaling Systems," Fourth Edition dated December 30, 1996 with revisions through October 22, 2003, Underwriters Laboratories Inc., Northbrook, IL, 2003.

Wakelin, A.J., "An Investigation of Correlations for Multi-Signal Fire Detectors," Master of Science Thesis, Worcester Polytechnic Institute, Worcester, MA, February 1997.

Wong, J.T., Gottuk, D.T., Rose-Pehrsson, S.L., Shaffer, R.E., Hart, S., Tatem, P.A., Williams, F.W., "Results of Multi-Criteria Fire Detection System Tests," Naval Research Laboratory, May 2000.